# Investigating the Control of Endogenous Respiration and Sulfite Oxidation in *Acidithiobacillus thiooxidans* and Ferric Iron Reduction by the Bacterium

By

Jerome Reuben Saba

A Thesis

Submitted to the Faculty of Graduate Studies

The University of Manitoba

In Partial Fulfillment

of the Requirements for the Degree

Master of Science

Department of Microbiology

The University of Manitoba

Winnipeg, Manitoba

2003

THE UNIVERSITY OF MANITOBA

FACULTY OF GRADUATE STUDIES

*****

COPYRIGHT PERMISSION PAGE

# Investigating the Control of Endogenous Respiration and Sulfite Oxidation in *Acidithiobacillus thiooxidans* and Ferric Iron Reduction by the Bacterium

BY

Jerome Reuben Saba

A Thesis/Practicum submitted to the Faculty of Graduate Studies of The University of Manitoba in partial fulfillment of the requirements of the degree of Master of Science

# Table of Contents

## Abstract

In the obligate chemolithoautotroph *Acidithiobacillus thiooxidans* (formerly *Thiobacillus thiooxidans*) strain ATCC 8085, two different responses were observed in the presence of chemical compounds known to collapse $\Delta p$ (uncouplers, permeant anions, weak organic acids). In the presence of these compounds, endogenous respiration rate (endogenous substrate(s) oxidation) was stimulated (measured by oxygen consumption and exogenous ferric iron reduction) but sulfite oxidation rate was inhibited (measured by oxygen consumption). The latter is the primary energy generating step via the electron transport chain. Results suggested that a normal, controlled respiratory system, similar to the mitochondrial electron transport system or that of heterotrophic bacteria, may be in operation for endogenous respiration. In such systems, the collapse of $\Delta p$ leads to the uncoupling of oxidation from phosphorylation with the oxidative component operating unhindered at its maximal rate. Whereas for sulfite oxidation, $\Delta p$ maintenance is essential. In the latter case, the coupling of substrate oxidation to reducing power generation for $CO_2$ fixation, via an energy requiring reversed electron transport, may be speculated. Additionally, an energy requiring step in the substrate oxidation pathway itself has been suggested for other autotrophs and may also be relevant to these observations.

Exogenous ferric iron reduction (ferrous iron formation) by endogenous substrate(s) oxidation was unexpected, since the bacterium does not oxidize ferrous iron. The coupling of endogenous respiration to exogenous ferric iron reduction was not complete, even in the presence of cyanide or when incubated anaerobically. Cell

concentration influenced exogenous ferric iron reduction. Exogenous ferric iron reduction by 5, 10, and 20 mg/mL cell concentrations followed normal Michaelis-Menten kinetics with respect to ferric iron concentration, while 40 and 80 mg/mL cell concentrations showed kinetics often associated with cooperativity or allosterism. Reduction of endogenous ferric iron by endogenous respiration was also observed. The coupling of exogenous substrate oxidation (sulfur, thiosulfate, formate) to exogenous ferric iron reduction was apparent aerobically and anaerobically. Ferric iron reduction by the bacterium may represent an inherent physiology of the bacterium to respire anaerobically, or possibly as a means of activating inert elemental sulfur, a preferred growth substrate for the bacterium.

## Acknowledgements

It is with great pleasure that I take this opportunity to express my profound gratitude to Dr. I. Suzuki, Professor Emeritus in the Department of Microbiology, for his gracious inspiration and expert guidance during the course of the research and the preparation of this thesis. I would also like to thank him for financial support.

My appreciation is also extended to Dr. R. Sparling and Dr. F. Wang for serving on my advisory committee and for reviewing this thesis.

Many thanks to the graduate students of the department for their friendship and assistance whenever needed.

Special thanks to my family for their love and support.

## List of Tables

Part I :

## List of Figures

Part I :

Part II :

## List of Abbreviations

| | |
|---|---|
| GSH | reduced glutathione |
| DMSO | dimethyl sulfoxide |
| DMSO/sulfur | precipitated elemental sulfur solubilized in dimethyl sulfoxide |
| Tween 80 sulfur | precipitated elemental sulfur suspension in polyoxyethylene (20) sorbitan monoleate |
| CCCP | carbonyl cyanide-m-chlorophenylhydrazone |
| 2,4-DNP | 2,4-dinitrophenol |
| NEM | *N*-ethylmaleimeide |
| HQNO | 2-heptyl-4-hydroxyquinoline-*N*-oxide |
| $TPB^-$ | tetraphenyl boron |

## Introduction

*Acidithiobacillus thiooxidans* (formerly *Thiobacillus thiooxidans*) is an aerobic, obligate chemolithoautotroph that obtains energy and reducing power necessary for growth from the oxidation of reduced inorganic sulfur compounds. The bacterium has played a pivotal role in the elucidation of the sulfur oxidation scheme. In the bacterium, the primary energy generating step is the oxidation of sulfite to sulfate via a membrane associated sulfite oxidoreductase which utilizes *c*-type cytochrome as the electron acceptor. The electrons are subsequently released into a cytochrome populated electron transport chain. Little, however, is known about the role of the proton motive force ($\Delta p = \Delta\Psi - 59\Delta pH$) in controlling sulfite oxidation by the bacterium. As a result, an investigation was undertaken to examine the control of sulfite oxidation, with respect to $\Delta p$, by using chemical compounds known to collapse this parameter. Chemicals tested include uncouplers, permeant anions, weak organic acids, and typical inhibitors of the electron transport chain. Additionally, the control of endogenous respiration was also examined as an alternate to exogenous substrate oxidation. Both endogenous respiration and sulfite oxidation were examined by oxygen consumption studies using a Clarke oxygen electrode and a Gilson oxygraph. Endogenous respiration was also examined by coupling to exogenous ferric iron reduction.

Ferric iron reduction by *A. thiooxidans* was unexpected since the bacterium does not oxidize ferrous iron. Thus ferric iron reduction by the bacterium presented an additional avenue for exploration.

# Historical

**General properties of the bacterium**

The γ-*Proteobacterium Acidithiobacillus thiooxidans* (formerly *Thiobacillus thiooxidans*) (Kelly and Wood, 2000) is an aerobic, Gram negative, rod shaped, motile, obligate chemolithoautotroph. Originally isolated from a compost of soil, sulfur, and rock phosphate (Waksman and Joffe, 1922), the bacterium is also distinguished by its ability to withstand extreme acid conditions (acidophile: growth optimum pH 1 - 3.5) and the ability to oxidize reduced inorganic sulfur compounds to sulfate to generate energy (ATP) and reducing power (NAD(P)H) required for growth and $CO_2$ fixation. *A. thiooxidans* grows optimally at 28-30 °C thus the bacterium is also classified as a mesophile. Standard taxanomical methods such as DNA analysis (Jackson *et al.*, 1968; Harrison, 1982) and fatty acid profile (Levin *et al.*, 1971) have been reported. Most importantly, the bacterium has served as one of the central microorganisms in the elucidation of the sulfur oxidation scheme (Suzuki 1974; 1999).

**Sulfur oxidation scheme**

The main pathway for the biological oxidation of reduced inorganic sulfur compounds is as follows (see Suzuki, 1999 for review) :

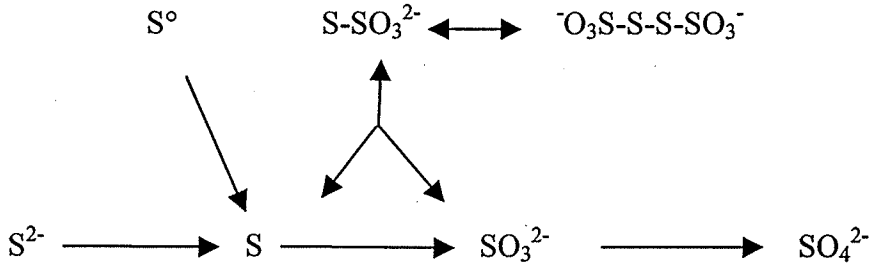

The pathway is initiated with the oxidation of sulfide ($S^{2-}$) to elemental sulfur (S) with sulfide oxidase catalyzing the initial step ($H_2S + ½ O_2 \rightarrow S + H_2O$). Subsequently, elemental sulfur is oxidized to sulfite ($SO_3^{2-}$) with the sulfur-oxidizing enzyme governing the reaction ($S + O_2 + H_2O \rightarrow H_2SO_3$). In the presence of *N*-ethylmaleimide (NEM), a sulfhydryl-binding inhibitor, sulfur oxidation is inhibited. The accumulating sulfur may condense non-enzymatically to form solid elemental sulfur ($S^o$), which assumes a stable sulfur octet ($S_8$) configuration. In cell-free systems, the sulfur-oxidizing enzyme requires a cofactor such as reduced glutathione (GSH) in catalytic amounts for the oxidation of solid elemental sulfur. GSH is suggested to carry out a nucleophilic attack on the sulfur octet to produce a linear glutathione polysulfide chain ($GS\text{-}S_n^-$) that is readily oxidized by a cell-free system to sulfite and glutathione polysulfide with a reduced sulfur chain length ($GS\text{-}S_{n-1}^-$) in a reaction catalyzed by the sulfur-oxidizing enzyme (Suzuki 1965; 1999). The role of GSH, aside from opening up the sulfur octet, is to maintain the terminal sulfur atom of glutathione polysulfide in the oxidation state of sulfide for enzymatic oxidation. The final step in the oxidation scheme is the main energy generating step and involves the oxidation of sulfite to sulfate ($SO_4^{2-}$) ($H_2SO_3 + ½ O_2 \rightarrow SO_4^{2-} + 2H^+ + 2e^-$). The oxidation may proceed via two different mechanisms governed by two different enzyme systems.

Sulfite may be oxidized to sulfate with a concomitant reduction of *c*-type cytochrome by sulfite oxidoreductase. The reduced cytochrome is oxidized with molecular oxygen by a cytochrome oxidase in the electron transport chain :

$$SO_3^{2-} + 2 \text{ Cyt } c\ Fe^{3+} + H_2O \rightarrow SO_4^{2-} + 2 \text{ Cyt } c\ Fe^{2+} + 2H^+$$

$$2 \text{ Cyt } c\ Fe^{2+} + ½ O_2 + 2H^+ \rightarrow 2 \text{ Cyt } c\ Fe^{3+} + H_2O$$

The membrane bound sulfite oxidoreductase has been shown to be present in *A. thiooxidans* (Nakamura *et al.*, 1995). In *Acidithiobacillus ferrooxidans* (formerly *Thiobacillus ferrooxidans*), *c*-type cytochrome is replaced by $Fe^{3+}$ (Sugio *et al.*, 1992).

Alternatively, sulfite may be oxidized by the adenosine phosphosulfate (APS) reductase pathway. In the APS reductase pathway, APS is formed from sulfite and adenosinemonophosphate (AMP) by APS reductase. Next, APS is converted to adenosine diphosphate (ADP) and sulfate in a substrate level phosphorylation reaction catalyzed by ADP sulfurylase. From the generated ADP molecules, ATP is produced in reactions catalyzed by adenylate kinase :

$2SO_3^{2-} + 2AMP \rightarrow 2APS + 4e^-$

$2APS + 2P_i \rightarrow 2SO_4^{2-} + 2ADP$

$2ADP \rightarrow ATP + AMP$

APS reductase pathway has not been identified in *A. thiooxidans* but it is present in other thiobacilli.

In the presence of 2-n-heptyl-4-hydroxyquinoline *N*-oxide (HQNO), a strong inhibitor of the electron transport chain, sulfite oxidation via the sulfite oxidoreductase is inhibited. In turn, the accumulating sulfite may non-enzymatically condense with free elemental sulfur to form thiosulfate ($S_2O_3^{2-}$). Thiosulfate metabolism may follow two different routes as well. Thiosulfate may be oxidized to tetrathionate ($S_4O_6^{2-}$) by thiosulfate oxidase ($2S_2O_3^{2-} + ½\ O_2 + 2H^+ \rightarrow S_4O_6^{2-} + H_2O$) or undergo decomposition to form elemental sulfur and sulfite by rhodanese (thiosulfate cleaving enzyme; sulfur transferase) ($S_2O_3^{2-} + 2H_2O \leftrightarrow S^o + H_2SO_3 + 2OH^-$). Elemental sulfur and sulfite produced from thiosulfate decomposition may re-enter the main sulfur oxidation scheme.

Tetrathionate hydrolysis, via tetrathionate hydrolase has also been proposed and it generates thiosulfate, sulfur, and sulfate as the end products ($S_4O_6^{2-} + H_2O \rightarrow S_2O_3^{2-} + S^o + SO_4^{2-} + 2H^+$). In *A. thiooxidans* at pH 5, thiosulfate cleavage to sulfur and sulfite was shown to occur, whereas at pH 3, thiosulfate oxidation and subsequent hydrolysis was shown to prevail (Masau *et al.*, 2001).

**Sulfite oxidoreductase**

Sulfite oxidoreductases are considered to be molybdenum containing enzymes that catalyze the oxidation of sulfite with the transfer of electrons to *c*-type cytochrome or other electron acceptors (ie. $Fe^{3+}$) (Suzuki, 1994; Kappler and Dahl, 2001.)

$$SO_3^{2-} + 2\ \text{Cyt}\ c\ Fe^{3+} + H_2O \rightarrow SO_4^{2-} + 2\ \text{Cyt}\ c\ Fe^{2+} + 2H^+$$

In general, the enzyme is responsible for the oxidation of sulfite to sulfate and the subsequent release of electrons to the electron transport chain (Suzuki, 1975; Yamanaka, 1981; Suzuki, 1994). The enzyme has been purified from several different thiobacilli including *Starkeya novella* (formerly *Thiobacillus novellus*) (Charles and Suzuki, 1966; Yamanaka *et al.*, 1981; Toghrol and Southerland, 1983; Kappler *et al.*, 2000), *Thiobacillus thioparus* (Lyric and Suzuki, 1970), *Paracoccus versutus* (formerly *Thiobacillus versutus*) (Lu and Kelly, 1984), *Acidiphilium acidophilum* (formerly *Thiobacillus acidophilus*) (de Jong *et al.*, 2000) and *A. ferrooxidans* (Vestal and Lundgren, 1971). In the aforementioned organisms, the enzyme has been purified from the soluble fraction of cell free extracts suggesting cytoplasmic or periplasmic location (Kappler and Dahl, 2001). In contrast, the sulfite oxidoreductase purified from *A.*

*thiooxidans* was isolated from the membrane fraction of cell free extracts (Nakamura *et al.*, 1995).

The sulfite oxidoreductase purified by Nakamura *et al.* (1995) required a detergent to be solubilized (n-Heptyl-$\beta$-D-thioglucoside) and also to prevent the loss of activity and aggregation once solubilized (Triton X-100). The enzyme had a molecular weight of 400 kDa and was composed of three different subunits ($M_r$ = 74, 70, and 62 kDa). The purified enzyme exhibited high specificity for sulfite as an electron donor and both *c*-type cytochrome and ferricyanide as electron acceptors. The purified enzyme did not use oxygen as an electron acceptor. The $K_m$ for sulfite was 1.95 mM and the enzyme was inhibited by sulfhydryl-binding agents. No prosthetic groups were described for this enzyme, and the near neutral pH optimum of 7.5 suggests a location on the cytoplasmic face of the plasma membrane. It is worth mentioning that the sulfite oxidoreductase of *A. thiooxidans* posses a higher molecular mass and more complex subunit structures than the enzymes purified from the soluble fraction of cell free extracts. For comparison, an enzyme also involved in sulfite oxidation and also purified from the membrane fraction, however in *A. ferrooxidans* and possessing $Fe^{3+}$ as an electron acceptor, has an equally large molecular weight of 650 kDa and two different subunits ($M_r$ = 61 and 59 kDa) (Sugio *et al.*, 1992).

**Cytochromes in *A. thiooxidans***

Earlier studies on the effects of inhibitors showed that sulfur oxidation by *A. thiooxidans* was clearly inhibited by low concentrations of cyanide, azide, and carbon monoxide (Vogler *et al.*, 1942). All of these are well known inhibitors of the cytochrome

system. The sensitivity to these inhibitors and additionally the aerobic nature of the entire process led to the assumption that the cytochrome system was involved in sulfur oxidation by *A. thiooxidans*. Evidences gathered ever since have substantiated this early claim.

Cook and Umbreit (1962) were one of the first to show evidence for the presence of a cytochrome system in the said bacterium. They identified *c*-type cytochrome in cell free extracts of sulfur grown cells. In addition, they detected cytochrome oxidase activity in the bacterium and also isolated ubiquinone.

Kodoma *et al.* (1970) identified *a*-, *b*-, and *c*-type cytochromes in the membrane fraction of an unidentified strain of this bacterium grown on sulfur. Additionally, *c*-type cytochrome was also identified in the soluble fraction. Sulfite was able to reduce all of the cytochromes of the membrane fraction and also the *c*-type cytochrome of the soluble fraction when catalytic amounts of membrane fraction were present.

Tano *et al.* (1982) working with the membrane fraction of strain ON106 grown on sulfur identified *a*-, *b*-, *c*-, and *d*-type cytochromes in the bacterium. They also showed that the amount of *a*- and *c*-type cytochromes decreased during growth whereas those of *b*- and *d*-type cytochromes increased. The increase in *b*- and *d*-type cytochromes during growth may be attributed to the higher affinity for oxygen by *d*-type cytochrome than by *a*-type (Yamanaka, 1992). This is especially true during growth when oxygen concentration must have decreased because of limited aeration rate and increased cell numbers (Masau *et al.*, 2001). Tano *et al.* did not propose a scheme for electron flow in the bacterium apart from mentioning *b*-type cytochrome to be an important intermediate carrier in the electron transport chain.

Nakamura *et al.* (1992) working with the membrane fraction of thiosulfate grown strain JCM 7814 showed that sulfite oxidation was followed by the reduction of cytochromes. Cytochromes identified in the bacterium included *a*-, *b*-, and *c*-type cytochromes.

Nogami *et al.* (1997) working with the membrane fraction of strain NB1-3 isolated from corroded concrete and grown on sulfur-salt medium showed the presence of only *a*- and *b*-type cytochromes. The researchers proposed that the *a*- and *b*-type cytochromes constituted an ubiquinol oxidase ($ba_3$) which also serves as the terminal oxidase in the bacterium. Cytochromes of the *c*-type were also identified by the group but it was present in the soluble fraction. Electron transport in the organism was strongly inhibited by cyanide, azide, and HQNO.

More recently, Masau *et al.* (2001) working with strain ATCC 8085 grown on thiosulfate (same strain and growth substrate as in the present research) identified *a*-, *b*-, *c*-, and *d*-type cytochromes in the bacterium. Results were therefore consistent with the earlier report by Tano *et al.* (1982). Cytochromes of the *b*-, *c*-, and *d*-type were more prominent than the *a*-type cytochrome. In the presence of substrates (sulfite, sulfur, thiosulfate), *c*-type cytochrome was always reduced first followed by the other cytochromes. This observation was consistent in both whole cells and cell free crude extracts. In the presence of respiratory chain uncouplers carbonyl cyanide-m-chlorophenylhydrazone (CCCP) and 2,4-dinitrophenol (2,4-DNP) only *c*-type cytochrome was reduced by the substrates tested in the whole cells whereas all the cytochromes identified were reduced in cell free crude extracts. In contrast, in the

presence of HQNO, only *c*-type cytochrome was reduced in both whole cells and cell free crude extracts.

In general, cytochromes are well defined in the electron transport chain of *A. thiooxidans*.

**Electron transport**

Bacterial respiratory chains are composed of a variety of electron transport constituents, such as flavoproteins, iron sulfur proteins, quinones, and cytochromes (Thöny-Meyer, 1997). Constituents of a respiratory chain are either part of or associated with the cytoplasmic membrane. Thus the transport of electrons through these constituents leads to the translocation of protons ($H^+$) from the cytoplasmic side of the cell to the periplasm of the cell and the subsequent formation across the cytoplasmic membrane of a proton electrochemical gradient which in turn can be used to drive ATP formation via the ATP synthase or used directly for transport or motility (Mitchel, 1976). The ATP generated can be used for various cellular purposes. Electron transport through these constituents most often flows from a carrier with the more electronegative redox potential to a carrier with the more electropositive redox potential. Oxygen has a redox potential of 820 mV and is therefore an ideal terminal electron acceptor (aerobic respiration) but in its absence numerous alternative terminal electron acceptors are available (anaerobic respiration). ATP synthesis coupled to electron transport can be driven by light (in phototrophs) or by the oxidation of both organic compounds (in organoheterotrophs) and inorganic ions (in chemolithotrophs (ie. *A. thiooxidans*)). Although there are differences in detail, the overall features of electron transport

dependent ATP synthesis are very similar in bacteria, in mitochondria and in photosynthetic bacteria (Haddock and Jones, 1977).

The Chemiosmotic Theory of Peter Mitchel requires that the proton translocating electron transport chain and proton translocating ATPase coexist in a membrane that is impermeable to most ions, including both $OH^-$ and $H^+$ ions. Thus the overall result of either electron transport or ATP hydrolysis is the generation across the plasma membrane of a pH gradient ($\Delta$pH) and an electrical potential gradient ($\Delta\Psi$). The sum of these two interconnected components is better known as the proton motive force ($\Delta p$). The components are described by the following equation :

$$\Delta p = \Delta\Psi - Z\Delta pH$$

$Z = 2.3\ RT/F$ where :

$R \rightarrow$ The gas constant ($8.3\ Jmol^{-1}K^{-1}$)

$F \rightarrow$ Faraday constant ($0.0965\ kJmol^{-1}\ mV^{-1}$)

$T \rightarrow$ absolute temperature (in K)

Z is assigned a numerical value of 59 mV at 25°C and the equation is re-written as :

$$\Delta p = \Delta\Psi - 59\Delta pH$$

**$CO_2$ fixation**

*A. thiooxidans* is classified as an autotroph based on its ability to reduce atmospheric $CO_2$ to organic carbon which in turn may be utilized for various metabolic and biosynthetic purposes. $CO_2$ fixation in autotrophs occurs mainly via the Calvin-Benson-Bassham Cycle (CBB cycle) (Shively *et al.*, 1998). $CO_2$ fixation by the CBB cycle is dependent on 13 enzymatic reactions. The enzyme responsible for the actual reduction of $CO_2$ is ribulose-1,5-bisphosphate carboxylase/oxygenase (RuBisCo). With

respect to $CO_2$ fixation, the enzyme catalyzes the carboxylation of ribulose-1,5-bisphosphate (RuBP) to form two molecules of 3-phosphoglyceric acid. The 3-phosphoglyceric acid molecules in turn may enter the glycolytic pathway. The other enzymes of the CBB cycle are involved in the regeneration of RuBP by a series of rearrangement reactions that consumes energy (ATP) and reduced pyridine nucleotides (NAD(P)H). The energy and reducing power required for the reactions of the CBB cycle are provided by the oxidation of substrate molecules (ie. reduced sulfur compounds in the case of *A. thiooxidans*). The gene encoding RuBisCo has been demonstrated in *A. thiooxidans* via heterologous hybridization using specific DNA probes (Shively *et al.*, 1986).

**Reversed electron flow**

ATP required for $CO_2$ fixation is generated from respiratory oxidation-reduction reactions of electrons derived from the oxidation of reduced inorganic sulfur compounds in *A. thiooxidans*. The flow of electrons is believed to occur via a thermodynamically favorable electron transport pathway to the terminal electron acceptor oxygen. The energy released during the course of the electron flow is first converted into a $\Delta p$ which is then used to drive ATP synthesis via the ATP synthase (Mitchel, 1976).

In contrast, the flow of electrons derived from the oxidation of reduced inorganic sulfur compounds for the synthesis of reduced pyridine nucleotides must take a thermodynamically unfavorable pathway (uphill or reversed electron transport pathway) to the site of pyridine nucleotide reduction. This is strictly based on the fact that most of the reduced inorganic sulfur compounds employed as substrates by this bacterium are

more electropositive than the redox potential of the pyridine nucleotides ($\sim E_o' = -320$ mV), and thus the latter cannot be reduced directly by the former. Electrons flow spontaneously only to the more electropositive acceptor. In order to make electrons flow from a reduced inorganic sulfur compound to the site of pyridine nucleotide reduction, the reversed electron transport pathway must be employed, which in turn requires the expenditure of energy. The source of energy is $\Delta p$. The inward flow of $H^+$ through the coupling sites down the $\Delta p$ gradient drives electron transport in reverse. Moreover, in the case of reduced inorganic sulfur compounds which are more electronegative than pyridine nucleotides (ie. $SO_3^{2-}$, $E_o' = -520$ mV), there is no evidence for the direct reduction of pyridine nucleotides by these compounds and possible pathways involving electron transport chain constituents must therefore exist.

Direct observation of reversed electron flow in obligate chemolithoautotrophs has been documented. Most notably in nitrifying and sulfur oxidizing bacteria. Specific observations of reversed electron flow in *A. thiooxidans*, however, remains sparse. Any assumptions made about reversed electron flow in the said bacterium must therefore be partly based on evidences presented in other chemolithoautotrophs. Since a variety of chemolithoautotrophs have been investigated with respect to reversed electron flow only selected works dealing with several other members of the γ-subclass of *Proteobacteria* will be briefly mentioned. Specifically, *Halothiobacillus neapolitanus* (formerly *Thiobacillus neapolitanus*) and *A. ferrooxidans*.

Reversed electron flow in *H. neapolitanus* has been shown in cell free extracts (Aleem, 1969; Saxena and Aleem, 1972) and whole cells of the bacterium (Roth *et al.*, 1973). Cell free preparations of the bacterium catalyzed the ATP dependent reduction of

pyridine nucleotides ($NAD^+$ and $NADP^+$) as well as flavins (FMN and FAD) by thiosulfate, sulfite, and ascorbate (Aleem, 1969; Saxena and Aleem, 1972). Saxena and Aleem (1972) showed that in cell free extracts the addition of ATP caused the initial reduction of FMN by thiosulfate oxidation and the subsequent oxidation of reduced FMN was accompanied with the concomitant reduction of $NAD^+$. The ATP driven reduction of flavins or that of pyridine nucleotides was inhibited by uncouplers and specific inhibitors of the electron transport chain (Aleem, 1969; Saxena and Aleem, 1972), an effect attributed to the inhibition of oxidative phosphorylation. Results obtained in cell free extracts was corroborated in whole cells even though cell free preparations are only about 1 % as active as the whole cells with respect to the reduction of NAD(P)H (Roth *et al.*, 1973).

Reversed electron flow in *A. ferrooxidans* has been reported on several different occasions. One of the first was by Aleem *et al.* (1963) who reported that cell free preparations of the bacterium required ATP for the reduction of $NAD^+$ using reduced horse heart cytochrome *c* as the electron donor. Tikhonova *et al.* (1967) later reported the reduction of $NAD^+$ by $Fe^{2+}$ which was driven by ATP hydrolysis in freeze thawed whole cells. It was reported that freeze thawing was not required for $Fe^{2+}$ oxidation but was required for the ATP effect. The system was however sensitive to amytal (complex I inhibitor). More recently, the presence of a $bc_1$-complex in *A. ferrooxidans* has been reported (Elbehti *et al.*, 1999; Brugna *et al.*, 1999; Brasseur *et al.*, 2002) and the existence of an electron transport pathway through the $bc_1$ complex and complex I has been proposed (Elbehti *et al.*, 2000).

Using spheroplasts of the bacterium and exogenous ferrocytochrome *c* as the electron donor, Elbehti *et al.* (2000) blocked off the terminal oxidase of the thermodynamically favorable forward electron transport pathway by cyanide and showed that reversed electron transport was stimulated by ATP but inhibited by complex I inhibitors (rotenone, amytal, atabrine) and also by a myriad of $bc_1$ complex inhibitors (HQNO, etc.). The system was also sensitive to inhibitors of ATP synthase (oligomycin, etc.) and uncouplers (CCCP, 2,4-DNP). The latter set of evidences further supports the requirement for the maintenance of oxidative phosphorylation and ATP synthesis for energy requiring reversed electron transport. In contrast, forward electron transport was only sensitive to cyanide. A proposal by Brasseur *et al.* (2002) that the $bc_1$ complex in the bacterium only functions in the reverse direction for reduced pyridine nucleotide synthesis further supports the observations made by Elbehti *et al.* (2000) where the $bc_1$ complex inhibitors did not inhibit the forward direction. A ubiquinol oxidase (*bd*) (Kamimura *et al.*, 2001) has been identified in the bacterium and may compensate for the proposed unidirectional operation of the $bc_1$ complex. To date, a $bc_1$ complex has not been identified in *A. thiooxidans* but ubiquinol oxidase (*bd*) activity has been detected (Nogami *et al.*, 1997) as well as ubiquinone (Cook and Umbreit, 1962). Ubiquinol oxidases in general, provide an alternate route for electron transport from ubiquinone to oxygen other than via a $bc_1$ complex. It is suggested that the electron transfer pathway involving a ubiquinol oxidase is not as effective in energy production as a pathway involving a $bc_1$ complex (if functioning in the forward direction) because the ubiquinol oxidase will be the sole proton-translocating complex (Thöny-Meyer, 1997).

**Research objective**

The objective of this research was to investigate the control of both endogenous respiration and sulfite oxidation in *A. thiooxidans* strain ATCC 8085 by using chemical compounds known to collapse $\Delta p$ ($\Delta\Psi$ - 59$\Delta$pH). Chemical compounds used in the research included uncouplers, permeant anions, weak organic acids, and typical electron transport chain inhibitors. Sulfite oxidation was chosen for substrate oxidation studies since it is the primary energy generating step in the bacterium utilizing the electron transport chain. Endogenous respiration and sulfite oxidation were measured by oxygen consumption rates. Alternatively, endogenous respiration was also measured by coupling to exogenous ferric iron reduction (rate of ferrous iron formation). Ferric iron reduction by strain ATCC 8085 was unexpected and a preliminary characterization was the second major undertaking of this research.

# Materials

## Bacterium

*Acidithiobacillus thiooxidans* strain ATCC 8085 was used throughout the research.

## Chemicals

All chemicals used were of the highest grade commercially available. Sodium thiosulfate ($Na_2S_2O_3 \cdot 5H_2O$) and precipitated elemental sulfur powder were obtained from British Drug Houses Inc., Toronto, Ontario, Canada. Potassium sulfite ($K_2SO_3$) was obtained from Matheson, Coleman, and Bell, Norwood, Ohio, and East Rutherford, New Jersey, U.S.A. .

Chemical compounds used to collapse $\Delta p$ were obtained from the following sources :

Uncouplers –

carbonyl cyanide-m-chlorophenylhydrazone (CCCP) – Sigma Chemical Co., St. Louis, Missouri, U.S.A.
2,4-dinitrophenol (2,4-DNP) – Calbiochem, San Diego, California, U.S.A.

Stock solutions were constituted in DMSO.

Permeant anions –

sodium tetraphenyl boron ($TPB^-$) – Aldrich Chemical Company. Inc., Milwaukee, Wisconsin, U.S.A.
potassium thiocyanate (KSCN) – Fisher Scientific Co., Fair Lawn, New Jersey, U.S.A.
potassium nitrate ($KNO_3$) – Fisher
potassium chloride (KCl) – Fisher
(methyltriphenylphosphonium bromide ($TPMP^+$) – Sigma)

Stock solutions were constituted in Milli-Q UF PLUS water except for $TPB^-$ and $TPMP^+$ which were constituted in acetone and DMSO respectively.

Weak organic acids –

citric acid (monohydrate) – Shawinigan, Distributed by the McArthur Chemical Co. Ltd., Montreal, Quebec, Canada.
90% formic acid – Fisher
100% butyric acid – Fisher
99% propionic acid – Fisher
glacial acetic acid – Baxter Corporation, Toronto, Ontario, Canada
D(-)-lactic acid – Shawanigan
succinic acid - Fisher
L-malic acid – Fisher
fumaric acid – Fisher
potassium fluoride (KF-HF) – Fisher

Stock solutions were prepared in Milli-Q UF PLUS water.

Terminal cytochrome oxidase inhibitors –

sodium azide ($NaN_3$) – BDH Chemicals Ltd., Poole, England
potassium cyanide (KCN) – J.T. Baker Chemical Co., Phillipsburg, New Jersey, U.S.A.

Stock solutions were constituted in Milli-Q UF PLUS water.

Complex I inhibitors –

amytal – Sigma
rotenone – Sigma
atabrine – Mann Research Laboratories Inc., New York, New York, U.S.A.

Stock solutions were constituted in DMSO except for atabrine which was constituted in Milli-Q UF PLUS water.

*bc*1 complex inhibitor –

2-heptyl-4-hydroxyquinoline-*N*-oxide (HQNO) – Sigma

Stock solution constituted in DMSO.

Sulfhydryl-binding inhibitors –

mercuric chloride ($HgCl_2$) – Matheson, Coleman, and Bell, Norwood, Ohio and East Rutherford, New Jersey, U.S.A.
*N*-ethylmaleimide (NEM) – Sigma

silver nitrate ($AgNO_3$) – Fisher

Stock solutions constituted in Milli-Q UF PLUS water.

Neutral electron donors –

ribitol – Sigma
glycerol – Fisher

Stock solutions were prepared in Milli-Q UF PLUS water.

The effect of the solvents used was also examined and found to be negligible when used in micro liter quantities (ie. $\leq 10$ μL) with the exception of acetone. The effect of acetone was therefore taken into consideration.

**Growth media**

**9K medium.** The primary growth medium was the basal 9K medium of Silverman and Lundgren (1959). The medium contained per liter of Milli-Q UF PLUS water: 3 g $(NH_4)_2SO_4$, 0.1 g KCl, 0.5 g $K_2HPO_4$, 0.5 g $MgSO_4 \cdot 7H_2O$, 0.014 g $Ca(NO_3) \cdot 4H_2O$, and 0.018 g $FeSO_4 \cdot 7H_2O$. The pH of the medium was adjusted to 5 with concentrated $H_2SO_4$. The medium was sterilized by autoclaving at 121°C for 20 min . Iron was Millipore filtered (10 mL of 1.8 g/L $FeSO_4 \cdot 7H_2O$ solution in pH 1.8 water adjusted with concentrated $H_2SO_4$) and added to the sterilized medium upon inoculation.

9K medium was supplemented with molybdenum (0.75 mg/L $Na_2MoO_4 \cdot 2H_2O$). Molybdenum was Millipore filtered (10 mL of 75 mg/L $Na_2MoO_4 \cdot 2H_2O$ solution) and added to the sterilized medium upon inoculation.

Thiosulfate (1 %) was used as the substrate for growth. Thiosulfate was Millipore filtered (100 mL of 10 g/100 mL $Na_2S_2O_3 \cdot 5H_2O$ solution) and added to the sterilized 9K medium upon inoculation.

**Starkey No. 1 medium.** When comparison to the sulfur grown version of the bacterium was needed, strain ATCC 8085 was cultivated on Starkey No. 1 medium. The medium contained per liter of Milli-Q UF PLUS water: 0.3 g $(NH_4)_2SO_4$, 0.5 g $MgSO_4 \cdot 7H_2O$, 3.5 g $KH_2PO_4$, 0.25 g $CaCl_2$, and 0.018 g $FeSO_4 \cdot 7H_2O$. The pH of the medium was adjusted to 2.3 with concentrated $H_2SO_4$. The medium was sterilized by autoclaving at 121°C for 20 min .

Precipitated elemental sulfur powder was used as the substrate for growth. Sulfur (10 g/L) was spread on the sterilized Starkey No. 1 medium upon inoculation.

**Substrates for oxidation studies (preparation of stock solutions)**

**DMSO/sulfur (soluble sulfur).** DMSO/sulfur was prepared by dissolving precipitated elemental sulfur powder (0.5 mg/mL) in DMSO.

**Tween 80 sulfur (sulfur suspension).** Tween 80 sulfur was prepared by suspending 32 g of precipitated elemental sulfur powder in 100 mL of Milli Q UF PLUS water containing 50 mg of Tween 80 (Polyoxyethylene (20) sorbitan monoleate).

**Thiosulfate.** Thiosulfate (10 mM) solution was prepared by dissolving sodium thiosulfate ($Na_2S_2O_3 \cdot 5H_2O$) in Milli Q UF PLUS water.

**Sulfite.** Sulfite (10 mM) solution was prepared by dissolving potassium sulfite ($K_2SO_3$) in Milli Q UF PLUS water that was initially subjected to 2 cycles of 7 min of degassing followed by 3 min of flushing with oxygen-free $N_{2\,(g)}$ (Welders Supplies,

Winnipeg, Manitoba, Canada). After sufite was added to the anaerobic water, the solution was once again subjected to 7 min of degassing followed by 3 min of flushing with $N_{2\,(g)}$. Sulfite was stored in a serum bottle capped with a Balch tube stopper secured with an aluminum crimp top.

**Formate**. Formate (10 mM) solution was prepared by diluting concentrated formic acid with Milli Q UF PLUS water.

## Methods

### Growth on thiosulfate

The bacterium was grown at 28°C on 9K medium in a 4L reactor equipped with an automated titrator (Radiometer, titartor 11 and pH meter 28, Copenhagen) to maintain the pH at 5 with 5 % $K_2CO_3$. The culture was continuously aerated through a glass sparger and a magnetic stirrer. Sodium thiosulfate (1 %) was added as the sole substrate. The cultivation was carried out every 36 h on a semi-continuous basis leaving 400 mL culture as the 10 % inoculum for a new 9K medium at pH 5 to start another 4L culture.

### Cell harvesting and washing

After 36 h of growth, the culture was centrifuged at 8,000 x g for 10 min and then twice washed in Milli-Q UF PLUS water with centrifugation in between (10,000 x g for 10 min). Washed cells were suspended in 0.1 M β-alanine-$H_2SO_4$ pH 3 at a concentration of 200 mg wet cells/mL. When not in use the cell suspension was stored at 4°C with gentle stirring to prevent the cells from settling out of suspension. Prolonged storage in

0.1 M β-alanine-$H_2SO_4$ pH 3 was not possible so cells were used as soon as they were harvested.

**Measuring oxygen consumption by endogenous respiration or by exogenous substrate oxidation**

Oxygen consumption by endogenous respiration or by exogenous substrate oxidation was followed in a Gilson oxygraph with a Clarke oxygen electrode at 25°C by measuring the decrease in dissolved oxygen. The initial linear rate of oxygen consumption (nmol/min) was reported as the oxidation rate. For oxygen consumption studies by endogenous respiration, the 1.2 mL reaction mixture consisted of 0.1 M β-alanine-$H_2SO_4$ pH 3 buffer and 25 mg of cells. For oxygen consumption studies by exogenous substrate oxidation, the desired substrate was added in microliter volumes to initiate the reaction. The effect of various electron transport chain inhibitors and uncouplers was observed by the addition of microliter volumes to the reaction mixture and particularly after 5 min of preincubation with the cells for the effect on exogenous substrate oxidation. Results were corrected for any non-biological oxidation rates. The oxygen consumption profiles depicted in the figures are based on the amount of oxygen consumed at various time intervals from the continuous oxygraph reading. To depict an oxygen consumption profile during endogenous oxygen consumption a 2.5 min interval was chosen where as for sulfite oxidation a 20 sec interval was chosen. Both intervals portray an accurate representation of the continuous oxidation profile generated by the oxygraph. The oxygraph readings which showed stimulation or inhibition were repeated on several different occasions to ensure that they were reproducible.

**Measuring exogenous ferric iron reduction by endogenous respiration**

The method used was based on the method reported by Suzuki *et al*, 1990 which in turn was based on the methods of Sugio *et al*, 1985 and Ballentine and Burford, 1957.

**Standard procedure**. Exogenous ferric iron reduction by endogenous respiration was measured in 1 mL reaction mixtures consisting of the assay buffer 0.1 M β-alanine-$H_2SO_4$ pH 3, 20 mg of cells, and 4 μmol $FeCl_3$ which were all stirred magnetically at 25°C in small glass vials capped loosely. Samples of 100 μL were taken at 15 min intervals using microsyringes over an allotted time (1 h) and mixed with 1 mL 0.1% 1,10-phenanthroline-$H_2SO_4$ pH 3. The mixtures were immediately centrifuged for 2 min to remove the cells. The supernatant was then diluted with 0.9 mL of the assay buffer and the red color formed was measured in a Hewlett-Packard 8452A diode array spectrophotometer at 510 nm after 10 min of incubation for stable color formation, using quartz cuvettes with a 1 cm light path. Absorbance readings at 510 nm were taken against a reagent blank and then compared to a standard curve developed using 20 – 200 nmol ferrous iron ($FeSO_4 \cdot 7H_2O$). Results were based on either 2 or 3 independent trials and reported as total ferrous iron formed (nmol).

For the measurement of exogenous ferric iron reduction by endogenous respiration during anaerobic incubation, the experiments were performed as previously stated but with one exception. Primarily, all reaction mixture components were made anaerobic (3 cycles of 7 min of degassing followed by 3 min of flushing with oxygen-free $N_{2\,(g)}$) in serum bottles capped with Balch tube stoppers secured with aluminum crimp tops, prior to combining in the serum bottles containing the specified amount of buffer. Each

component was added to the reaction mixture using microsyringes cleaned with anaerobic water in between each addition.

**Measuring endogenous ferric iron reduction by endogenous respiration**

The method used was based on the method reported by Suzuki *et al.*, 1990 (specific for the measurement of exogenous ferric iron reduction) which in turn was based on the methods of Sugio *et al*, 1985 and Ballentine and Burford, 1957.

**Standard procedure.** For the measurement of endogenous ferric iron reduction by endogenous respiration, the experiments were performed as already stated under the standard procedure for the measurement of exogenous ferric iron reduction by endogenous respiration, but with several exceptions. Initially, exogenous ferric iron was not added to the reaction mixture since endogenous iron was being measured. Secondly, the volume sampled from the 1 mL reaction mixtures was only 50 μL. Thirdly, the sampled volume was mixed with an equal volume of 1 M $HNO_3$ and allowed to stand for 10 min to allow for complete extraction of total endogenous iron from the cells. Fourthly, 50 μL of 10 % $NH_2OH$-HCl was added when total iron (ferrous + ferric) was required as it reduces ferric to ferrous iron. Fifthly, reduction was observed over a much longer time (approximately 30-40 h). Absorbance readings at 510 nm were taken against a reagent blank and then compared to a standard curve developed using 20 - 200 nmol ferrous iron. Results were based on either 2 or 3 independent trials and reported as total ferrous iron formed (nmol).

For the measurement of endogenous ferric iron reduction by endogenous respiration during anaerobic incubation, the experiments were performed as previously

stated but with one exception. Primarily, all reaction mixture components were made anaerobic (3 cycles of 7 min of degassing followed by 3 min of flushing with $N_{2\,(g)}$) prior to combining to initiate the reaction under anaerobic incubation.

**Measuring exogenous ferric iron reduction by exogenous substrate oxidation**

The method used was based on the method reported by Suzuki *et al.*, 1990 which in turn was based on the methods of Sugio *et al*, 1985 and Ballentine and Burford, 1957.

**Standard procedure.** For the measurement of exogenous ferric iron reduction by exogenous substrate oxidation, the experiments were performed as already stated under the standard procedure for the measurement of exogenous ferric iron reduction by endogenous respiration, but with several exceptions. Initially, the reactions were performed in the reaction chamber of the oxygraph to permit additional measurement of ferrous iron formed by the oxygraph (the decrease measured from the amount of expected oxygen uptake can be correlated to the total ferrous iron formed by multiplying the difference by 4 to account for 4 electrons equivalent to one molecular oxygen consumed ($O_2 + 4e^- + 4H^+ \rightarrow 2H_2O$)). Secondly, the volume of the reaction mixtures was 1.4 mL which in turn allowed for ferrous iron measurement before the initiation of the reaction (200 μL was sampled for initial reading allowing 1.2 mL of the reaction mixture to be analyzed via the oxygraph, thus keeping the volume of the reaction mixture consistent with the specific volume required for the operation of the oxygraph) and also after the completion of the reaction (another 200 μL was sampled for ferrous iron formed during the course of the reaction). The volume of the reaction mixtures was increased to 1.6 mL when sulfite formed measurements were need alongside the ferrous iron formed

measurements (ie. 200 µL sampled for both ferrous iron and sulfite determination before the reaction and also after the reaction). Thirdly, exogenous substrates at concentrations of 156 nmol for DMSO/sulfur, 1 mmol for Tween 80 sulfur, and 100 nmol for each of thiosulfate, sulfite, and formate were utilized. Fourthly, reactions were initiated with the addition of the substrate and terminated 15 min later. Fifthly, ferrous iron formed from the reduction of exogenous ferric iron by endogenous respiration during the allotted time was also determined. Results were reported as total ferrous iron formed (nmol).

For the measurement of exogenous ferric iron reduction by exogenous substrate oxidation during anaerobic incubation, the experiments were performed as previously stated but with several exceptions. Initially, the reactions were not performed in the reaction chamber of the oxygraph. Secondly, all reaction mixture components were made anaerobic (3 cycles of 7 min of degassing followed by 3 min of flushing with $N_{2\ (g)}$) prior to combining to initiate the reaction under anaerobic incubation.

**Sulfite determination**

Sulfite was measured according to the method of West and Gaeke (1956). Initially, 200 µL was sampled from a reaction mixture and mixed with 5 mL of 0.1 M sodium tetrachloromercurate II which was then centrifuged (10,000 x g for 15 min) to remove the cells. To the supernatant, 0.5 mL of 0.2 % formaldehyde and 0.5 mL of HCl-bleached pararosaniline (0.04 %) was added, with mixing in between. After 30 min of incubation, the absorbance at 550 nm was taken against a reagent blank and compared to a standard curve developed using 20 – 200 nmol sulfite ($K_2SO_3$). Results were reported as total sulfite formed (nmol).

**Total endogenous iron (ferric + ferrous) and endogenous ferrous iron determination**

Total endogenous iron (ferric + ferrous) in the cells was measured by initially diluting (in 0.1M β-alanine $H_2SO_4$ pH 3) a stock cell suspension (200 mg/mL) to the desired cell concentration (ie. 5,10, 20, 40, 80 mg/mL), in a final volume of 1 mL. Next, 50 µL was removed from the cell suspension and mixed with an equal volume of 1 M $HNO_3$ and allowed to stand for 10 min, after which time the mixture was treated with 50 µL of 10 % $NH_2OH$-HCl to reduce extracted ferric iron to ferrous iron. The sample was then mixed with 1 mL of 1,10-phenanthroline and immediately centrifuged for 2 min to remove the cells. The supernatant was then diluted with 0.85 mL of the assay buffer and the red color (corresponding to total endogenous iron (ferric + ferrous)) was measured in a Hewlett-Packard 8452A diode array spectrophotometer at 510 nm after 10 min of incubation for stable color formation. Absorbance readings at 510 nm were taken against a reagent blank and then compared to a standard curve developed using 20 – 200 nmol ferrous iron ($FeSO_4 \cdot 7H_2O$). Endogenous ferrous iron in the cells was measured according to the previously mentioned method but 10 % $NH_2OH$-HCl was not added during the procedure. Total iron (ferrous + ferric) and ferrous iron in the supernatant of the cell suspension was measured according to the previously mentioned method, however cells were removed through centrifugation prior to the measurement. Results were reported as total iron (ferrous + ferric) and ferrous iron present (nmol).

**Absorption spectra of cell-free crude extracts**

The cells suspended in 0.1 M β-alanine-$H_2SO_4$ pH 3 were washed once in 0.1 M Tris-HCl pH 7.5 buffer and suspended in the same buffer at a wet cell concentration of 200 mg/mL. The suspension was passed through a French pressure cell three times at 110 MPa to break the cells and was centrifuged at 10,000 x g for 10 min to obtain cell-free crude extracts. The supernatant of thiosulfate grown cells was translucent with a reddish/brown color whereas the supernatant of the sulfur grown cells was somewhat beige/white in color.

To obtain a difference spectrum (reduced – oxidized spectrum) the cell free crude extract was diluted 4-fold in 0.1 M Tris-HCl pH 7.5 at a final volume of 1 mL. The 1 mL dilution (oxidized extract) was used as the reference blank for the reduced spectrum. To prepare reduced extracts, few grains of sodium dithionite was added to the 1 mL dilution and gently inverted several times for mixing while capped with parafilm. Absorbance readings (400-800 nm) were taken using a Hewlett-Packard 8452A diode array spectrophotometer in a quartz cuvette with a 1 cm light path.

## Growth of the bacterium

*Acidithiobacillus thiooxidans* strain ATCC 8085 was grown on 9K medium of Silverman and Lundgren at pH 5 using 1 % thiosulfate as the sole energy source, as reported by Masau *et al* (2001), based on the initial work of Nakamura *et al* (1990). However, unlike Masau *et al.*, the growth medium was supplemented with a minute amount of molybdenum (0.75 mg $Na_2MoO_4 \cdot H_2O$)/L) which resulted in a much higher cell offering. In the present research, a yield of approximately 0.75-1 g of wet cells/L was not unusual, compared to an average yield of 0.425 g of wet cells/L by Masau *et al* (2001). Additionally, a survey of thiosulfate, sulfite, and sulfur (soluble sulfur - DMSO/sulfur and precipitated elemental sulfur - Tween 80 sulfur) oxidation activities at various time intervals during growth (12-96 h) revealed that peak substrate oxidation activities were present after only 36 h of growth. As a result, cells were routinely harvested for study after 36 h of growth. Masau *et al.* (2001) routinely harvested their cells every 72-96 h .

The rapid cell proliferation and the resulting increase in cell yield may be most likely due to molybdenum supplementation. Molybdenum has been reported to increase specific growth rate and final cell yield of *A. thiooxidans* by 2- and 4-fold respectively, at minute concentrations (0.3 ppm) in the growth medium (Takakuwa *et al*, 1977). The role of molybdenum as a cofactor of enzymes is also well known and has been reported in such enzymes as hepatic sulfite oxidase (Cohen *et al.*, 1971), xanthine oxidase (Bray, 1963), aldehyde oxidase (Rajagopalan *et al.*, 1962), and in formate dehydrogenase in *E. coli* (Enoch and Lester, 1975 , Pinset, 1954). More specifically, molybdenum has also

been identified as a component of sulfite oxidase in several thiobacilli ( Kessler and Rajagopalan, 1972; Southerland and Toghrol, 1983; Kappler *et al.*, 2000).

# Part I

## Part I : Investigating the control of endogenous respiration and sulfite oxidation in *Acidithiobacillus thiooxidans*

### Introduction

The respiratory control of both endogenous substrate(s) oxidation (endogenous respiration) and exogenous substrate oxidation in *A. thiooxidans* strain ATCC 8085 was investigated using chemical compounds known to collapse $\Delta p$ ($\Delta\Psi$ - 59$\Delta$pH). Sulfite ($K_2SO_3$) was chosen as the substrate for exogenous substrate oxidation studies since it is suspected of being the key energy-generating reaction, via the electron transport chain, in the sulfur to sulfate oxidation scheme ($H_2SO_3 + \frac{1}{2}O_2 \rightarrow SO_4^{2-} + 2H^+ + 2e^-$) (Suzuki, 1999; Masau *et al.*, 2001). At this juncture, the nature of the substrate(s) responsible for endogenous respiration is not yet known.

Endogenous respiration and sulfite oxidation were both investigated by oxygen consumption studies. Alternatively, endogenous respiration was also investigated with exogenous ferric iron serving as the terminal electron acceptor (ferrous iron formation). The coupling of endogenous respiration to exogenous ferric iron reduction was unexpected in the bacterium and was therefore investigated in the second part of this research.

The control of endogenous respiration and sulfite oxidation was investigated at pH 3 (in 0.1 M β-alanine-$H_2SO_4$ buffer) to prevent chemical oxidation of ferrous iron which increases with increasing pH (Pronk and Johnson, 1992). Furthermore, the solubility of ferric iron also decreases with increasing pH (Pronk and Johnson, 1992). The chemicals used to investigate the role of $\Delta p$ in the control of both endogenous and exogenous

substrate oxidation by the bacterium included uncouplers, permeant anions, weak organic acids, terminal oxidase inhibitors, complex I inhibitors, $bc_1$ complex inhibitors, and sulfhydryl-binding agents. Additionally, pH 3 is also a typical growth pH for the bacterium especially when elemental sulfur is utilized as the substrate.

Throughout the investigation, a fixed concentration of cells was maintained (20 mg/mL) for both endogenous respiration and sulfite oxidation studies so as to allow a direct comparison between the two. The amount of sulfite used in the investigation was especially crucial at pH 3 as higher amounts of the substrate was found to be inhibitory, which was indicated by a lag in the substrate oxidation profile (Figure 1). At higher concentrations of the substrate, the lag was found to be more pronounced. The inhibition of sulfite oxidation, at higher concentrations of the substrate at low pH, may be related to the chemical form of the substrate as it enters the cell from the external environment. Takeuchi and Suzuki (1994) have suggested that sulfite enters the cells in the form of undissociated (or protonated) sulfurous acid ($H_2SO_3$) or as sulfur dioxide gas ($SO_{2\,(g)} + H_2O$), at acidic pH. Sulfite ion ($SO_3^{2-}$) may be protonated to bisulfite ion ($SO_3^{2-} + H^+ \leftrightarrow HSO_3^-$, $K_{a2} = 1.02 \times 10^{-7}$ or $pK_{a2} = 7$) and further to sulfurous acid ($HSO_3^- + H^+ \leftrightarrow H_2SO_3$, $K_{a1} = 1.54 \times 10^{-2}$ or $pK_{a1} = 1.81$) as it passes through the outer membrane and periplasmic space to reach the site of sulfite oxidation. Therefore, the lag may be due to the acidification of cells by protonated sulfite. To avoid complications arising from substrate inhibition, 100 nmol of $K_2SO_3$ (per 1.2 mL of reaction mixture) was used throughout the research. In most instances, 100 nmol of $K_2SO_3$ generated a linear rate of substrate oxidation and facilitated stoichiometric measurement of substrate oxidation ($H_2SO_3 + \frac{1}{2}O_2 \rightarrow SO_4^{2-} + 2H^+ + 2e^-$).

**Effect of uncouplers**

Uncouplers, 2,4-DNP and CCCP, are classified as protonophores or proton translocators (Nicholls and Ferguson, 1992 ; Lehninger *et al.*, 1993). Both of the uncouplers have dissociable protons and permeate bilayers either in their protonated or deprotonated forms. The ability of the anionic form to permeate across hydrophobic bilayers is said to be made possible by the presence of an extensive π-orbital system which is believed to delocalize the negative charge, such that lipid solubility is retained (Nicholls and Ferguson, 1992). By carrying protons across the membrane, the uncouplers can catalyze the net electrical uniport of protons and therefore increase the proton conductance of the membrane (Nicholls and Fergusson, 1992). This is primarily mediated by the dissociation of a proton from the uncoupler due to the near neutral pH of the cytoplasm ($pH_{in} > pK_a$ of uncoupler; $pK_a = 4$ for 2,4-DNP) and by the subsequent cycling of the uncoupler between the internal and external environments. In the external environment, the uncoupler is reprotonated ($pH_{out} < pK_a$ of uncoupler). The cycling continues until the internal pH of the cell equilibrates with the pH of the external environment so that $59\Delta pH$ equals $\Delta\Psi$ (ie. $\Delta p$ approaches zero). The collapse of $\Delta p$ allows the oxidative component (substrate oxidation) of respiration to be uncoupled from the constraints imposed by the phosphorylating component (ATP synthesis) and results in stimulation of substrate oxidation rate.

**2,4-DNP.** The effect of 2,4-DNP on the rate of exogenous ferric iron reduction by endogenous respiration was stimulatory (Table 1,Figure 2 (a)). The uncoupler exhibited increased effectiveness at increasing concentrations. At higher concentrations, however, reduced stimulation was also apparent. Peak stimulation was observed around 10 μM 2,4-

DNP. The effect of the uncoupler on the rate of oxygen consumption by endogenous respiration was consistent with exogenous ferric iron reduction studies (Table 1, Figure 2 (b)). The uncoupler stimulated endogenous respiration but at higher concentrations exerted a reduced stimulatory or an inhibitory effect. The uncoupler concentration range at which peak stimulation was observed (0.5 → 10 μM) was consistent with the ferric iron reduction studies, although the extent of the stimulation was less.

The effect of 2,4-DNP on the rate of sulfite oxidation was inhibitory. The uncoupler exhibited increased effectiveness at increasing concentrations (Table 1). The uncoupler concentration which caused peak stimulation of endogenous respiration rate in both iron reduction (10 μM) and oxygen consumption (0.5 → 10 μM) studies inhibited sulfite oxidation (Figure 2 (c) ).

**CCCP.** The effect of CCCP on the rate of exogenous ferric iron reduction by endogenous respiration was stimulatory (Table 2, Figure 3 (a)). The uncoupler exhibited increased effectiveness at increasing concentrations. However, at higher concentrations, reduced stimulation was also apparent. Peak stimulation was observed around 10 μM CCCP. The effect of CCCP on the rate of oxygen consumption by endogenous respiration was also stimulatory, but at higher concentrations of the uncoupler, it was less stimulatory and even inhibitory (Table 2, Figure 3 (b)). Peak stimulation was observed around 1 μM CCCP. The extent of the stimulation in oxygen consumption studies was less than that in exogenous ferric iron reduction studies.

The effect of CCCP on the rate of sulfite oxidation was inhibitory (Table 2). The uncoupler exhibited increased effectiveness at increasing concentrations. A typical inhibitory response to CCCP during sulfite oxidation is illustrated in Figure 3 (c).

The uncouplers, in general, stimulated endogenous respiration, but at very high concentrations were less stimulatory or even inhibitory. The stimulation of endogenous respiration was most likely due to the collapse of $\Delta p$ which was mediated by $H^+$ translocation into the cell and thus leading to the uncoupling of oxidation from phosphorylation. Without the constraints of the phosphorylating component of the electron transport system, the oxidative component operates unhindered at its maximal rate. The proton pumping system operates to re-establish the $\Delta p$. However, at very high concentrations of the uncoupler, $H^+$ leaking in is too fast in comparision to the $H^+$ being pumped out, thus decreasing the cytoplasmic pH to non-physiological levels (acidification of the cytoplasm) leading to reduced activities. Stimulation of endogenous respiration by the uncouplers was consistent with what would be expected from a mitochondrial electron transport system or in heterotrophic bacteria, thus suggesting a control for endogenous respiration similar to those systems. In contrast, sulfite oxidation was strictly inhibited by the uncouplers. Results implicate a control strongly dependent on the maintenance of an energy transducing membrane ($\Delta p$ maintenance) for substrate oxidation by the bacterium.

**Effect of anions**

The ability to use anions to collapse the $\Delta\Psi$ component of $\Delta p$ is possible only if $\Delta\Psi$ is positive inside the cell. An inside positive $\Delta\Psi$ has been determined for numerous acidophiles (Hsung and Haug, 1977a; 1977b; Krulwich *et al.*, 1978; Cox *et al.*, 1979; Matin *et al.*, 1982; Alexander *et al.*, 1987). In acidophiles, the $\Delta\Psi$ values vary but the polarity remains the same (positive inside). Thiocyanate (KSCN) is a permeant anion

suspected of distributing electrophoretically according to $\Delta\Psi$ based on the $pK_a$ value of -1.85 for thiocyanic acid (HSCN). Therefore, at assay pH 3, almost all proportion of KSCN would be in dissociated form ($SCN^-$). Tetraphenylboron ($TPB^-$), on the other hand, is a lipophillic anion whose negative charge is sufficiently delocalized by the $\pi$-orbital system and screened with hydrophobic groups to enable it to permeate lipid bilayers (Nicholls and Ferguson, 1992). Both thiocyanate and $TPB^-$ have been used as probes to determine $\Delta\Psi$ in microorganisms. Other anions tested include nitrate ($KNO_3$) ($pK_a$ = -1.44 for $HNO_3$) and chloride (KCl) ($pK_a$ = -7.0 for HCl).

**Thiocyanate.** The effect of potassium thiocyanate (KSCN) on the rate of exogenous ferric iron reduction by endogenous respiration was stimulatory (Table 3, Figure 4 (a)). Thiocyanate exhibited increased effectiveness at increasing concentrations. At higher concentrations of the anion, reduced stimulation and inhibition were also observed. Peak stimulation was observed at 0.2 mM KSCN. The effect of thiocyanate on the rate of oxygen consumption by endogenous respiration was similar to the ferric iron reduction studies except the degree of stimulation was less in oxygen consumption studies (Table 3, Figure 4 (b)). Peak stimulation was observed around 0.2 → 0.5 mM KSCN, whereas at higher concentrations of the anion, reduced stimulation or inhibition was observed.

The effect of thiocyanate on the rate of sulfite oxidation was inhibitory (Table 3). The anion exhibited increased effectiveness at increasing concentrations. A typical inhibitory response to thiocyanate during sulfite oxidation is illustrated in Figure 4 (c).

**$TPB^-$.** Tetraphenyl boron ($TPB^-$) was constituted in acetone. Acetone had no effect on the rate of endogenous respiration measured by either exogenous ferric iron reduction

or by oxygen consumption, but exerted a strong inhibitory effect on the rate of sulfite oxidation. Sulfite oxidation results were therefore corrected for the effect of acetone. For all the $TPB^-$ concentrations tested in endogenous respiration and substrate oxidation studies, the acetone concentration was approximately 1 % (v/v).

The effect of $TPB^-$ on the rate of exogenous ferric iron reduction by endogenous respiration was stimulatory (Table 4, Figure 5 (a)). The anion exhibited increased effectiveness at increasing concentrations but reduced stimulation and inhibition were also apparent. Peak stimulation was observed around 0.5 → 1 mM $TPB^-$. The effect of $TPB^-$ on the rate of oxygen consumption by endogenous respiration was not very informative with respect to stimulation. However, inhibition of endogenous respiration at higher concentrations of the anion was consistent with the trend observed in exogenous ferric iron reduction studies (Table 4).

The effect of $TPB^-$ on the rate of sulfite oxidation was clearly inhibitory (Table 4, Figure 5 (b)). An increased effectiveness at increasing concentrations was observed with lipophillic the anion. A typical inhibitory response to $TPB^-$ during sulfite oxidation is illustrated in Figure 5 (b).

**Nitrate.** The effect of potassium nitrate ($KNO_3$) on the rate of exogenous ferric iron reduction by endogenous resiration was determined to be stimulatory. However, at higher concentrations of the anion, initial stimulation followed by inhibition was also noticed. Peak stimulation was observed around 5 mM $KNO_3$ (Table 5, Figure 6 (a)). Stimulation at 5 mM $KNO_3$ elicited a biphasic ferric iron reduction pattern such that initial stimulation was followed by further stimulation in the latter stages of incubation. In contrast, at 25 mM $KNO_3$, initial stimulation was followed by complete inhibition of

endogenous respiration in the remaining time of incubation. The effect of nitrate on the rate of oxygen consumption by endogenous respiration was also stimulatory (Table 5, Figure 6 (b)). The anion exhibited increased effectiveness at increasing concentrations. The stimulation of oxygen consumption rate in the presence of nitrate was time dependent. The time required for stimulation decreased with increasing anion concentration (Figure 6 (b)). Stimulation of endogenous respiration by nitrate appeared to be greater in exogenous ferric iron reduction studies than in oxygen consumption studies.

The effect of nitrate on the rate of sulfite oxidation was inhibitory (Table 5). The anion exhibited increased effectiveness at increasing concentrations. Inhibition of sulfite oxidation rate in the presence of nitrate was distinct in comparison to other anions tested, since an initial lag was noticed during substrate oxidation. The duration of the lag increased with increasing anion concentration. Some typical inhibitory responses to nitrate during sulfite oxidation is illustrated in Figure 6 (c).

**Chloride.** The effect of potassium chloride (KCl) on the rate of endogenous respiration and substrate oxidation was investigated. In general, chloride had no effect on endogenous respiration rate (either by exogenous ferric iron reduction measurements or by oxygen consumption measurements) and also on sulfite oxidation rate.

The possibility of anions collapsing $\Delta\Psi$ of cells is strictly dependent on the ability of anions to enter cells. The only way anions can enter cells electrophoretically is if $\Delta\Psi$ was of opposite polarity (positive inside). In the research, the cation methyltriphenylphosphonium ($TPMP^{+}$) had no effect on endogenous respiration and sulfite oxidation. It may be that the cation was excluded from the cells since it is of the same polarity as the $\Delta\Psi$ of the cells. Additionally, previous reports have suggested a

positive $\Delta\Psi$ for acidophiles (Cox *et al.*, 1979 ; Matin *et al.*, 1982 ; Alexander *et al.*, 1987). As a result, it may be safe to assume that in *A. thiooxidans* strain ATCC 8085 the $\Delta\Psi$ value is of positive polarity, and the ability of anions to enter cells and collapse $\Delta\Psi$ is very much a reality.

In the research, the permeant anion thiocyanate and the lipohillic anion $TPB^-$ both stimulated endogenous respiration and inhibited sulfite oxidation. The stimulation of endogenous respiration was much more obvious in the ferric iron reduction studies involving $TPB^-$ but clearly obvious in both ferric iron reduction studies and oxygen consumption studies involving thiocyanate. The anions probably collapsed $\Delta p$ by neutralizing the positive $\Delta\Psi$ component and therefore permitting $H^+$ to leak in from the acidic outside (outside pH = 3). The proton pumping system operates to re-establish $\Delta p$ but as more $H^+$ enter at high anion concentration, it becomes overwhelmed. The collapse in $\Delta p$ most likely initiated the uncoupling of oxidation from phosphorylation, leading to the oxidative component operating unhindered. The stimulation of endogenous respiration and inhibition of substrate oxidation by respiratory uncoupling suggests once again two different types of controls in operation. For endogenous respiration, the control often associated with a mitochondrial electron transport system or that of heterotrophic cells may be proposed, whereas for substrate oxidation, the energized state of the cell or $\Delta p$ maintenance exerts a strong control.

The effect mediated by nitrate was consistent with the results obtained with the other anions tested (stimulation of endogenous respiration rate and inhibition of substrate oxidation rate). However, it was also unusual in certain aspects. The time dependent stimulation of endogenous respiration and the prominent lag during substrate oxidation

may indicate a slow permeability of the anion across the cell membrane. In comparision, thiocyanate and $TPB^-$ generated effects that were much more instantaneous, suggesting a more rapid permeation into the cell.

The inability of chloride to exert an effect may be due to complete exclusion of the anion from the cell.

Additionally, it was interesting to note that the degree of stimulation of endogenous respiration and inhibition of sulfite oxidation followed the order $SCN^- > NO_3^- > Cl^-$ (with $Cl^-$ exhibiting virtually no effect). The order is similar to that of the Hofmeister series for chaotrophic anions (Parasegian, 1995 ; Leberman and Soper, 1995 ; Suzuki *et al.*, 1999). Perhaps, the degree of permeability of these anions across the plasma membrane of strain ATCC 8085 may be reflected in their order in the Hofmeister series.

**Effect of weak acids**

The ΔpH component of $\Delta p$ may be collapsed by using weak acids. Weak acids dissociate ($HA \leftrightarrow H^+ + A^-$) based on their dissociation constants ($pK_a$). The protonated form (HA) passes freely back and forth across the cell membrane, whereas the deprotonated form ($A^-$) does not. At a pH value equal to the $pK_a$, equal proportions of HA and $A^-$ will be present. At pH values above the $pK_a$, the proportion of $A^-$ increases with increasing pH. In contrast, at pH values below the $pK_a$, HA predominates. Once the weak acid diffuses into a cell, internal HA will dissociate based on intracellular pH. The dissociation lowers internal HA concentration as well as the pH. Subsequently, a new round of equilibration is initiated resulting in further internal accumulation of HA. The cycle is continued until internal pH is equal to external pH. Therefore, the net effect is the

collapse of the ΔpH component of $\Delta p$. The intracellular pH for acidophiles has been determined to be near neutrality (Ingledew, 1982) over a wide range of external pH in such organisms as *A. ferrooxidans* (Cox *et al.*, 1979 ; Alexander *et al.*, 1987), *Bacillus acidocaldarius* (Oshima *et al.*, 1977 ; Krulwich *et al.*, 1978) and *Thermoplasma acidophilum* (Hsung and Haug, 1975 ; Searcy, 1976). Weak acids used in the research included hydrofluoric acid, monocarboxylic acids – acetic acid, propionic acid, butyric acid, lactic acid, formic acid, dicarboxylic acids – fumaric acid, malic acid, succinic acid, and the tricarboxylic acid – citric acid.

**Acetic acid.** The $pK_a$ of acetic acid is 4.75. Acetic acid (50 μM → 25 mM) had no effect on the rate of exogenous ferric iron reduction by endogenous respiration. In contrast, the weak acid seemed to show some stimulation of the rate of oxygen consumption by endogenous respiration (Table 6, Figure 7 (a)).

The effect of acetic acid on the rate of sulfite oxidation was clearly inhibitory. The weak acid exhibited increased effectiveness at increasing concentrations (Table 6). A typical inhibitory response to the weak acid during sulfite oxidation is illustrated in Figure 7 (b).

**Hydrofluoric acid.** The $pK_a$ of hydrofluoric acid is 3.45 . Hydrofluoric acid inhibited the rate of exogenous ferric iron reduction by endogenous respiration (Table 7, Figure 8 (a)). The weak acid exhibited increased effectiveness at increasing concentrations. Likewise, hydrofluoric acid inhibited the rate of oxygen consumption by endogenous respiration (Table 7, Figure 8 (b)).

The effect on the rate of sulfite oxidation by hydrofluoric acid was also inhibitory (Table 7). The weak acid exhibited increased effectiveness at increasing concentrations.

A typical inhibitory response to the weak acid during sulfite oxidation is illustrated in Figure 8 (c).

**Propionic acid.** The $pK_a$ of propionic acid is 4.89 . Propionic acid (1 μM → 10 mM) had no effect on the rate of exogenous ferric iron reduction by endogenous respiration. In contrast, the weak acid seemed to show some stimulation of the rate of oxygen consumption by endogenous respiration (Table 8, Figure 9 (a)).

The effect on the rate of sulfite oxidation by propionic acid was clearly inhibitory (Table 8). The weak acid exhibited increased effectiveness at incresing concentrations. A typical inhibitory response to the weak acid during sulfite oxidation is illustrated in Figure 9 (b).

**Butyric acid.** The $pK_a$ of butyric acid is 4.82 . Butyric acid (1 μM → 10 mM) had no effect on the rate of exogenous ferric iron reduction by endogenous respiration. However, the weak acid did appear to stimulate the rate of oxygen consumption by endogenous respiration (Table 9, Figure 10 (a)).

Butyric acid clearly inhibited the rate of sulfite oxidation (Table 9). The weak acid exhibited increased effectiveness at increasing concentrations. A typical inhibitory response to the weak acid during sulfite oxidation is illustrated in Figure 10 (b).

**Lactic acid.** The $pK_a$ of lactic acid is 3.86 . Lactic acid (1 μM → 10 mM) exerted very little influence on the rate of exogenous ferric iron reduction by endogenous respiration. At 10 mM lactic acid, however, some inhibition of the reaction rate was noticed (Table 10). Lactic acid exerted very little influence on the rate of oxygen consumption by endogenous respiration. However, at 8.3 mM lactic acid, some inhibition of oxygen consumption rate was also noticed (Table 10).

The effect on sulfite oxidation rate by lactic acid was clearly inhibitory (Table 10). Lactic acid exhibited increased effectiveness at increasing concentrations. A typical inhibitory response to the weak acid during sulfite oxidation is illustrated in Figure 11 (c).

**Formic acid.** The $pK_a$ of formic acid is 3.74 . The effect exerted by formic acid was distinct in comparison to other weak acids tested. In the experiments, the weak acid was stoichiometrically oxidized by the bacterium ($HCOOH + ½O_2 \rightarrow CO_2 + H_2O$) (Table 11, Figure 12 (a)). The rate of oxidation increased with increasing concentrations of the compound, however, at higher concentrations, a decrease in the rate of oxidation was also noted. Results suggested that the role of formic acid may be that of a substrate rather than that of a weak acid, but at higher concentrations the inhibition may be due to the acidification of the cells. It is worth mentioning that *A. ferrooxidans* has been shown to grow on formic acid when the substrate supply was growth limiting (Pronk *et al.*, 1991). Formic acid oxidation by whole cells of the bacterium was strongly inhibited at substrate concentrations above 100 μM which is in agreement with results obtained with *A. thiooxidans* (formic acid concentrations >170 μM appeared to be inhibitory). Pronk *et al.* (1991) also reported that the oxidation of formic acid by cell extracts was NAD(P) independent.

The possibility of formic acid behaving as a substrate was further investigated using an uncoupler (CCCP). In the presence of an uncoupler, the rate of substrate oxidation is expected to be inhibited, as previously demonstrated with sulfite (Table 2, Figure 3(c)). Therefore, if formic acid was really behaving as a substrate, then the rate of oxidation would be inhibited upon CCCP addition. Results revealed an inhibition in

oxygen consumption upon CCCP addition to cells actively oxidizing formic acid (Figure 13 (a)), thus providing some confirmation for the role of formic acid as that of a substrate.

The addition of exogenous ferric iron to cells actively oxidizing formic acid also resulted in an inhibition of oxygen consumption (Figure 13 (b)). Results suggested that the transfer of electrons from formic acid oxidation to exogenous ferric iron reduction may be possible. The coupling of formic acid oxidation to exogenous ferric iron reduction was investigated in the next part of this thesis.

**Malic acid.** The $pK_a$'s of malic acid are 3.4 and 5.05. Malic acid (100 nM → 10 mM) had no effect on the rate of exogenous ferric iron reduction by endogenous respiration. Malic acid did however appear to stimulate slightly the rate of oxygen consumption by endogenous respiration (Table 12, Figure 14 (a)).

The effect of malic acid on the rate of sulfite oxidation is shown in (Table 12). Malic acid exhibited weak inhibition up to 0.83 mM, but strong inhibition above 4.2 mM. A typical inhibitory response to malic acid during sulfite oxidation is illustrated in Figure 14 (b).

**Succinic acid.** The $pK_a$'s of succinic acid are 4.19 and 5.57 . Succinic acid clearly stimulated the rate of exogenous ferric iron reduction by endogenous respiration (Table 13, Figure 15 (a)). Peak stimulation was observed at 0.2 mM succinate. At higher concentrations of the weak acid, reduced stimulation and inhibition were also prevalent. The effect of the weak acid on the rate of oxygen consumption by endogenous respiration was also clearly stimulatory (Table 13, Figure 15 (b)). Peak stimulation was observed around 0.17 → 0.83 mM succinic acid.

The effect of succinic acid on the rate of sulfite oxidation was inhibitory (Table 13). The weak acid Succinate exhibited increased effectiveness at increasing concentrations. A typical inhibitory response to the weak acid during sulfite oxidation is illustrated in Figure 15 (c).

**Fumaric acid.** The $pK_a$'s of fumaric acid are 3.03 and 4.47. Fumaric acid stimulated the rate of exogenous ferric iron reduction by endogenous respiration (Table 14, Figure 16 (a)). Peak stimulation was observed around 0.1 → 0.5 mM. The effect of fumaric acid on the rate of oxygen consumption by endogenous respiration was also clearly stimulatory (Table 14, Figure 16 (b)). Peak stimulation was observed at 0.1 → 0.2 mM fumaric acid.

The effect of fumaric acid on the rate of sulfite oxidation was inhibitory (Table 15). The weak acid exhibited increased effectiveness at increasing concentrations. A typical inhibitory response to the weak acid during sulfite oxidation is illustrated in Figure 16 (c).

**Citric acid.** The $pK_a$'s of citric acid are 3.06, 4.74, and 5.4 . Citric acid (10 μM → 10 mM) exerted very little effect on the rate of exogenous ferric iron reduction by endogenous respiration. However, at 10 mM citric acid, some inhibition of ferric iron reduction rate was apparent (Table 15, Figure 17). Possibly, the inhibition may be due to the chelation of ferric iron by citric acid, thus making ferric iron unavailable for reaction. It is noteworthy, that when the cells were suspended in 0.1 M sodium citrate pH 3, ferric iron reduction was not possible, thus giving some weight to the previous claim. Citric acid (83 μM → 8.3 mM) also exerted very little effect on the rate of oxygen consumption by endogenous respiration. However, when the cells were suspended in a citrate buffer

(0.1 M Na-Citrate pH 3) the rate of oxygen consumption by endogenous respiration was faster than the rate in 0.1 M β-alanine-$H_2SO_4$ pH 3 buffer. Possibly, at this high concentration of citric acid, the cells were uncoupled and stimulation is apparent. Addition of uncouplers to cells suspended in citrate buffer resulted in the inhibition of endogenous respiration (as measured by oxygen consumption) (data not shown).

Citric acid (83 μM → 8.3 mM) exerted very little influence on the rate of sulfite oxidation. Cells suspended in citrate buffer generated sulfite oxidation rates similar to cells suspended in β-alanine buffer of equal concentration. The rate of sulfite oxidation in citrate buffer suspended cells was also inhibited by uncouplers (data not shown).

Of all the weak acids tested, the highest degree of stimulation of endogenous respiration rate was observed in the presence of succinic acid and fumaric acid. Additionally, the concentrations causing peak stimulation were low (0.1 → 0.2 mM) in comparison to other weak acids tested. Therefore, the possibility of succinic acid and fumaric acid behaving as substrates rather than as weak acids was investigated. For the investigation, the uncouplers (2,4-DNP, CCCP) were used in the presence of either of these two acids. Two outcomes were possible in the presence of an uncoupler. Initially, the rate of endogenous respiration may be further stimulated as a result of a cumulative effect with an uncoupler, thus implicating these compounds as weak acids. Alternatively, the observed stimulation in the presence of these compounds may be inhibited upon an uncoupler addition, thus suggesting the role of these compounds as substrates and analogous to sulfite and now possibly formic acid oxidation. In general, results revealed that the stimulation caused by either succinic acid or fumaric acid was not inhibited by uncoupler addition (Figures 18 (a) and (b), Figures 19 (a) and (b)), however a cumulative

effect was also not very easily observed. There is some evidence that in the presence of 2,4-DNP and succinic acid or fumaric acid a cumulative effect may be present in the oxygen consumption studies (Figures 18 (b) and 19 (b)). In general, the stimulation in the presence of an uncoupler and either succinic acid or fumaric acid was similar to the stimulation in the presence of an uncoupler alone.

The data presented, with respect to the weak acids tested, provides some evidence for the maintenance of the intracellular pH of *A. thiooxidans* strain ATCC 8085 at a pH higher than the external pH of 3, and possibly even near neutrality, as in other acidophiles. This is so because at a pH below the $pK_a$ of a weak acid, the acid is expected to enter cells in undissociated form down its concentration gradient and only once inside does it dissociate based on intracellular pH ($pH_{in} > pK_a$). The dissociation of the weak acid inside the cell permits the entry of more acid in order to re-establish an equilibrium. The overall effect, however, is a decrease in the intracellular pH of the cell and the collapse of the $\Delta$pH component of $\Delta p$.

The ability to collapse the $\Delta p$ of the cells by collapsing the $\Delta$pH component was achieved with some of the weak acids tested. This was suggested by the stimulation of endogenous respiration and the inhibition of substrate oxidation. The stimulation, however, was not as apparent as in the previous studies with uncouplers and anions. Nevertheless, stimulation of endogenous respiration by the uncoupling of oxidation from phosphorylation once again supports the hypothesis that the respiratory control of endogenous respiration is reminiscent of mitochondrial electron transport system or that of heterotrophic bacteria. In such systems, the uncoupling of oxidation from phosphorylation results in the oxidative component operating unhindered at its maximal

rate. The collapse of $\Delta p$ and the subsequent inhibition of sulfite oxidation and now possibly formate, reiterates the importance of maintaining an energized state of the cell for substrate oxidation in this bacterium.

The peculiarity observed with hydrofluoric acid where both the rate of endogenous respiration and that of substrate oxidation were strongly inhibited by the weak acid may be due to an adversarial effect exhibited by the fluoride anion upon particular intracellular enzyme(s) possibly required for the viability of the cells. The behavior of the fluoride anion as an enzyme poison has been previously mentioned (Marquis, 1995).

**Effect of terminal cytochrome oxidase inhibitors**

Cyanide (KCN) and azide ($NaN_3$) were utilized in the research to elucidate the effect of terminal cytochrome oxidase inhibitors on the control of endogenous respiration and substrate oxidation. Cyanide is toxic to most living organisms owing to the high affinity of the chemical to iron of the heme protein (Knowles, 1976; Knowles and Bunch, 1986; Chena Liu, 1999). As a result, cyanide is commonly used to inhibit the activities of terminal cytochrome oxidases. The degree of cyanide binding to an oxidase is often affected by the prosthetic groups of the porphyrin ring structure of the heme protein (Chena and Liu, 1999). Like cyanide, azide is also commonly used as a standard inhibitor of terminal oxidases.

**Cyanide.** Potassium cyanide (KCN) (10 μM → 10 mM) had no effect on the rate of exogenous ferric iron reduction by endogenous respiration. In contrast, cyanide exhibited an inhibitory effect on the rate of oxygen consumption by endogenous

respiration (Table 16, Figure 20 (a)). The effectiveness of cyanide as an inhibitor of oxygen consumption rate increased at increasing concentrations.

The effect of cyanide on the rate of sulfite oxidation was also inhibitory (Table 16). Cyanide exhibited increased effectiveness at increasing concentrations. However, complete inhibition of the rate of sulfite oxidation was not observed (Figure 20 (b)).

**Azide.** The effect of sodium azide ($NaN_3$) on the rate of exogenous ferric iron reduction by endogenous respiration was stimulatory (Table 17, Figure 21 (a)). Azide exhibited increased effectiveness at increasing concentrations. At higher concentrations of azide, however, stimulation in the early stages of incubation was apparent with reduced stimulation or inhibition in the latter stages of incubation. Peak stimulation of the rate of exogenous ferric iron reduction by endogenous respiration throughout the allotted incubation period was observed at 12 mM $NaN_3$. At 16 mM $NaN_3$, however, stimulation in the early stages of incubation was higher than that at 12 mM $NaN_3$ but decreased with time. The effect of azide on the rate of oxygen consumption by endogenous respiration was also stimulatory (Table 17, Figure 21 (b)). Azide exhibited increased effectiveness at increasing concentrations. Peak stimulation was observed around 13 $\rightarrow$ 21 mM $NaN_3$. Reduced stimulation by azide was also noticed at higher concentrations.

The effect of azide on the rate of sulfite oxidation was inhibitory (Table 17). Azide exhibited increased effectiveness at increasing concentrations. Unlike cyanide, complete inhibition of the sulfite oxidation rate was possible with azide. A typical inhibitory response to azide during sulfite oxidation is illustrated in Figure 21 (c).

Known inhibitors of terminal oxidases, cyanide and azide, acted differently with respect to the endogenous respiration rate but similarly towards sulfite oxidation rate. The

effect exhibited by cyanide on endogenous respiration rate differed when measured by either exogenous ferric iron reduction or by oxygen consumption. The inhibition of oxygen consumption rate by endogenous respiration was as expected since cyanide is a potent inhibitor of terminal cytochrome oxidases. The rate of ferric iron reduction from endogenous respiration was not at all inhibited by cyanide suggesting that the electron pathway to ferric iron from endogenous electron source may deviate from the pathway to oxygen.

The inability to completely inhibit oxygen consumption by endogenous respiration and also sulfite oxidation by cyanide is worth noting. With respect to sulfite oxidation, Masau *et al.* (2001) suggested that the ability of cyanide to form complex ions of some metals (ie. $Cu^{+1}$ (Dean, 1985)) may in turn stimulate the chemical oxidation of sulfite. Since sulfite was prepared in anaerobic water as opposed to an EDTA solution (sulfite in an EDTA solution minimizes free radical oxidation of the substrate particularly in the presence of metals (Harahuc and Suzuki, 2001)), then there may exist a possibility for the presence of such metals in the reaction mixture. However, the presence of cyanide tolerant *d*-type cytochrome in thiosulfate grown strain ATCC 8085 (Masau *et al.*, 2001) and the possibility of it conferring some cyanide tolerance to the organism should not be easily dismissed either. The role of *d*-type cytochrome conferring cyanide tolerance to the bacterium may provide a more unifying explanation for both endogenous respiration and sulfite oxidation results where cyanide was not a complete inhibitor of electron flow.

Azide stimulation of endogenous respiration may be due to the inhibitor behaving as a weak acid and thus uncoupling oxidation from phosphorylation by collapsing the ΔpH component of $\Delta p$. The $pK_a$ of hydrazoic acid ($HN_3$) is 4.7 , therefore it can flow

down its concentration gradient and dissociate to generate $H^+$ and $N_3^-$ in the higher pH of the internal environment. The inhibition of sulfite oxidation by azide may be due to its weak acid role especially at higher concentrations but at lower concentrations its role as a terminal oxidase inhibitor is more applicable.

Data procured with azide further supports the concept of the maintenance of $\Delta p$ or energized state of the cell for exogenous substrate oxidation, however, the dissipation of this parameter results in the inhibition of exogenous substrate oxidation and stimulation of endogenous substrate(s) oxidation.

**Effect of complex I inhibitors**

Complex I catalyzes the transfer of electrons from the oxidation of reduced pyridine nucleotides (NADP(H)) to ubiquinone in a reaction that is associated with proton translocation across the membrane. There are a wide variety of complex I inhibitors acting at or close to the ubiquinone reduction site. One of the most widely used inhibitors of complex I is rotenone. Rotenone consists of a five-ring structure (A- to E-rings) in which the entire stereochemical structure is said to influence its inhibitory potency (Miyoshi 1998). In addition to rotenone, the barbiturate amytal has also been shown to exert an equally effective inhibitory response on complex I. The effect of complex I inhibitors on the control of endogenous substrate(s) oxidation and exogenous substrate oxidation was therefore investigated.

**Rotenone.** The effect of rotenone on the rate of exogenous ferric iron reduction by endogenous respiration was inhibitory (Table 18, Figure 22 (a)). Inhibition with rotenone, however, was only observed after 5 min of preincubation with the cells prior to initiation

of the reaction by exogenous ferric iron addition. In the absence of preincubation, rotenone (5 μM → 0.5 mM) had no effect on the rate of endogenous respiration measured by exogenous ferric iron reduction. With preincubation, rotenone exhibited increased effectiveness at increasing concentrations. The effect of rotenone on the rate of oxygen consumption by endogenous respiration was analogous to the ferric iron reduction studies (Table 18, Figure 22 (b)).

The effect of rotenone on the rate of sulfite oxidation was inhibitory (Table 18). Rotenone exhibited increased effectiveness at increasing concentrations. A typical inhibitory response by rotenone during sulfite oxidation is illustrated in Figure 22 (b).

**Amytal.** The effect of amytal on the rate of exogenous ferric iron reduction by endogenous respiration was stimulatory (Table 19, Figure 23 (a)). Amytal exhibited increased effectiveness at increasing concentrations. However, at higher concentrations of amytal, reduced stimulation was also noticed. Peak stimulation was observed around 1 mM amytal. The effect of amytal on the rate of oxygen consumption by endogenous respiration was also stimulatory (Table 19, Figure 23 (b)). Similar to the exogenous ferric iron reduction studies, high concentrations of amytal were less stimulatory and even inhibitory. Peak stimulation was observed around 0.83 → 1.3 mM amytal.

Amytal (4.2 μM → 8.3 mM) had no effect on the rate of sulfite oxidation.

**Atabrine.** Atabrine is also a common complex I inhibitor. Atabrine, however, had no effect on the rate of endogenous respiration measured by either exogenous ferric iron reduction (0.1 μM → 1 mM) or by oxygen consumption (83 nM → 0.83 mM). The inhibitor (4.2 μM → 0.42 mM) also exerted very little effect on the rate of sulfite oxidation by the bacterium.

The inhibition of endogenous respiration rate by rotenone may suggest the involvement of complex I in endogenous respiration. Possibly, reduced pyridine nucleotides (NAD(P)H) serving as the source for endogenous electron flow. The inhibition of sulfite oxidation rate by rotenone may imply some coupling between substrate oxidation and NAD(P)H synthesis. Sulfite oxidation donating electrons for $NAD(P)^+$ reduction may be a reasonable explanation for this observation. To date, evidence for the direct reduction of pyridine nucleotides ($E_o'$ of $NAD^+$/NADH couple = -320 mV; $NADP^+$/NADPH couple = -324 mV) by sulfite oxidation ( $E_o' = SO_3^{2-}/SO_4^{2-}$ couple = -516 mV) is not known and therefore it may only occur through reversed electron transport using electron transport chain constituents. Also at this stage, the flux of electrons from substrate oxidation for $NAD(P)^+$ reduction is not yet known. Roth *et al.* (1973) have reported that the rate of pyridine nucleotide reduction by thiosulfate oxidation to be less than 1% the rate of thiosulfate oxidation by oxygen, in the autotroph *H. neapolitanus*.

Corroboration of the results obtained with rotenone by amytal proved to be futile as the inhibitor stimulated the rate of endogenous respiration and had no effect on the rate of sulfite oxidation. Stimulation of endogenous respiration rate by amytal may be due to the collapse of $\Delta p$. An uncoupling action by amytal (~ 4 mM) has been previously suggested (Boonstra *et al.*, 1979). It appears that the uncoupling may be due to the behavior of amytal as a weak acid which is said to exist in the proton complexes $H_2$-amytal and H-amytal$^-$ (Boonstra *et al.*, 1979). Both $H_2$-amytal and H-amytal$^-$ are also said to be membrane permeable. It is possible that one of the forms enters cells down its concentration gradient and dissociates to generate $H^+$, in the process collapsing the $\Delta$pH

component of $\Delta p$ and thus uncoupling oxidation from phosphorylation. It was surprising to note that sulfite oxidation rate was not at all inhibited by amytal, even with the possibility of the inhibitor behaving as an uncoupler of oxidative phosphorylation. In previous examples, exogenous substrate oxidation rate was readily inhibited upon the collapse of $\Delta p$. The stimulation of endogenous respiration rate by the collapse of $\Delta p$ was however consistent with the results observed so far.

**Effect of $bc_1$ complex inhibitor**

The $bc_1$ complex is a key component of both mitochondrial and bacterial respiratory chains. A functionally similar but structurally simpler version of the mitochondrial $bc_1$ complex is said to be located in the plasma membrane of a wide variety of bacterial cells (Darrouzet *et al.*, 1999 ; Hunte *et al.*, 2003). The functional core of the enzyme was found to be made up of three subunits containing two *b*-type hemes ($b_H$ and $b_L$; cytochrome *b*), a *c*-type cytochrome (cytochrome $c_1$), and [2Fe-2S] cluster called the Rieske center. The role of the $bc_1$ complex is to catalyze the transfer of two electrons from their substrate, ubiquinol, to the one-electron acceptor cytochrome *c*, concomitantly with the generation of an electrochemical gradient across the membrane (Darrouzet *et al.*, 1999 ; Hunte *et al.*, 2003). It is generally accepted that $bc_1$ complexes function via the modified Q-cycle mechanism, the key feature being the bifurcation of electrons (Mitchel, 1976). A common inhibitor of the $bc_1$ complex is 2-heptyl-4-hydroxyquinoline-*N*-oxide (HQNO).

**HQNO.** The effect of HQNO on the rate of exogenous ferric iron reduction by endogenous respiration was stimulatory (Table 20, Figure 24 (a)). The inhibitor exhibited

increased effectiveness at increasing concentrations. However, at higher concentrations, initial stimulation followed by inhibition and also just inhibition of iron reduction rate were observed. HQNO exerted little effect on the rate of oxygen consumption by endogenous respiration, except at the highest concentration of the inhibitor tested, where the rate of oxygen consumption by endogenous respiration did appear to be inhibited (Table 20, Figure 24 (b)).

The effect of HQNO on the rate of sulfite oxidation was clearly inhibitory (Table 20). The inhibitor exhibited increased effectiveness at increasing concentrations. A typical inhibitory response to HQNO during sulfite oxidation is illustrated in Figure 24 (c).

The inhibitory effect exerted by HQNO on the rate of sulfite oxidation was consistent with previous efforts in which the chemical was recognized as a potent inhibitor of sulfite oxidation by *A. thiooxidans* (Takakuwa, 1976 ; Tano *et al.*, 1982 ; Suzuki *et al.*, 1992 ; Nogami *et al.*, 1997). The inhibitory effect of HQNO is said to be mediated at the $Q_N$ site of the $bc_1$ complex, specifically by blocking the flow of electrons from the heme-$b_H$ centre of cytochrome *b* to UQ (von Jagow and Link, 1986). In effect, HQNO is strong inhibitor of *b*-type cytochromes (Tano, 1982 ; Masau *et al.*, 2001). The involvement of *b*-type cytochromes along with cytochromes of *a*-, *c*-, and *d*-type in the conductance of electrons derived from sulfite oxidation in *A. thiooxidans* has been suggested (Kodoma *et al.*, 1970 ; Takakuwa, 1976 ; Tano *et al.*, 1982 ; Nakamura *et al.*, 1992). Furthermore, working with whole cells of strain ATCC 8085, Masau *et al.* (2001) showed that only *c*-type cytochromes were reduced by substrates in the presence of HQNO but in the absence of the inhibitor all of the cytochromes were reduced with *c*-

type cytochromes always being reduced first. Therefore, in the present study, the inhibition of sulfite oxidation rate by HQNO was also probably due to the inhibition of the reduction of *b*-type cytochrome by reduced *c*-type cytochrome, thus blocking the flow of electrons to the terminal electron acceptor (oxygen).

The stimulation of endogenous respiration rate by HQNO was unexpected. A possible role for HQNO as an uncoupler of oxidative phosphorylation has been previously suggested ( 100 – 200 μM by Oleskin and Samuilov, 1988) and therefore may provide the much needed explanation for this observation. However, the precise mechanism of uncoupling is yet to be resolved, but the presence of OH groups and hydrophilic and hydrophobic structures in the molecules of this inhibitor may play an important role (Oleskin and Samuilov, 1988).

In the case of HQNO, one can also argue that the collapse of $\Delta p$ was responsible for the inhibition of sulfite oxidation as in the case of classical uncouplers (2,4-DNP and CCCP), weak acids, or anions. The primary reason being that concentrations of HQNO which caused stimulation of endogenous respiration also inhibited sulfite oxidation (Table 20).

In cell free systems, HQNO has been shown to inhibit sulfite oxidation (Takakuwa *et al.*, 1976 ; Tano *et al.*, 1982 ; Nogami *et al.*, 1997). Additionally, working with a cell free system of strain ATCC 8085, Masau *et al.* (2001) showed that only *c*-type cytochrome was reduced in the presence of HQNO. In a cell free system, the sulfite oxidation system is physically exposed without the constraints of closed cell membranes ($\Delta p$) and the substrate can be oxidized without any restrictions. However, the inhibition

by HQNO can therefore only be attributed to the blocking effect of the inhibitor on electron transport at *b*-type cytochrome, in the cell free system.

**Effect of sulfhydryl-binding inhibitors**

N-ethylmaleimide (NEM) along with $Ag^+$ and $Hg^{2+}$ are generally considered as sulfhydryl-binding inhibitors due to their specificity to bind the protein thiol sulfur. The effect of sulfhydryl-binding inhibitors on the control of endogenous substrate(s) oxidation and exogenous substrate oxidation was therefore investigated.

**NEM.** The effect of NEM on the rate of exogenous ferric iron reduction by endogenous respiration was inhibitory at lower concentrations and stimulatory at higher concentrations (Table 21, Figure 25 (a)). The inhibition of endogenous respiration rate at lower concentrations of the inhibitor was not complete. The effect of NEM on the rate of oxygen consumption by endogenous respiration was also inhibitory at lower concentrations and stimulatory at higher concentrations (Table 21, Figure 25 (b)).

The effect of NEM on the rate of sulfite oxidation was strictly inhibitory (Table 21). The inhibitor exhibited increased effectiveness at increasing concentrations. A typical inhibitory response to NEM during sulfite oxidation is illustrated in Figure 25 (c).

**$Ag^+$.** The effect of $Ag^+$ ($AgNO_3$) on the rate of exogenous ferric iron reduction by endogenous respiration was inhibitory at lower concentrations and stimulatory at higher concentrations (Table 22, Figure 26 (a)). However, at a very high concentration of $Ag^+$, inhibition of the rate was also apparent. The inhibition observed with $Ag^+$ at the lower concentration tested was not complete. The effect of $Ag^+$ on the rate of oxygen consumption by endogenous respiration generated results similar to the exogenous ferric

iron reduction studies but with some unique features (Table 22, Figure 26 (b)). The inhibitory responses at lower concentrations of $Ag^+$ were exemplified by a lag period prior to the initiation of oxygen consumption. The duration of the lag period decreased with increasing $Ag^+$ concentrations. On the other hand, the stimulatory response was exemplified by an initial linear rate of oxygen consumption followed by a decrease in oxygen consumption. At higher concentrations of $Ag^+$, the initial linear rate of oxygen consumption also decreased.

The effect of $Ag^+$ on the rate of sulfite oxidation was strictly inhibitory (Table 22). The inhibitor exhibited increased effectiveness at increasing concentrations. A typical inhibitory response to $Ag^+$ during sulfite oxidation is illustrated in Figure 26 (c).

**$Hg^{2+}$.** The effect of $Hg^{2+}$ ($HgCl_2$) was strictly inhibitory on both endogenous respiration rate (exogenous ferric iron reduction studies, oxygen consumption studies) and sulfite oxidation rate (Table 23, Figures 27 (a), (b), and (c)).

A partial inhibition of endogenous respiration by low concentrations of NEM suggests the involvement of sulfhydryl groups in the oxidation of endogenous substrate(s). The effect of high concentrations of NEM as a stimulator of endogenous respiration rate was unexpected. Possible explanations for this phenomenon may be found in reports which have suggested that NEM may behave as a strong oxidizing agent of respiratory chain components or as an uncoupler of oxidative phosphorylation. However, the actual mechanism by which the inhibitor exerts its effects has yet to be resolved. Initially, in the absence of any biological system, spontaneous oxidation of ferrocyanide (Marzulli *et al.*, 1985(a)) and *N,N,N',N'*- tetramethylphenylenediamine (TMPD) (Marzulli *et al.*, 1985 (a) and (b)) was greatly increased by NEM. Moreover,

NEM was shown to promote the oxidation of mitochondrial respiratory intermediates. In the presence of azide, however, the oxidizing effect was completely inhibited, suggesting that the stimulation cannot be ascribed to an irreversible damage of mitochondrial intactness (Zanotti *et al.*, 1985 (a)). Secondly, in rat liver mitochondria, the gradient of protons set up across the inner membrane during $Ca^{2+}$ uptake was completely reversed upon NEM addition (Lofrumento and Zanotti, 1978 ; Lofrumento *et al.*, 1979). Therefore, it is possible that in the present research, the stimulation of endogenous respiration rate may also be due to these documented observations. At lower concentrations, NEM may be behaving as a sulfhydryl-binding inhibitor (inhibition of endogenous respiration), but at higher concentrations, the possibility of NEM behaving as an oxidizing agent or as an uncoupler of oxidative phosphorylation (stimulation of endogenous respiration) may be realized.

The stimulatory effect exerted by $Ag^{+}$ on endogenous respiration rate may also be due to the uncoupling of oxidative phoshorylation in the bacterium. Reports documenting uncoupler-like effects by $Ag^{+}$ on energy transducing membranes have appeared (Chappell and Greville, 1954 ; Dibrov *et al.*, 2002). The inhibitory effect at lower concentrations of $Ag^{+}$ was most likely due to its role as a sulfhydryl-binding inhibitor.

The inhibitory effect exerted by $Hg^{2+}$ on both endogenous respiration and substrate oxidation rates at all the concentrations tested suggests that it may be a more potent sulfhydryl-binding inhibitor than both NEM or $Ag^{+}$.

In general, the stimulatory effect exerted by both NEM and $Ag^{+}$ was unexpected. Stimulation, in turn, may be related to their uncoupling effects. Furthermore, the possibility of NEM behaving as a strong oxidizing agent of respiratory chain components

may be considered as well. The inhibition of sulfite oxidation was apparent even with the lowest concentrations of inhibitor tested thus implicating sulfhydryl-binding as the probable cause. Additionally, inhibition of sulfite oxidoreductase by sulfhydryl-binding inhibitors is well known (Suzuki, 1994). However, at higher concentrations of NEM and $Ag^+$, the possibility of an uncoupled membrane ($\Delta p$ collapsed) inhibiting substrate oxidation, as it has been previously demonstrated, should not be overlooked either.

**Implication of results**

The control of both endogenous respiration and sulfite oxidation in *A. thiooxidans* strain ATCC 8085 was investigated using chemical compounds that are known to collapse $\Delta p$ ($\Delta\Psi$ - 59$\Delta$pH). Endogenous respiration and sulfite oxidation were examined by oxygen consumption. Alternatively, endogenous respiration was also examined by coupling to exogenous ferric iron reduction (ferrous iron formation). Of the two methods employed for the examination of endogenous respiration, exogenous ferric iron reduction by endogenous respiration seemed to be more sensitive to the various chemical compounds tested allowing for stimulation to be observed much more readily. Secondly, the technique used for analysis allowed for many separate experiments to be carried out at once, which in turn afforded numerous trials of a given experiment, thus paving the way for better statistical accuracy.

In general, results showed that uncouplers, CCCP and 2,4-DNP, stimulated endogenous respiration. Stimulation of endogenous respiration by uncouplers is consistent with what would be expected from a mitochondrial electron transport system or in heterotrophic bacteria. In these systems, the collapse of $\Delta p$ by the translocation of

$H^+$ into the cell cytoplasm by the action of the protonophores, leads to the uncoupling of oxidation from phosphorylation. Without the constraints of the phosphorylating component of the electron transport chain the oxidative component operates unhindered at its maximal rate. Other chemicals which stimulated endogenous respiration included the permeant anions, some of the weak organic acids, and unexpectedly some typical electron transport chain inhibitors. Specifically, HQNO, amytal, azide, NEM, and $AgNO_3$. Uncoupling effects or weak acid roles may be suggested for these conventional inhibitors, as previously discussed. Therefore, it can be safely assumed that the bacterium has a normal, controlled respiratory system, similar to the mitochondrial system or that of heterotrophic cells, specifically for the oxidation of endogenous substrate(s). In *A. thiooxidans*, endogenous respiration may be the most basic form of respiration and probably essential for the maintenance and survival of the bacterium. The identity of the endogenous substrate(s) is not yet known but the partial inhibition of endogenous electron flow by rotenone may indicate that endogenous respiration may proceed through complex I, and possibly involve reduced pyridine nucleotides (NAD(P)H) . The contribution to the reduced pyridine nucleotide pool by the oxidation of several different neutral electron donors such as glycerol (10 μM → 10 mM) and ribitol (1 μM → 1 mM) was investigated in the research. In the case of ribitol, ribitol dehydrogenase can generate NADH from $NAD^+$ via the oxidation of ribitol to ribulose. The latter can then be converted to ribulose-5-phosphate which can enter the CBB pathway. Unfortunately, neither of the compounds was found to increase endogenous respiration in the whole cells. It should be noted that for *A. ferrooxidans*, poly (β-hydroxybutyrate) has been suggested to be a major storage product (Ingledew, 1982). Future investigations should

therefore focus on determining the nature of the endogenous substrate(s) in the bacterium.

In contrast, the inhibition of sulfite oxidation by compounds that are known to collapse $\Delta p$, suggests a respiratory system unlike that of the mitochondrial system or that of heterotrophic cells, for exogenous substrate oxidation. Inhibition by these compounds suggests a strong requirement for the maintenance of the energized state of the cell for substrate oxidation. That is, $\Delta p$ must remain intact. The requirement for an energized state of the cell during substrate oxidation may reflect the need of the cell to carry out energetically uphill reaction(s), possibly in the substrate oxidation pathway itself and/or substrate oxidation may be coupled to reducing power generation (NAD(P)H), which is energetically uphill and essential for autotrophic growth. The partial inhibition of sulfite oxidation by rotenone provides some evidence for the coupling between sulfite oxidation and reducing power generation catalyzed by complex I . Evidence for the presence of an energetically uphill reaction in the substrate oxidation pathway itself can be found in the report by Masau *et al.* (2001). Masau *et al.* showed that in whole cells of strain ATCC 8085, uncouplers prevented the reduction of *bd* cytochromes by reduced *c*-type cytochrome. Possibly, the flow of electrons from *c*-type cytochrome to *b*-type cytochrome is an energy requiring step in the bacterium and not possible when $\Delta p$ is dissipated. Similarly, in *A. ferrooxidans*, there is a report of a potentially uphill reaction between rusticyanin and cytochrome $c_4$ (Giudici-Orticoni *et al.*, 1999). Furthermore, in *Nitrobacter*, electrons from nitrite ($NO_2^-$) oxidation have to go through an energetically uphill reaction between cytochrome $a_1$ ($E_o' = 350$ mV) to cytochrome *c* ($E_o' = 270$ mV) (Kiesow, 1967 ; Aleem, 1977 ; Cobly, 1976a ; 1976b). In *A. thiooxidans*, exogenous

substrate oxidation (ie. $SO_3^{2-}$) is probably essential for the growth of the bacterium such as in the generation of reducing power for $CO_2$ fixation. Future investigations should delve more into quantifying the changes in $\Delta\Psi$ and $\Delta$pH in the presence of chemical compounds that affect $\Delta p$. Such an undertaking can only further substantiate the present claims.

# Tables

**Table 1** The effect of 2,4-dinitrophenol (2,4-DNP) on the initial rate of endogenous respiration and sulfite oxidation

| | Endogenous respiration | | Sulfite oxidation |
|---|---|---|---|
| Conc. of 2,4-DNP | Initial rate of exogenous ferric iron reduction (nmol/min) | Initial rate of oxygen consumption (nmol/min) | Initial rate of oxygen consumption (nmol/min) |
| - | 3.8 | 3.4 | 79.4 (50) |
| 50 nM | | 3.6 | |
| 83 nM | | | 76.8 (51) |
| 0.1 μM | 4.5 | 3.8 | |
| 0.5 μM | | 4.2 | |
| 0.83 μM | | | 65.6 (54) |
| 1 μM | 5.7 | 4.4 | |
| 4.2 μM | | | 17.8 (47) |
| 5μM | 6.2 | 4.2 | |
| 8.3 μM | | | 14.6 (nd) |
| 10 μM | 7.6 | 4.2 | |
| 20 μM | | 3.4 | |
| 50 μM | 5.6 | 2.6 | |
| 83 μM | | | 6.8 (nd) |
| 0.83 mM | | | 2.2 (nd) |

Some of the results are illustrated in Figures 2 (a), (b), and (c).
The numbers in parentheses indicate the total amount of oxygen consumed by the oxidation of 100 nmol of $K_2SO_3$ ($H_2SO_3 + ½O_2 \rightarrow SO_4^{2-} + 2H^+ + 2e^-$).
nd – not determined

**Table 2** The effect of carbonyl cyanide-m-chlorophenylhydrazone (CCCP) on the initial rate of endogenous respiration and sulfite oxidation

| | Endogenous respiration | | Sulfite oxidation |
|---|---|---|---|
| Conc. of CCCP | Initial rate of exogenous ferric iron reduction (nmol/min) | Initial rate of oxygen consumption (nmol/min) | Initial rate of oxygen consumption (nmol/min) |
| - | 4.0 | 3.6 | 94.2 (50) |
| 50 nM | 3.8 | 4.0 | |
| 83 nM | | | 64.8 (50) |
| 0.1 μM | | 4.2 | |
| 0.5 μM | | 4.4 | |
| 0.83 μM | | | 21.1 (47) |
| 1 μM | 4.6 | 4.8 | |
| 5μM | 6.3 | 4.2 | |
| 8.3 μM | | | 19.2 (nd) |
| 10 μM | 7.3 | 4.2 | |
| 20 μM | | 3.4 | |
| 50 μM | 6.8 | 3.8 | |
| 83 μM | | 3.6 | 16.0 (nd) |
| 0.1 mM | 5.2 | | |
| 0.83 mM | | 2.2 | 5.4 (nd) |

Some of the results are illustrated in Figures 3 (a), (b), and (c).
The numbers in parentheses indicate the total amount of oxygen consumed by the oxidation of 100 nmol of $K_2SO_3$ ($H_2SO_3 + ½O_2 \rightarrow SO_4^{2-} + 2H^+ + 2e^-$).
nd – not determined

**Table 3** The effect of potassium thiocyanate (KSCN) on the initial rate of endogenous respiration and sulfite oxidation

| | Endogenous respiration | | Sulfite oxidation |
|---|---|---|---|
| Conc. of KSCN | Initial rate of exogenous ferric iron reduction (nmol/min) | Initial rate of oxygen consumption (nmol/min) | Initial rate of oxygen consumption (nmol/min) |
| - | 5.7 | 3.0 | 83.6 (50) |
| 8.3 μM | | | 70.0 (50) |
| 40 μM | 7.1 | | |
| 50 μM | | 4.2 | |
| 83 μM | | | 23.4 (50) |
| 0.2 mM | 9.5 | 5.0 | |
| 0.4 mM | | | 4.0 (nd) |
| 0.5 mM | | 5.0 | |
| 0.83 mM | | 4.0 | 2.8 (nd) |
| 1 mM | 6.6 | | |
| 4.2 mM | | | 4.0 (nd) |
| 5 mM | 0.0 | 1.4 | |
| 8.3 mM | | | 4.0 (nd) |

Results are illustrated in Figures 4 (a), (b), and (c).
The numbers in parentheses indicate the total amount of oxygen consumed by the oxidation of 100 nmol of $K_2SO_3$ ($H_2SO_3 + ½O_2 \rightarrow SO_4^{2-} + 2H^+ + 2e^-$).
nd – not determined

**Table 4** The effect of tetraphenyl boron ($TPB^-$) on the initial rate of endogenous respiration and sulfite oxidation

| Conc. of $TPB^-$ | Endogenous respiration: Initial rate of exogenous ferric iron reduction (nmol/min) | | Endogenous respiration: Initial rate of oxygen consumption (nmol/min) | Sulfite oxidation: Initial rate of oxygen consumption (nmol/min) |
|---|---|---|---|---|
| - | 5.1 | *4.9* | 2.2 | 40.0 [a] (50) |
| 0.83 nM | | | | 39.2 (48) |
| 8.3 nM | | | | 39.6 (50) |
| 83 nM | | | | 40.4 (50) |
| 0.5 µM | | | 2.4 | |
| 0.83 µM | | | | 39.2 (50) |
| 1 µM | | | 2.2 | |
| 8.3 µM | | | | 29.6 (50) |
| 10 µM | | | 2.4 | |
| 42 µM | | | | 13.8 (52) |
| 50 µM | | | 2.4 | |
| 83 µM | | *5.1* | | 4.0 (nd) |
| 0.1 mM | | | 2.0 | |
| 0.2 mM | | 5.2 | | |
| 0.5 mM | 7.0 | | 1.4 | |
| 0.83 mM | | | | 1.8 (nd) |
| 1 mM | 7.3 | *6.2* | 1.0 | |
| 1.5 mM | 5.7→2.0 | | | |
| 2 mM | 3.3→1.5 | | | |
| 5 mM | | *0.0* | | |

Results are illustrated in Figures 5 (a) and (b).
Italicized results are from a different experiment performed under similar conditions (not depicted graphically).
The numbers in parentheses indicate the total amount of oxygen consumed by the oxidation of 100 nmol of $K_2SO_3$ ($H_2SO_3 + ½O_2 \rightarrow SO_4^{2-} + 2H^+ + 2e^-$).
nd – not determibed
a) Rate of sulfite oxidation in the presence of 1 % (v/v) acetone. In the absence of acetone the control was 104.8 nmol/min .

**Table 5** The effect of potassium nitrate ($KNO_3$) on the initial rate of endogenous respiration and sulfite oxidation

| Conc. of $KNO_3$ | Endogenous respiration | | | Sulfite oxidation |
|---|---|---|---|---|
| | Initial rate of exogenous ferric iron reduction (nmol/min) | | Initial rate of oxygen consumption (nmol/min) | Initial rate of oxygen consumption (nmol/min) |
| - | 3.8 | *3.4* | 3.8 | 128.0 (50) |
| 50 µM | 3.8 | | | |
| 83 µM | | | | 132.0 (48) |
| 0.2 mM | 4.5 | | | |
| 0.83 mM | | | 3.6 | 106.4 (50) |
| 1 mM | 4.8 | *4.7* | | |
| 5 mM | 6.5→12.6 | | | |
| 8.3 mM | | | 3.8 | 28.0→68.8 (50) |
| 10 mM | | *11.0* | | |
| 13 mM | | | | 21.6→56.0 (48) |
| 17 mM | | | 2.8→4.2 | |
| 20 mM | | *8.7 → 0.0* | | |
| 21 mM | | | | 15.6→41.2 (45) |
| 25 mM | 10.5→0.0 | *14.0 → 0.0* | 3.0→5.6 | |
| 33 mM | | | 2.8→6.0 | |
| 42 mM | | | 3.0→6.6 | 10.4→23.0 (nd) |
| 83 mM | | | 2.2→7.4 | |

Some of the results are illustrated in Figures 6 (a), (b), and (c).
Italicized results are from a different experiment performed under similar conditions (not depicted graphically).
The numbers in parentheses indicate the total amount of oxygen consumed by the oxidation of 100 nmol of $K_2SO_3$ ($H_2SO_3 + ½O_2 \rightarrow SO_4^{2-} + 2H^+ + 2e^-$).
nd – not determined

**Table 6** The effect of acetic acid on the initial rate of endogenous respiration and sulfite oxidation

| | Endogenous respiration | Sulfite oxidation |
|---|---|---|
| Conc. of acetic acid | Initial rate of oxygen consumption (nmol/min) | Initial rate of oxygen consumption (nmol/min) |
| - | 2.6 | 143.2 (50) |
| 83 μM | | 128.0 (50) |
| 0.42 mM | | 107.2 (50) |
| 0.83 mM | | 84.0 (50) |
| 4.2 mM | 2.8 | 19.0 (43) |
| 8.3 mM | 3.2 | 9.0 (42) |
| 12.5 mM | 3.0 | |
| 16.7 mM | 3.0 | |
| 25 mM | 2.6 | |

Some of the results are illustrated in Figures 7 (a) and (b).
The numbers in parentheses indicate the total amount of oxygen consumed by the oxidation of 100 nmol of $K_2SO_3$ ($H_2SO_3 + ½O_2 \rightarrow SO_4^{2-} + 2H^+ + 2e^-$).

**Table 7** The effect of hydrofluoric acid on the initial rate of endogenous respiration and sulfite oxidation

| | Endogenous respiration | | | Sulfite oxidation |
|---|---|---|---|---|
| Conc. of hydrofluoric acid | Initial rate of exogenous ferric iron reduction (nmol/min) | | Initial rate of oxygen consumption (nmol/min) | Initial rate of oxygen consumption (nmol/min) |
| - | 6.5 | *7.0* | 2.4 | 112.8 (50) |
| 4.2 μM | | | | 104.0 (52) |
| 8.3 μM | | | | 92.0 (50) |
| 42 μM | | | | 34.8→80.0 (50) |
| 50 μM | | *6.1* | 2.0 | |
| 83 μM | | | | 20.8→49.4 (48) |
| 0.2 mM | | *5.9* | 1.8 | |
| 0.42 mM | | | | 5.4 (43) |
| 0.83 mM | | | | 3.6 (nd) |
| 1 mM | | *5.4* | 1.4 | |
| 2.5 mM | 4.8 | | | |
| 4.2 mM | | | | 2.0 (nd) |
| 5 mM | 3.4 | *2.6* | 1.2 | |
| 7.5 mM | 3.1 | | | |
| 8.3 mM | | | | 1.8 (nd) |
| 10 mM | 2.2 | | 1.2 | |
| 12.5 mM | 1.5 | | | |
| 25 mM | | *1.0* | 1.0 | |

Some of the results are illustrated in Figures 8 (a), (b), and (c).
Italicized results are from a different experiment performed under similar conditions (not depicted graphically).
The numbers in parentheses indicate the total amount of oxygen consumed by the oxidation of 100 nmol of $K_2SO_3$ ($H_2SO_3 + ½O_2 \rightarrow SO_4^{2-} + 2H^+ + 2e^-$).
nd – not determined

**Table 8** The effect of propionic acid on the initial rate of endogenous respiration and sulfite oxidation

| | Endogenous respiration | Sulfite oxidation |
|---|---|---|
| Conc. of propionic acid | Initial rate of oxygen consumption (nmol/min) | Initial rate of oxygen consumption (nmol/min) |
| - | 2.4 | 116.0 (50) |
| 83 μM | | 99.2 (50) |
| 0.42 mM | | 42.4→94.4 (53) |
| 0.83 mM | 2.2 | 34.4→72.8 (50) |
| 4.2 mM | 2.8 | 16.2 (46) |
| 8.3 mM | 3.0 | |
| 12.5 mM | 3.0 | |
| 16.7 mM | 2.8 | |
| 25 mM | 2.6 | |

Some of the results are illustrated in Figures 9 (a) and (b).
The numbers in parentheses indicate the total amount of oxygen consumed by the oxidation of 100 nmol of $K_2SO_3$ ($H_2SO_3 + ½O_2 \rightarrow SO_4^{2-} + 2H^+ + 2e^-$).

**Table 9** The effect of butyric acid on the initial rate of endogenous respiration and sulfite oxidation

| | Endogenous respiration | Sulfite oxidation |
|---|---|---|
| Conc. of butyric acid | Initial rate of oxygen consumption (nmol/min) | Initial rate of oxygen consumption (nmol/min) |
| - | 2.8 | 112.0 (50) |
| 83 μM | | 92.0 (46) |
| 0.42 mM | | 97.6 (50) |
| 0.83 mM | 2.4 | 34.4→74.4 (50) |
| 4.2 mM | 3.0 | 12.0→15.4 (48) |
| 8.3 mM | 3.4 | 6.6 (50) |
| 12.5 mM | 3.2 | |
| 17 mM | 3.2 | |
| 25 mM | 2.6 | |

Some of the results are illustrated in Figures 10 (a) and (b).
The numbers in parentheses indicate the total amount of oxygen consumed by the oxidation of 100 nmol of $K_2SO_3$ ($H_2SO_3 + ½O_2 \rightarrow SO_4^{2-} + 2H^+ + 2e^-$).

**Table 10** The effect of lactic acid on the initial rate of endogenous respiration and sulfite oxidation

| | Endogenous respiration | | Sulfite oxidation |
|---|---|---|---|
| Conc. of lactic acid | Initial rate of exogenous ferric iron reduction (nmol/min) | Initial rate of oxygen consumption (nmol/min) | Initial rate of oxygen consumption (nmol/min) |
| - | 5.6 | 3.2 | 104.0 (48) |
| 1 μM | 5.5 | | |
| 8.3μM | | 3.2 | |
| 10 μM | 5.8 | | 65.6 (54) |
| 42 μM | | 3.4 | |
| 83 μM | | 3.4 | 72.8 (49) |
| 0.1 mM | 5.7 | | |
| 0.25 mM | | 3.0 | |
| 0.42 mM | | 3.0 | 14.0→27.2 (46) |
| 0.83 mM | | 3.4 | 7.6 (38) |
| 1 mM | 5.9 | | |
| 4.2 mM | | | 3.4 (nd) |
| 8.3 mM | | 2.4 | 0.0 |
| 10 mM | 4.1 | | |

Some of the results are illustrated in Figures 11 (a), (b), and (c).
The numbers in parentheses indicate the total amount of oxygen consumed by the oxidation of 100 nmol of $K_2SO_3$ ($H_2SO_3 + ½O_2 \rightarrow SO_4^{2-} + 2H^+ + 2e^-$).
nd – not determined

**Table 11** The stoichiometric oxidation of formic acid by *A. thiooxidans* strain ATCC 8085

| Amount of formic acid added | Initial rate of oxygen consumption (nmol/min) | Amount of oxygen consumed (nmol) |
|---|---|---|
| 0 | 2.9 | na |
| 25 nmol | 7.6 | 16 (12.5) |
| 50 nmol | 8.6 | 25 (25) |
| 100 nmol | 9.4 | 48 (50) |
| 200 nmol | 9.4 | 90 (100) |
| 400 nmol | 9.0 | 161 (200) |
| 1 µmol | 6.6 | nd |
| 5 µmol | 4.0 | nd |
| 10 µmol | 3.0 | nd |
| 15 µmol | 3.0 | nd |
| 20 µmol | 2.8 | nd |
| 30 µmol | 2.6 | nd |

Some of the results are presented in Figure 12.
The numbers in parenthesis indicate the expected oxygen uptake (nmol) from the complete oxidation of the amount of formic acid added ($HCOOH + \frac{1}{2}O_2 \rightarrow CO_2 + H_2O$).
na – not applicable
nd – not determined

**Table 12** The effect of malic acid on the initial rate of endogenous respiration and sulfite oxidation

| | Endogenous respiration | Sulfite oxidation |
|---|---|---|
| Conc. of malic acid | Initial rate of oxygen consumption (nmol/min) | Initial rate of oxygen consumption (nmol/min) |
| - | 3.0 | 19.2→69.6 (66) |
| 8.3 μM | 3.0 | 21.6→62.4 (66) |
| 42 μM | 3.4 | 18.0→59.2 (68) |
| 83 μM | 3.6 | 25.6→41.6 (68) |
| 0.42 mM | 3.6 | 17.6→58.4 (68) |
| 0.83 mM | 3.6 | 16.0→40.0 (66) |
| 1.7 mM | 3.6 | |
| 3.3 mM | 3.8 | |
| 4.2 mM | 3.6 | 8.4 (68) |
| 8.3 mM | | 0.0 |

Some of the results are illustrated in Figures 14 (a) and (b).
The numbers in parentheses indicate the total amount of oxygen consumed by the oxidation of 100 nmol of $K_2SO_3$ ($H_2SO_3 + ½O_2 \rightarrow SO_4^{2-} + 2H^+ + 2e^-$).

**Table 13** The effect of succinic acid on the initial rate of endogenous respiration and sulfite oxidation

| | Endogenous respiration | | Sulfite oxidation |
|---|---|---|---|
| Conc. of succinic acid | Initial rate of exogenous ferric iron reduction (nmol/min) | Initial rate of oxygen consumption (nmol/min) | Initial rate of oxygen consumption (nmol/min) |
| - | 5.8 | 2.6 | 40.4→104.0 (64) |
| 8.3 μM | | 2.8 | 25.6→92.8 (62) |
| 42 μM | | 4.0 | 25.6→64.0 (64) |
| 50 μM | 7.0 | | |
| 83 μM | | 4.0 | 14.4→46.4 (62) |
| 0.1 mM | 7.4 | | |
| 0.17 mM | | 4.4 | |
| 0.2 mM | 7.9 | | |
| 0.42 mM | | 4.6 | 6.4→11.2 (50) |
| 0.5 mM | 6.9 | | |
| 0.83 mM | | 4.6 | 5.2 (48) |
| 1 mM | 5.9 | | |
| 2 mM | 5.5 | | |
| 3.3 mM | | 2.4 | |
| 8.3 mM | | | 0.0 |

Some of the results are illustrated in Figures 15 (a), (b), and (c).
The numbers in parentheses indicate the total amount of oxygen consumed by the oxidation of 100 nmol of $K_2SO_3$ ($H_2SO_3 + ½O_2 \rightarrow SO_4^{2-} + 2H^+ + 2e^-$).

**Table 14** The effect of fumaric acid on the initial rate of endogenous respiration and sulfite oxidation

| | Endogenous respiration | | Sulfite oxidation |
|---|---|---|---|
| Conc. of fumaric acid | Initial rate of exogenous ferric iron reduction (nmol/min) | Initial rate of oxygen consumption (nmol/min) | Initial rate of oxygen consumption (nmol/min) |
| - | 4.2 | 3.0 | 20.0→68.0 (64) |
| 1 μM | | 2.6 | 20.0→66.4 (66) |
| 5 μM | | | 18.0→58.4 (64) |
| 10 μM | | 3.6 | 19.2→55.2 (64) |
| 50 μM | 5.7 | 4.0 | 10.8→28.8 (66) |
| 0.1 mM | 7.0 | 4.2 | 0.0 |
| 0.2 mM | | 4.4 | |
| 0.25 mM | 6.8 | | |
| 0.5 mM | 6.9 | 3.6 | |
| 1 mM | | 2.6 | |

Some of the results are illustrated in Figures 16 (a), (b), and (c).
The numbers in parentheses indicate the total amount of oxygen consumed by the oxidation of 100 nmol of $K_2SO_3$ ($H_2SO_3 + ½O_2 \rightarrow SO_4^{2-} + 2H^+ + 2e^-$).

**Table 15** The effect of citric acid on the initial rate of endogenous respiration

| | Endogenous respiration |
|---|---|
| Conc. of citric acid | Initial rate of exogenous ferric iron reduction (nmol/min) |
| - | 4.5 |
| 10 μM | 5.0 |
| 0.1 mM | 4.9 |
| 1 mM | 5.1 |
| 10 mM | 3.2 |

Some of the results are illustrated in Figure 17.

**Table 16** The effect of potassium cyanide (KCN) on the initial rate of endogenous respiration and sulfite oxidation

| | Endogenous respiration | Sulfite oxidation |
|---|---|---|
| Conc. of KCN | Initial rate of oxygen consumption (nmol/min) | Initial rate of oxygen consumption (nmol/min) |
| - | 3.8 | 110.0 (50) |
| 0.83 μM | | 80.0 (50) |
| 8.3 μM | 3.4 | 82.0 (46) |
| 42 μM | 3.0 | |
| 83 μM | 2.8 | 40.0 (50) |
| 0.17 mM | 2.4 | |
| 0.42 mM | 1.8 | |
| 0.83 mM | 1.9 | 27.3 (48) |
| 1.7 mM | 1.4 | |
| 8.3 mM | | 31.6 (50) |

Some of the results are illustrated in Figures 20 (a) and (b).
The numbers in parentheses indicate the total amount of oxygen consumed by the oxidation of 100 nmol of $K_2SO_3$ ($H_2SO_3 + ½O_2 \rightarrow SO_4^{2-} + 2H^+ + 2e^-$).

**Table 17** The effect of sodium azide ($NaN_3$) on the initial rate of endogenous respiration and sulfite oxidation

| Conc. of $NaN_3$ | Endogenous respiration | | Sulfite oxidation |
|---|---|---|---|
| | Initial rate of exogenous ferric iron reduction (nmol/min) | Initial rate of oxygen consumption (nmol/min) | Initial rate of oxygen consumption (nmol/min) |
| - | 5.3 *3.1* | 3.4 | 22.0→62.0 (50) |
| 83 nM | | | 26.0→67.2 (48) |
| 0.83 μM | | | 22.0→30.0 (50) |
| 8.3 μM | | | 20.4→48.0 (50) |
| 50 μM | *3.9* | | |
| 83 μM | | | 11.6→16.0 (48) |
| 0.2 mM | *5.3* | | |
| 0.83 mM | | | 2.2 (nd) |
| 4.2 mM | *7.9* | 5.2 | |
| 5 mM | | | |
| 8 mM | 9.3 | | |
| 8.3 mM | | 5.8 | 2.4 (nd) |
| 12 mM | 11.3 | | |
| 13 mM | | 7.6 | |
| 16 mM | 14.7→8.7 | | |
| 20 mM | 11.7→5.5 | | |
| 21 mM | | 7.8 | |
| 24 mM | 7.8→3.1 | | |
| 33 mM | | 6.6 | |

Some of the results are illustrated in Figures 21 (a), (b), and (c).
Italicized results are from a different experiment performed under similar conditions (not depicted graphically).
The numbers in parentheses indicate the total amount of oxygen consumed by the oxidation of 100 nmol of $K_2SO_3$ ($H_2SO_3 + ½O_2 \rightarrow SO_4^{2-} + 2H^+ + 2e^-$).
nd – not determined

**Table 18** The effect of rotenone on the initial rate of endogenous respiration and sulfite oxidation

| | Endogenous respiration | | Sulfite oxidation |
|---|---|---|---|
| Conc. of rotenone | Initial rate of exogenous ferric iron reduction (nmol/min) | Initial rate of oxygen consumption (nmol/min) | Initial rate of oxygen consumption (nmol/min) |
| - | 4.1 | 3.2 | 87.2 (50) |
| 1 μM | | 3.2 | |
| 4.2 μM | | | 34.4→86.4 (48) |
| 10 μM | 3.6 | 3.0 | |
| 21 μM | | | 33.6→71.2 (50) |
| 42 μM | | | 24.8→54.0 (48) |
| 50 μM | 3.2 | 2.6 | |
| 83 μM | | | 28.0→58.4 (49) |
| 0.1 mM | 3.0 | 2.2 | |
| 0.21 mM | | | 26.4→56.0 (48) |
| 0.42 mM | | | 22.4→47.2 (48) |
| 0.5 mM | 3.1 | 2.4 | |

Some of the results are illustrated in Figures 22 (a), (b), and (c).
The numbers in parentheses indicate the total amount of oxygen consumed by the oxidation of 100 nmol of $K_2SO_3$ ($H_2SO_3 + ½O_2 \rightarrow SO_4^{2-} + 2H^+ + 2e^-$).

**Table 19** The effect of amytal on the initial rate of endogenous respiration

| Conc. of amytal | Endogenous respiration | |
|---|---|---|
| | Initial rate of exogenous ferric iron reduction (nmol/min) | Initial rate of oxygen consumption (nmol/min) |
| - | 3.8 | 3.6 |
| 1 μM | 4.2 | |
| 10 μM | 4.8 | |
| 83 μM | | 4.0 |
| 0.1 mM | 6.1 | |
| 0.42 mM | | 4.2 |
| 0.63 mM | | 4.0 |
| 0.83 mM | | 4.4 |
| 1 mM | 6.9 | |
| 1.3 mM | | 4.6 |
| 2.5 mM | | 3.8 |
| 4.2 mM | | 3.2 |
| 10 mM | 5.7 | |

Some of the results are illustrated in Figure 23 (a) and (b).

**Table 20** The effect of 2-heptyl-4-hydroxyquinoline-*N*-oxide (HQNO) on the initial rate of endogenous respiration and sulfite oxidation

| | Endogenous respiration | | Sulfite oxidation |
|---|---|---|---|
| Conc. of HQNO | Initial rate of exogenous ferric iron reduction (nmol/min) | Initial rate of oxygen consumption (nmol/min) | Initial rate of oxygen consumption (nmol/min) |
| - | 4.4 | 2.4 | 133.6 (47) |
| 0.67 nM | | 2.4 | |
| 0.8nM | 5.3 | | |
| 6.7 nM | | 2.4 | |
| 8 nM | 5.6 | | |
| 33 nM | | 2.6 | 117.6 (48) |
| 67 nM | | 2.6 | |
| 80 nM | 6.2 | | |
| 0.17 μM | | | 89.6 (46) |
| 0.32 μM | | | 22.4 → 60.8 (43) |
| 0.33 μM | | 2.6 | |
| 0.67 μM | | 2.6 | |
| 0.8 μM | 7.8 → 4.1 | | |
| 0.83 μM | | | 7.8 → 20.0 (45) |
| 1.6 μM | | | 0.0 |
| 6.7 μM | | 2.4 | |
| 8 μM | 3.5 → 1.9 | | |
| 67 μM | | 1.4 | |

Some of the results are illustrated in Figures 24 (a), (b), and (c).
The numbers in parentheses indicate the total amount of oxygen consumed by the oxidation of 100 nmol of $K_2SO_3$ ($H_2SO_3 + ½O_2 \rightarrow SO_4^{2-} + 2H^+ + 2e^-$).

**Table 21** The effect of *N*-ethylmaleimide (NEM) on the initial rate of endogenous respiration and sulfite oxidation

| Conc. of NEM | Endogenous respiration | | Sulfite oxidation |
|---|---|---|---|
| | Initial rate of exogenous ferric iron reduction (nmol/min) | Initial rate of oxygen consumption (nmol/min) | Initial rate of oxygen consumption (nmol/min) |
| - | 4.7 *6.2* | 2.2 | 30.4 → 54.0 (50) |
| 1 μM | *5.9* | | |
| 8.3 μM | | | 22.0 → 48.8 (48) |
| 10 μM | *5.8* | | |
| 42 μM | | | 15.2 → 37.6 (47) |
| 83 μM | | 1.8 | 18.0 → 36.0 (48) |
| 0.1 mM | 4.0 *4.9* | | |
| 0.42 mM | | 1.6 | 12.8 → 21.6 (44) |
| 0.5 mM | 3.3 | | |
| 0.83 mM | | 1.8 | 14.0 → 25.2 (50) |
| 1 mM | 4.1 *5.1* | | |
| 4.2 mM | | 2.4 | 14.4 (26) |
| 5 mM | 6.3 | | |
| 8.3 mM | | 3.0 | 7.6 (nd) |
| 10 mM | 6.9 | | |

Some of the results are illustrated in Figures 25 (a), (b), and (c).
Italicized results are from a different experiment performed under similar conditions (not depicted graphically).
The numbers in parentheses indicate the total amount of oxygen consumed by the oxidation of 100 nmol of $K_2SO_3$ ($H_2SO_3 + ½O_2 \rightarrow SO_4^{2-} + 2H^+ + 2e^-$).
nd – not determined

**Table 22** The effect of silver nitrate ($AgNO_3$) on the initial rate of endogenous respiration and sulfite oxidation

| | Endogenous respiration | | Sulfite oxidation |
|---|---|---|---|
| Conc. of $AgNO_3$ | Initial rate of exogenous ferric iron reduction (nmol/min) | Initial rate of oxygen consumption (nmol/min) | Initial rate of oxygen consumption (nmol/min) |
| - | 4.0 *4.3* | 2.4 | 91.2 (50) |
| 8.3 μM | *3.4* | 2.4 | |
| 83 μM | | 1.0 | 89.6 (50) |
| 0.1 mM | *3.0* | | |
| 0.42 mM | | 0.0 (5 min) → 2.0 | 61.6 (50) |
| 0.5 mM | 3.1 | | |
| 0.63 mM | | | 30.0 → 43.2 (48) |
| 0.83 mM | | 0.0 (2.5 min) → 2.2 | 0.8 (nd) |
| 1 mM | 4.7 *4.2* | | |
| 2 mM | 3.8 | | |
| 4 mM | 2.5 | | |
| 4.2 mM | | 2.4 → 1.0 | |
| 8.3 mM | | 1.6 → 0.0 | |
| 10 mM | *0.8* | | |

Some of the results are illustrated in Figures 26 (a), (b), and (c).
Italicized results are from a different experiment performed under similar conditions (not depicted graphically).
The numbers in parentheses indicate the total amount of oxygen consumed by the oxidation of 100 nmol of $K_2SO_3$ ($H_2SO_3 + ½O_2 \rightarrow SO_4^{2-} + 2H^+ + 2e^-$).

**Table 23** The effect of mercuric chloride ($HgCl_2$) on the initial rate of endogenous respiration and sulfite oxidation

| | Endogenous respiration | | Sulfite oxidation |
|---|---|---|---|
| Conc. of $HgCl_2$ | Initial rate of exogenous ferric iron reduction (nmol/min) | Initial rate of oxygen consumption (nmol/min) | Initial rate of oxygen consumption (nmol/min) |
| - | 3.9 | 3.2 | 35.2 → 80.0 (53) |
| 0.83 μM | | 2.8 | |
| 8.3 μM | | 2.0 | 30.6 → 61.6 (54) |
| 10 μM | 3.4 | | |
| 21 μM | | | 11.2 → 32.0 (50) |
| 42 μM | | 1.0 | 8.4 → 18.4 (55) |
| 83 μM | | 0.0 | 2.6 (nd) |
| 0.1 mM | 0.0 | | |
| 0.83 mM | | | 0.0 |

Some of the results are illustrated in Figures 27 (a), (b), and (c).
The numbers in parentheses indicate the total amount of oxygen consumed by the oxidation of 100 nmol of $K_2SO_3$ ($H_2SO_3 + ½O_2 \rightarrow SO_4^{2-} + 2H^+ + 2e^-$).
nd – not determined

# Figures

**Figure 1** Sulfite oxidation by *A. thiooxidans* strain ATCC 8085. The reactions were performed at 25°C in 0.1 M β-alanine-$H_2SO_4$ pH 3 and contained 25 mg of cells. $K_2SO_3$ at the amounts specified were added at the arrows. The volume of the reaction mixtures was 1.2 mL .

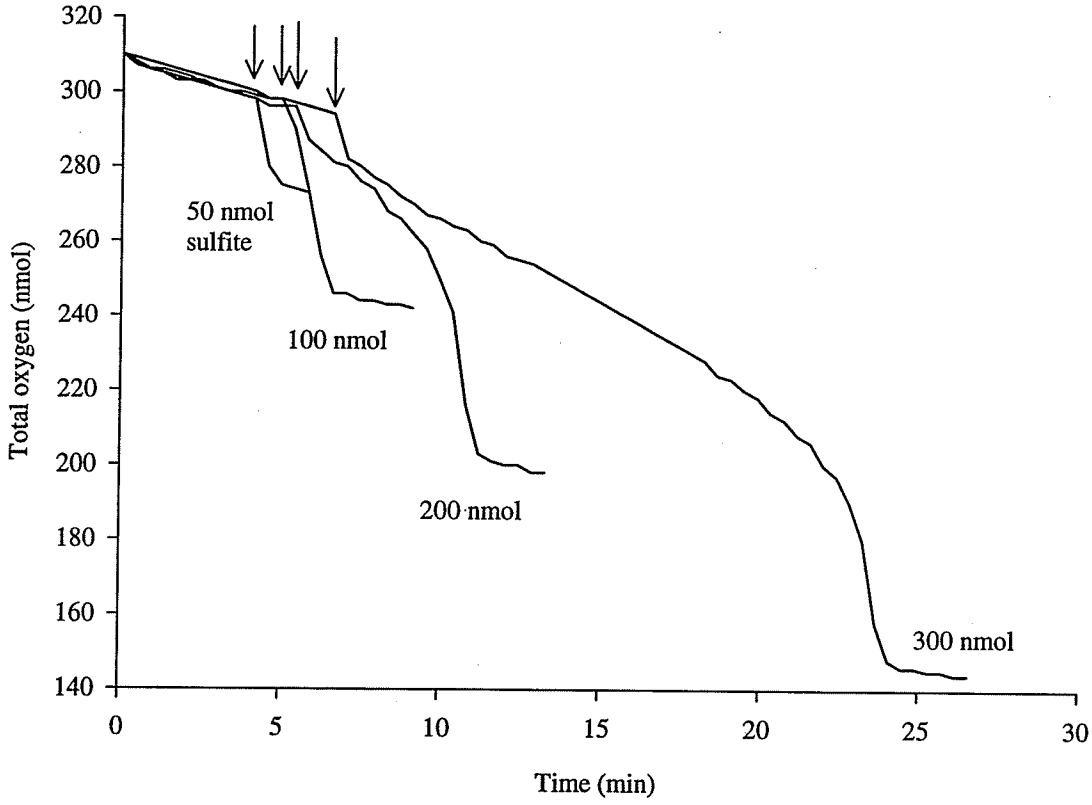
320
300
280
260
240
220
200
180
160
140
Total oxygen (nmol)
50 nmol
sulfite
100 nmol
200 nmol
300 nmol
0
5
10
15
20
25
30
Time (min)

**Figure 2 (a)** The effect of 2,4-dinitrophenol (2,4-DNP) on the rate of exogenous ferric iron reduction by endogenous respiration. The reactions were performed at 25°C in 0.1 M β-alanine-$H_2SO_4$ pH 3 and contained 20 mg of cells, 4 μmol $FeCl_3$, and 2,4-DNP at the concentrations specified. The volume of the reaction mixtures was 1 mL . The results were based on 2 separate trials. The error bars are the standard deviation of the 2 trials.

**Figure 2 (b)** The effect of 2,4-DNP on the rate of oxygen consumption by endogenous respiration. The reactions were performed at 25°C in 0.1 M β-alanine-$H_2SO_4$ pH 3 and contained 25 mg of cells and 2,4-DNP at the concentrations specified. The volume of the reaction mixtures was 1.2 mL .

**2 (a)**

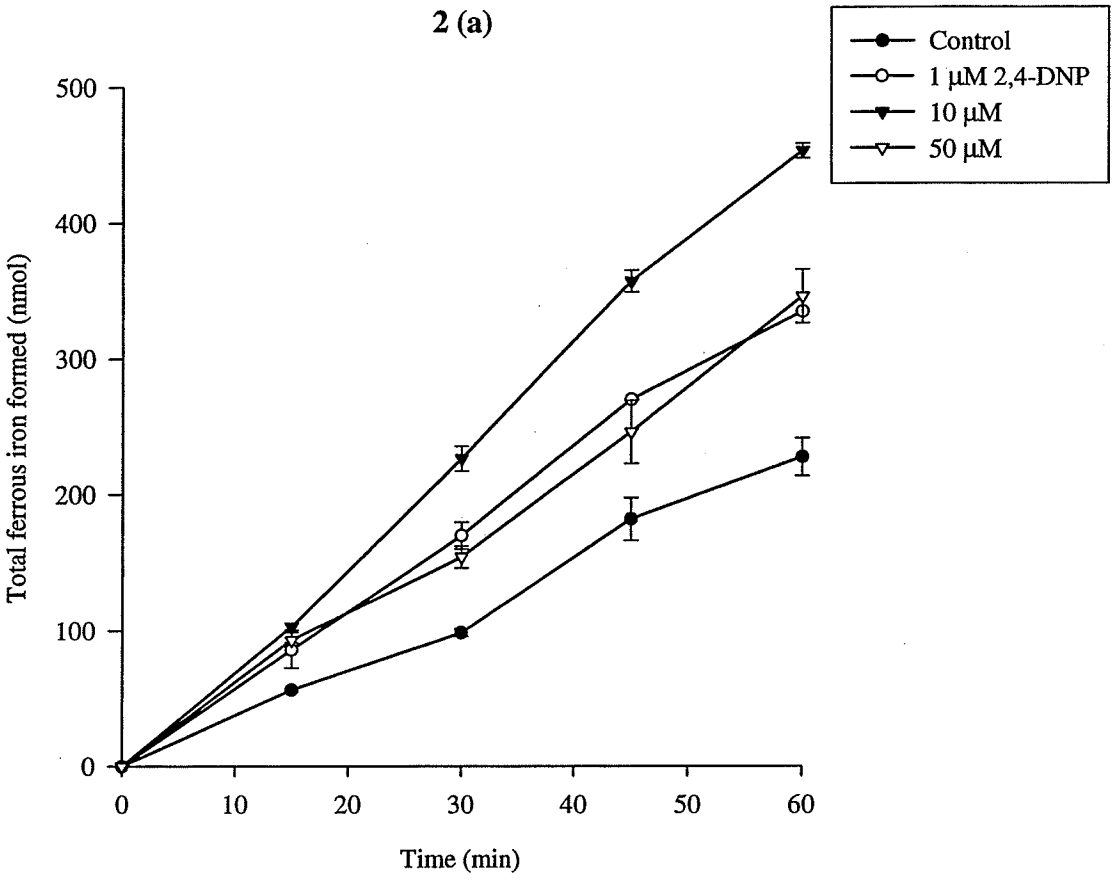
Control
1 µM 2,4-DNP
10 µM
50 µM
Total ferrous iron formed (nmol)
500
400
300
200
100
0
0
10
20
30
40
50
60
Time (min)

**2 (b)**

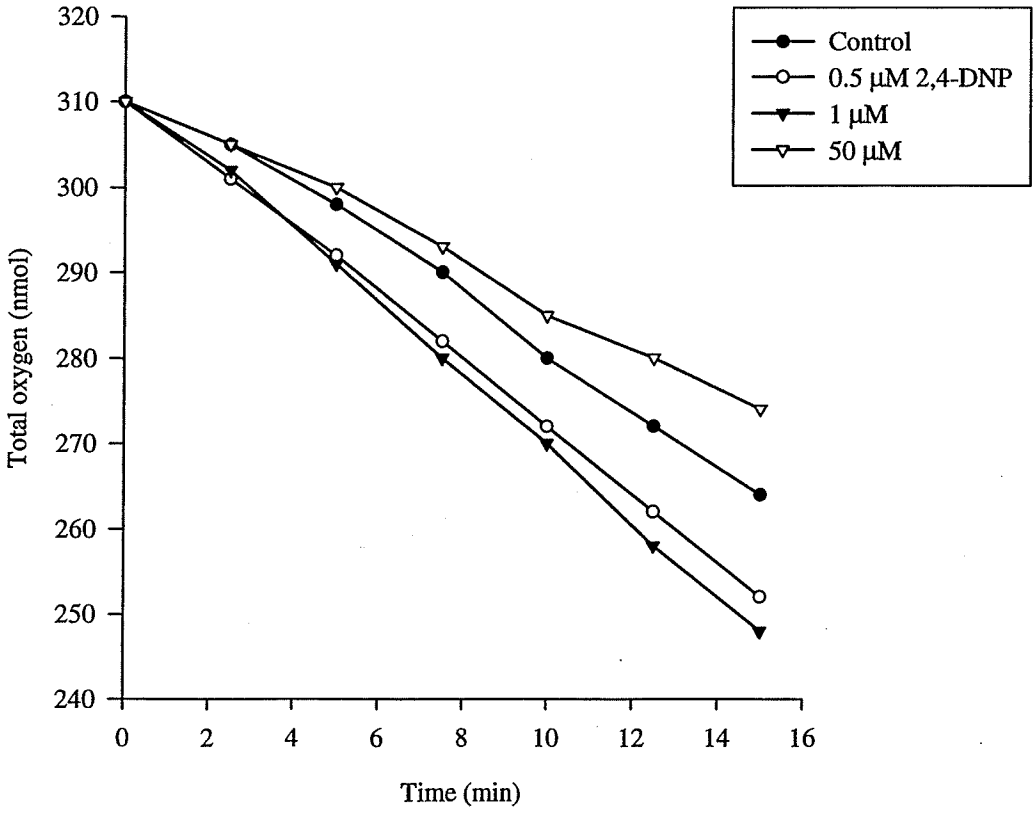
Control
0.5 µM 2,4-DNP
1 µM
50 µM
Total oxygen (nmol)
320
310
300
290
280
270
260
250
240
0
2
4
6
8
10
12
14
16
Time (min)

**Figure 2 (c)** The effect of 2,4-DNP on the rate of sulfite oxidation. The reactions were performed at 25°C in 0.1 M β-alanine-$H_2SO_4$ pH 3 and contained 25 mg of cells and 2,4-DNP at the concentrations specified. $K_2SO_3$ (100 nmol) was added at the arrows after 5 min of preincubation between the cells and 2,4 DNP. The volume of the reaction mixtures was 1.2 mL .

**2 (c)**

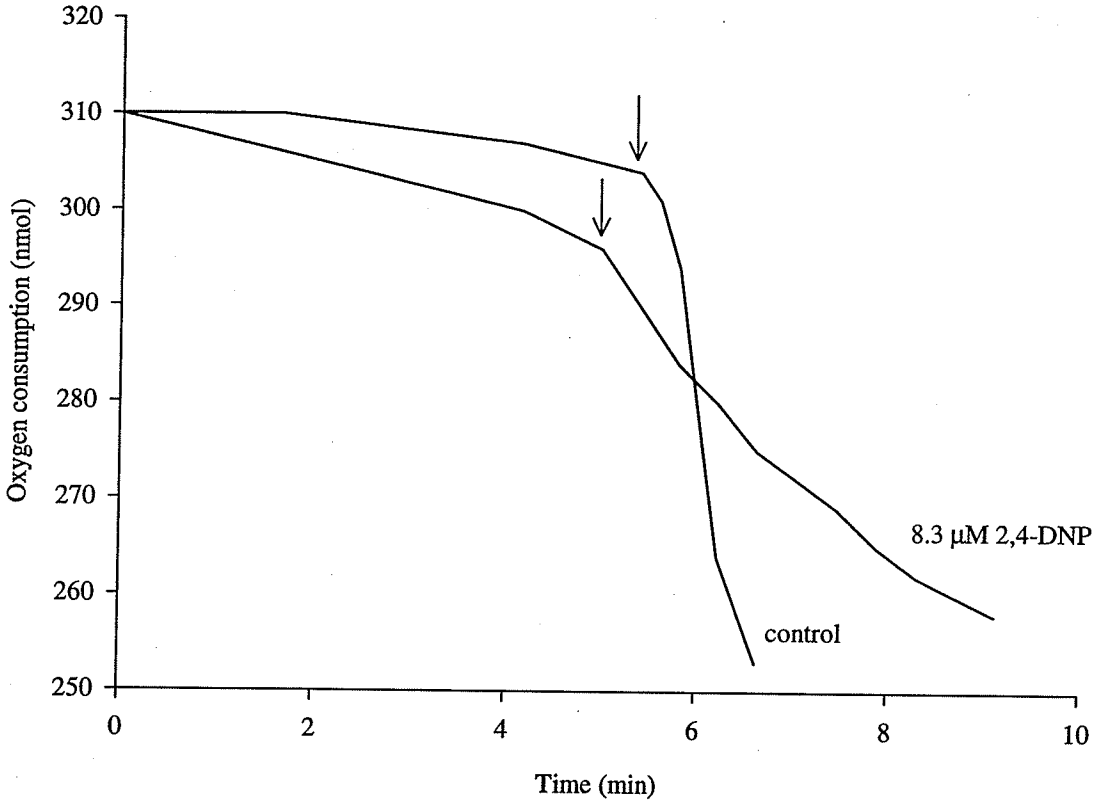
320
310
300
290
280
270
260
250
Oxygen consumption (nmol)
0
2
4
6
8
10
Time (min)
8.3 µM 2,4-DNP
control

**Figure 3 (a)** The effect of carbonyl cyanide-m-chlorophenylhydrazone (CCCP) on the rate of exogenous ferric iron reduction by endogenous respiration. The reactions were performed at 25°C in 0.1 M β-alanine-$H_2SO_4$ pH 3 and contained 20 mg of cells, 4 μmol of $FeCl_3$, and CCCP at the concentrations specified. The volume of the reaction mixtures was 1 mL . The results were based on 2 separate trials. The error bars are the standard deviation of the 2 trials.

**Figure 3 (b)** The effect of CCCP on the rate of oxygen consumption by endogenous respiration. The reactions were performed at 25°C in 0.1 M β-alanine-$H_2SO_4$ pH 3 and contained 25 mg of cells and CCCP at the concentrations specified. The volume of the reaction mixtures was 1.2 mL .

**3 (a)**

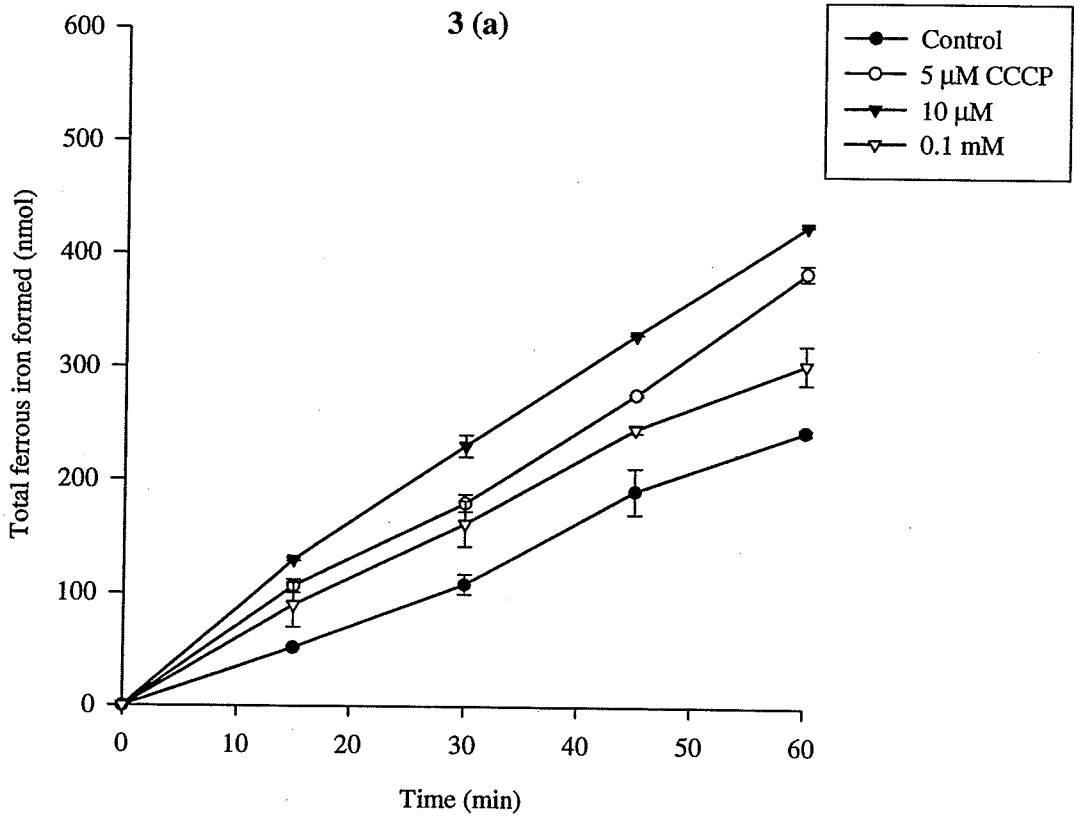
Control
5 µM CCCP
10 µM
0.1 mM
Total ferrous iron formed (nmol)
600
500
400
300
200
100
0
0
10
20
30
40
50
60
Time (min)

**3 (b)**

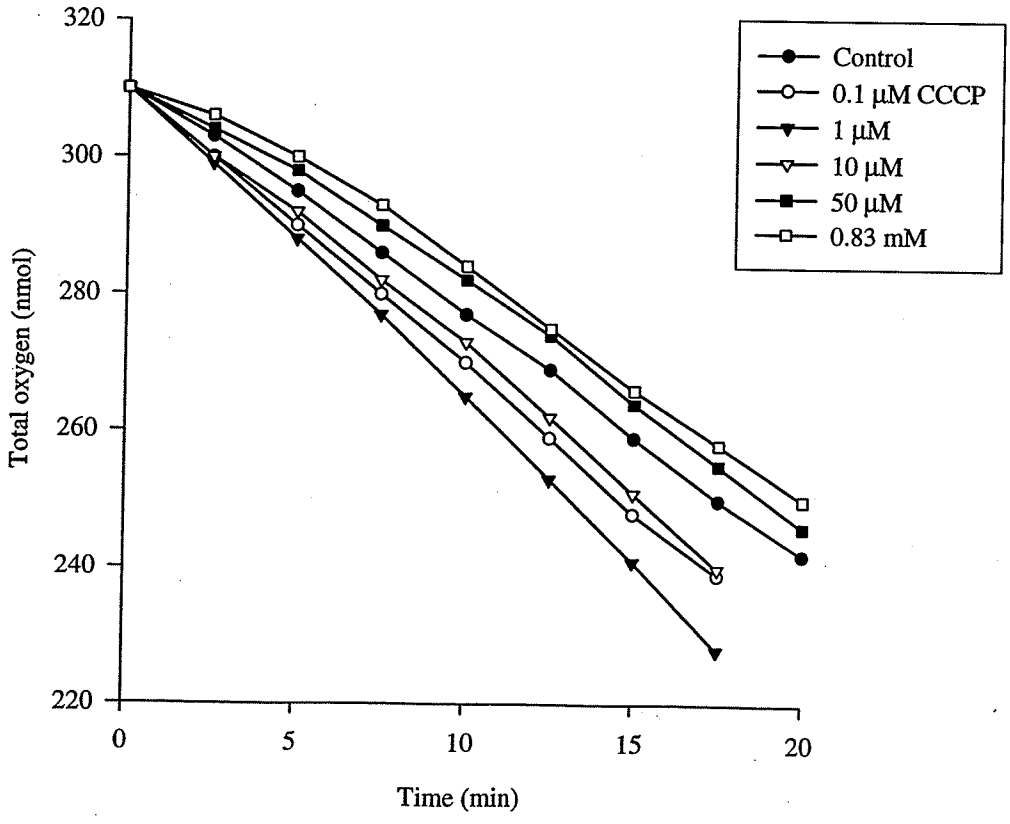
Control
0.1 µM CCCP
1 µM
10 µM
50 µM
0.83 mM
Total oxygen (nmol)
320
300
280
260
240
220
0
5
10
15
20
Time (min)

**Figure 3 (c)** The effect of CCCP on the rate of sulfite oxidation. The reactions were performed at 25°C in 0.1 M β-alanine-$H_2SO_4$ pH 3 and contained 25 mg of cells and CCCP at the concentration specified. $K_2SO_3$ (100 nmol) was added at the arrows after 5 min of preincubation between the cells and CCCP. The volume of the reaction mixtures was 1.2 mL .

**3 (c)**

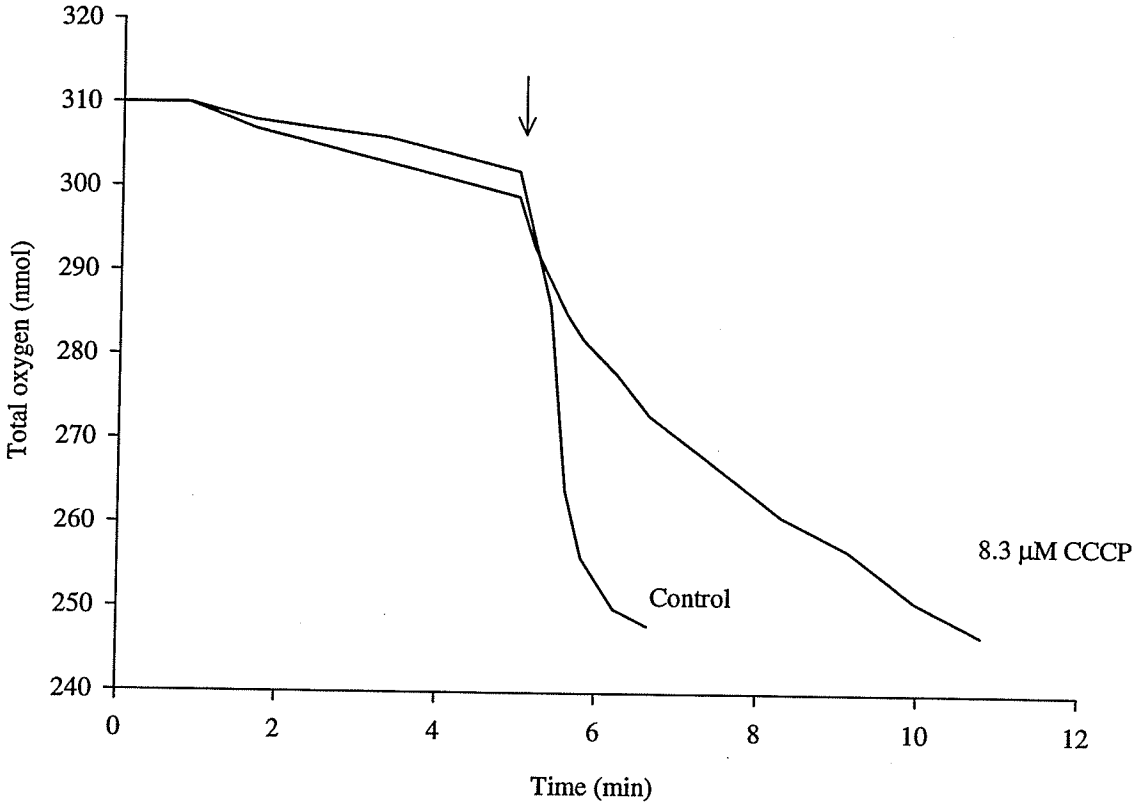
320
310
300
290
280
270
260
250
240
Total oxygen (nmol)
0
2
4
6
8
10
12
Time (min)
8.3 µM CCCP
Control

**Figure 4 (a)** The effect of potassium thiocyanate (KSCN) on the rate of exogenous ferric iron reduction by endogenous respiration. The reactions were performed at 25°C in 0.1 M β-alanine-$H_2SO_4$ pH 3 and contained 20 mg of cells, 4 μmol $FeCl_3$, and KSCN at the concentrations specified. The volume of the reaction mixtures was 1 mL . The results were based on 2 separate trials. The error bars are the standard deviation of the 2 trials.

**Figure 4 (b)** The effect of KSCN on the rate of oxygen consumption by endogenous respiration. The reactions were performed at 25°C in 0.1 M β-alanine-$H_2SO_4$ pH 3 and contained 25 mg of cells and KSCN at the concentrations specified. The volume of the reaction mixtures was 1.2 mL .

**4 (a)**

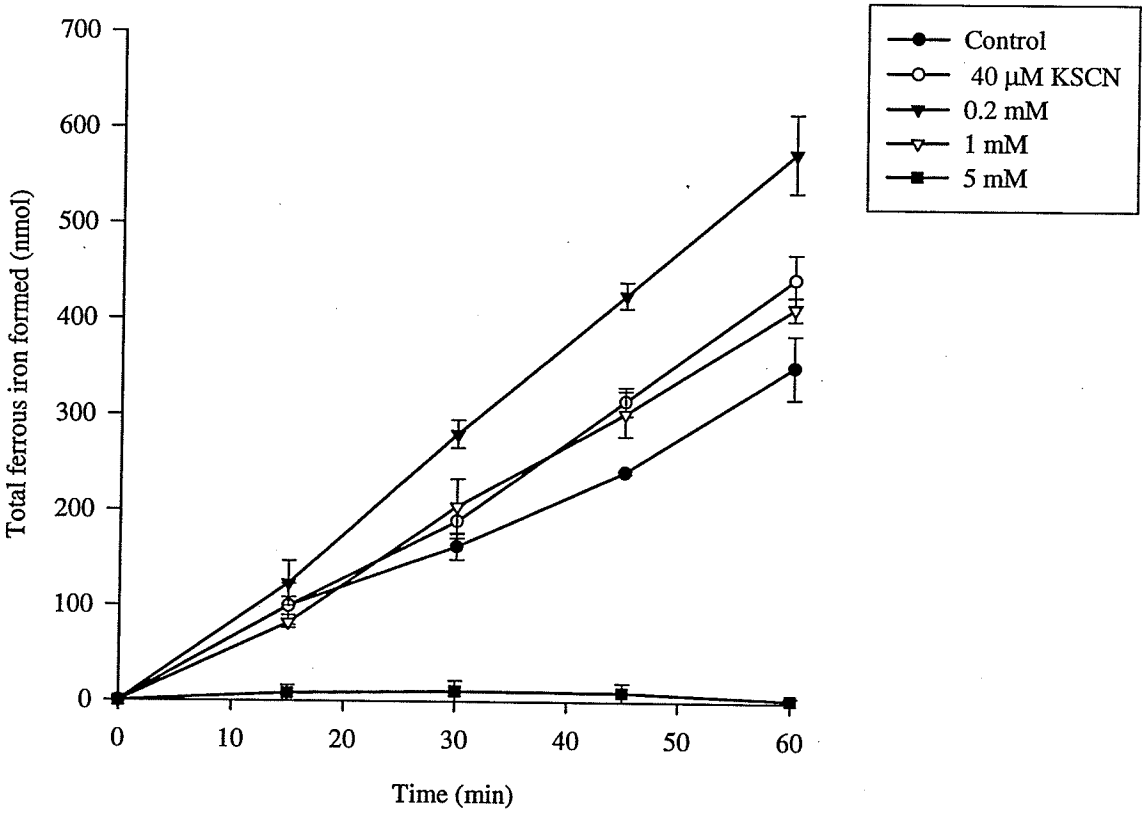
Total ferrous iron formed (nmol)
700
600
500
400
300
200
100
0
0
10
20
30
40
50
60
Time (min)
Control
40 µM KSCN
0.2 mM
1 mM
5 mM

**4 (b)**

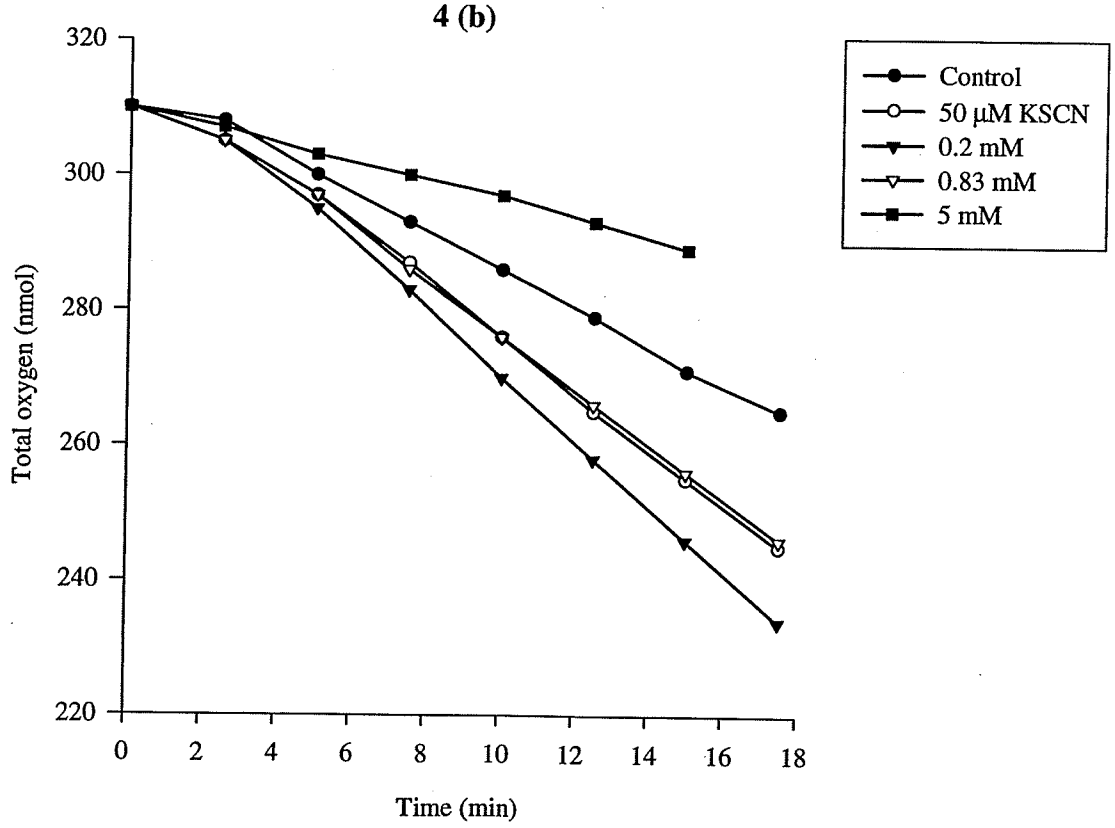
Total oxygen (nmol)
320
300
280
260
240
220
0
2
4
6
8
10
12
14
16
18
Time (min)
Control
50 µM KSCN
0.2 mM
0.83 mM
5 mM

**Figure 4 (c)** The effect of KSCN on the rate of sulfite oxidation. The reactions were performed at 25°C in 0.1 M β-alanine-$H_2SO_4$ pH 3 and contained 25 mg of cells and KSCN at the concentrations specified. $K_2SO_3$ (100 nmol) was added at the arrows after 5 min of preincubation between the cells and KSCN. The volume of the reaction mixtures was 1.2 mL .

**4 (c)**

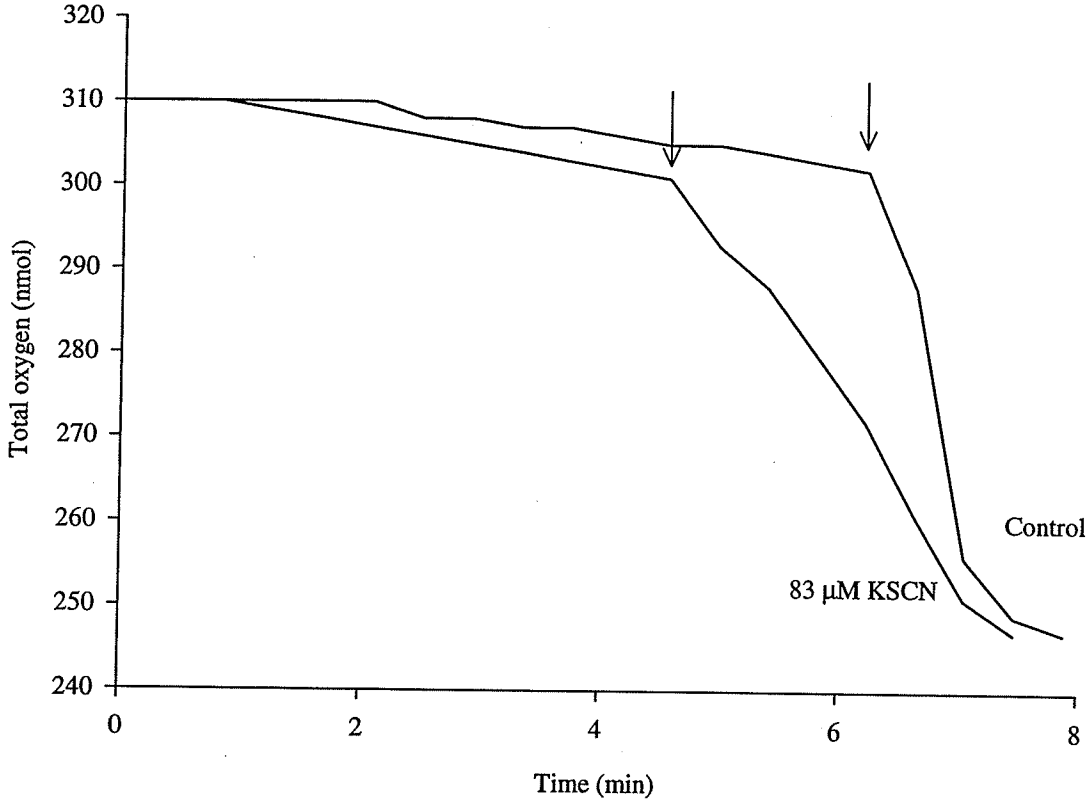
320
310
300
290
280
270
260
250
240
Total oxygen (nmol)
0
2
4
6
8
Time (min)
Control
83 µM KSCN

**Figure 5 (a)** The effect of tetraphenyl boron ($TPB^-$) on the rate of exogenous ferric iron reduction by endogenous respiration. The reactions were performed at 25°C in 0.1 M β-alanine-$H_2SO_4$ pH 3 and contained 20 mg of cells, 4 μmol $FeCl_3$, and $TPB^-$ at the concentrations specified. The volume of the reaction mixtures was 1 mL . Results were based on 2 separate trials. The error bars are the standard deviation of the 2 trials.

**5 (a)**

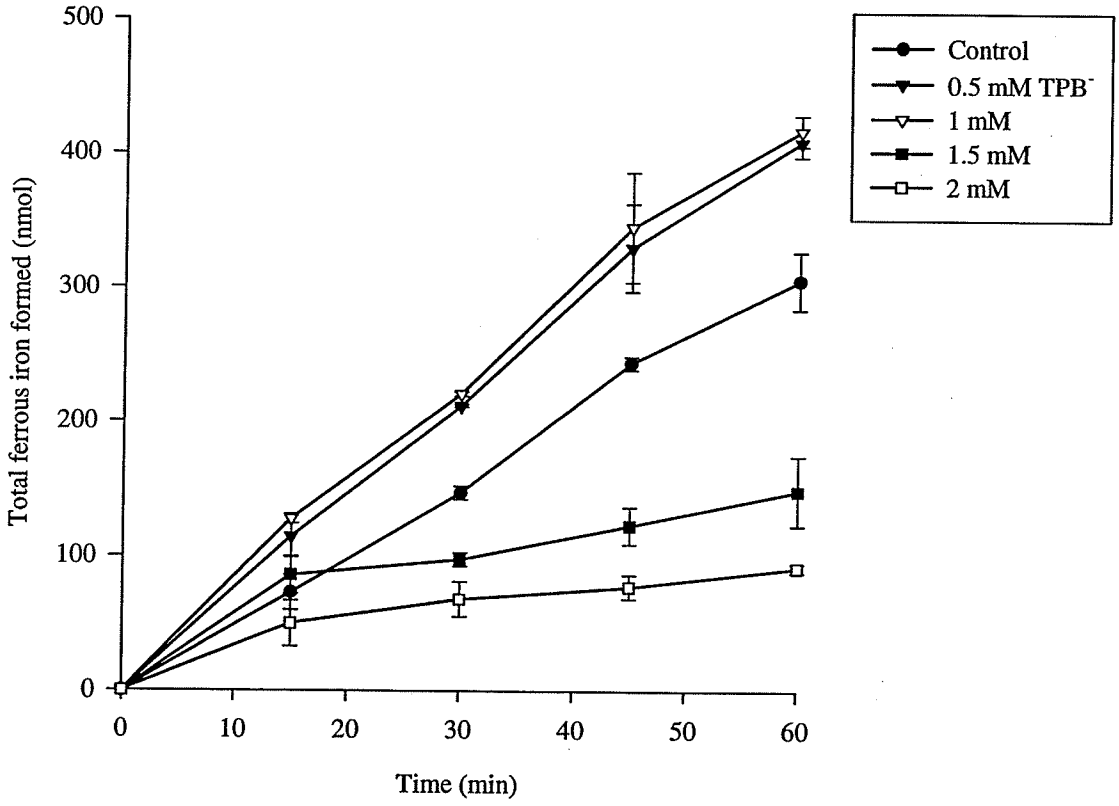
500
400
300
200
100
0
Total ferrous iron formed (nmol)
0
10
20
30
40
50
60
Time (min)
Control
0.5 mM TPB⁻
1 mM
1.5 mM
2 mM

**Figure 5 (b)** The effect of $TPB^-$ on the rate of sulfite oxidation. The reactions were performed at 25°C in 0.1 M β-alanine-$H_2SO_4$ pH 3 and contained 25 mg of cells and $TPB^-$ at the concentration specified. $K_2SO_3$ (100 nmol) was added at the arrows after 5 min of preincubation between the cells and $TPB^-$. A control with 1 % (v/v) acetone is also shown. The volume of the reaction mixtures was 1.2 mL .

**5 (b)**

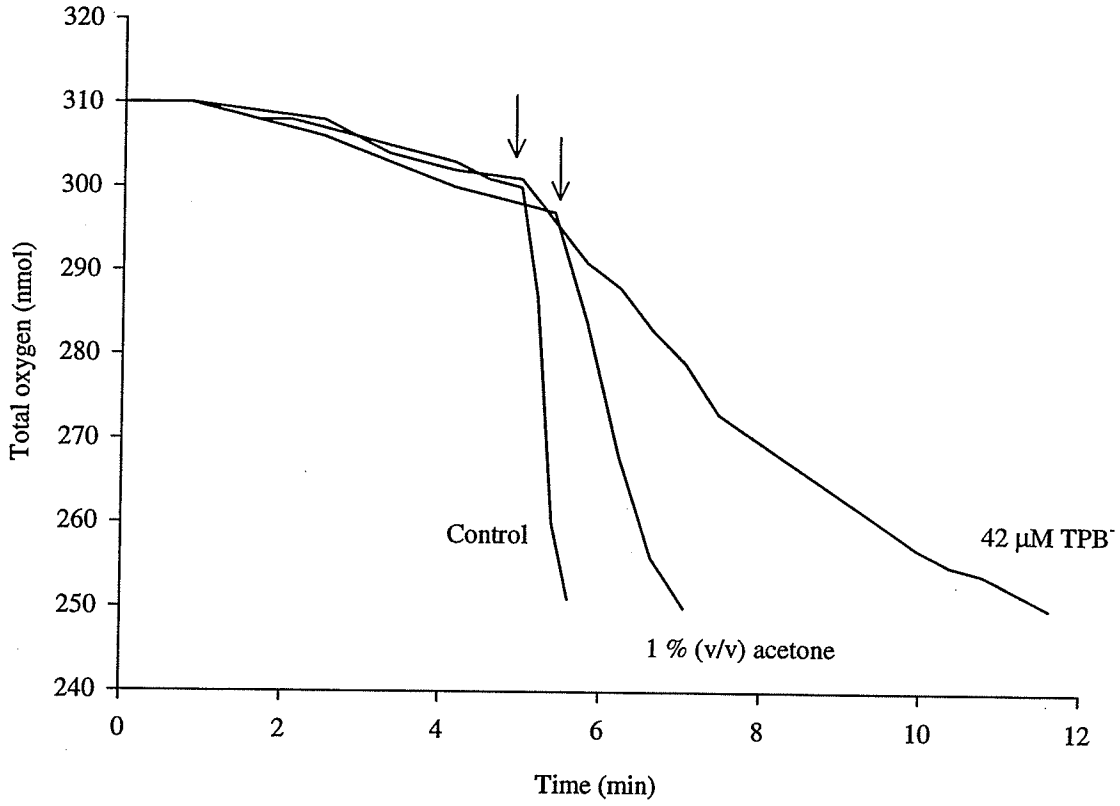
320
310
300
290
280
270
260
250
240
Total oxygen (nmol)
0
2
4
6
8
10
12
Time (min)
Control
1 % (v/v) acetone
42 µM TPB⁻

**Figure 6 (a)** The effect of potassium nitrate ($KNO_3$) on the rate of exogenous ferric iron reduction by endogenous respiration. The reactions were performed at 25°C in 0.1 M β-alanine-$H_2SO_4$ pH 3 and contained 20 mg of cells, 4 μmol $FeCl_3$, and $KNO_3$ at the concentrations specified. The volume of the reaction mixtures was 1 mL . The results were based on 2 separate trials. The error bars are the standard deviation of the 2 trials.

**Figure 6 (b)** The effect of $KNO_3$ on the rate of oxygen consumption by endogenous respiration. The reactions were performed at 25°C in 0.1 M β-alanine-$H_2SO_4$ pH 3 and contained 25 mg of cells and $KNO_3$ at the concentrations specified. The volume of the reaction mixtures was 1.2 mL .

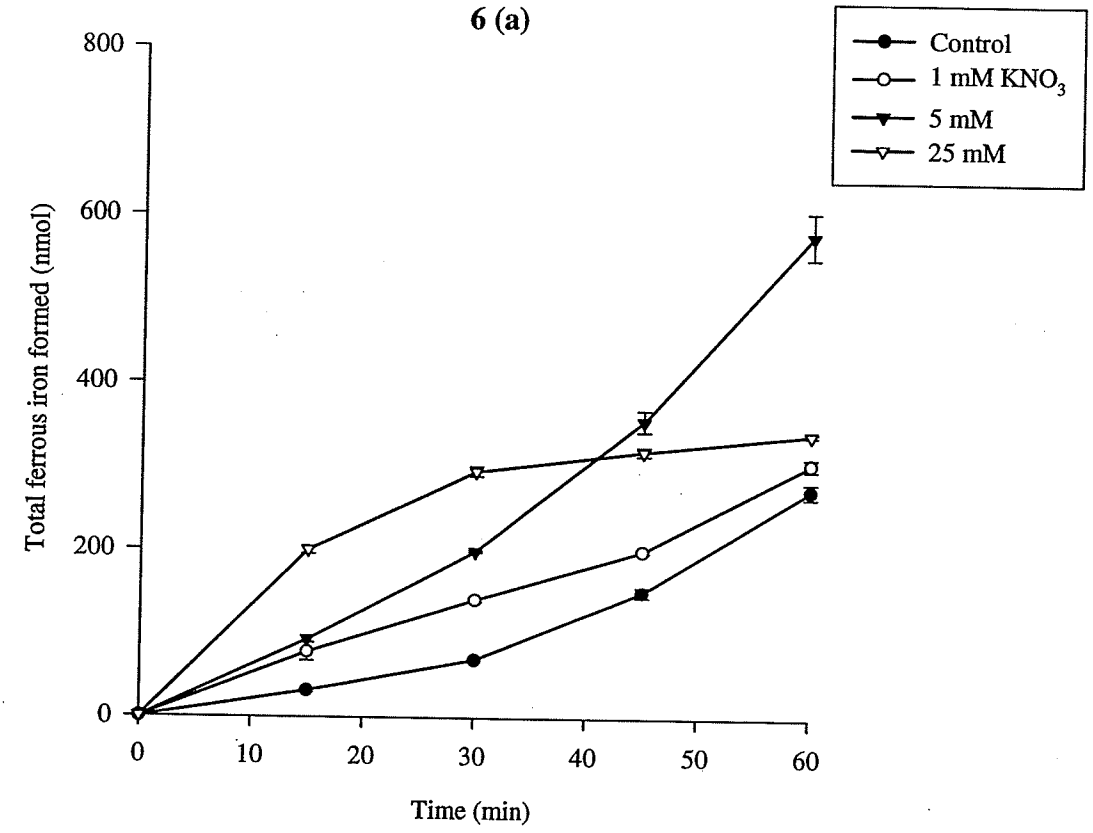
6 (a)
Control
1 mM KNO3
5 mM
25 mM
Total ferrous iron formed (nmol)
800
600
400
200
0
0
10
20
30
40
50
60
Time (min)

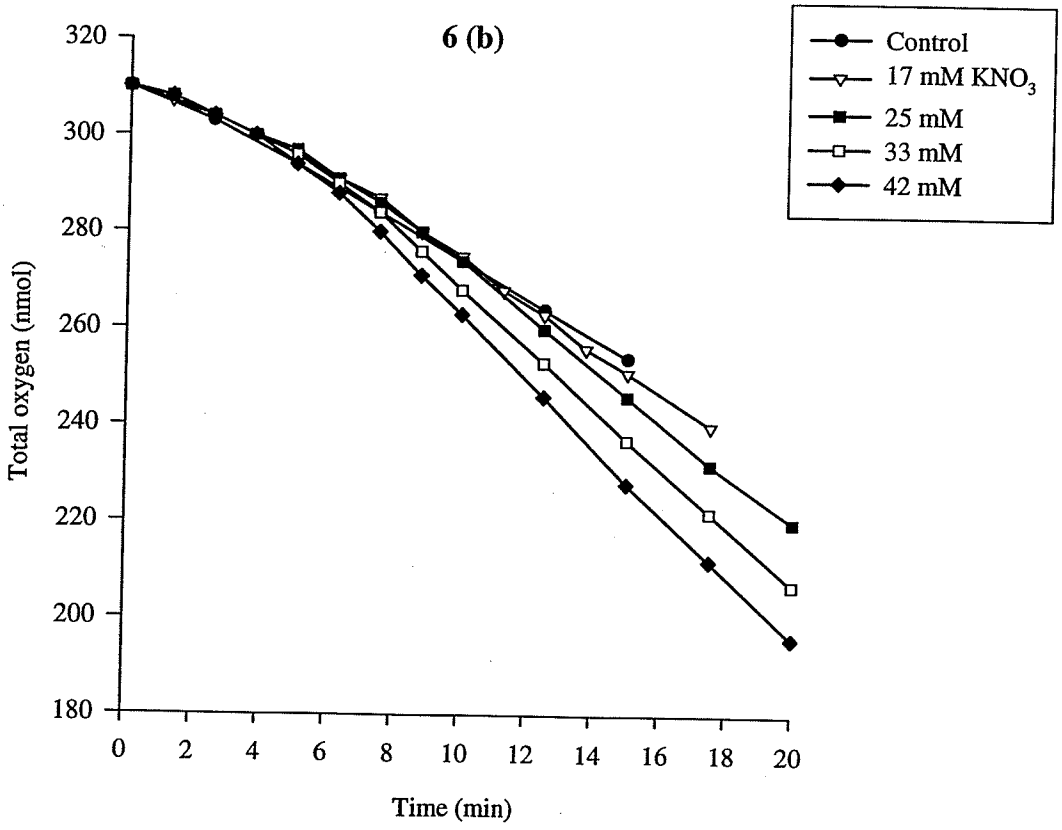
6 (b)
Control
17 mM KNO3
25 mM
33 mM
42 mM
Total oxygen (nmol)
320
300
280
260
240
220
200
180
0
2
4
6
8
10
12
14
16
18
20
Time (min)

**Figure 6 (c)** The effect of potassium nitrate ($KNO_3$) on the rate of sulfite oxidation. The reactions were performed at 25°C in 0.1 M β-alanine-$H_2SO_4$ pH 3 and contained 25 mg of cells and $KNO_3$ at the concentrations specified. Sulfite (100 nmol) was added at the arrows after 5 min of preincubation between the cells and $KNO_3$. The volume of the reaction mixtures was 1.2 mL .

**6 (c)**

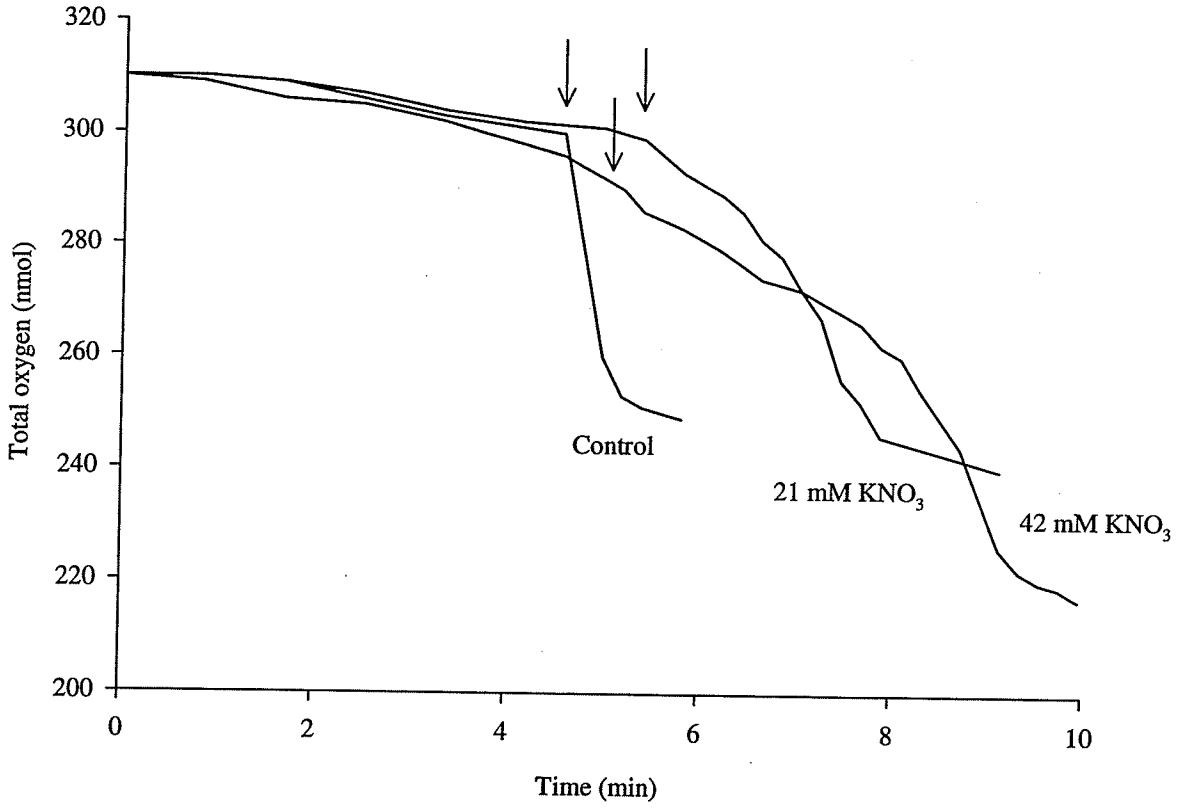
320
300
280
260
240
220
200
Total oxygen (nmol)
0
2
4
6
8
10
Time (min)
Control
21 mM KNO3
42 mM KNO3

**Figure 7 (a)** The effect of acetic acid on the rate of oxygen consumption by endogenous respiration. The reactions were performed at 25°C in 0.1 M β-alanine-$H_2SO_4$ pH 3 and contained 25 mg of cells and acetic acid at the concentrations specified. The volume of the reaction mixtures was 1.2 mL .

**7(a)**

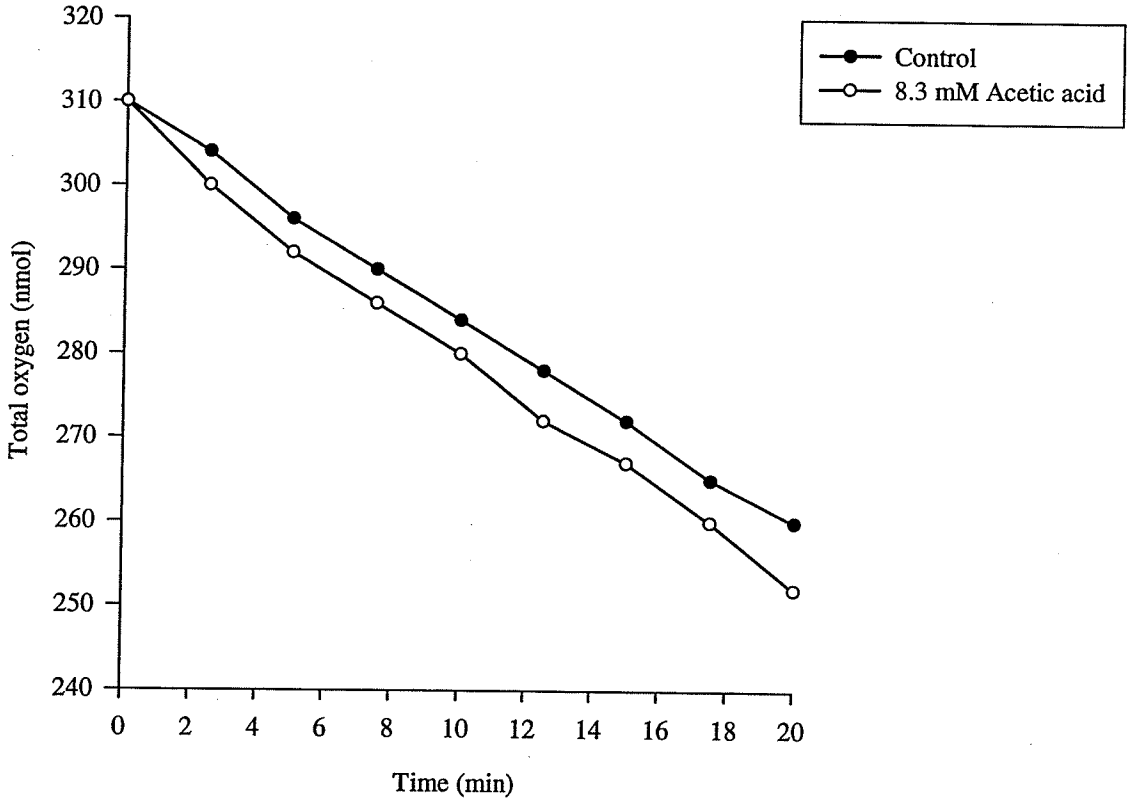
320
310
300
290
280
270
260
250
240
Total oxygen (nmol)
0
2
4
6
8
10
12
14
16
18
20
Time (min)
Control
8.3 mM Acetic acid

**Figure 7 (b)** The effect of acetic acid on the rate of sulfite oxidation. The reactions were performed at 25°C in 0.1 M β-alanine-$H_2SO_4$ pH 3 and contained 25 mg of cells and acetic acid at the concentrations specified. Sulfite (100 nmol) was added at the arrows after 5 min of preincubation between the cells and acetic acid. The volume of the reaction mixtures was 1.2 mL .

**7 (b)**

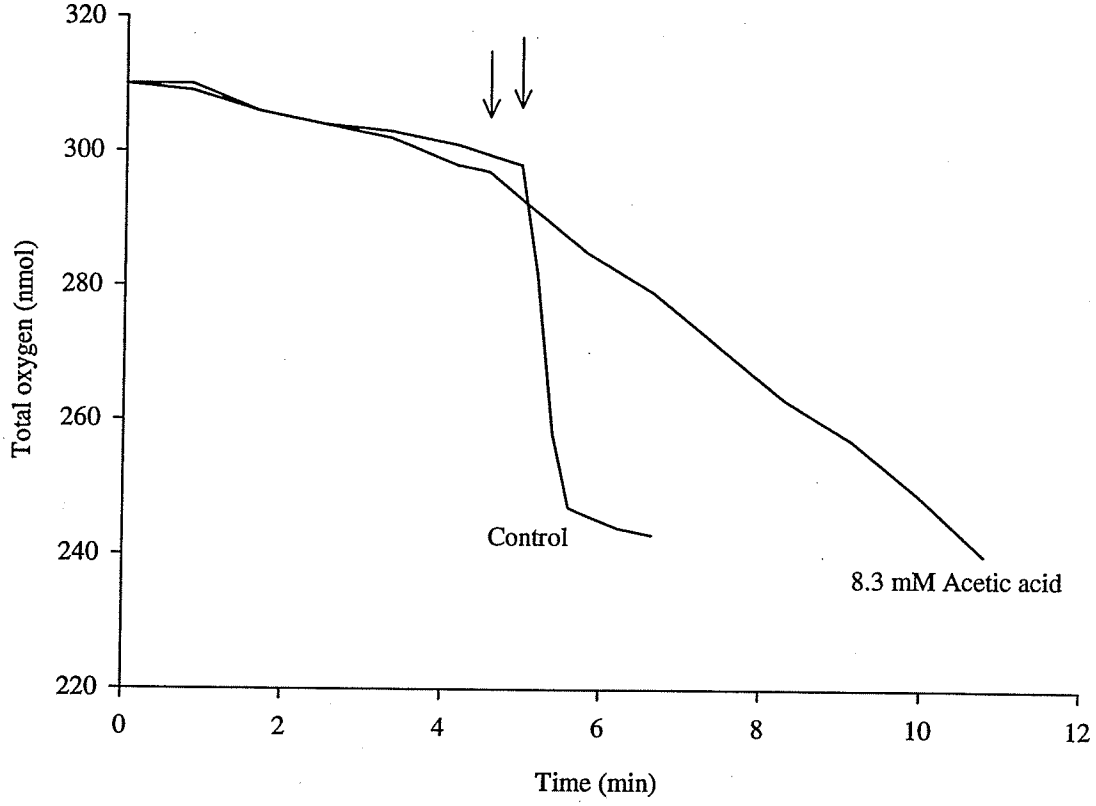
320
300
280
260
240
220
Total oxygen (nmol)
0
2
4
6
8
10
12
Time (min)
Control
8.3 mM Acetic acid

**Figure 8 (a)** The effect of hydrofluoric acid on the rate of exogenous ferric iron reduction by endogenous respiration. The reactions were performed at 25°C in 0.1 M β-alanine-$H_2SO_4$ pH 3 and contained 20 mg of cells, 4 μmol $FeCl_3$, and hydrofluoric acid at the concentrations specified. The volume of the reaction mixtures was 1 mL . The results were based on 2 separate trials. The error bars are the standard deviation of the 2 trials.

**Figure 8 (b)** The effect of hydrofluoric acid on the rate of oxygen consumption by endogenous respiration. The reactions were performed at 25°C in 0.1 M β-alanine-$H_2SO_4$ pH 3 and contained 25 mg of cells and hydrofluoric acid at the concentrations specified. The volume of the reaction mixtures was 1.2 mL .

**8 (a)**

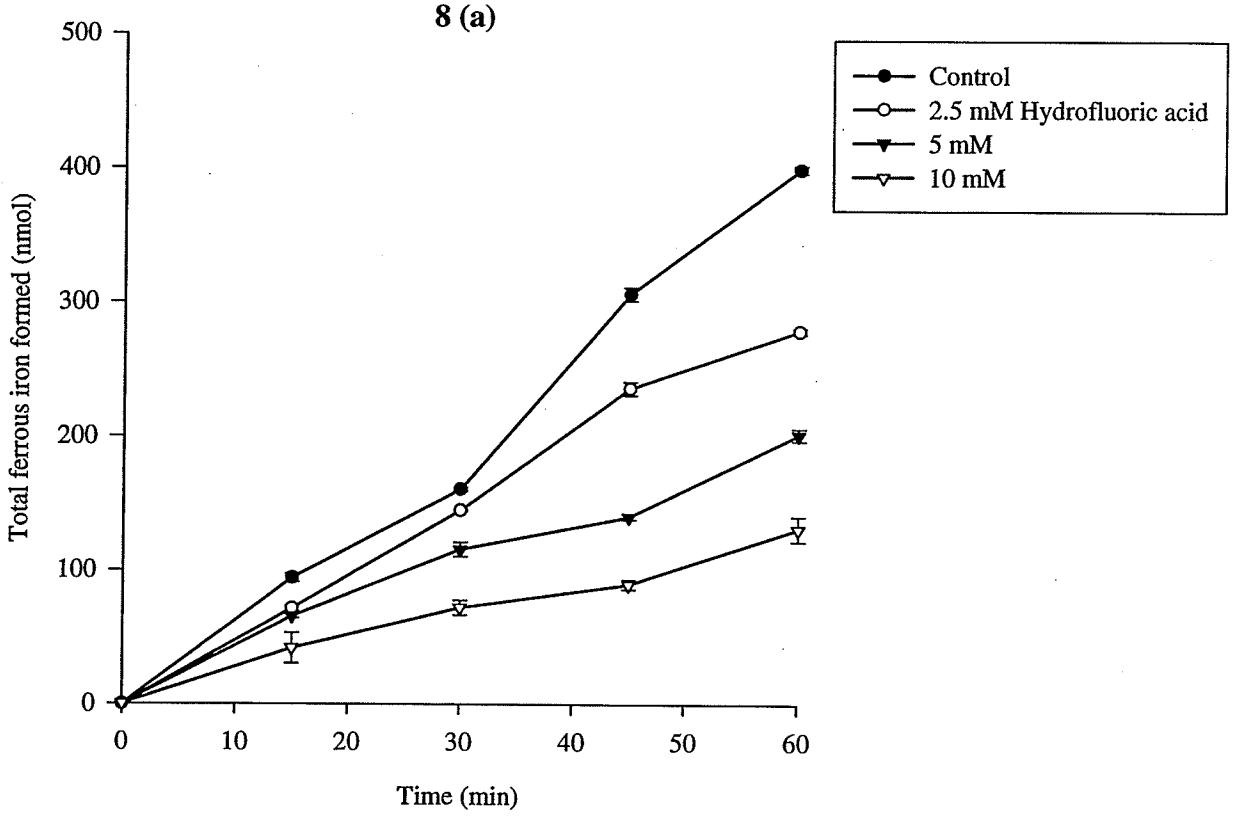
Control
2.5 mM Hydrofluoric acid
5 mM
10 mM
Total ferrous iron formed (nmol)
500
400
300
200
100
0
0
10
20
30
40
50
60
Time (min)

**8 (b)**

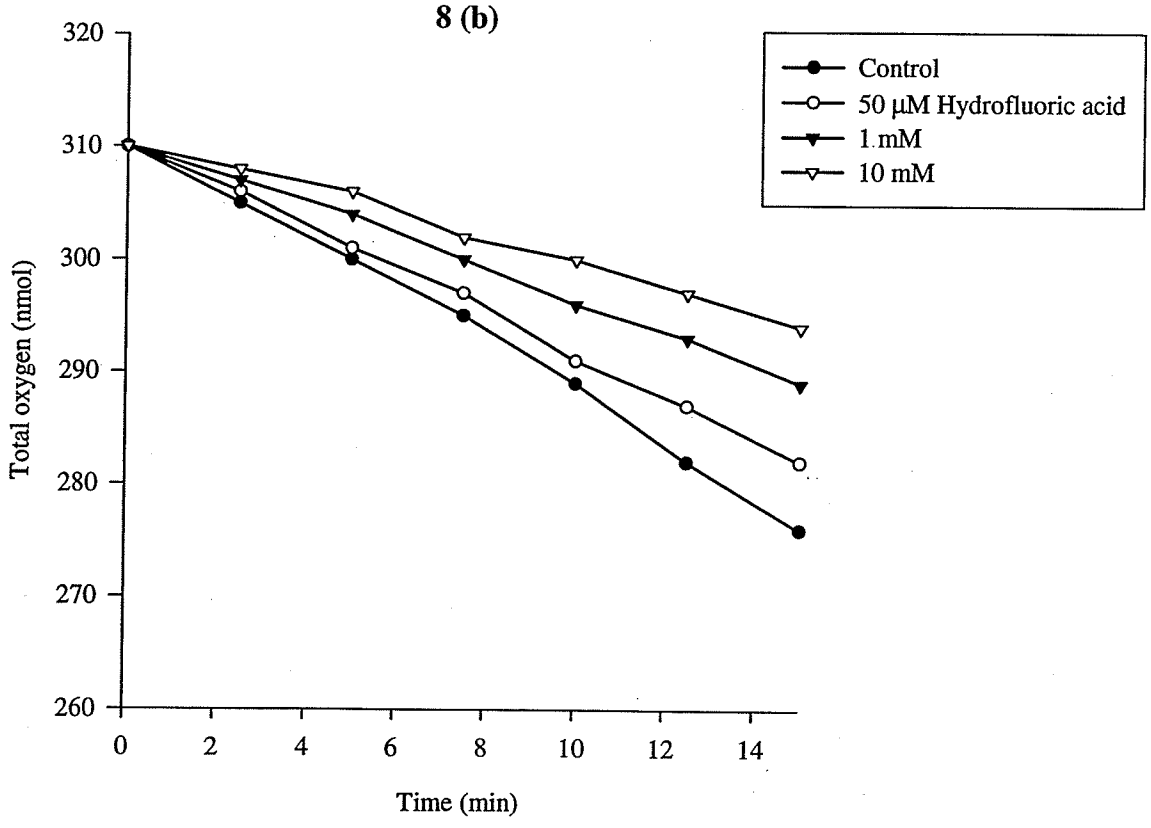
Control
50 µM Hydrofluoric acid
1 mM
10 mM
Total oxygen (nmol)
320
310
300
290
280
270
260
0
2
4
6
8
10
12
14
Time (min)

**Figure 8 (c)** The effect of hydrofluoric acid on the rate of sulfite oxidation. The reactions were performed at 25°C in 0.1 M β-alanine-$H_2SO_4$ pH 3 and contained 25 mg of cells and hydrofluoric acid at the concentration specified. $K_2SO_3$ (100 nmol) was added at the arrows after 5 min of preincubation between the cells and hydrofluoric acid. The volume of the reaction mixtures was 1.2 mL .

**8 (c)**

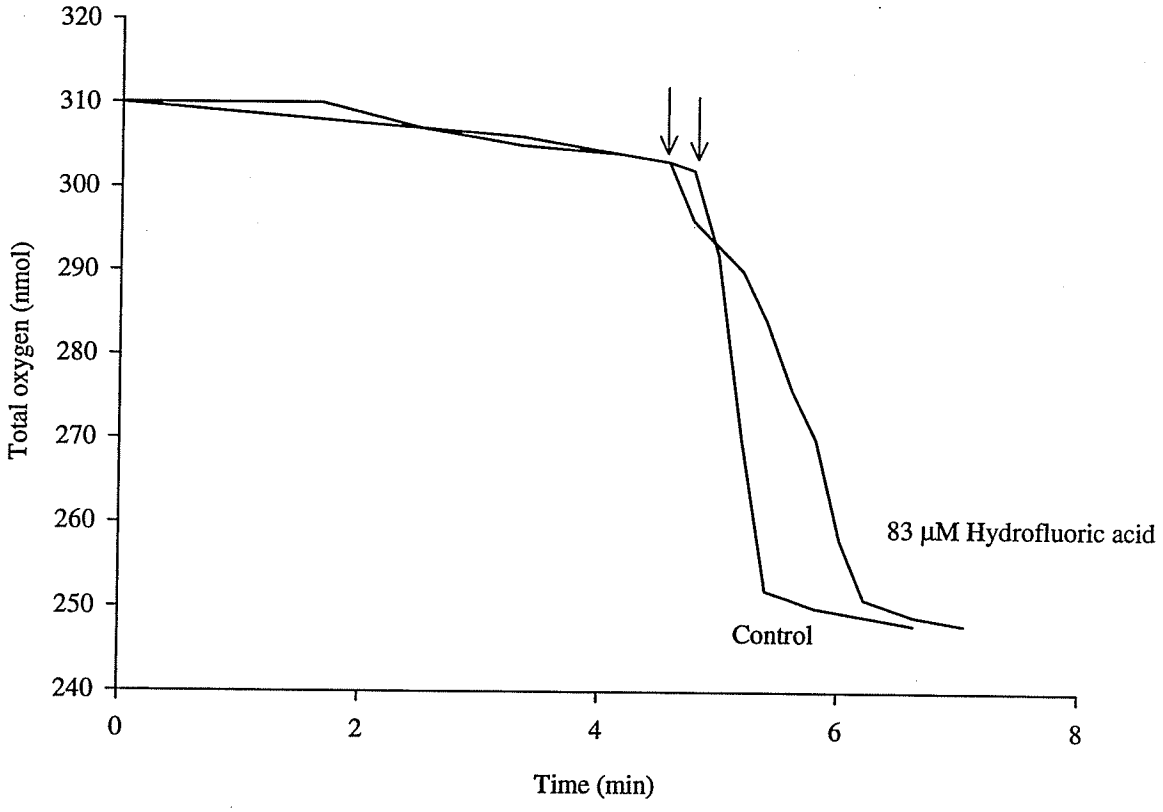
320
310
300
290
280
270
260
250
240
Total oxygen (nmol)
0
2
4
6
8
Time (min)
83 μM Hydrofluoric acid
Control

**Figure 9 (a)** The effect of propionic acid on the rate of oxygen consumption by endogenous respiration. The reactions were performed at 25°C in 0.1 M β-alanine-$H_2SO_4$ pH 3 and contained 25 mg of cells and propionic acid at the concentrations specified. The volume of the reaction mixtures was 1.2 mL .

**9 (a)**

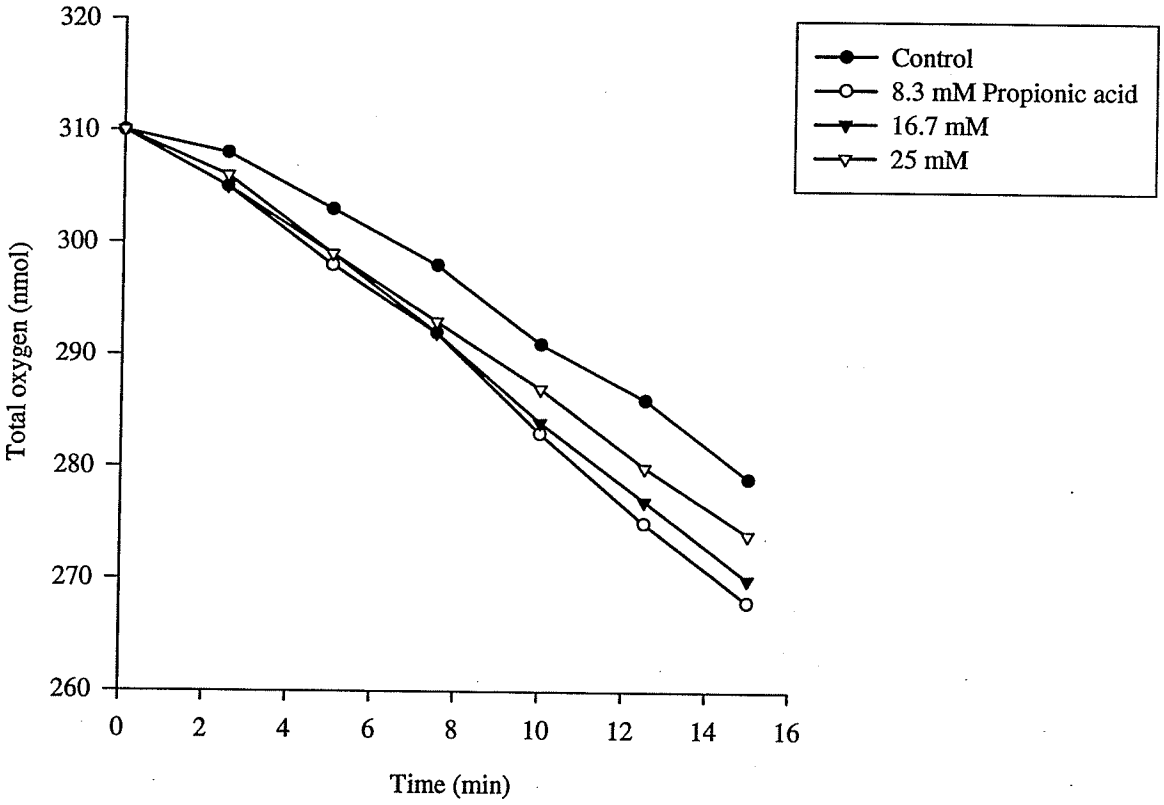
320
310
300
290
280
270
260
Total oxygen (nmol)
0
2
4
6
8
10
12
14
16
Time (min)
Control
8.3 mM Propionic acid
16.7 mM
25 mM

**Figure 9 (b)** The effect of propionic acid on the rate of sulfite oxidation. The reactions were performed at 25°C in 0.1 M β-alanine-$H_2SO_4$ pH 3 and contained 25 mg of cells and propionic acid at the concentrations specified. $K_2SO_3$ (100 nmol) was added at the arrows after 5 min of preincubation between the cells and propionic acid. The volume of the reaction mixtures was 1.2 mL .

**9 (b)**

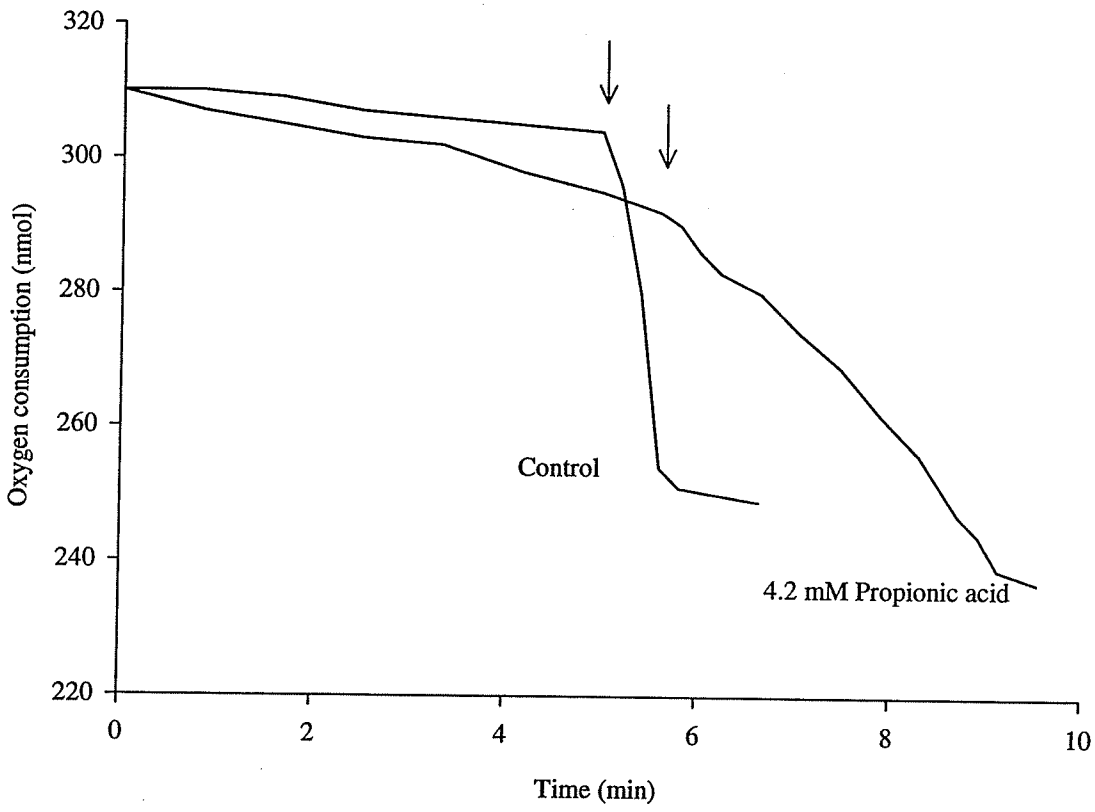
320
300
280
260
240
220
Oxygen consumption (nmol)
0
2
4
6
8
10
Time (min)
Control
4.2 mM Propionic acid

**Figure 10 (a)** The effect of butyric acid on the rate of oxygen consumption by endogenous respiration. The reactions were performed at 25°C in 0.1 M β-alanine-$H_2SO_4$ pH 3 and contained 25 mg of cells and butyric acid at the concentrations specified. The volume of the reaction mixtures was 1.2 mL .

**10 (a)**

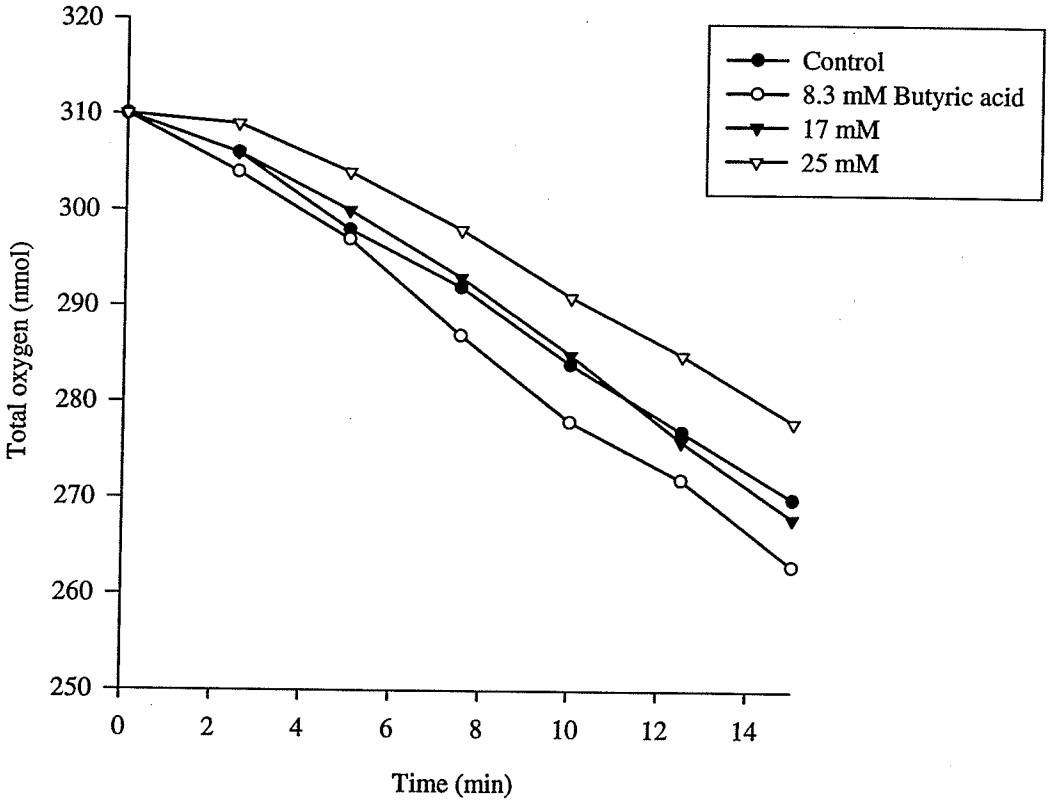
320
310
300
290
280
270
260
250
Total oxygen (nmol)
0
2
4
6
8
10
12
14
Time (min)
Control
8.3 mM Butyric acid
17 mM
25 mM

**Figure 10 (b)** The effect of butyric acid on the rate of sulfite oxidation. The reactions were performed at 25°C in 0.1 M β-alanine-$H_2SO_4$ pH 3 and contained 25 mg of cells and butyric acid at the concentrations specified. $K_2SO_3$ (100 nmol) was added at the arrows after 5 min of preincubation between the cells and butyric acid. The volume of the reaction mixtures was 1.2 mL .

**10 (b)**

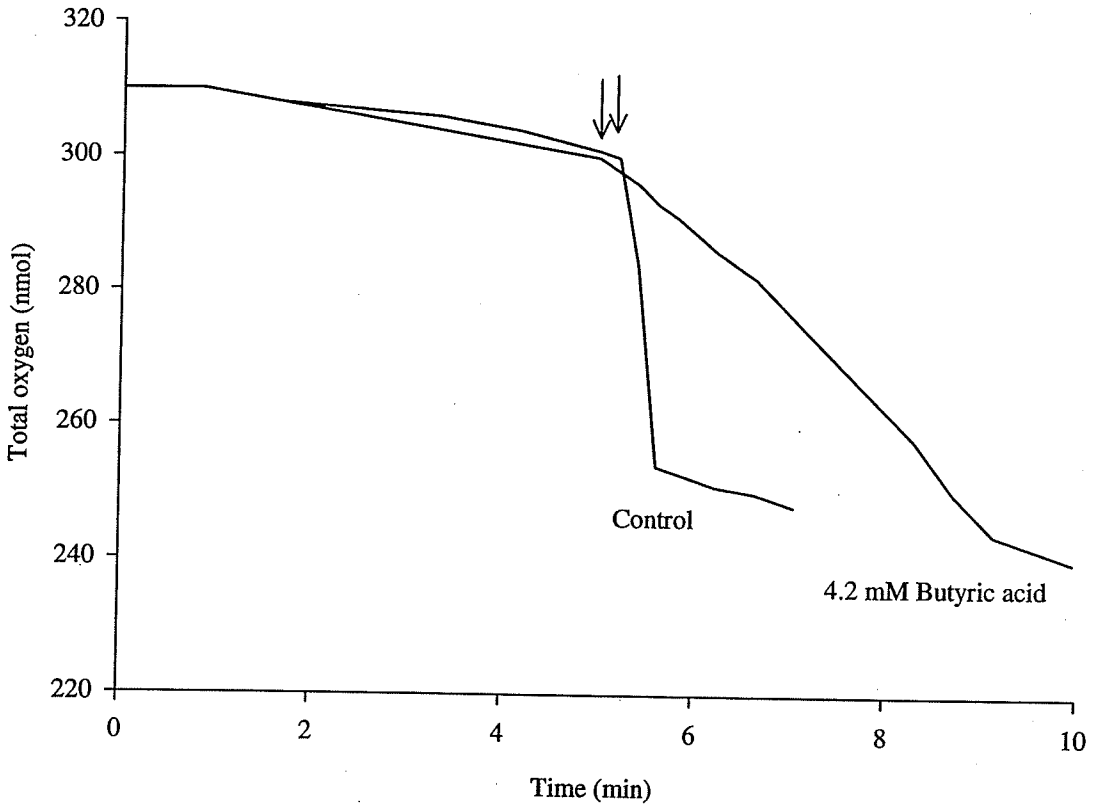
320
300
280
260
240
220
Total oxygen (nmol)
0
2
4
6
8
10
Time (min)
Control
4.2 mM Butyric acid

**Figure 11 (a)** The effect of lactic acid on the rate of exogenous ferric iron reduction by endogenous respiration. The reactions were performed at 25°C in 0.1 M β-alanine-$H_2SO_4$ pH 3 and contained 20 mg of cells, 4 μmol of $FeCl_3$, and lactic acid at the concentrations specified. The volume of the reaction mixtures was 1 mL . The results were based on 2 separate trials. The error bars are the standard deviation of the 2 trials.

**Figure 11 (b)** The effect of lactic acid on the rate of oxygen consumption by endogenous respiration. The reactions were performed at 25°C in 0.1 M β-alanine-$H_2SO_4$ pH 3 and contained 25 mg of cells and lactic acid at the concentrations specified. The volume of the reaction mixtures was 1.2 mL .

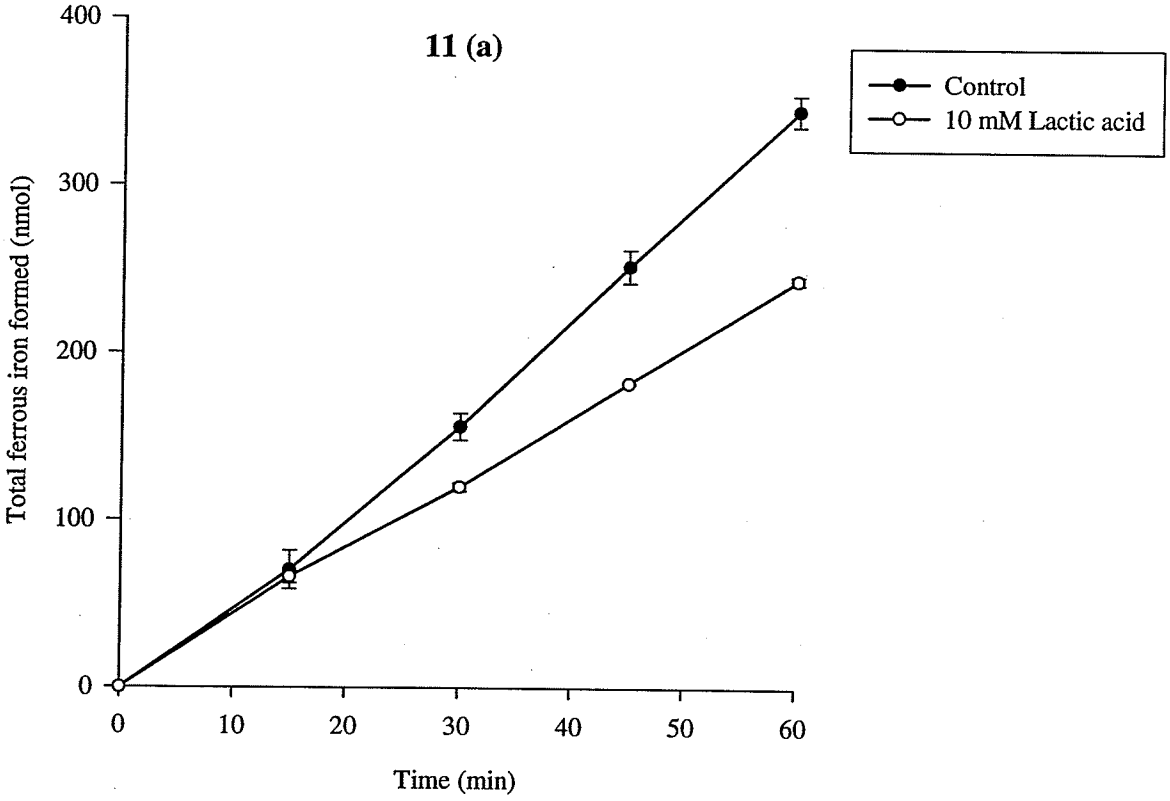
11 (a)
Control
10 mM Lactic acid
Total ferrous iron formed (nmol)
400
300
200
100
0
0
10
20
30
40
50
60
Time (min)

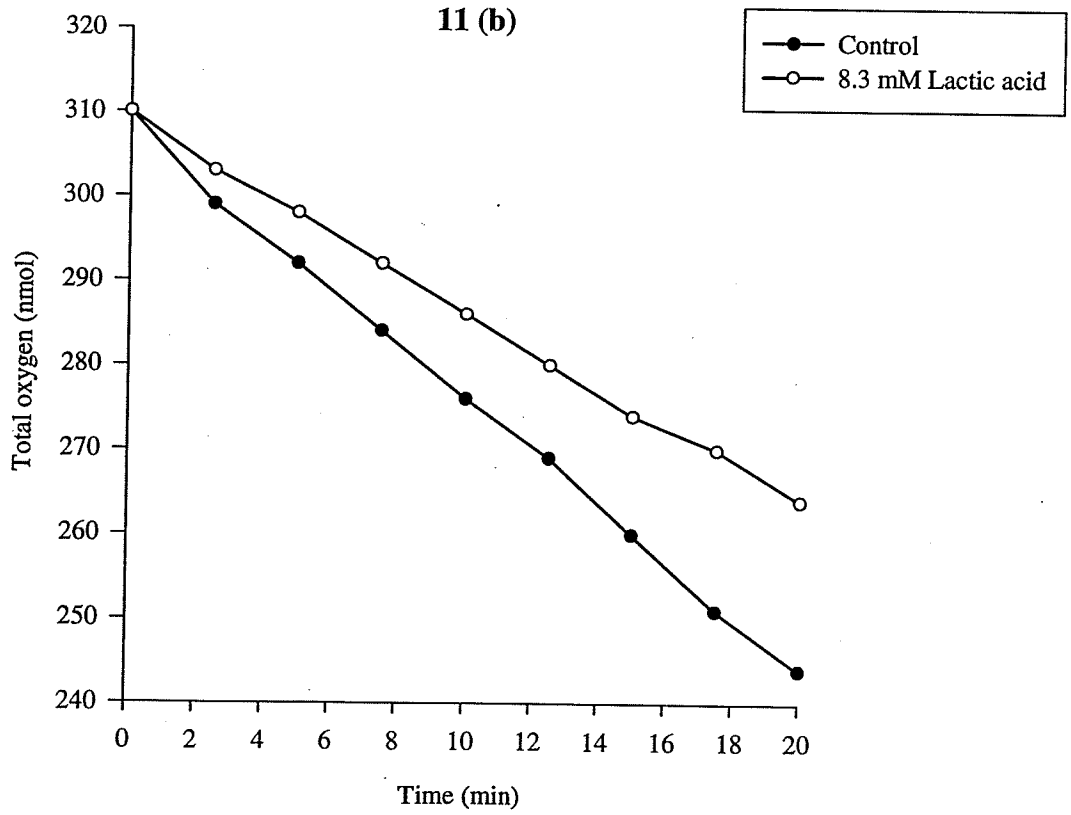
11 (b)
Control
8.3 mM Lactic acid
Total oxygen (nmol)
320
310
300
290
280
270
260
250
240
0
2
4
6
8
10
12
14
16
18
20
Time (min)

**Figure 11 (c)** The effect of lactic acid on the rate of sulfite oxidation. The reactions were performed at 25°C in 0.1 M β-alanine-$H_2SO_4$ pH 3 and contained 25 mg of cells and lactic acid at the concentrations specified. $K_2SO_3$ (100 nmol) was added at the arrows after 5 min of preincubation between the cells and lactic acid. The volume of the reaction mixtures was 1.2 mL .

**11 (c)**

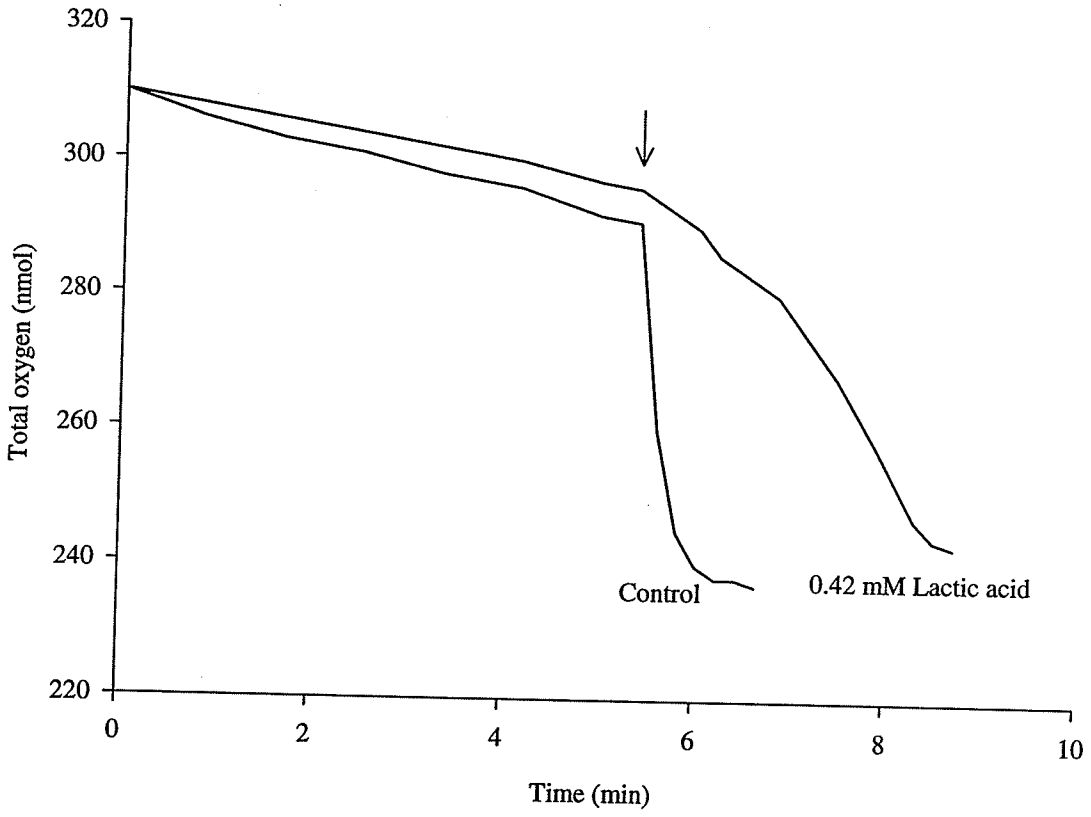
320
300
280
260
240
220
Total oxygen (nmol)
0
2
4
6
8
10
Time (min)
Control
0.42 mM Lactic acid

**Figure 12** The stoichiometric oxidation of formic acid by *A. thiooxidans* strain ATCC 8085. The reactions were performed at 25°C in 0.1 M β-alanine-$H_2SO_4$ pH 3 and contained 25 mg of cells. Formic acid was added at the arrows at the amounts specified. The volume of the reaction mixtures was 1.2 mL .

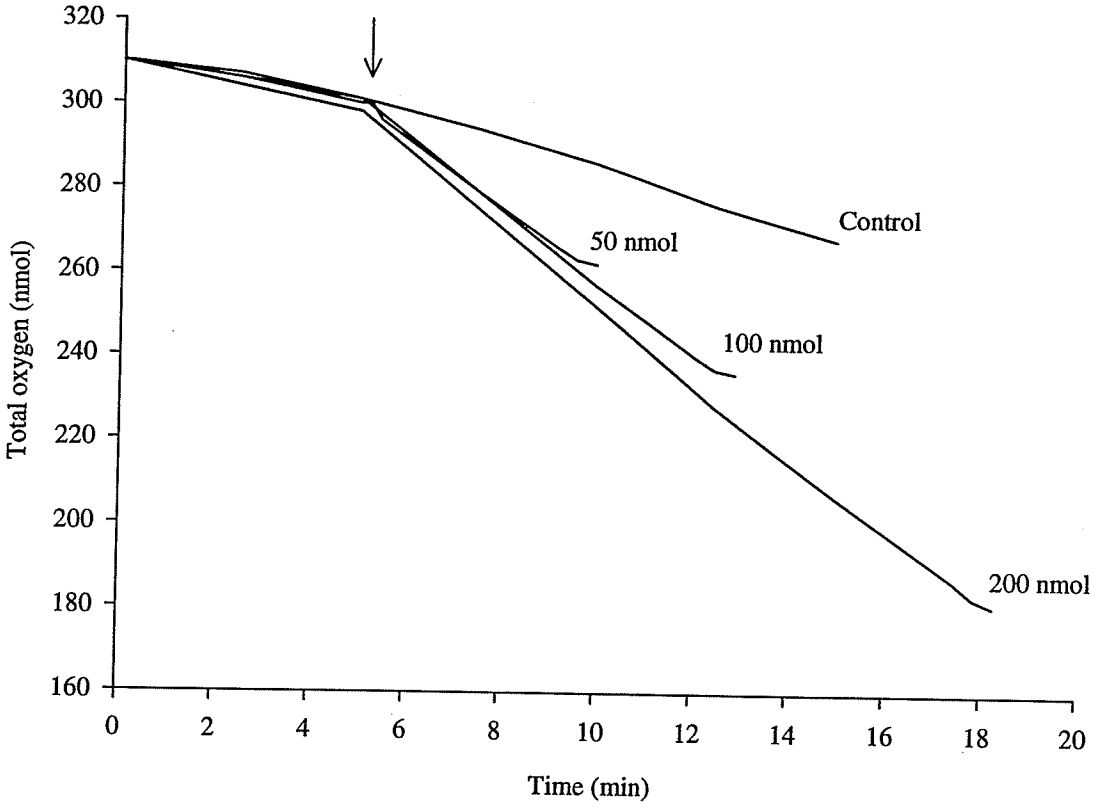
320
300
280
260
240
220
200
180
160
Total oxygen (nmol)
0
2
4
6
8
10
12
14
16
18
20
Time (min)
Control
50 nmol
100 nmol
200 nmol

**Figure 13** Formic acid oxidation in the presence of **(a)** CCCP and **(b)** exogenous ferric iron. The reactions were performed at 25°C in 0.1 M β-alanine-$H_2SO_4$ pH 3 and contained 25 mg of cells and CCCP or exogenous ferric iron at the concentrations specified. Formic acid (200 nmol) was added at the initial arrows. CCCP and exogenous ferric iron were added at the final arrows. The volume of the reaction mixtures was 1.2 mL.

**13 (a)**

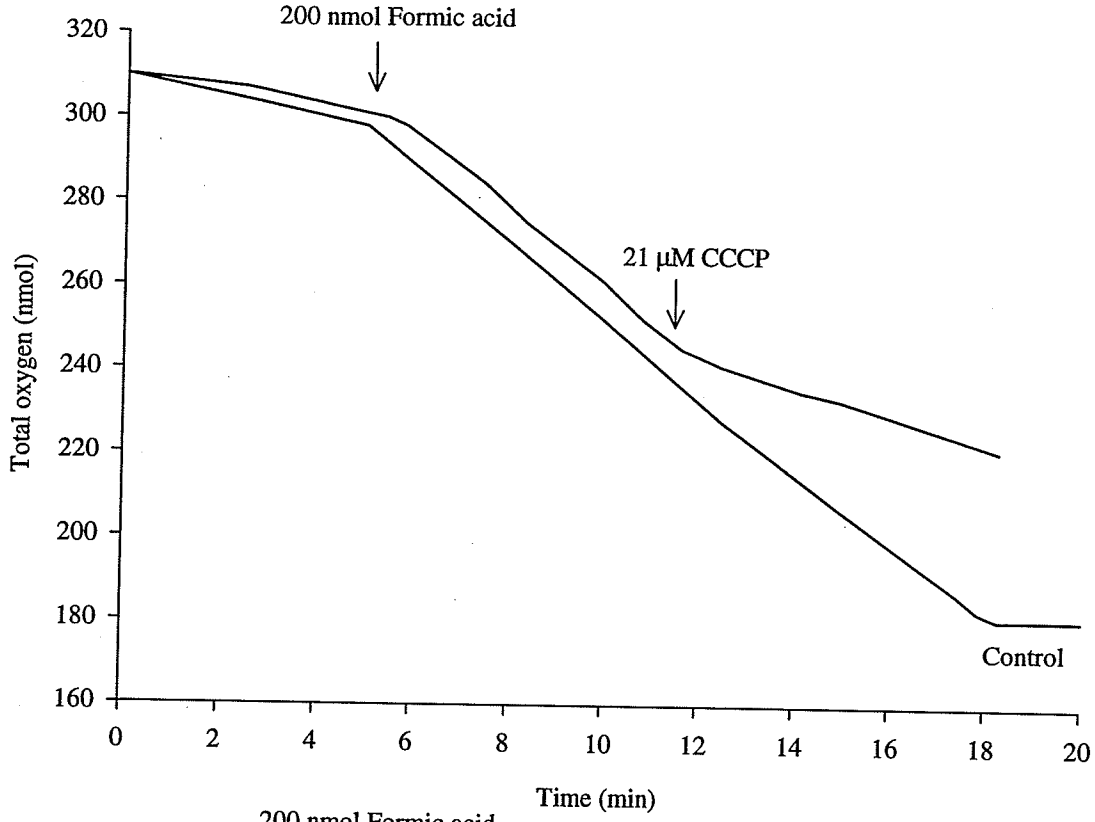
200 nmol Formic acid
21 µM CCCP
Control
Total oxygen (nmol)
320
300
280
260
240
220
200
180
160
0
2
4
6
8
10
12
14
16
18
20
Time (min)

**13 (b)**

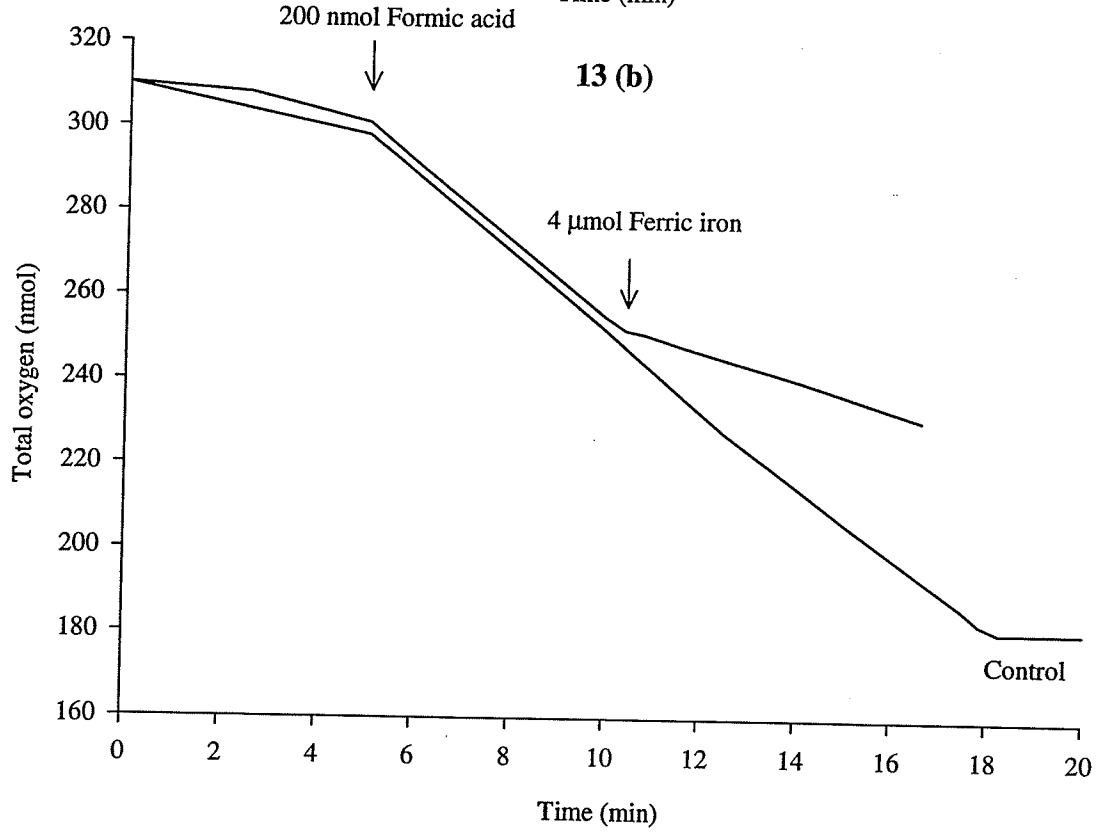
200 nmol Formic acid
4 µmol Ferric iron
Control
Total oxygen (nmol)
320
300
280
260
240
220
200
180
160
0
2
4
6
8
10
12
14
16
18
20
Time (min)

**Figure 14 (a)** The effect of malic acid on the rate of oxygen consumption by endogenous respiration. The reactions were performed at 25°C in 0.1 M β-alanine-$H_2SO_4$ pH 3 and contained 25 mg of cells and malic acid at the concentrations specified. The volume of the reaction mixtures was 1.2 mL .

**14 (a)**

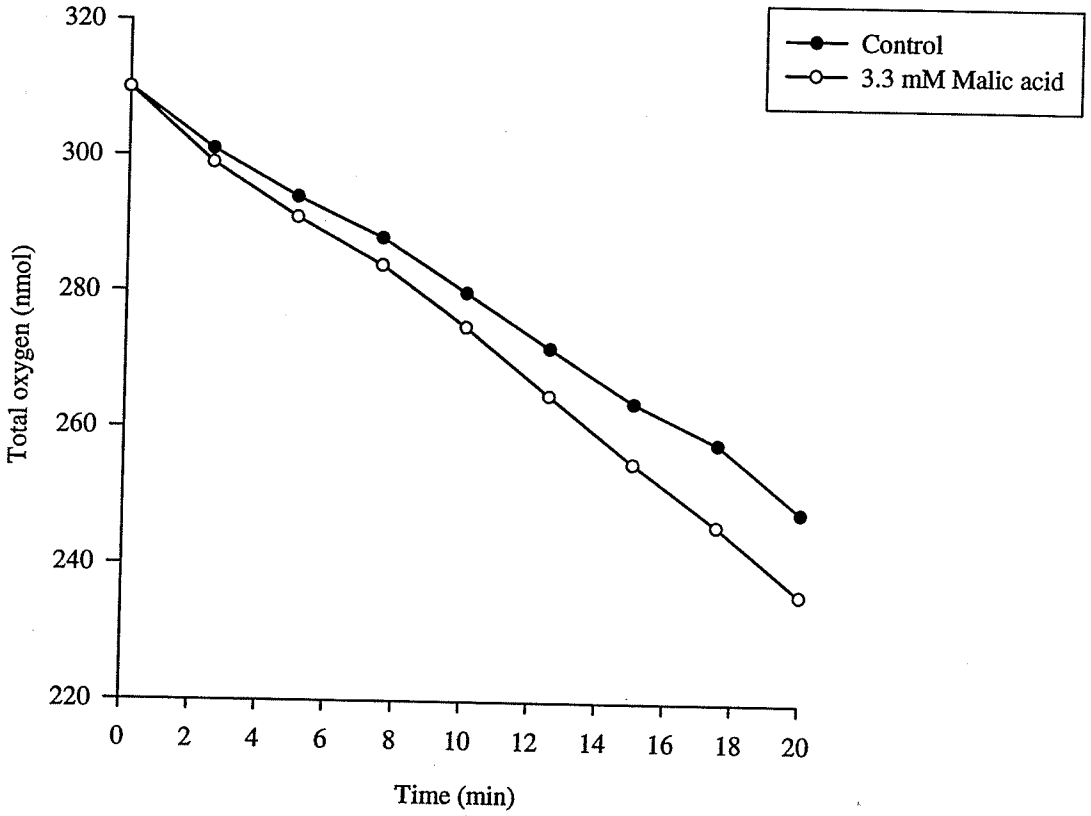
Control
3.3 mM Malic acid
Total oxygen (nmol)
320
300
280
260
240
220
0
2
4
6
8
10
12
14
16
18
20
Time (min)

**Figure 14 (b)** The effect of malic acid on the rate of sulfite oxidation. The reactions were performed at 25°C in 0.1 M β-alanine-$H_2SO_4$ pH 3 and contained 25 mg of cells and malic acid at the concentrations specified. $K_2SO_3$ (100 nmol) was added at the arrows after 5 min of preincubation between the cells and malic acid. The volume of the reaction mixtures was 1.2 mL .

**14 (b)**

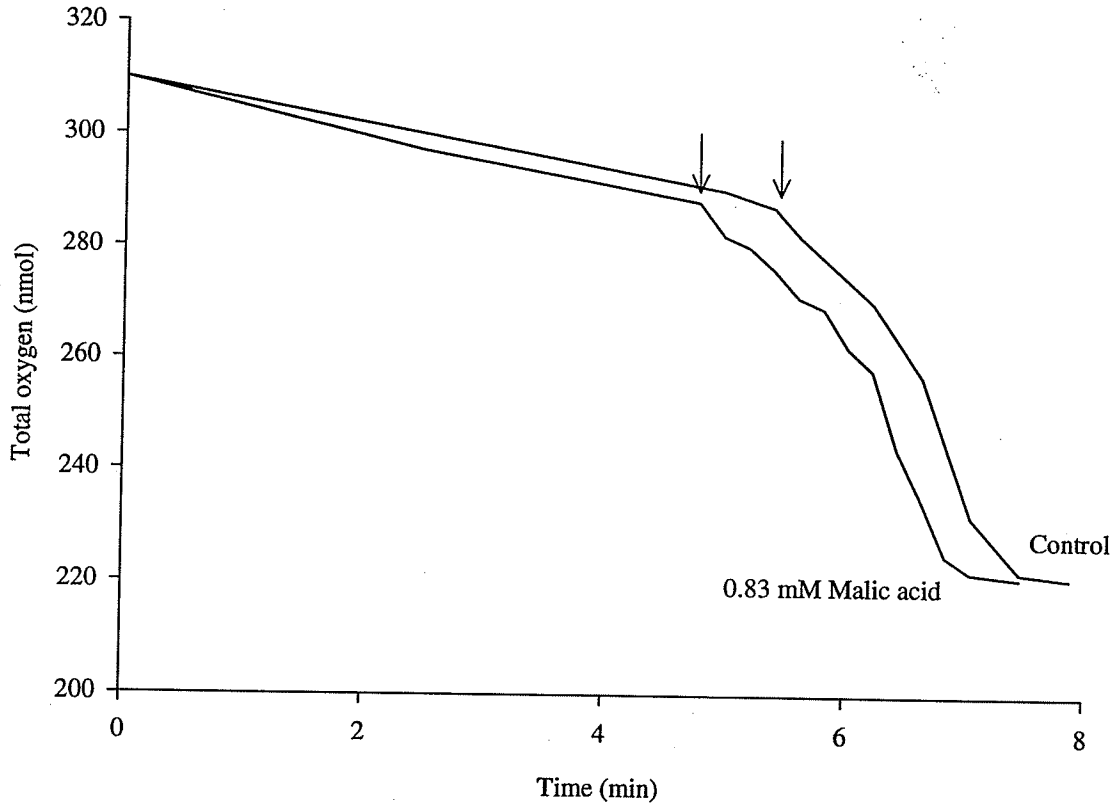
320
300
280
260
240
220
200
Total oxygen (nmol)
0
2
4
6
8
Time (min)
Control
0.83 mM Malic acid

**Figure 15 (a)** The effect of succinic acid on the rate of exogenous ferric iron reduction by endogenous respiration. The reactions were performed at 25°C in 0.1 M β-alanine-$H_2SO_4$ pH 3 and contained 20 mg of cells, 4 μmol $FeCl_3$, and succinic acid at the concentrations specified. The volume of the reaction mixtures was 1 mL . The results were based on 2 separate trials. The error bars are the standard deviation of the 2 trials.

**Figure 15 (b)** The effect of succinic acid on the rate of oxygen consumption by endogenous respiration. The reactions were performed at 25°C in 0.1 M β-alanine-$H_2SO_4$ pH 3 and contained 25 mg of cells and succinic acid at the concentrations specified. The volume of the reaction mixtures was 1.2 mL .

**15 (a)**

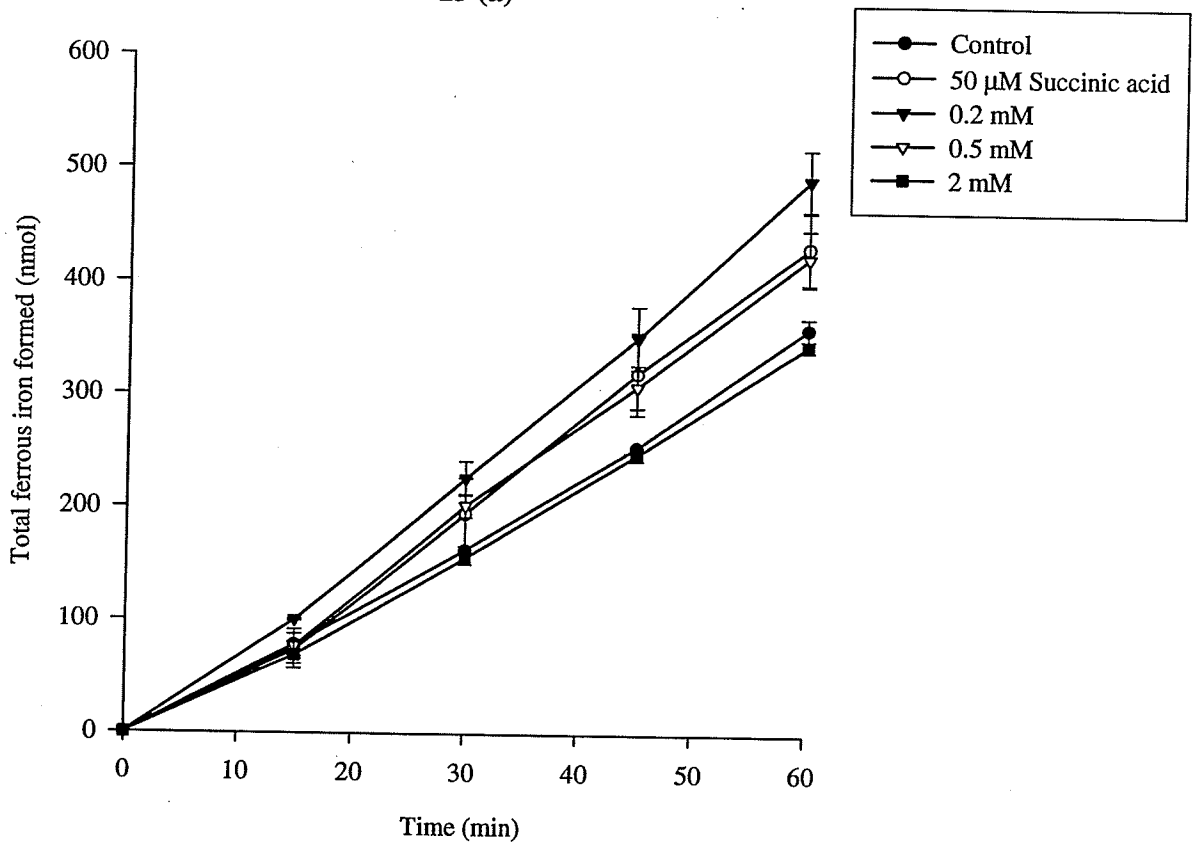
Control
50 µM Succinic acid
0.2 mM
0.5 mM
2 mM
Total ferrous iron formed (nmol)
600
500
400
300
200
100
0
0
10
20
30
40
50
60
Time (min)

**15 (b)**

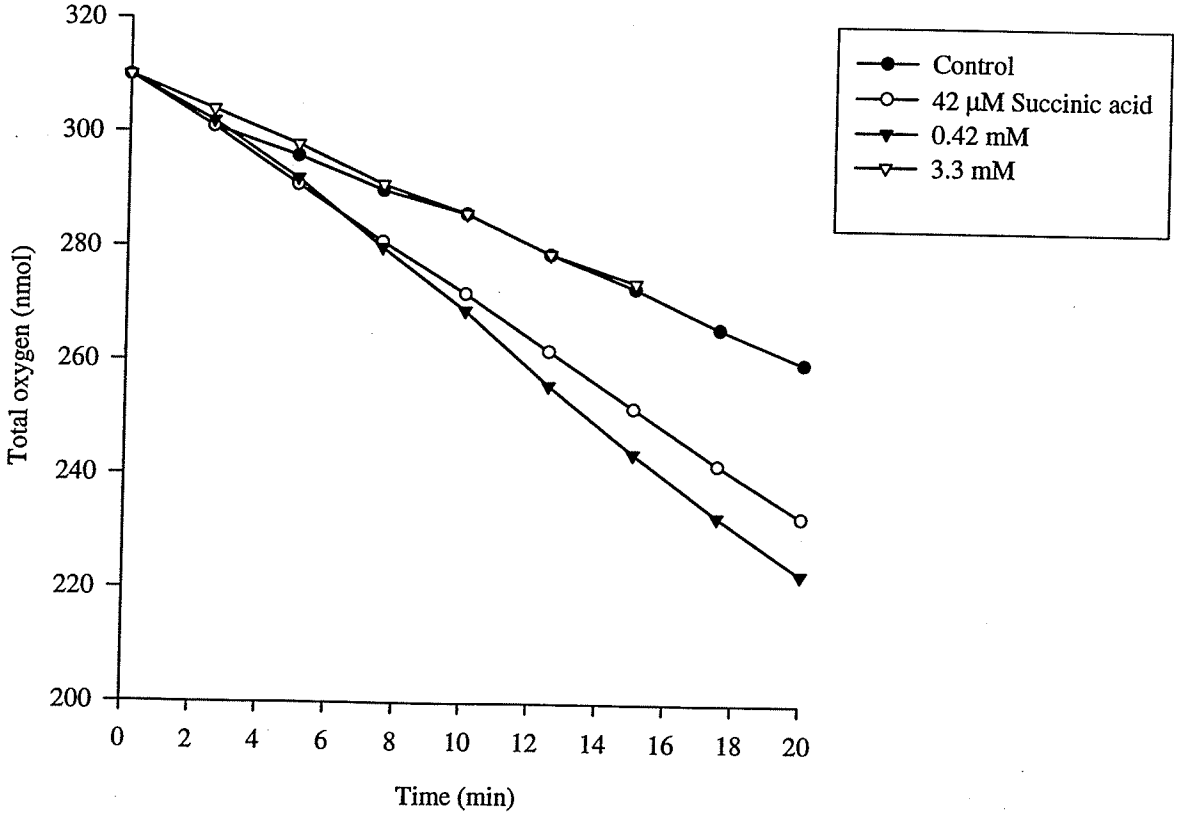
Control
42 µM Succinic acid
0.42 mM
3.3 mM
Total oxygen (nmol)
320
300
280
260
240
220
200
0
2
4
6
8
10
12
14
16
18
20
Time (min)

**Figure 15 (c)** The effect of succinic acid on the rate of sulfite oxidation. The reactions were performed at 25°C in 0.1 M β-alanine-$H_2SO_4$ pH 3 and contained 25 mg of cells and succinic acid at the concentrations specified. $K_2SO_3$ (100 nmol) was added at the arrows after 5 min of preincubation between the cells and succinic acid. The volume of the reaction mixtures was 1.2 mL .

**15 (c)**

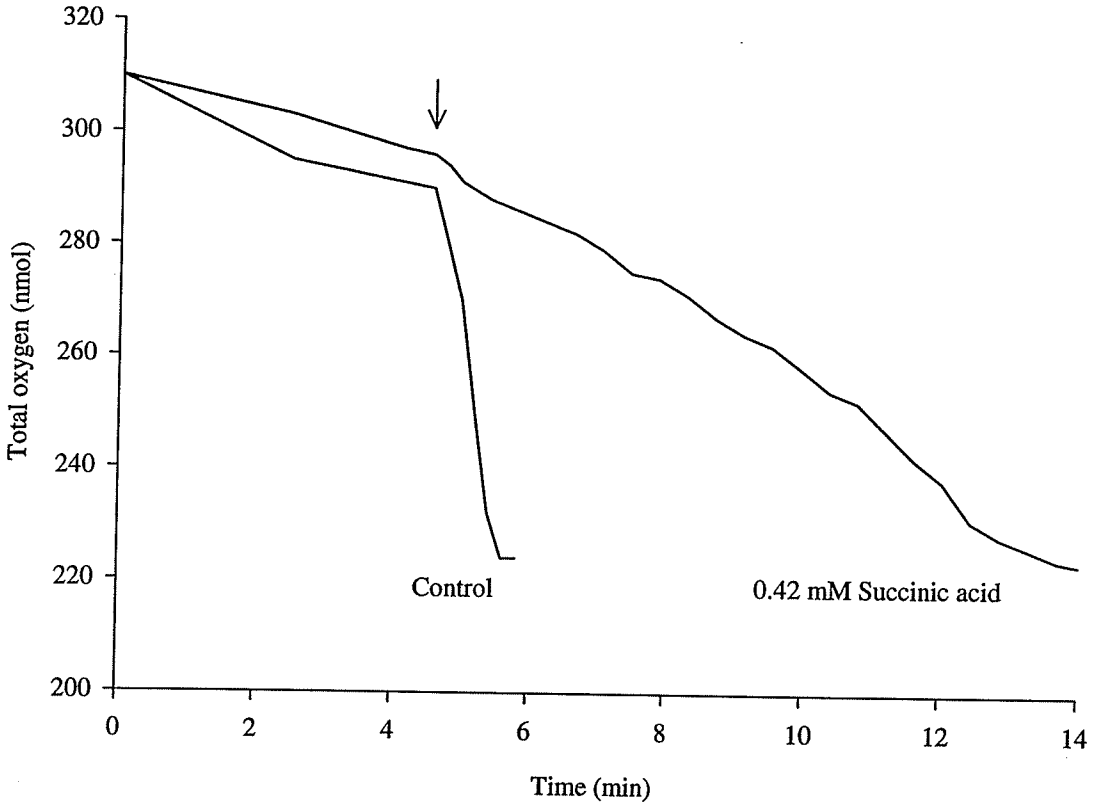
320
300
280
260
240
220
200
Total oxygen (nmol)
0
2
4
6
8
10
12
14
Time (min)
Control
0.42 mM Succinic acid

**Figure 16 (a)** The effect of fumaric acid on the rate of exogenous ferric iron reduction by endogenous respiration. The reactions were performed at 25°C in 0.1 M β-alanine-$H_2SO_4$ pH 3 and contained 20 mg of cells, 4 μmol $FeCl_3$, and fumaric acid at the concentrations specified. The volume of the reaction mixtures was 1 mL . The results were based on 2 separate trials. The error bars are the standard deviation of the 2 trials.

**Figure 16 (b)** The effect of fumaric acid on the rate of oxygen consumption by endogenous respiration. The reactions were performed at 25°C in 0.1 M β-alanine-$H_2SO_4$ pH 3 and contained 25 mg of cells and fumaric acid at the concentrations specified. The volume of the reaction mixtures was 1.2 mL .

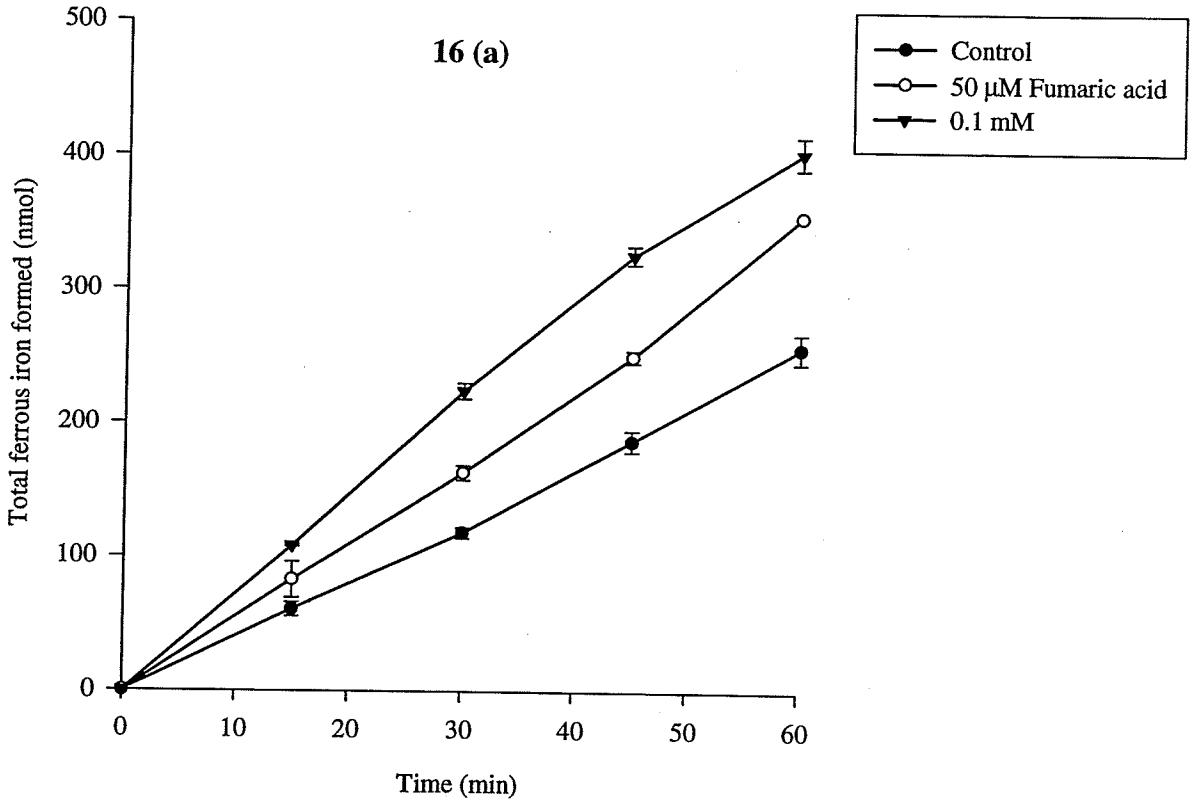
16 (a)
Control
50 µM Fumaric acid
0.1 mM
Total ferrous iron formed (nmol)
500
400
300
200
100
0
0
10
20
30
40
50
60
Time (min)

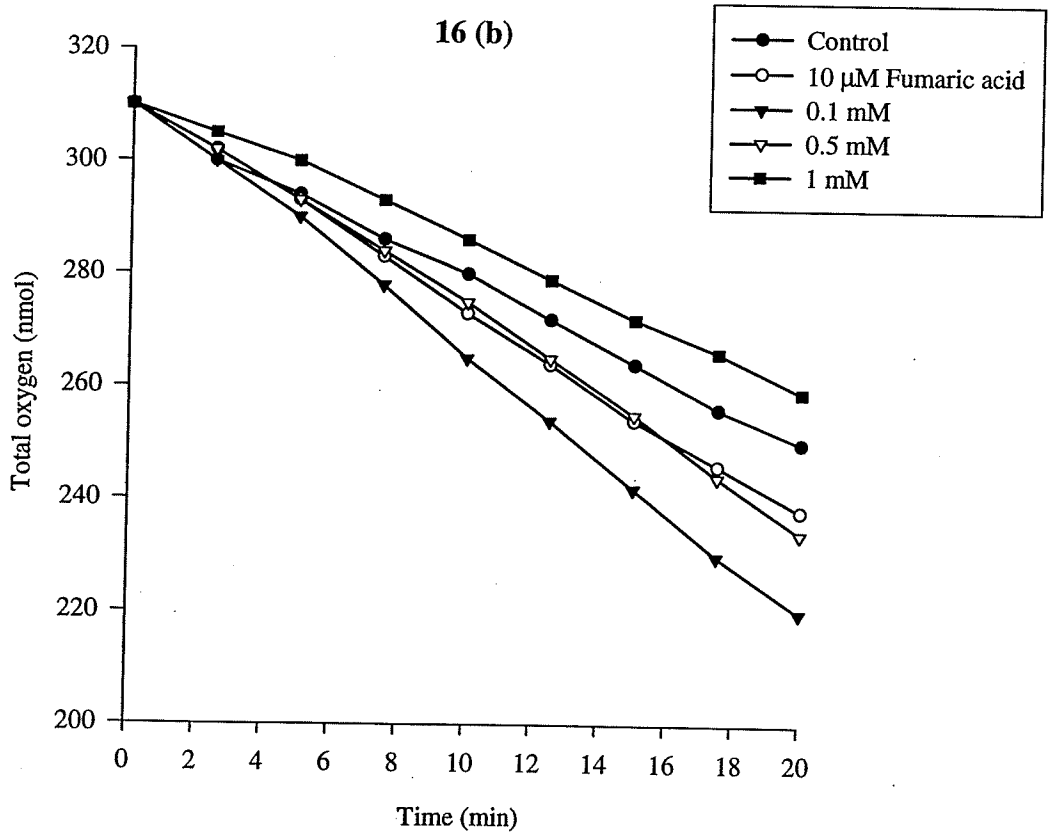
16 (b)
Control
10 µM Fumaric acid
0.1 mM
0.5 mM
1 mM
Total oxygen (nmol)
320
300
280
260
240
220
200
0
2
4
6
8
10
12
14
16
18
20
Time (min)

**Figure 16 (c)** The effect of fumaric acid on the rate of sulfite oxidation. The reactions were performed at 25°C in 0.1 M β-alanine-$H_2SO_4$ pH 3 and contained 25 mg of cells and fumaric acid at the concentrations specified. $K_2SO_3$ (100 nmol) was added at the arrows after 5 min of preincubation between the cells and fumaric acid. The volume of the reaction mixtures was 1.2 mL .

**16 (c)**

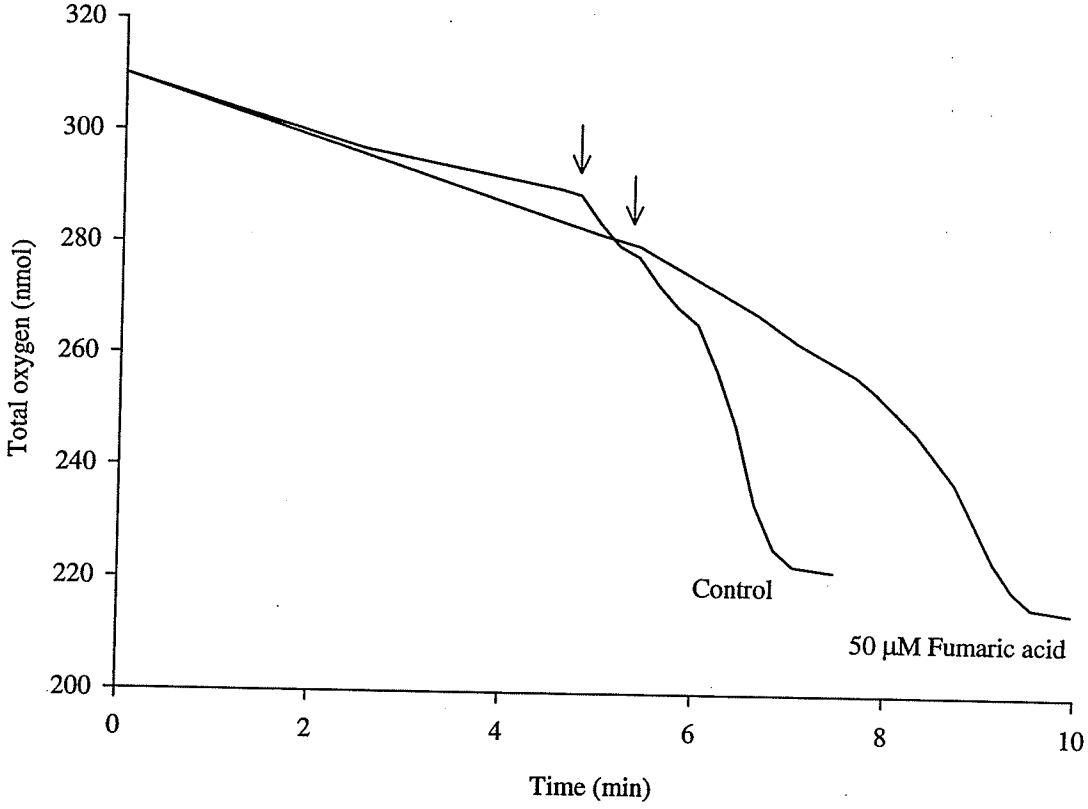
320
300
280
260
240
220
200
Total oxygen (nmol)
0
2
4
6
8
10
Time (min)
Control
50 µM Fumaric acid

**Figure 17** The effect of citric acid on the rate of exogenous ferric iron reduction by endogenous respiration. The reactions were performed at 25 in 0.1 M β-alanine-$H_2SO_4$ pH 3 and contained 20 mg of cells, 4 μmol $FeCl_3$, and citric acid at the concentrations specified. The volume of the reaction mixtures was 1 mL . The results were based on 2 separate trials. The error bars are the standard deviation of the 2 trials.

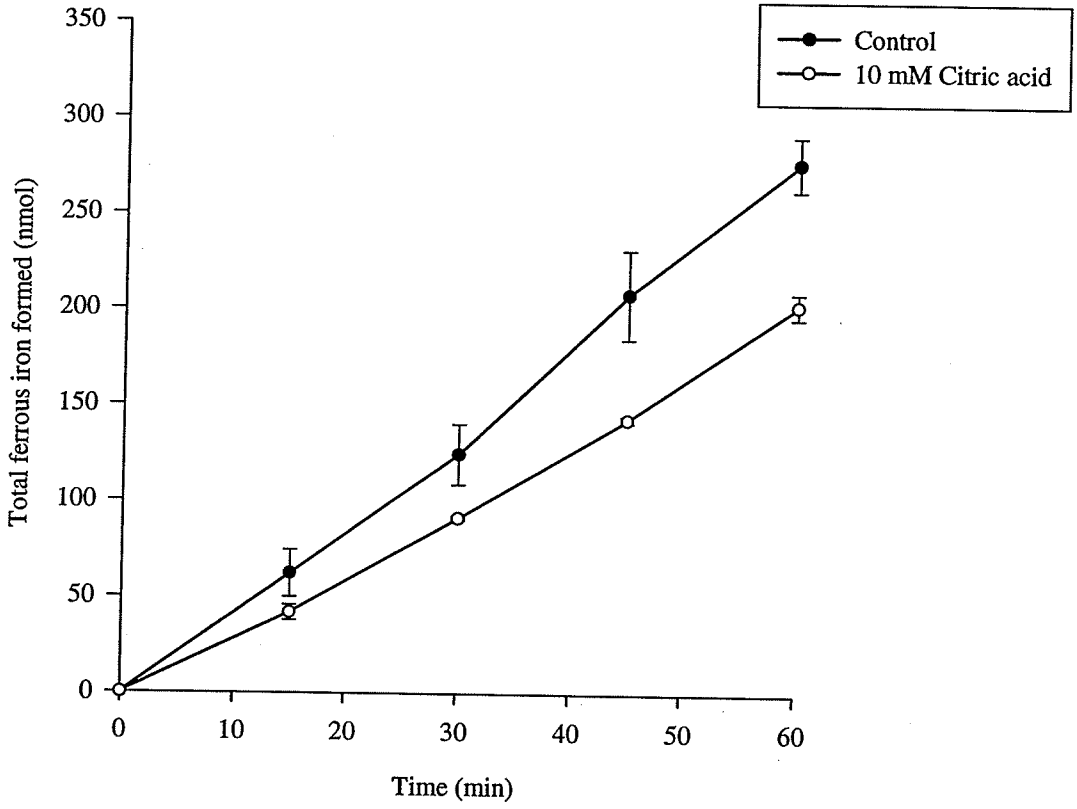
Control
10 mM Citric acid
Total ferrous iron formed (nmol)
350
300
250
200
150
100
50
0
0
10
20
30
40
50
60
Time (min)

**Figure 18 (a)** The effect of succinic acid on the rate of exogenous ferric iron reduction by endogenous respiration in the presence of uncouplers, 2,4-DNP and CCCP. The reactions were performed at 25°C in 0.1 M β-alanine-$H_2SO_4$ pH 3 and contained 20 mg of cells, 4 μmol $FeCl_3$, and succinic acid and uncouplers at the concentrations specified. The volume of the reaction mixtures was 1 mL . The results were based 2 separate trials. The error bars are the standard deviation of the 2 trials.

**Figure 18 (b)** The effect of succinic acid on the rate of oxygen consumption by endogenous respiration in the presence of uncouplers, **(i)** 2,4-DNP and **(ii)** CCCP. The reactions were performed at 25°C in 0.1 M β-alanine-$H_2SO_4$ pH 3 and contained 25 mg of cells and succinic acid and uncouplers at the concentrations specified. The volume of the reaction mixtures was 1.2 mL .

**18 (a)**

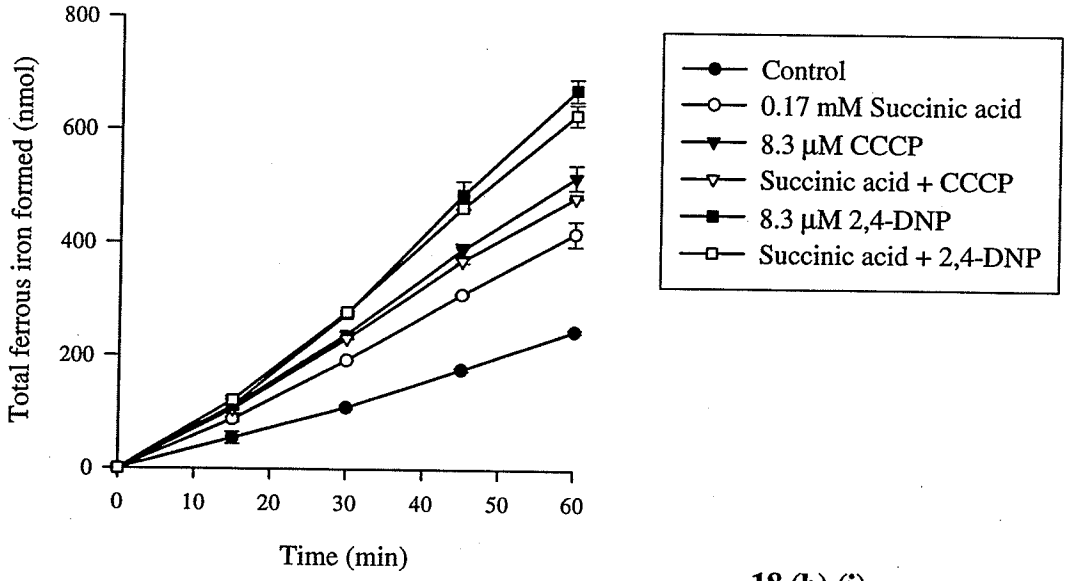


**18 (b) (i)**

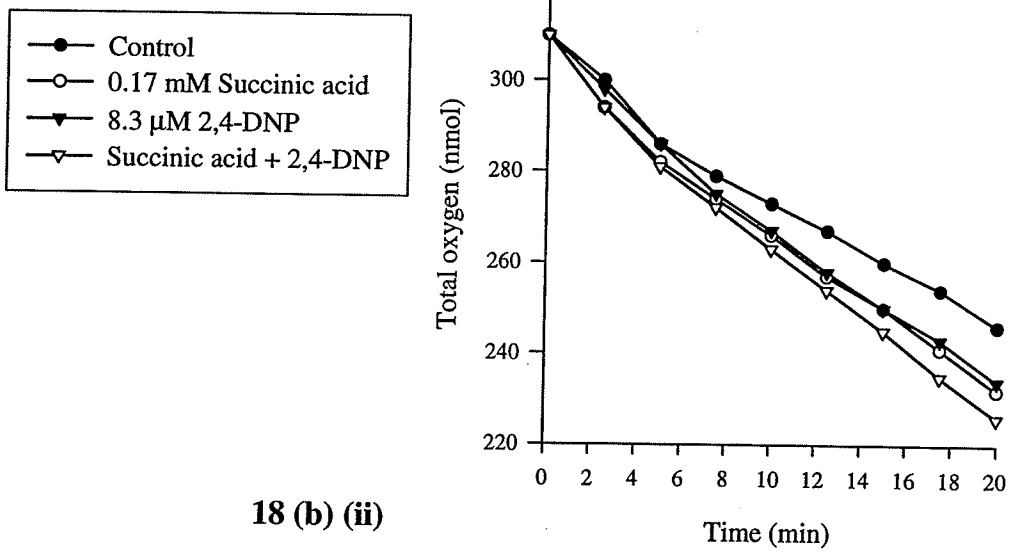


**18 (b) (ii)**

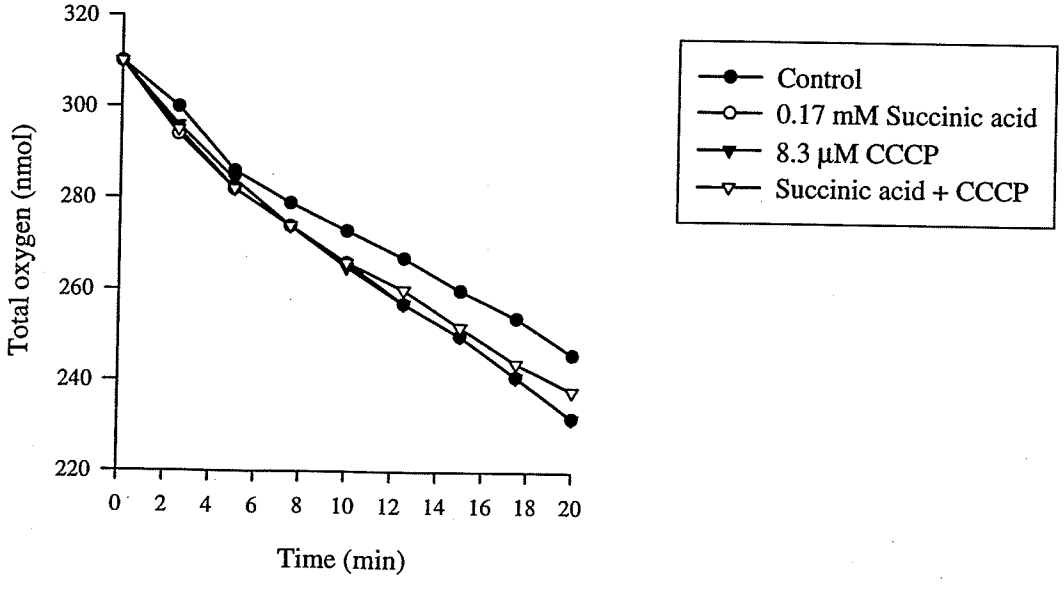

**Figure 19 (a)** The effect of fumaric acid on the rate of exogenous ferric iron reduction by endogenous respiration in the presence of uncouplers, 2,4-DNP and CCCP. The reactions were performed at 25°C in 0.1 M β-alanine-$H_2SO_4$ pH 3 and contained 20 mg of cells, 4 μmol $FeCl_3$, and fumaric acid and uncouplers at the concentrations specified. The volume of the reaction mixtures was1 mL . The results were based on 2 separate trials. The error bars are the standard deviation of the 2 trials.

**Figure 19 (b)** The effect of fumaric acid on the rate of oxygen consumption by endogenous respiration in the presence of uncouplers, **(i)** 2,4-DNP and **(ii)** CCCP. The reactions were performed at 25°C in 0.1 M β-alanine-$H_2SO_4$ pH 3 and contained 25 mg of cells and fumaric acid and uncouplers at the concentrations specified. The volume of the reaction mixtures was1.2 mL .

**19 (a)**

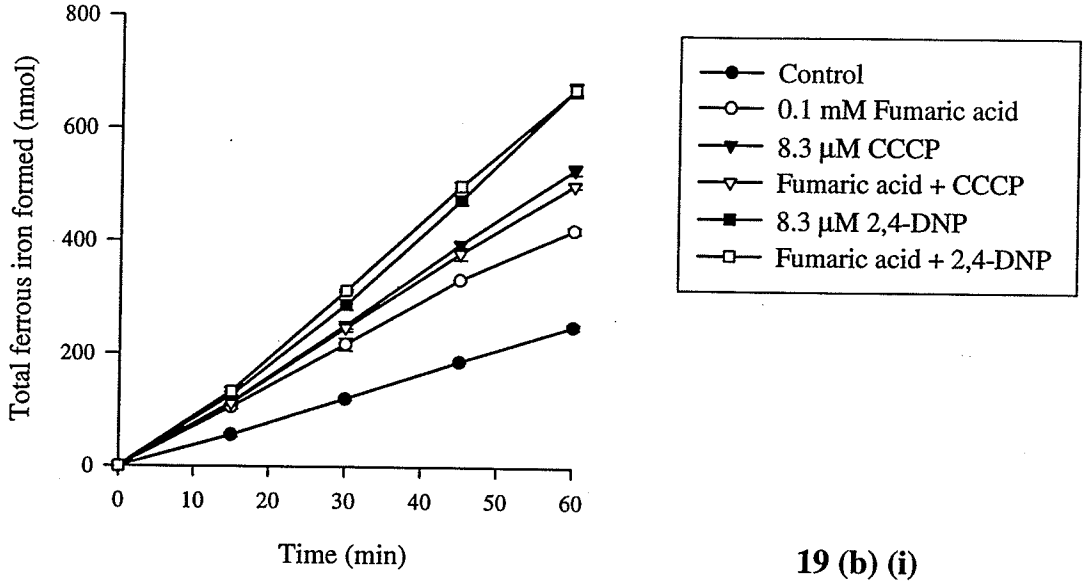


**19 (b) (i)**

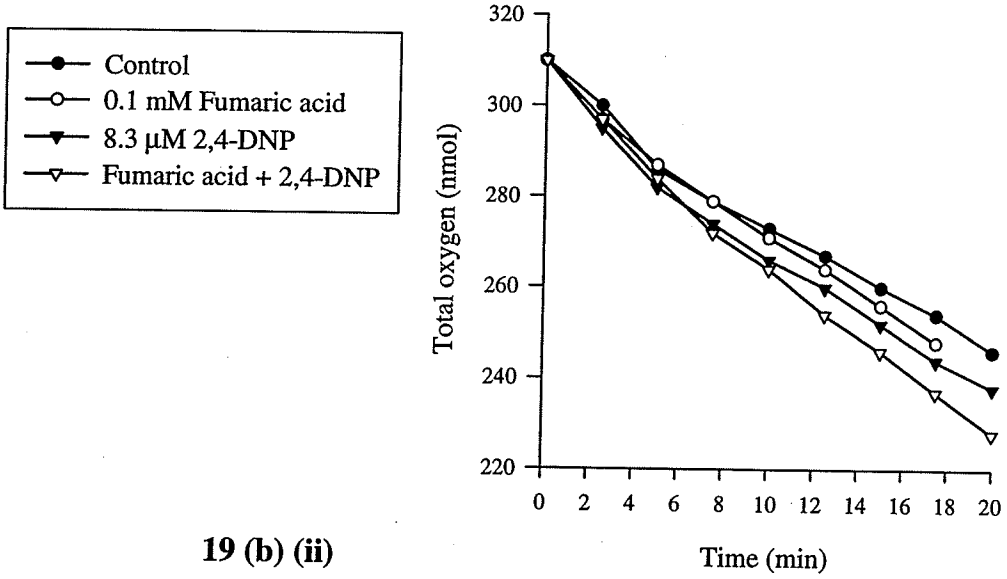


**19 (b) (ii)**

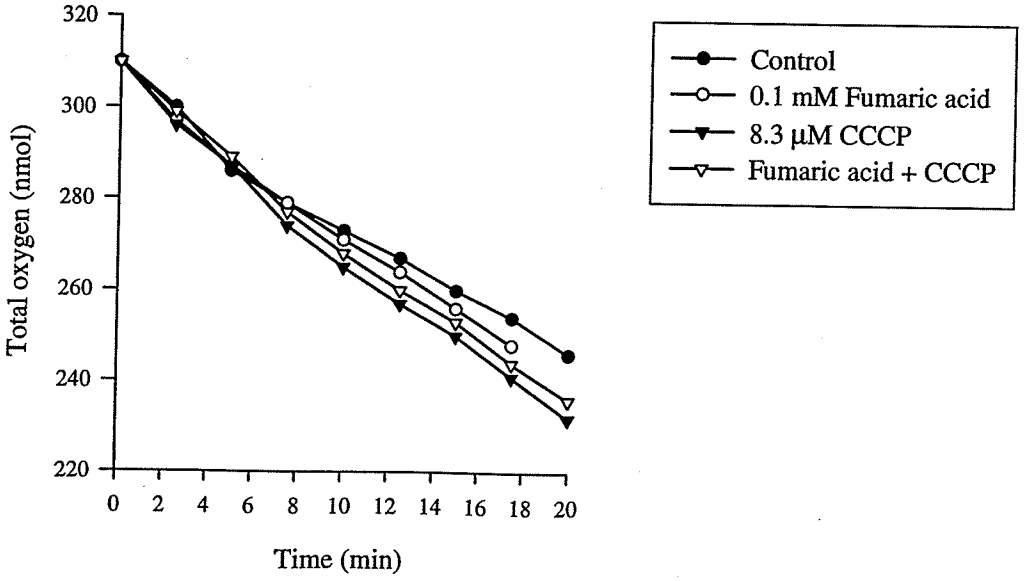

**Figure 20 (a)** The effect of potassium cyanide (KCN) on the rate of oxygen consumption by endogenous respiration. The reactions were performed at 25°C in 0.1 M β-alanine-$H_2SO_4$ pH 3 and contained 25 mg of cells and KCN at the concentrations specified. The volume of the reaction mixtures was1.2 mL .

**20 (a)**

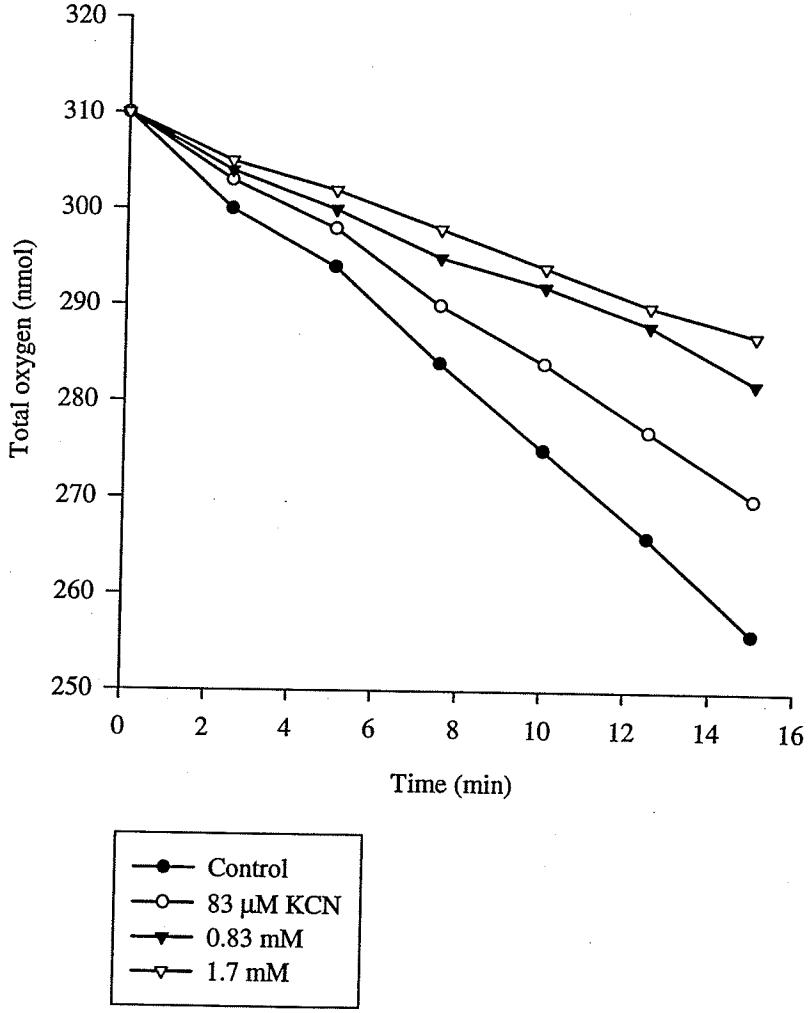
320
310
300
290
280
270
260
250
Total oxygen (nmol)
0
2
4
6
8
10
12
14
16
Time (min)
Control
83 µM KCN
0.83 mM
1.7 mM

**Figure 20 (b)** The effect of KCN on the rate of sulfite oxidation. The reactions were performed at 25°C in 0.1 M β-alanine-$H_2SO_4$ pH 3 and contained 25 mg of cells and KCN at the concentrations specified. $K_2SO_3$ (100 nmol) was added at the arrows after 5 min of preincubation between cells and KCN. The volume of the reaction mixtures was1.2 mL .

**20 (b)**

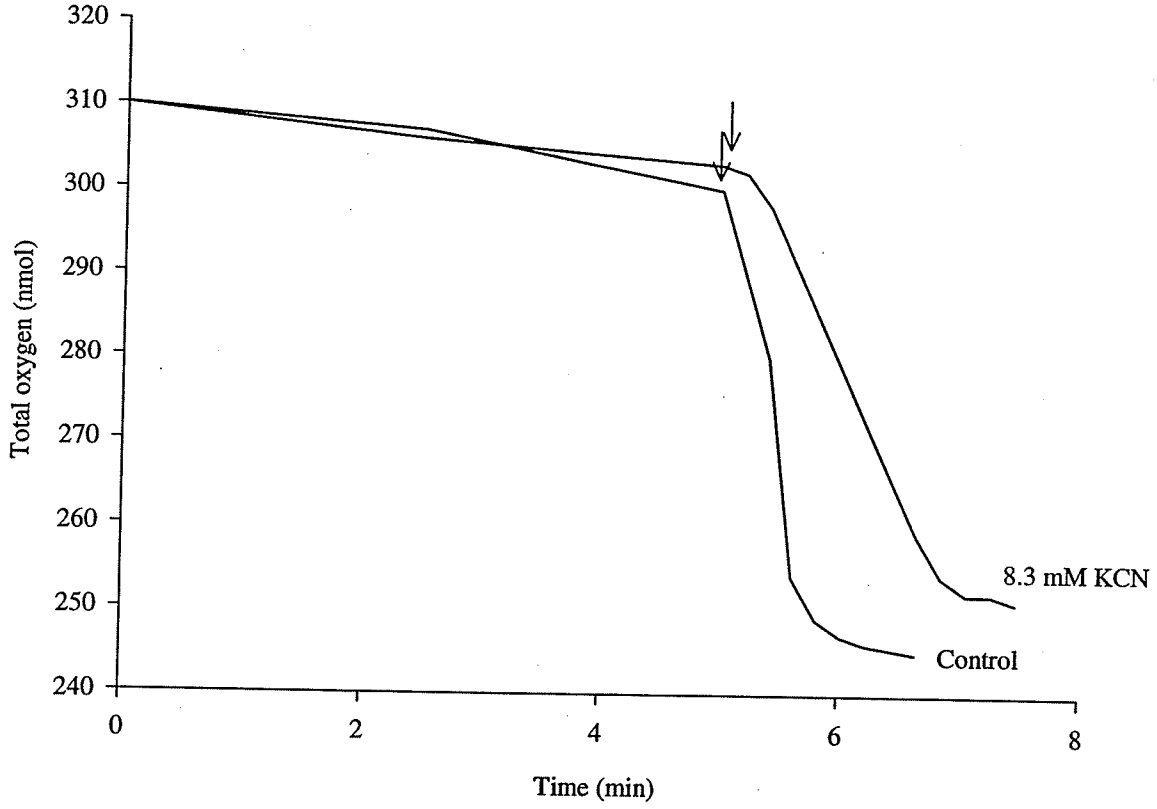
320
310
300
290
280
270
260
250
240
Total oxygen (nmol)
0
2
4
6
8
Time (min)
8.3 mM KCN
Control

**Figure 21 (a)** The effect of sodium azide ($NaN_3$) on the rate of exogenous ferric iron reduction by endogenous respiration. The reactions were performed at 25°C in 0.1 M β-alanine-$H_2SO_4$ pH 3 and contained 20 mg of cells, 4 μmol $FeCl_3$, and $NaN_3$ at the concentrations specified. The volume of the reaction mixtures was1 mL . The results were based on 2 separate trials. The error bars are the standard deviation of the 2 trials.

**Figure 21 (b)** The effect of $NaN_3$ on the rate of oxygen consumption by endogenous respiration. The reactions were performed at 25°C in 0.1 M β-alanine-$H_2SO_4$ pH 3 and contained 25 mg of cells and $NaN_3$ at the concentrations specified. The volume of the reaction mixtures was1.2 mL .

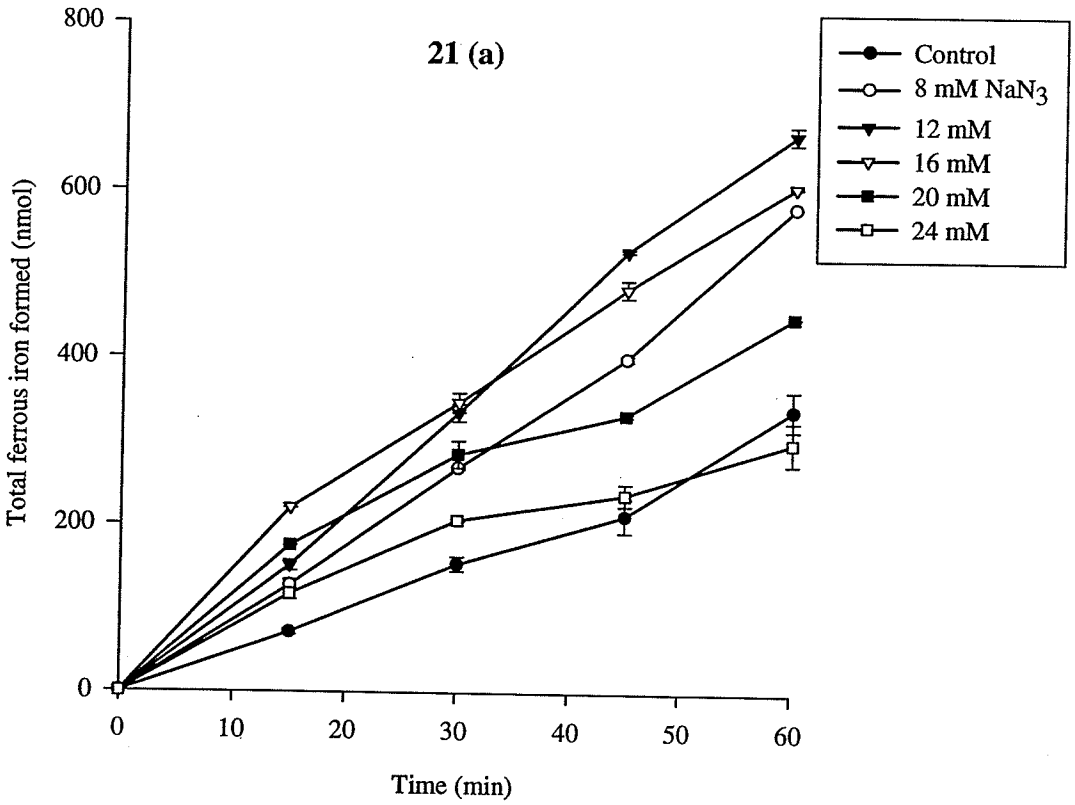
21 (a)
Control
8 mM NaN3
12 mM
16 mM
20 mM
24 mM
Total ferrous iron formed (nmol)
800
600
400
200
0
0
10
20
30
40
50
60
Time (min)

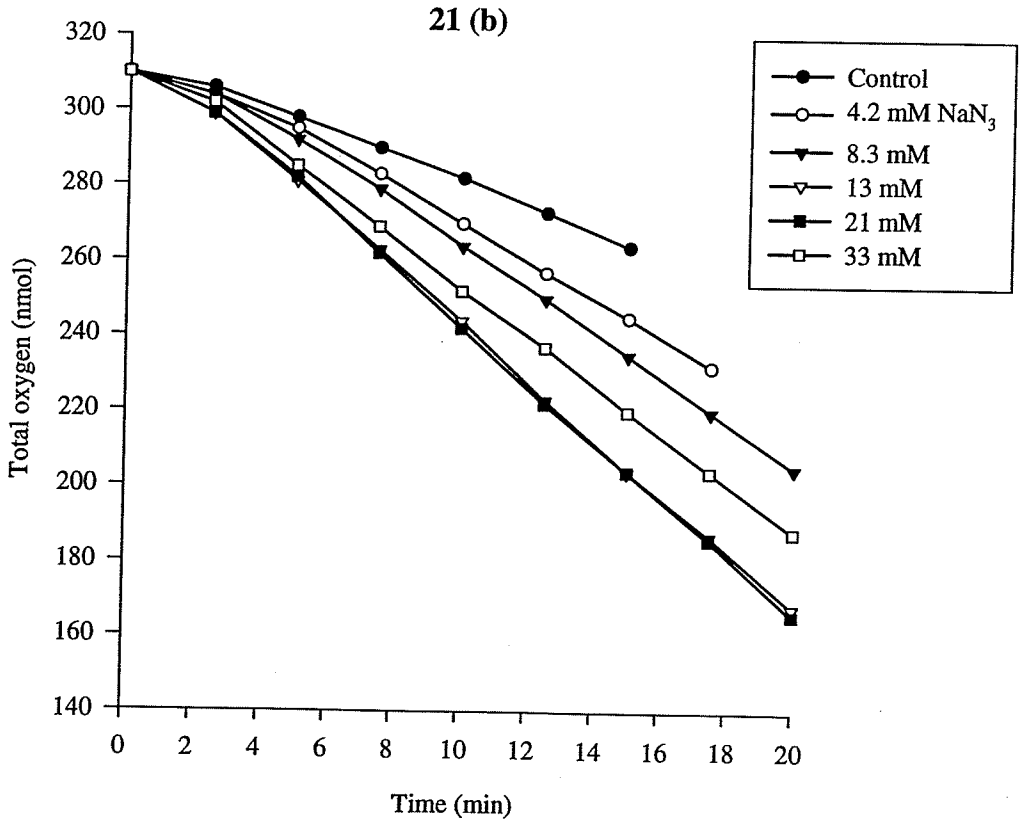
21 (b)
Control
4.2 mM NaN3
8.3 mM
13 mM
21 mM
33 mM
Total oxygen (nmol)
320
300
280
260
240
220
200
180
160
140
0
2
4
6
8
10
12
14
16
18
20
Time (min)

**Figure 21 (c)** The effect of $NaN_3$ on the rate of sulfite oxidation. The reactions were performed at 25°C in 0.1 M β-alanine-$H_2SO_4$ pH 3 and contained 25 mg of cells and $NaN_3$ at the concentrations specified. $K_2SO_3$ (100 nmol) was added at the arrows after 5 min of preincubation between the cells and $NaN_3$. The volume of the reaction mixtures was1.2 mL .

**21 (c)**

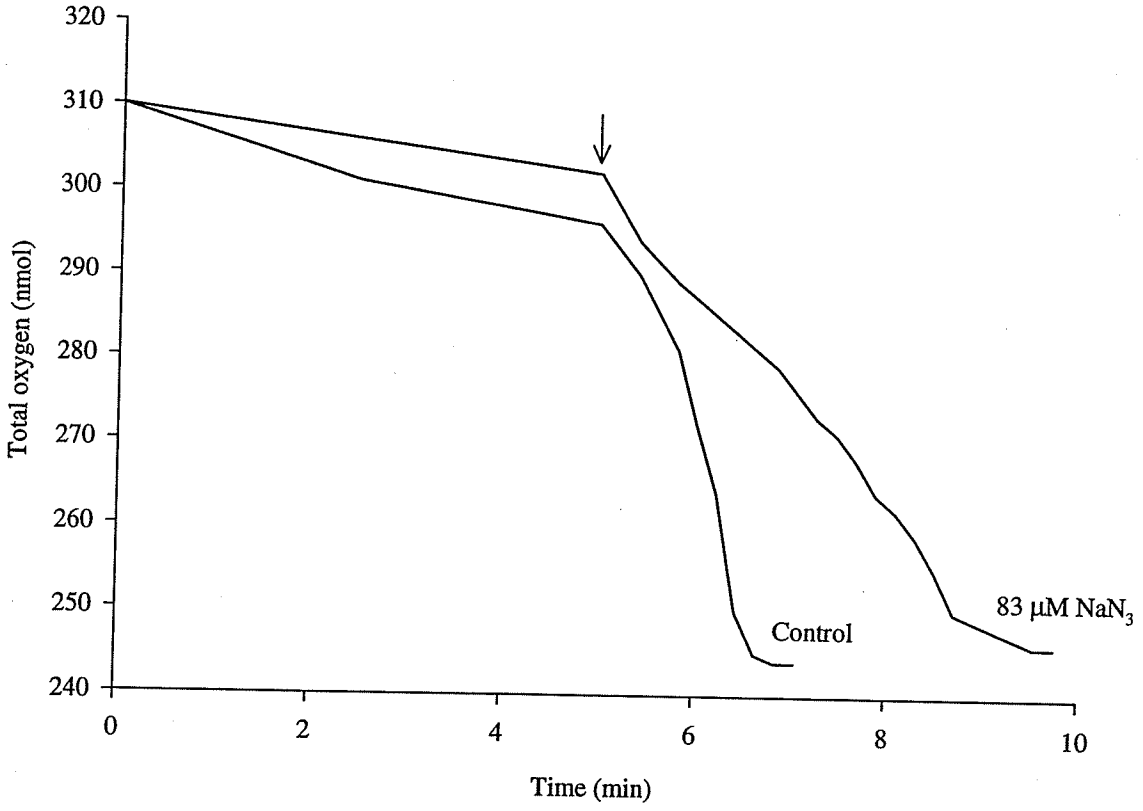
320
310
300
290
280
270
260
250
240
Total oxygen (nmol)
0
2
4
6
8
10
Time (min)
Control
83 µM $NaN_3$

**Figure 22 (a)** The effect of rotenone on the rate of exogenous ferric iron reduction by endogenous respiration. The reactions were performed at 25°C in 0.1 M β-alanine-$H_2SO_4$ pH 3 and contained 20 mg of cells, 4 μmol $FeCl_3$, and rotenone at the concentrations specified. The volume of the reaction mixtures was1 mL . The results were based on 2 separate trials. The error bars are the standard deviation of the 2 trials.

**Figure 22 (b)** The effect of rotenone on the rate of oxygen consumption by endogenous respiration. The reactions were performed at 25°C in 0.1 M β-alanine-$H_2SO_4$ pH 3 and contained 25 mg of cells and rotenone at the concentrations specified. The volume of the reaction mixtures was1.2 mL .

**22 (a)**

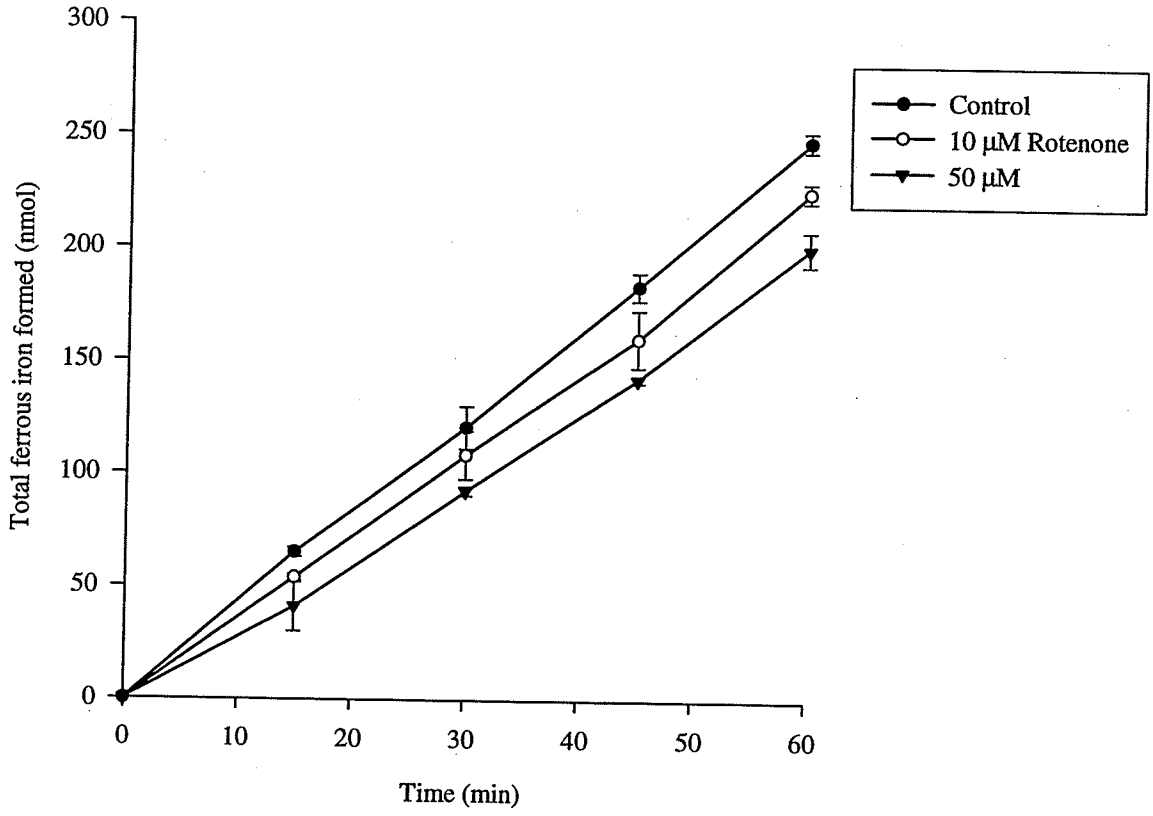
Total ferrous iron formed (nmol)
300
250
200
150
100
50
0
0
10
20
30
40
50
60
Time (min)
Control
10 µM Rotenone
50 µM

**22 (b)**

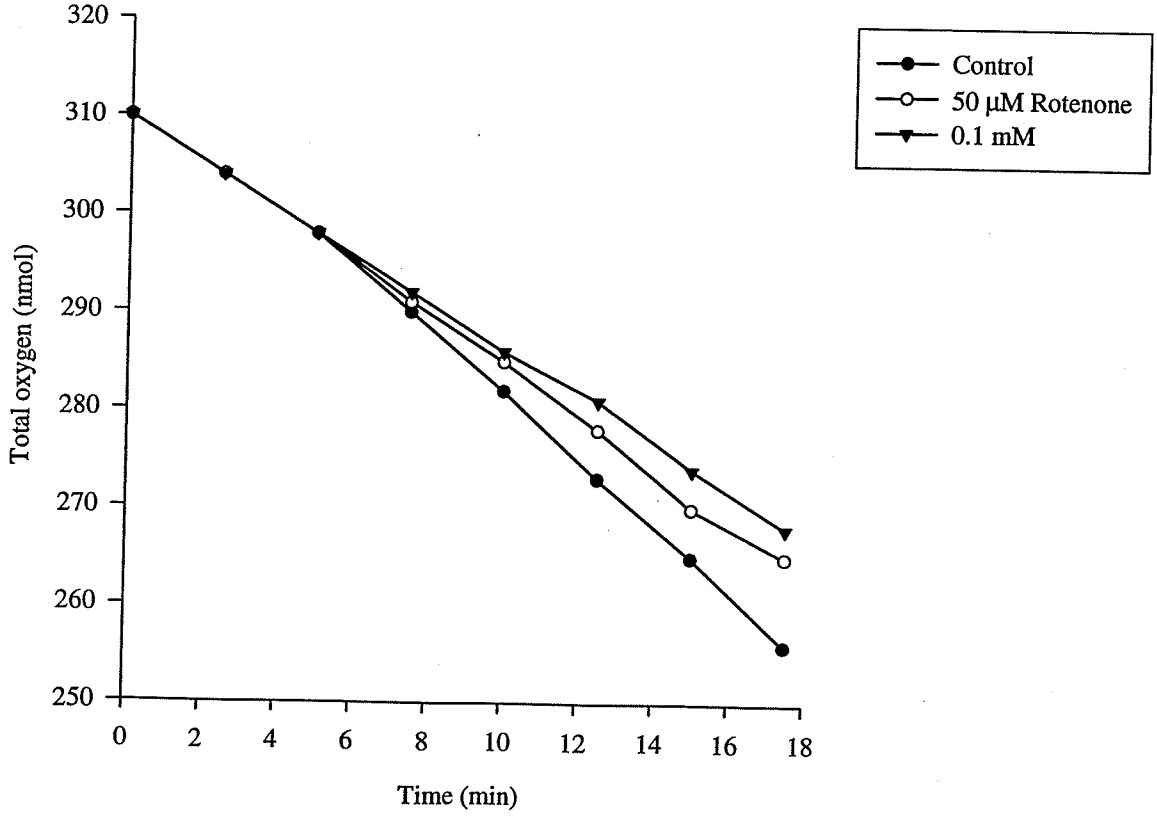
Total oxygen (nmol)
320
310
300
290
280
270
260
250
0
2
4
6
8
10
12
14
16
18
Time (min)
Control
50 µM Rotenone
0.1 mM

**Figure 22 (c)** The effect of rotenone on the rate of sulfite oxidation. The reactions were performed at 25°C in 0.1 M β-alanine-$H_2SO_4$ pH 3 and contained 25 mg of cells and rotenone at the concentrations specified. $K_2SO_3$ (100 nmol) was added at the arrows after 5 min of preincubation between the cells and rotenone. The volume of the reaction mixtures was 1.2 mL .

**22 (c)**

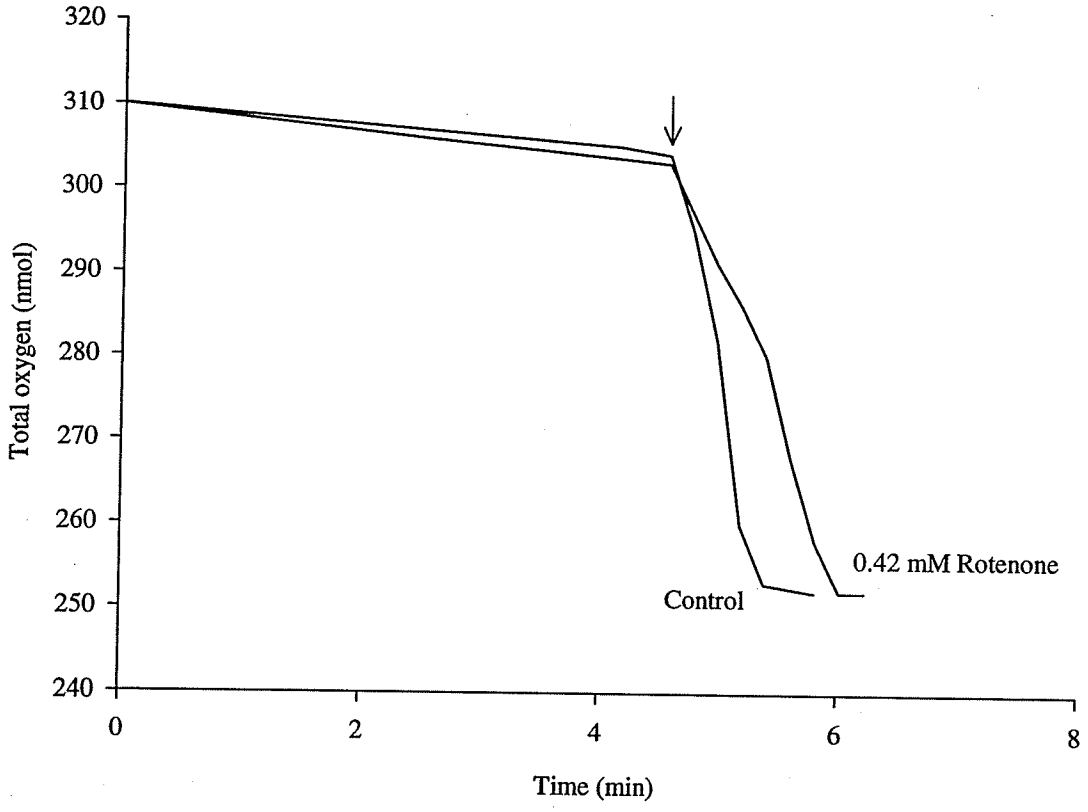
320
310
300
290
280
270
260
250
240
Total oxygen (nmol)
0
2
4
6
8
Time (min)
0.42 mM Rotenone
Control

**Figure 23 (a)** The effect of amytal on the rate of exogenous ferric iron reduction by endogenous respiration. The reactions were performed at 25°C in 0.1 M β-alanine-$H_2SO_4$ pH 3 and contained 20 mg of cells, 4 μmol $FeCl_3$, and amytal at the concentrations specified. The volume of the reaction mixtures was1 mL . The results were based on 2 separate trials. The error bars are the standard deviation of the 2 trials.

**Figure 23 (b)** The effect of amytal on the rate of oxygen consumption by endogenous respiration. The reactions were performed at 25°C in 0.1 M β-alanine-$H_2SO_4$ pH 3 and contained 25 mg of cells and amytal at the concentrations specified. The volume of the reaction mixtures was1.2 mL .

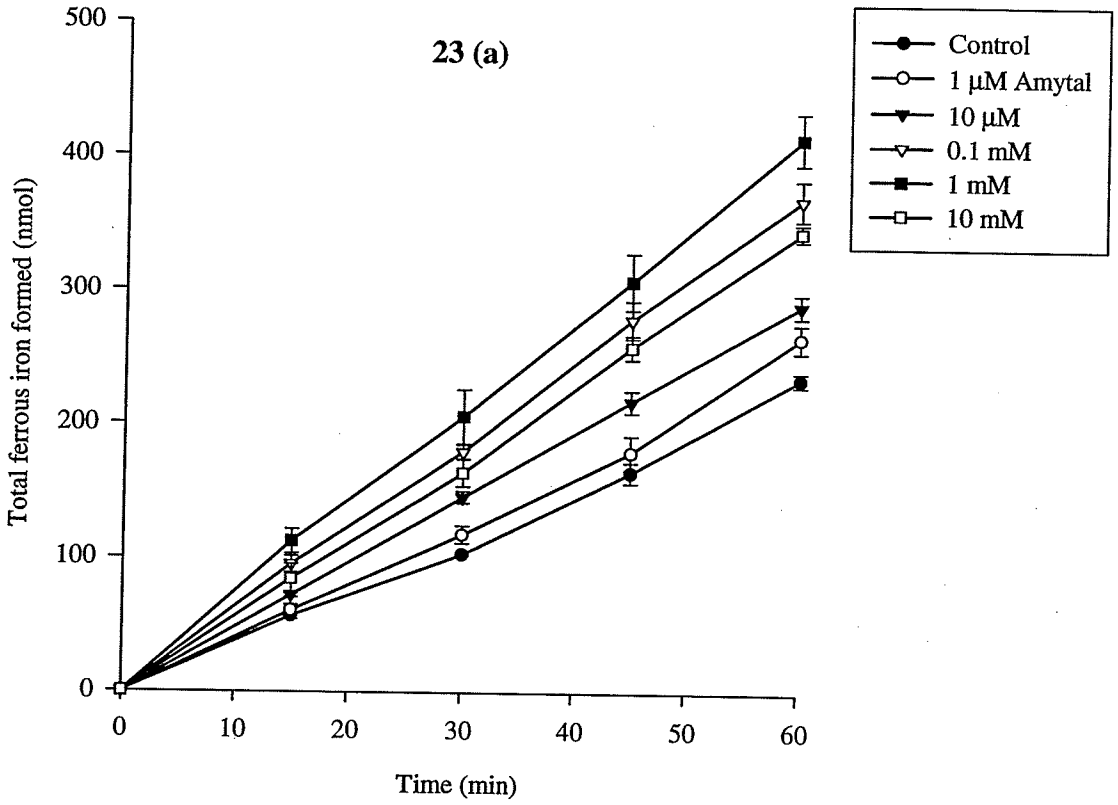
23 (a)
Control
1 µM Amytal
10 µM
0.1 mM
1 mM
10 mM
Total ferrous iron formed (nmol)
500
400
300
200
100
0
0
10
20
30
40
50
60
Time (min)

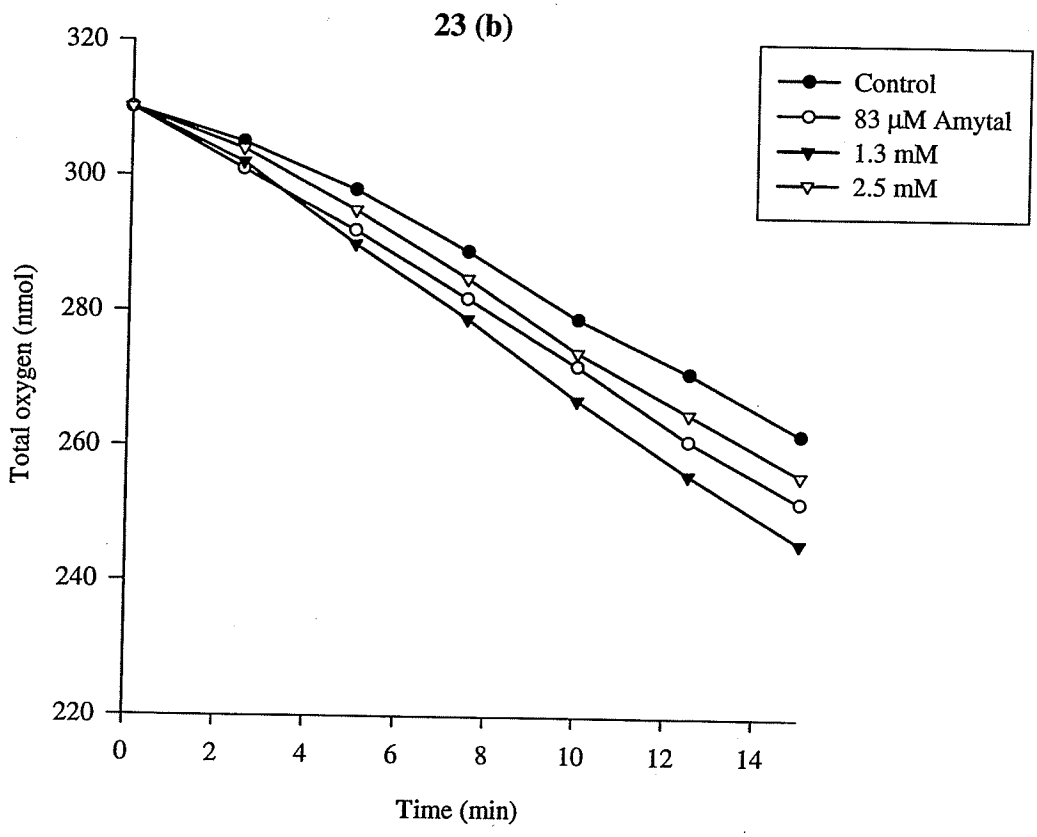
23 (b)
Control
83 µM Amytal
1.3 mM
2.5 mM
Total oxygen (nmol)
320
300
280
260
240
220
0
2
4
6
8
10
12
14
Time (min)

**Figure 24 (a)** The effect of 2-heptyl-4-hydroxyquinoline-*N*-oxide (HQNO) on the rate of exogenous ferric iron reduction by endogenous respiration. The reactions were performed at 25°C in 0.1 M β-alanine-$H_2SO_4$ pH 3 and contained 20 mg of cells, 4 μmol $FeCl_3$, and HQNO at the concentrations specified. The volume of the reaction mixtures was 1 mL. Results were based on two separate trials. The error bars are the standard deviation of the 2 trials.

**Figure 24 (b)** The effect of HQNO on the rate of oxygen consumption by endogenous respiration. The reactions were performed at 25°C in 0.1 M β-alanine-$H_2SO_4$ pH 3 and contained 25 mg of cells and HQNO at the concentrations specified. The volume of the reaction mixtures was 1.2 mL.

**24 (a)**

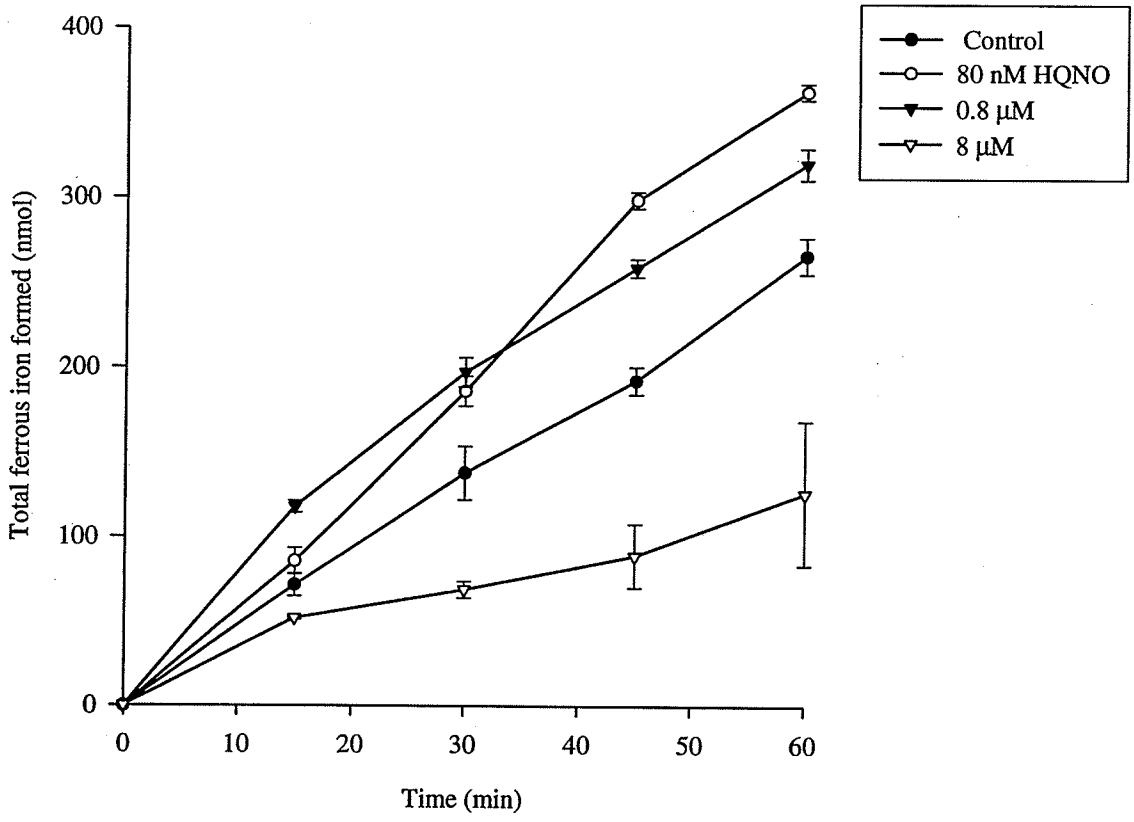
Control
80 nM HQNO
0.8 µM
8 µM
Total ferrous iron formed (nmol)
400
300
200
100
0
0
10
20
30
40
50
60
Time (min)

**24 (b)**

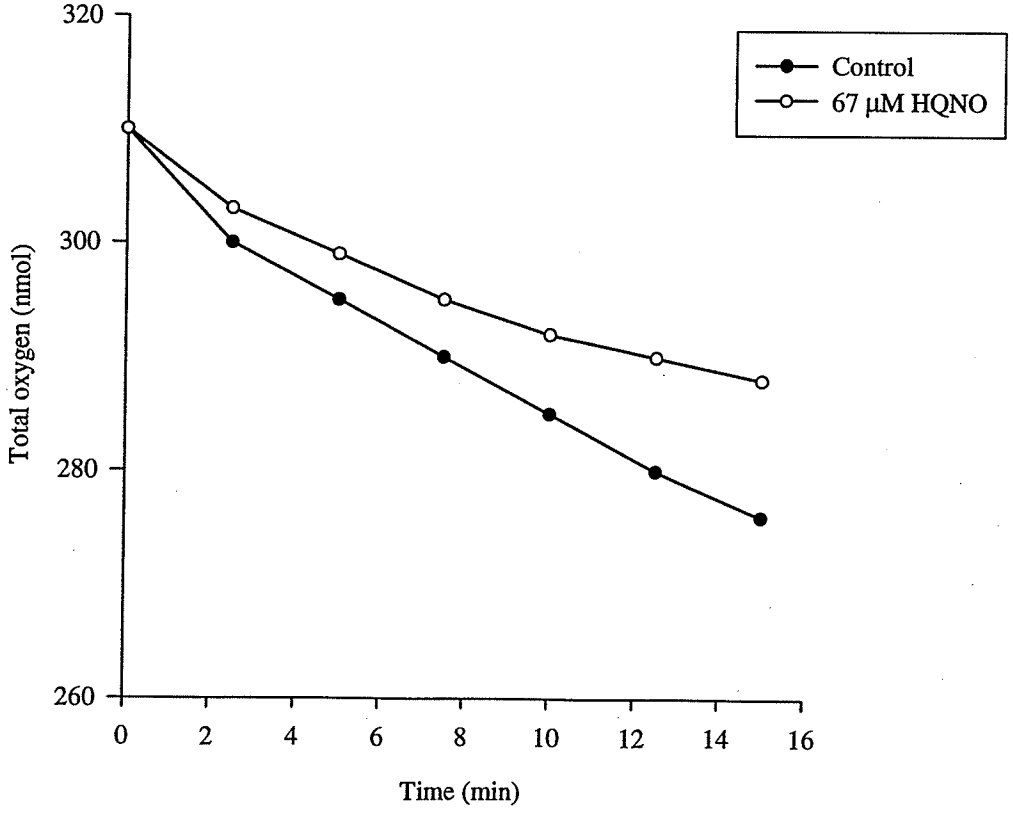
Control
67 µM HQNO
Total oxygen (nmol)
320
300
280
260
0
2
4
6
8
10
12
14
16
Time (min)

**Figure 24 (c)** The effect of HQNO on the rate of sulfite oxidation. The reactions were performed at 25°C in 0.1 M β-alanine-$H_2SO_4$ pH 3 and contained 25 mg of cells and HQNO at the concentrations specified. $K_2SO_3$ (100 nmol) was added at the arrows after 5 min of preincubation between the cells and HQNO. The volume of the reaction mixtures was 1.2 mL .

**24 (c)**

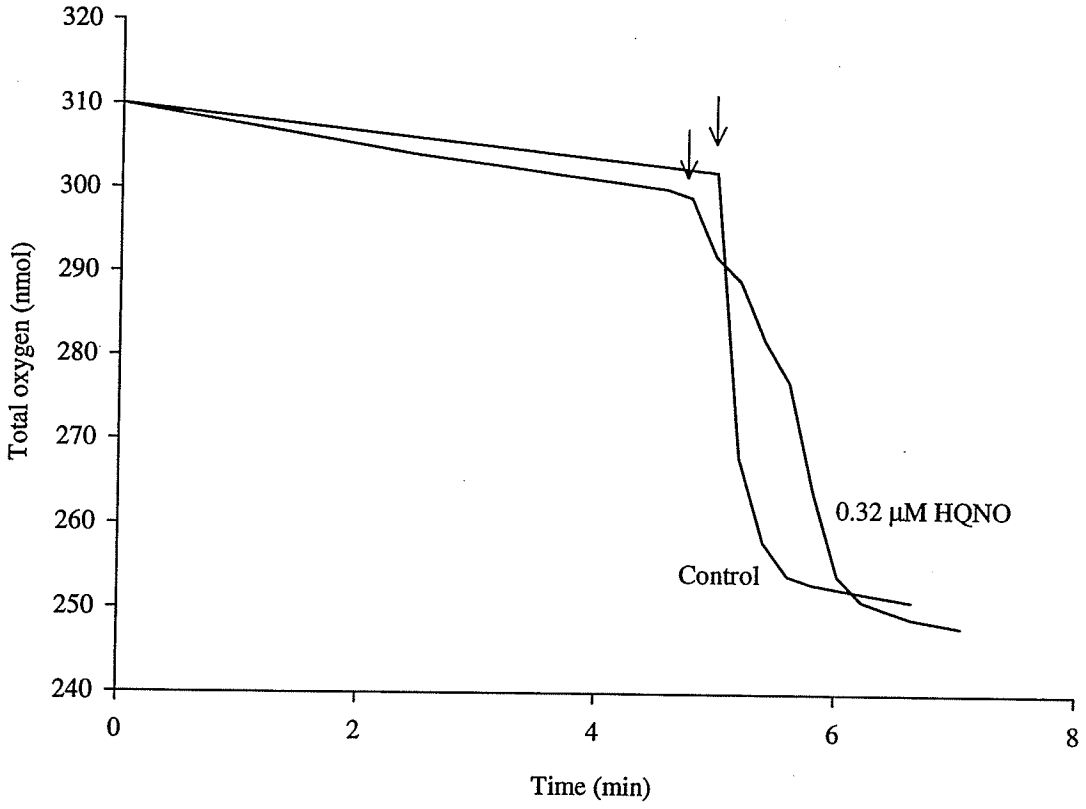
320
310
300
290
280
270
260
250
240
Total oxygen (nmol)
0
2
4
6
8
Time (min)
0.32 µM HQNO
Control

**Figure 25 (a)** The effect of *N*-ethymaleimide (NEM) on the rate of exogenous ferric iron reduction by endogenous respiration. The reactions were performed at 25°C in 0.1 M β-alanine-$H_2SO_4$ pH 3 and contained 20 mg of cells, 4 μmol $FeCl_3$, and NEM at the concentrations specified. The volume of the reaction mixtures was 1 mL . Results were based on two separate trials. The error bars are the standard deviation of the 2 trials.

**Figure 25 (b)** The effect of NEM on the rate of oxygen consumption by endogenous respiration. The reactions were performed at 25°C in 0.1 M β-alanine-$H_2SO_4$ pH 3 and contained 25 mg of cells and NEM at the concentrations specified. The volume of the reaction mixtures was 1.2 mL .

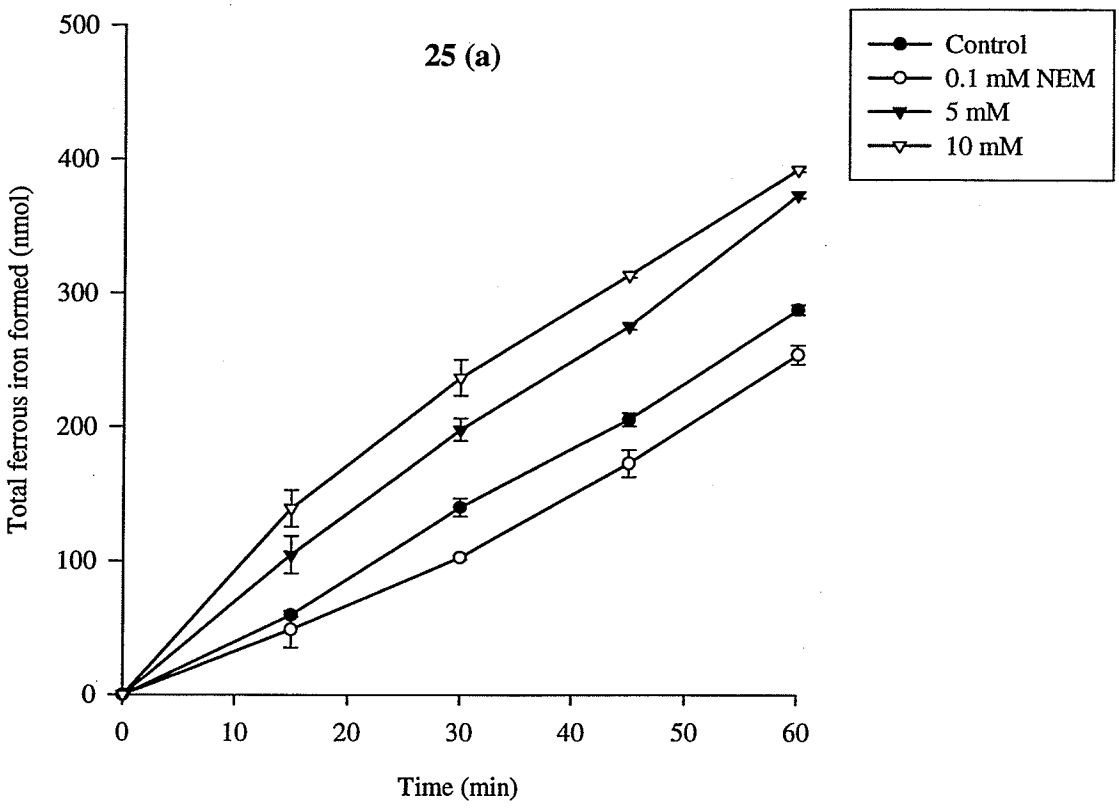
25 (a)
Control
0.1 mM NEM
5 mM
10 mM
Total ferrous iron formed (nmol)
500
400
300
200
100
0
0
10
20
30
40
50
60
Time (min)

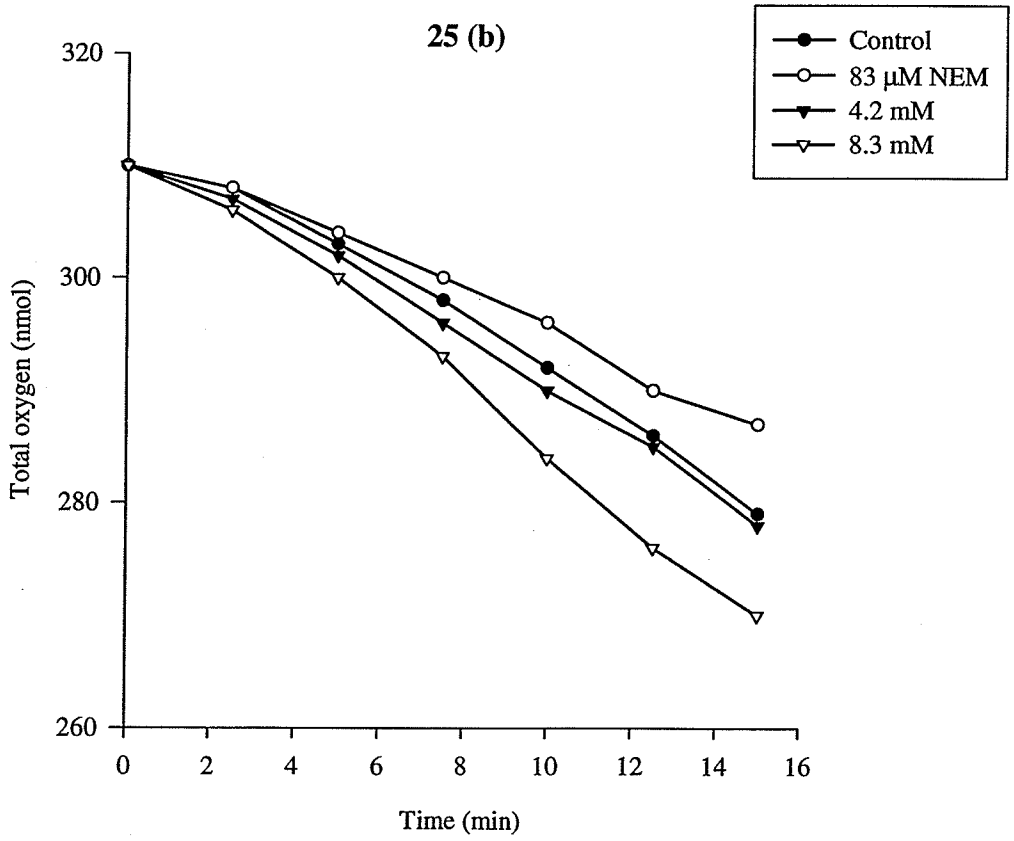
25 (b)
Control
83 µM NEM
4.2 mM
8.3 mM
Total oxygen (nmol)
320
300
280
260
0
2
4
6
8
10
12
14
16
Time (min)

**Figure 25 (c)** The effect of NEM on the rate of sulfite oxidation. The reactions were performed at 25°C in 0.1 M β-alanine-$H_2SO_4$ pH 3 and contained 25 mg of cells and NEM at the concentrations specified. $K_2SO_3$ (100 nmol) was added at the arrows after 5 min of preincubation between the cells and NEM. The volume of the reaction mixtures was 1.2 mL .

**25 (c)**

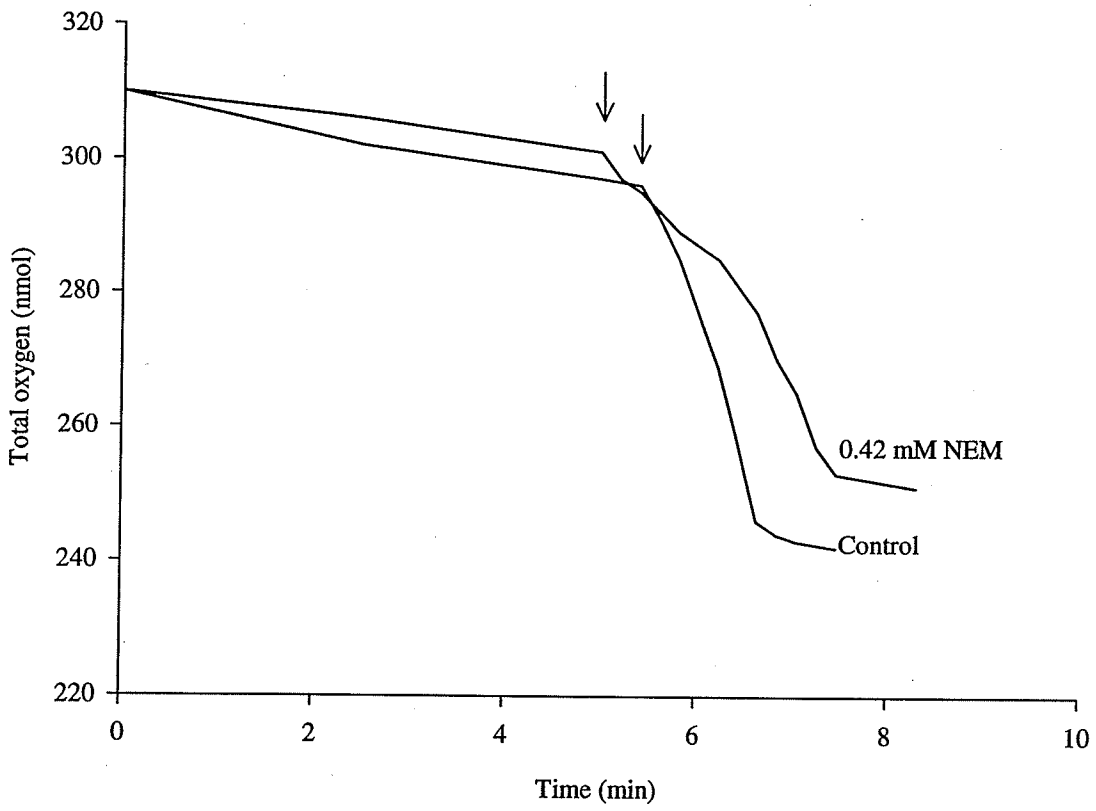
320
300
280
260
240
220
Total oxygen (nmol)
0
2
4
6
8
10
Time (min)
0.42 mM NEM
Control

**Figure 26 (a)** The effect of silver nitrate ($AgNO_3$) on the rate of exogenous ferric iron reduction by endogenous respiration. The reactions were performed at 25°C in 0.1 M β-alanine-$H_2SO_4$ pH 3 and contained 20 mg of cells, 4 μmol $FeCl_3$, and $AgNO_3$ at the concentrations specified. The volume of the reaction mixtures was 1 mL . Results were based on two separate trials. The error bars are the standard deviation of the 2 trials.

**Figure 26 (b)** The effect of $AgNO_3$ on the rate of oxygen consumption by endogenous respiration. The reactions were performed at 25°C in 0.1 M β-alanine-$H_2SO_4$ pH 3 and contained 25 mg of cells and $AgNO_3$ at the concentrations specified. The volume of the reaction mixtures was 1.2 mL .

**26 (a)**

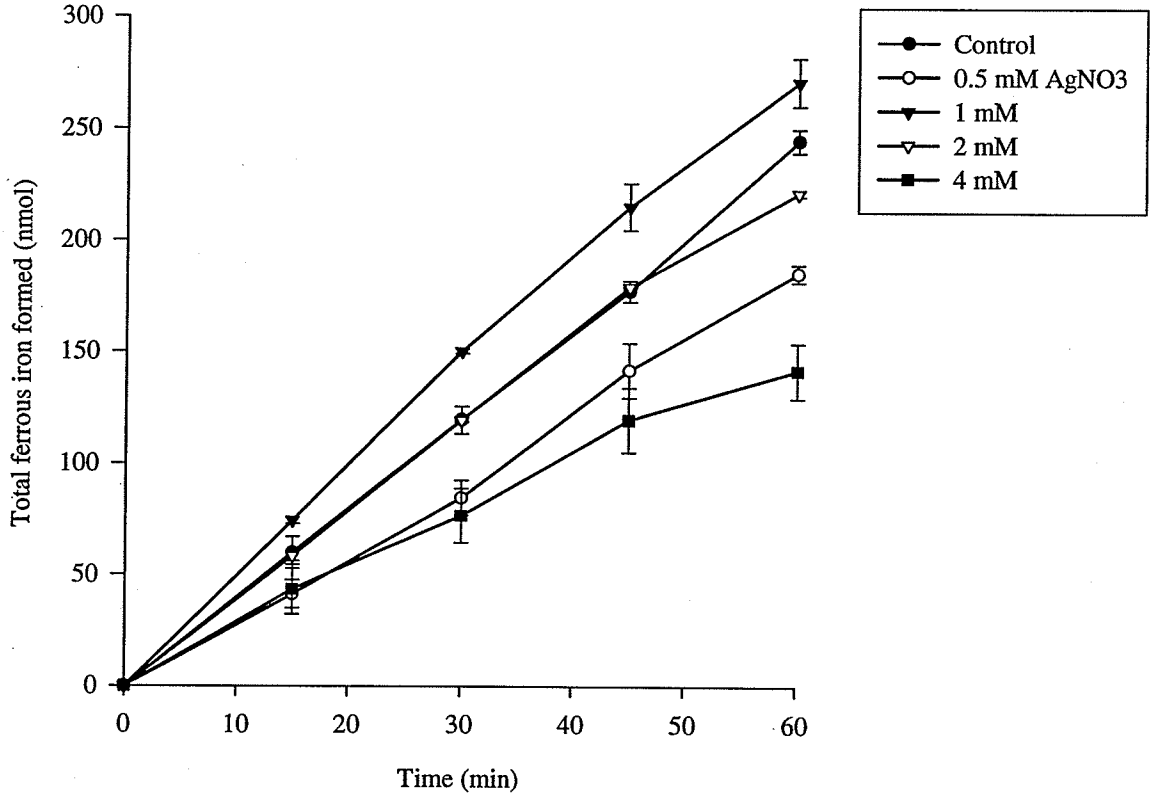
Total ferrous iron formed (nmol)
300
250
200
150
100
50
0
0
10
20
30
40
50
60
Time (min)
Control
0.5 mM AgNO3
1 mM
2 mM
4 mM

**26 (b)**

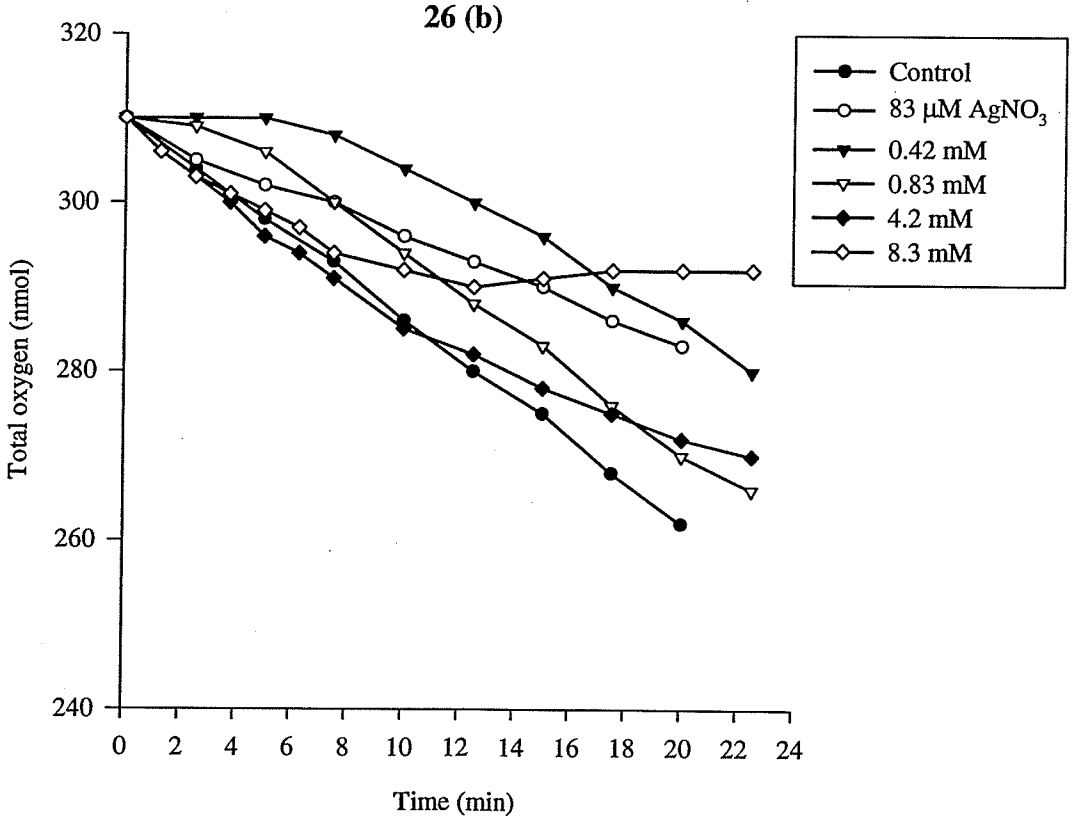
Total oxygen (nmol)
320
300
280
260
240
0
2
4
6
8
10
12
14
16
18
20
22
24
Time (min)
Control
83 μM AgNO3
0.42 mM
0.83 mM
4.2 mM
8.3 mM

**Figure 26 (c)** The effect of $AgNO_3$ on the rate of sulfite oxidation. The reactions were performed at 25°C in 0.1 M β-alanine-$H_2SO_4$ pH 3 and contained 25 mg of cells and $AgNO_3$ at the concentrations specified. $K_2SO_3$ (100 nmol) was added at the arrows after 5 min of preincubation between the cells and $AgNO_3$. The volume of the reaction mixtures was 1.2 mL .

**26 (c)**

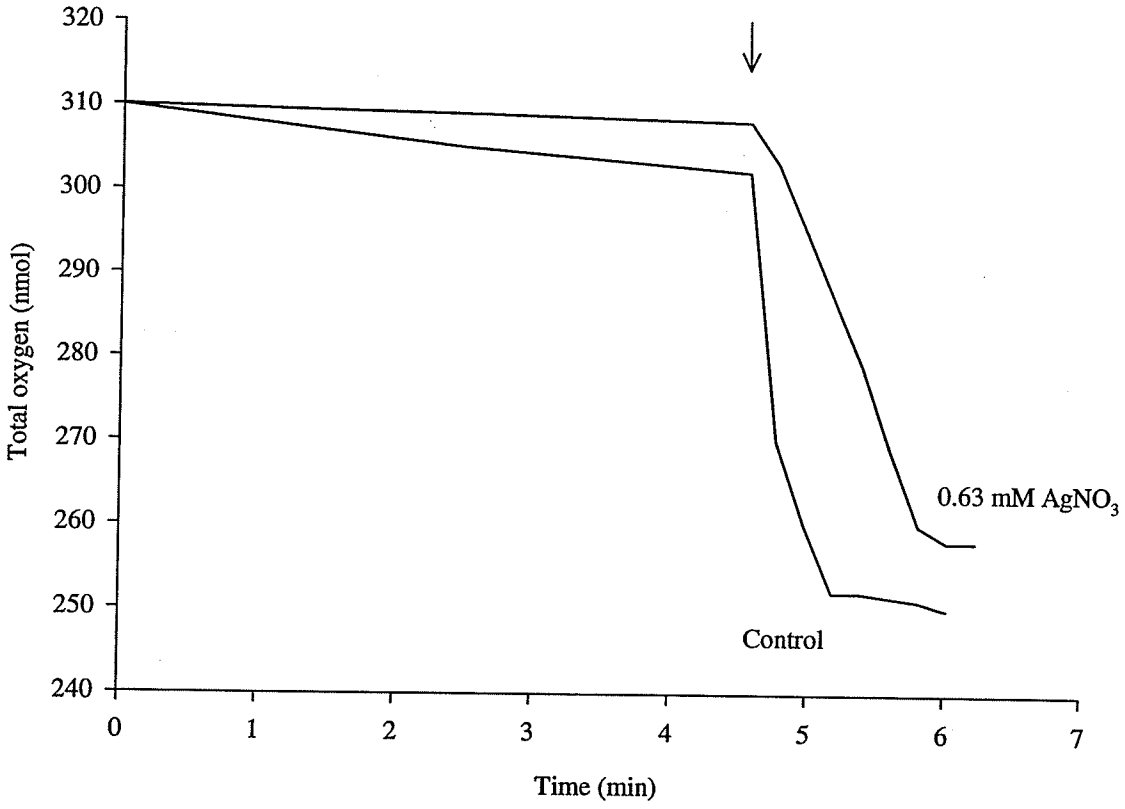
320
310
300
290
280
270
260
250
240
Total oxygen (nmol)
0
1
2
3
4
5
6
7
Time (min)
0.63 mM $AgNO_3$
Control

**Figure 27 (a)** The effect of mercuric chloride ($HgCl_2$) on the rate of exogenous ferric iron reduction by endogenous respiration. The reactions were performed at 25°C in 0.1 M β-alanine-$H_2SO_4$ pH 3 and contained 20 mg of cells, 4 μmol $FeCl_3$, and $HgCl_2$ at the concentrations specified. The volume of the reaction mixtures was 1 mL . Results were based on two separate trials. The error bars are the standard deviation of the 2 trials.

**Figure 27 (b)** The effect of $HgCl_2$ on the rate of oxygen consumption by endogenous respiration. The reactions were performed at 25°C in 0.1 M β-alanine-$H_2SO_4$ pH 3 and contained 25 mg of cells and $HgCl_2$ at the concentrations specified. The volume of the reaction mixtures was 1.2 mL .

**27 (a)**

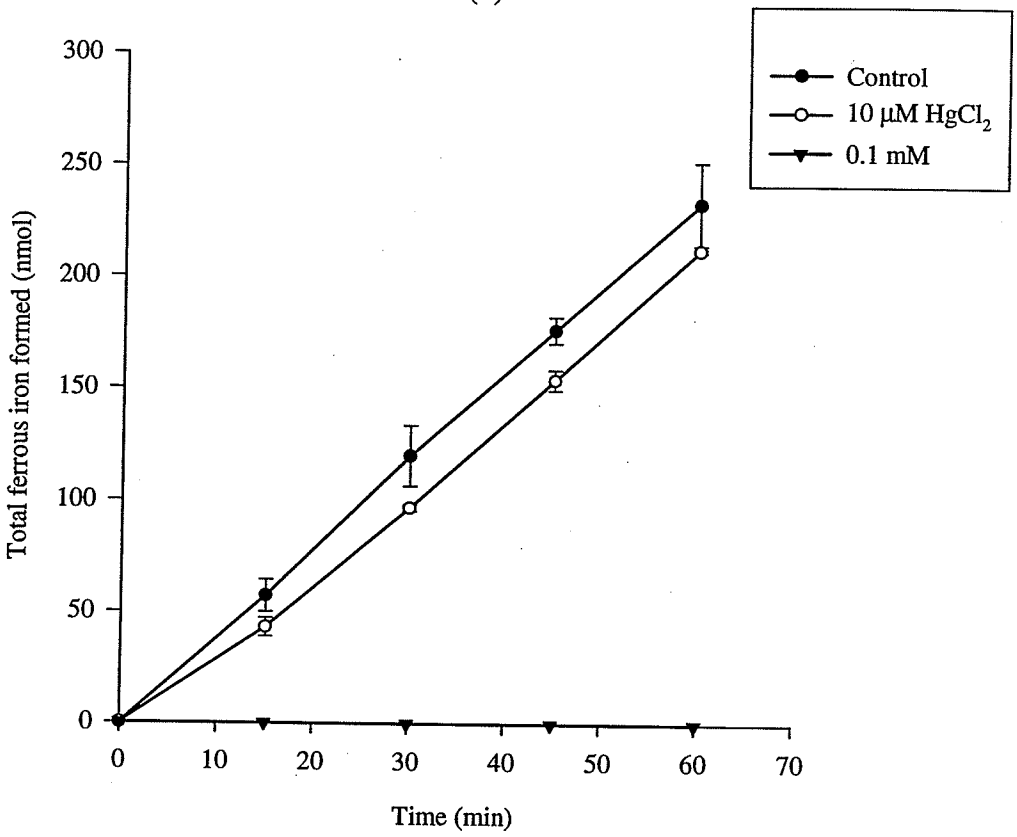
Control
10 µM HgCl2
0.1 mM
Total ferrous iron formed (nmol)
300
250
200
150
100
50
0
0
10
20
30
40
50
60
70
Time (min)

**27 (b)**

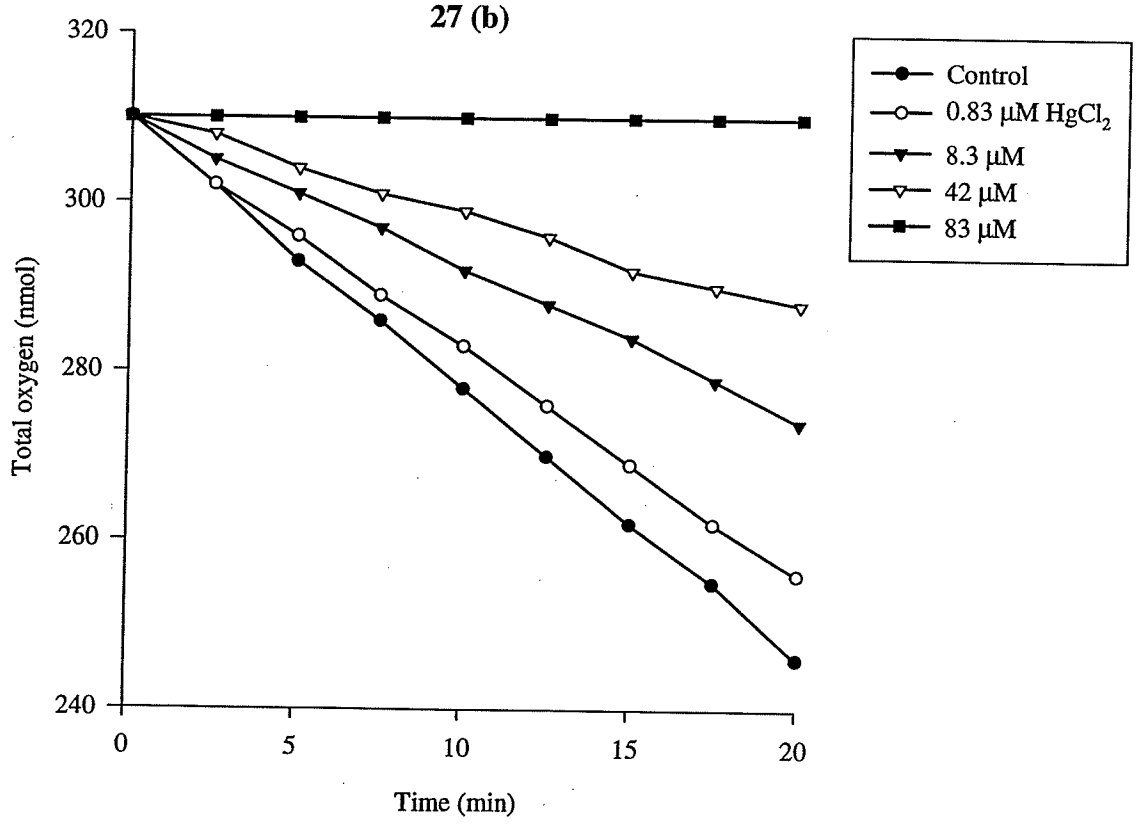
Control
0.83 µM HgCl2
8.3 µM
42 µM
83 µM
Total oxygen (nmol)
320
300
280
260
240
0
5
10
15
20
Time (min)

**Figure 27 (c)** The effect of $HgCl_2$ on the rate of sulfite oxidation. The reactions were performed at 25°C in 0.1 M β-alanine-$H_2SO_4$ pH 3 and contained 25 mg of cells and $HgCl_2$ at the concentrations specified. $K_2SO_3$ (100 nmol) was added at the arrows after 5 min of preincubation between the cells and $HgCl_2$. The volume of the reaction mixtures was 1.2 mL .

**27 (c)**

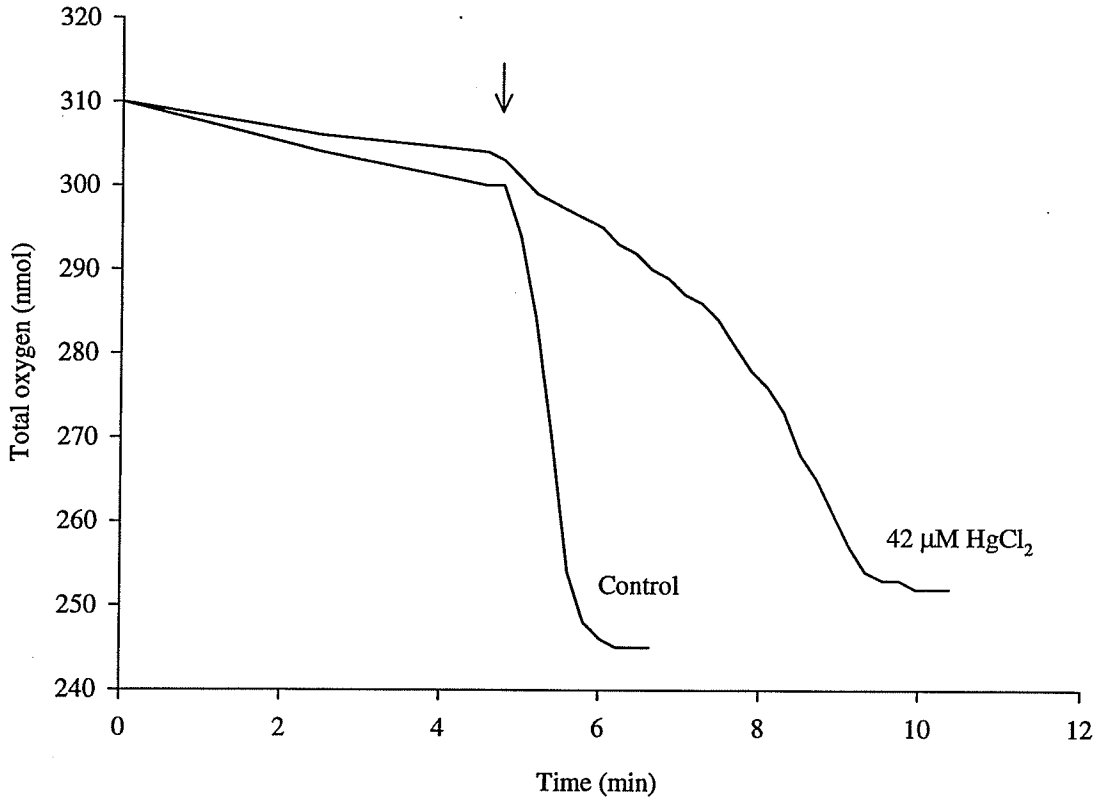
320
310
300
290
280
270
260
250
240
Total oxygen (nmol)
0
2
4
6
8
10
12
Time (min)
42 µM HgCl2
Control

# Part II

## Part II : Investigating ferric iron reduction by *Acidithiobacillus thiooxidans*

### Introduction

In the literature, only two instances of ferric iron reduction by *A. thiooxidans* (Brock and Gustafson, 1976; Kino and Usami, 1982) have been reported. The sparse attention paid to this subject matter may be due to the fact that the bacterium is not known for oxidizing ferrous iron for growth.

Brock and Gustafson (1976) using an unidentified strain of the bacterium showed that complete reduction of exogenous ferric iron was possible when aerobically grown on elemental sulfur. The pH of the culture medium was maintained at 1.6 and it was gently shaken during incubation. Brock and Gustafson did not propose an explanation for this physiological activity but suggested that future investigations should focus on possibly growing the bacterium under anerobic conditions with ferric iron serving as the sole terminal electron acceptor.

Heeding the words of Brock and Gustafson, Kino and Usami (1982) tried but were mainly unsuccessful in growing strain WU-79A on elemental sulfur under anerobic conditions with ferric iron as the electron acceptor. However, like the earlier reaserchers, they too observed exogenous ferric iron reduction during aerobic growth on elemental sulfur. In the same report, Kino and Usami suggested that unspecified reducing substrates formed during growth may be responsible for the reduction of exogenous ferric iron. To date, no evidence for the reduction of exogenous ferric iron by endogenous substrate(s) oxidation in thiobacilli have been reported.

In the present research, the coupling of endogenous respiration to exogenous ferric iron reduction was consistently observed under aerobic conditions. The initial motivation to observe endogenous respiration in this manner arose from similar observations in a strain of *A. ferrooxidans* in the lab. In the latter specie, the presence of an iron oxidase is common knowledge, as is the utilization of ferrous iron as an oxidizable substrate for growth via the electron transport chain (Ingledew, 1982). Since *A. thiooxidans* strain ATCC 8085 offered a rather unique physiology for investigation it was worth looking at.

Ferric iron reduction by the bacterium was characterized at pH 3 due to increased solubility of ferric iron at low pH and decreased chemical oxidation of the formed product - ferrous iron (Pronk and Johnson, 1992).

**Influence of buffer and buffer concentration**

The influence of various assay buffers on exogenous ferric iron reduction by the bacterium was investigated. The buffers tested included: 0.1 M β-alanine-$H_2SO_4$ pH 3, 0.1 M K-phosphate pH 3, 0.1 M sodium citrate pH 3 and 9K medium pH 3 . Ferric iron reduction was not observed in K-phosphate buffer or 9K medium. In either case, precipitation occurred upon ferric iron addition. The said observation is consistent with the affinity of phosphate to interact with metals. The degree of precipitation was greater in 0.1 M phosphate buffer than in the 9K medium which contained only 3 mM phosphate. Ferric iron reduction was slow in sodium citrate buffer, in agreement with the metal chelating property of citrate. In comparison to these buffers, ferric iron reduction was much faster in β-alanine-$H_2SO_4$ which was therefore selected as the buffer for further investigation of this physiology (Figure 1).

Different concentrations of β-alanine-$H_2SO_4$ pH 3 buffer were also tested in an effort to identify the optimal buffer concentration to observe exogenous ferric iron reduction by the bacterium (Figure 2). Optimum buffer concentrations were at or below 0.1 M . At 0.5 and 1 M, however, a dramatic decrease in ferric iron reduction rate was observed, which in turn may be attributed to an increased hypertonic effect exerted on the cells by the buffer. Throughout the research, 0.1 M β-alanine-$H_2SO_4$ pH 3 buffer was utilized. In the absence of cells in the reaction mixture (buffer + ferric iron), there was no detection of ferrous iron, suggesting the requirement of cells for this process. However, in the presence of cells alone in the reaction mixture (buffer + cells), some ferrous iron was detected but it was considerably less than in the presence of exogenous ferric iron. Most probably, the ferrous iron detected in the reaction mixture must have originated from the cells.

**Proportion of endogenous respiration that can be diverted for exogenous ferric iron reduction**

The proportion of endogenous respiration that can be used for exogenous ferric iron reduction was investigated using a 80 mg/mL cell concentration and by monitoring for changes to the amount of oxygen consumed by the cells in the presence of ferric iron, as well as by detecting for any ferrous iron formed (Figure 3 (a) and (b)). The primary reason for using a large concentration of cells was that any change in the amount of oxygen consumed by the cells, specifically any inhibition in the presence of exogenous ferric iron, may be measured much more easily at a higher cell concentration than at a lower concentration, since oxygen consumption by endogenous respiration increased with

increasing cell concentration (Figure 4). However, it was not feasible to use a large concentration of cells all the time. In general, the amount of oxygen consumed by cells decreased when exogenous ferric iron concentration was increased (Figure 3 (a)) with a corresponding increase in ferrous iron formed (Figure 3 (b)). At higher exogenous ferric iron concentrations, both the decrease in the amount of oxygen consumed and increase in ferrous iron formed appeared to level off. Thus, the maximal coupling of endogenous respiration to exogenous ferric iron reduction represented roughly 50 % of endogenous respiration measured by oxygen consumption studies ($O_2 + 4e^- + 4H^+ \rightarrow 2H_2O$ ; $Fe^{3+} + e^- \rightarrow Fe^{2+}$). A similar degree of coupling was also observed with 40 mg/mL and 20 mg/mL cell concentrations (data not shown). In general, the coupling of endogenous respiration to exogenous ferric iron reduction was not complete and full diversion of endogenous respiration to exogenous ferric iron reduction was not possible, even at higher ferric iron concentrations. Therefore, any generalizations drawn about endogenous respiration from exogenous ferric iron reduction studies should also take into consideration endogenous respiration measurements made by oxygen consumption studies, since the latter appears to measure a higher proportion of endogenous respiration.

**Influence of anaerobic incubation**

The influence of anaerobic incubation on exogenous ferric iron reduction was investigated using reaction mixtures incubated anaerobically (under $N_{2\,(g)}$) (Figure 5). The main goal of this investigation was to determine if the amount of ferric iron reduced by the bacterium increased during anaerobic incubation, when oxygen is eliminated as a terminal electron acceptor. Results illustrated that little difference existed between

aerobic and anaerobic incubation. The data obtained is in contrast to *A. ferrooxidans* where an anaerobic environment was essential for the observation of ferric iron reduction by the bacterium (Brock and Gustafson, 1976 ; Suzuki *et al.*, 1990). The strict requirement for an anaerobic environment for the observation of exogenous ferric iron reduction by *A. ferrooxidans* may be closely related to its physiological ability to oxidize ferrous iron by molecular oxygen via the electron transport chain for growth. Therefore, by blocking ferrous iron oxidation, the accumulation of this product would be more apparent.

During aerobic incubation, employing the terminal cytochrome oxidase inhibitor cyanide, an anaerobic environment was simulated to investigate ferric iron reduction by the bacterium. With the addition of cyanide, the ability of the bacterium to use oxygen as a terminal electron acceptor was impaired (In Part I, see Table 16 and Figure 20). Results, however, showed that cyanide had virtually no effect on ferric iron reduction by the bacterium (Figure 6).

Results from the anaerobic incubation of the reaction mixture suggested that the bacterium may perform ferric iron reduction regardless of the degree of oxygen tension in the environment, since the amount of exogenous ferric iron reduced by the bacterium did not change under anaerobic incubation (Figure 5). Additionally, the insensitivity to cyanide (Figure 6) suggested that the electron pathway to exogenous ferric iron, from endogenous electron source, may deviate from the pathway using oxygen as the terminal electron acceptor, since the latter showed some sensitivity to cyanide.

In general, *A. thiooxidans* is not known for oxidizing ferrous iron, therefore, precautionary measures to inhibit biological oxidation of the formed ferrous iron such as

anaerobic incubation or cyanide to block off the terminal cytochrome oxidase was not necessary. Additionally, the low pH of the reaction mixture was sufficient to prevent the chemical oxidation of the ferrous iron formed.

**Influence of cell concentration**

The influence of an increasing cell concentration on exogenous ferric iron reduction was investigated in 0.1 M β-alanine-$H_2SO_4$ pH 3 using 5, 10, 20, 40, and 80 mg/mL cell concentrations (Figures 7, 8, 9, 10, 11 and results summarized in Table 1). At 5, 10, and 20 mg/mL cell concentrations, normal Michaelis-Menten kinetics often associated with enzymes was observed, such that a hyperbolic increase in the velocity of the reaction occurred with an increase in substrate concentration. However, high concentrations of ferric iron were also inhibitory, particularly in experiments involving the 5 mg/mL cell concentration (Figure 7 (a)). The apparent $V_{max}$ (nmol of ferric iron reduced/min) doubled when the cell concentration was doubled but the apparent specific $V_{max}$ (nmol of ferric iron reduced/min/mg of cells) remained relatively constant. The apparent $V_{max}$ for the 5, 10, and 20 mg/mL cell concentrations was 0.84, 1.7, and 3 nmol of ferric iron reduced/min, respectively, whereas the apparent specific $V_{max}$ was 0.17, 0.17, and 0.15 nmol of ferric iron reduced/min/mg of cells, respectively (Figures 7 (b), 8 (b), 9 (b)). The apparent $K_m$ also remained relatively constant at 0.30, 0.31, and 0.37 mM for the 5, 10, and 20 mg/mL cell concentrations, respectively (Figures 7 (b), 8 (b), 9 (b)). For the 5 mg/mL cell concentration, however, the apparent $K_i$ (substrate inhibition constant ) was 1.8 mM, only slightly higher than the apparent $K_m$ value of 0.30 mM

(Figure 7 (c)). For the 10 mg/mL cell concentration, the apparent $K_i$ value of 72 mM was much higher than the apparent $K_m$ value of 0.31 mM (Figure 8 (c)).

It is not uncommon to find enzymes that show normal Michaelis-Menten kinetics at low substrate concentrations, while at high substrate concentrations, the velocity falls off (Dixon and Webb, 1979). This effect may be due to a number of reasons but one of the most important to be considered may be the overcrowding of substrate molecules onto the active site of the enzyme (Dixon and Webb, 1979). In such instances, the tendency to form ineffective enzyme-substrate complexes increases as two or more substrate molecules combine with an active site that is only destined to bind a single substrate (Dixon and Webb, 1979). In this particular instance with whole cells, one may consider the overcrowding of ferric iron molecules onto ferric iron binding site(s) of the cells as responsible for the decrease in velocity at high ferric iron concentrations (ie. 5 mg/mL cell concentration). However, as cell concentration increases, there will be more cells to interact with the excess ferric iron and instances of overcrowding of ferric iron molecules at ferric iron binding site(s) may become less frequent (ie. 10 and 20 mg/mL).

For the 40 and 80 mg/mL cell concentrations, a different type of kinetics was very much apparent (Figure 10 (a), 11 (a)). A sigmoidal increase in the velocity of the reaction was noticed when the substrate concentration was increased, thus suggesting kinetics often associated with cooperativity or allosterism. The sigmoidicity of the substrate versus velocity plot was more apparent with 80 mg/mL cell concentration (Figure 11 (a)). The analysis of the kinetic behavior of the 40 and 80 mg/mL cell concentrations via Lineweaver-Burk Plot analysis revealed that the plots were non-linear (Figures 10 (b), 11 (b)). The observation is consistent with cooperative or allosteric kinetics where the

double reciprocal plot is curved and approaches a horizontal line which intersects the 1/velocity axis at $1/V_{max}$ (Segel, 1975). The apparent $V_{max}$ was determined to be 6.3 nmol of ferric iron reduced/min for the 40 mg/mL cell concentration and 20.9 nmol of ferric iron reduced/min for the 80 mg/mL cell concentration. Not necessarily doubling of the kinetic parameter when the cell concentration was doubled, but nevertheless, an increase in $V_{max}$. The apparent specific $V_{max}$ was 0.16 nmol of ferric iron reduced/min/mg of cells for the lower cell concentration and 0.26 nmol of ferric iron reduced/min/mg of cells for the higher cell concentration.

Data suspected of illustrating cooperativity or allosterism is often analyzed using the Hill Model. The model of Hill takes into consideration that in order to show cooperativity an enzyme must have more than one binding site for a substrate (Dixon and Webb, 1979). Based on this assumption, the Hill model suggests that the binding of H molecules of a substrate (S) to an enzyme occurs in a single step ($E + HS = ES_H$) and that there are no stable intermediates in the system (ie. no $ES_{H-1}$, $ES_{H-2}$, etc) (Segel, 1975 , Dixon and Webb, 1979). The value of H obtained from such an analysis would correspond to the number of binding sites on the enzyme (H = n). The model of Hill predicts that a plot of $v/V_{max}$-v against substrate concentration on a log-log scale, where v is the velocity of the reaction, would be linear (Segel, 1975 , Dixon and Webb, 1979). However, most often, experimental data show that the plot is not linear over the entire range of substrate concentration, specifically at very low and very high concentrations of the substrate (Segel, 1975 , Dixon and Webb, 1979). At very low substrate concentrations when one is proceeding from a state where no sites are occupied on any given molecule of enzyme one would expect to see no cooperativity, and similarly at very high

concentrations of the substrate, when there is only one site remaining to be filled, there will also be no cooperativity (Segel, 1975 , Dixon and Webb, 1979). Thus one would expect the slope of the Hill plot to approach values of n = 1 at very low and high concentrations of substrate. A Hill plot slope of n = 1 reflects enzymes showing non-cooperativity or normal Michaelis-Menten kinetics. Despite its limitations, the Hill model of analysis is often used as an empirical method of estimating the degree of cooperativity, especially from about 10 → 90 % enzyme saturation.

With the experimental data, the Hill plot deviated from linearity at low and high substrate concentrations as expected (Figure 10 (c), 11 (c)). The deviation from linearity was clearly evident at high substrate concentrations in both the 40 and 80 mg/mL cell concentrations. In both instances, the apparent n value at higher substrate concentrations was approximately 1 . It was difficult to determine the apparent n values at lower substrate concentrations for the 40 and 80 mg/mL cell concentrations without additional readings but the genesis of a deviation is evident, especially with the 40 mg/mL cell concentration (apparent n = 0.7). The portion of the plots that did follow the Hill model showed an apparent n value of 4.8 for both the 40 and 80 mg/mL cell concentration. However, the substrate concentration required for $0.5V_{max}$ ($[S]_{0.5}$) was only 0.5 mM for the 40 mg/mL cell concentration and slightly more than doubled that for the 80 mg/mL cell concentration at 1.2 mM.

In general, sigmoid kinetic behavior most often reflects cooperative interaction between the subunits of an oligomeric protein. Changes in the structural and/or electronic feature(s) of one subunit are translated into changes in adjacent subunits, an effect that is mediated by non-covalent interactions at the subunit interface. Therefore, the binding of

one molecule of substrate greatly enhances the binding of other molecules of the same substrate to other subunits of the enzyme.

In this particular instance of sigmoidal kinetic behavior, one may consider a collection of cells possibly initiated by cell-cell interaction at high cell concentration as showing cooperativity. The binding of one or more molecules of ferric iron and/or subsequent reduction by a cell in an interaction may greatly enhance the binding of ferric iron molecule(s) to other cells involved in the interaction. A possibility may be that ferric iron binding to one particular cell confers structural and/or electronic change(s) to that cell leading to a slight dispersal of the cell from the collection and therefore opening up ferric iron binding site(s) in adjacent cells which may have been temporarily obstructed during cell-cell interaction. Therefore, a stepwise dispersal of cells may be responsible for the observed cooperativity or allosterism at high cell concentration. The tendency of strain ATCC 8085 cells to settle out of suspension was often noticed, especially at high cell concentrations. This tendency may have been due to an ability of the cells to interact or possibly even to aggregate. In the 40 and 80 mg/mL cell concentrations, at least 4.8 cells may be interacting in a cooperative or allosteric manner (apparent $n = 4.8$).

In previous studies on this bacterium, Lizama and Suzuki (1991) illustrated competitive inhibition of sulfur oxidation by other ATCC 8085 cells, in a series of experiments using various sulfur and cell concentrations. It was suggested that cells may compete with sulfur molecules for the sulfur-binding sites of active cells. The nature of the cell-cell competitive inhibition was not clear but a suggestion was put forth that the interaction may be related to the mechanism of sulfur oxidation which is thought to occur

at the cell surface. Since the cell is suited for adhesion to sulfur, then it may interact with the surface of a similarly endowed cell and thus obstruct the sulfur-binding site.

**Endogenous ferric iron reduction by endogenous respiration**

To observe endogenous ferric iron reduction by endogenous respiration it was imperative to determine the total iron (ferrous + ferric) present in the cells, as well as the proportion of ferrous iron to ferric iron. Total iron (ferrous + ferric) in the cell was determined by $HNO_3$ extraction of ferrous and ferric iron followed by $NH_2OH$-HCl treatment to reduce ferric iron to ferrous iron so that it may be detected by 1,10-phenanthroline. The total ferrous iron was determined as just stated but without $NH_2OH$-HCl treatment. Results revealed that on average 46 nmol of iron (ferrous + ferric) was present per mg of cells (Table 2). Of the total iron present in the cells, less than 5 % was in ferrous iron form, thus leaving ample room to observe endogenous ferric iron reduction by endogenous respiration.

Endogenous ferric iron reduction was investigated in 0.1 M β-alanine-$H_2SO_4$ pH 3 using 5, 10, 20, 40, 80, and 200 mg/mL cell concentrations (Figure 12). Unlike exogenous ferric iron reduction which was quite fast, endogenous ferric iron reduction was rather slow and was observed over a much longer period of time (approximately 30 h).

At cell concentrations of 5, 10, and 20 mg/mL, endogenous ferric iron reduction was observed during the allotted time (Figure 12 (a)). The 5 mg/mL cell suspension showed nearly 80 % increase in ferrous iron during the allotted time (Figure 12 (c)). In contrast, at higher cell concentrations of 40, 80, and 200 mg/mL, there was barely any

increase in ferrous iron during the same time (Figure 12 (c)). Interestingly, in the 5 mg/mL cell concentration, most of the ferrous iron formed appeared extracellularly in the supernatant and most of the iron found in the supernatant was in the ferrous form in most experiments (Figure 12 (b)). The results may provide some clues as to the probable mode of exogenous ferric iron reduction.

It may be argued that exogenous ferric iron is reduced by endogenous ferrous iron. The main drawback to this argument is that endogenous ferric iron reduction is a slow time consuming process whereas exogenous ferric iron reduction can be easily observed in a much shorter time. However, if the addition of exogenous ferric iron somehow promotes rapid endogenous ferric iron reduction, possibly by exchanging the endogenously reduced iron with externally added ferric iron, then the argument may be plausible.

The inability of the high cell concentrations to perform endogenous ferric iron reduction was further investigated. It was assumed that possibly some deleterious compound(s) may be released by the concentrated cell suspensions during the course of the prolonged incubation, which in turn may inhibit endogenous ferric iron reduction.

Fresh cells (5 → 200 mg/mL) were suspended in the supernatant of a week old 200 mg/mL cell suspension and endogenous ferric iron reduction was studied over a 30 h period and the results were compared to those of normal assay (data not shown). The low cell concentration suspensions exhibited the same ferric iron reduction activities regardless of the type of suspension buffer used. Therefore it was safe to assume that no inhibitor was present in the supernatant of highly concentrated cell suspensions. Additionally, spectrophotometric analysis of the week old supernatant revealed the

presence of absorption peaks at 260, 280, and 410 nm, corresponding to nucleic acid, protein, and *c*-type cytochromes, respectively. The observed peaks may be attributed to age related cell lysis which would be prevalent in an older cell suspension.

It would be tempting to speculate that the cooperative or allosteric effect observed with high cell concentrations in exogenous ferric iron reduction studies may somehow be involved in the observed endogenous ferric iron reduction phenomena. A possible cell-cell interaction preventing endogenous ferric iron reduction in the absence of high concentrations of exogenous ferric iron would be an ideal explanation for these observations. It is noteworthy in Figure 12 that the iron concentration in the supernatant does not increase much when the cell concentration was increased from 5 to 200 mg/mL .

**Influence of anaerobic incubation on endogenous ferric iron reduction by endogenous respiration**

The influence of anaerobic incubation on endogenous ferric iron reduction by endogenous respiration was investigated using reaction mixtures incubated anaerobically (under $N_{2\,(g)}$) (Figure 13). Figure 13 reveals that very little difference existed between aerobic and anerobic incubation. The results were identical to exogenous ferric iron reduction which was determined to behave similarly under aerobic and anaerobic incubation (Figure 3). It was interesting to note that endogenous ferrous iron concentration increases linearly up to around 1000 – 1100 nmol in 30-35 h and levels off beyond that. The observed level of ferrous iron formed was nearly identical to the total level of iron (ferrous + ferric) predicted for a 20 mg/mL cell suspension (Table 2). Additionally, the 0-time reading of around 60 nmol of ferrous iron was in close

approximation to the total ferrous iron concentration predicted for this particular cell concentration as well (Table 2). In general, it appears that endogenous ferric iron reduction by endogenous respiration proceeds until most of the extractable cellular ferric iron is reduced to ferrous iron, and oxygen tension in the environment exerts very little influence.

**Reduction of exogenous ferric iron by exogenous substrate oxidation**

The reduction of exogenous ferric iron by the oxidation of exogenous substrates such as sulfur (soluble sulfur – DMSO/sulfur, precipitated elemental sulfur – Tween 80 sulfur), thiosulfate, sulfite, and formate was investigated. In general, all of the aforementioned substrates, with the exception of sulfite, can couple to exogenous ferric iron reduction, however the degree by which they couple varies. In the case of sulfite, non-biological oxidation of the substrate was observed in the presence of ferric iron without the formation of ferrous iron. In this research, degree of coupling was defined as: (Total number of electrons transferred to exogenous ferric iron from the oxidation of the exogenous substrate ÷ Total number of electrons available from the oxidation of the exogenous substrate) x 100 % . Electron count was based on 4 electrons equivalent to one molecular oxygen consumed ($O_2 + 4e^- + 4H^+ \rightarrow 2H_2O$) and one electron for ferric iron reduction ($Fe^{3+} + e^- \rightarrow Fe^{2+}$). For example, the complete oxidation of 156 nmol of DMSO/sulfur ($S + 1½O_2 + H_2O \rightarrow SO_4^{2-} + 2H^+$) consumes 234 nmol of oxygen, therefore the consumption of 234 nmol of oxygen is made possible by 936 nmol of electrons. Similarly, with 100 nmol of thiosulfate ($S_2O_3^{2-} + 2O_2 + H_2O \rightarrow 2SO_4^{2-} + 2H^+$)

800 nmol of electrons were available, and with 100 nmol of formate ($HCOOH + ½ O_2 \rightarrow H_2O + CO_2$) 200 nmol of electrons were available.

**Reduction of exogenous ferric iron by sulfur oxidation.** The reduction of exogenous ferric iron by both DMSO/sulfur (Table 3) and Tween 80 sulfur (Table 4) oxidation was observed. With both types of sulfur, the degree of coupling increased with increasing ferric iron concentration. However, complete coupling was not observed, even at higher ferric iron concentrations. The highest degree of coupling observed was 34 % with DMSO/sulfur and up to 63 % with Tween 80 sulfur, at 8.6 mM ferric iron concentration.

At 8.6 mM ferric iron concentration, the amount of oxygen consumed by the cells in the presence of DMSO/sulfur was similar to the amount of oxygen consumed when sulfur is oxidized to sulfite ($S + O_2 + H_2O \rightarrow SO_3^{2-} + 2H^+$) (Table 5). The biological oxidation of sulfur to sulfite without further oxidation to sulfate ($SO_3^{2-} + 2H^+ + ½ O_2 \rightarrow SO_4^{2-} + 2H^+ + 2e^-$) can be observed in the presence of the $bc_1$ complex inhibitor, HQNO (Suzuki *et al.*, 1992). The implication is that the observed coupling between sulfur and ferric iron, may actually occur at the level of sulfite, after the initial oxidation of sulfur to sulfite. As a result, the 34 % coupling observed for DMSO/sulfur oxidation at ferric iron concentration of 8.6 mM is in agreement with the proportion of total electrons that would be available from sulfite oxidation alone, in the sulfur to sulfate oxidation scheme (1/3 of total available electrons). Corroboration with Tween 80 sulfur proved to be futile as sulfur suspensions are rarely used for stoichiometric studies primarily due to the difficulty in controlling the amount of substrate that is added. If the implication is indeed correct, then it would be interesting to

note that externally added sulfite reacts non-biologically with exogenous ferric iron without the formation of ferrous iron even in the presence of cells, whereas sulfite generated from sulfur oxidation by the cells can be coupled to exogenous ferric iron reduction with a near stoichiometric production of ferrous iron. The results raise the possibility of an intarcellular location for the formed sulfite, which in turn may permit the observed coupling. In the presence of both HQNO and ferric iron, sulfite produced from sulfur probably came out of the cell and was oxidized chemically with oxygen catalyzed by ferric iron. HQNO, after all, has some uncoupling effects on whole cells (Oleskin and Samuilov, 1988). Possibly this uncoupling may be due to some physical alteration of the integrity of the plasma membrane which also permits the release of sulfite.

**Reduction of exogenous ferric iron by thiosulfate oxidation.** The reduction of exogenous ferric iron by thiosulfate oxidation was also observed (Table 6). The degree of coupling increased with increasing ferric iron concentration. Like sulfur, complete coupling was not observed, even at higher ferric iron concentrations. The highest degree of coupling with thiosulfate was 34 %, at 8.6 mM ferric iron concentration.

Once again, the results confirm the hypothesis that the coupling during the oxidation of a reduced sulfur compound to ferric iron reduction, may occur at the level of sulfite (Table 7). At pH 3, thiosulfate oxidation is expected to occur via the thiosulfate oxidizing enzyme pathway ($S_2O_3^{2-} + 2O_2 + H_2O \rightarrow 2SO_4^{2-} + 2H^+$) (Pathway B in Masau *et al.*, 2001). In the said pathway, the presence of an inhibitory concentration of HQNO will result in approximately 75 % of the total available electrons from thiosulfate oxidation being utilized by oxygen with the remaining electrons accumulating at the level of sulfite ($S_2O_3^{2-} + 1½O_2 + 2H^+ \rightarrow H_2SO_3 + SO_4^{2-}$). As a result, the 34 % coupling

observed for thiosulfate oxidation at ferric iron concentration of 8.6 mM (Table 6) is in close approximation with the proportion of total electrons that would be available from sulfite oxidation alone, in the thiosulfate to sulfate oxidation scheme (1/4 of total available electrons).

Results from sulfur and thiosulfate coupling to exogenous ferric iron reduction suggest the possible presence of a ferric iron-dependent sulfite oxidase in *A. thiooxidans* strain ATCC 8085. The existence of a sulfite oxidoreductase which directly utilizes ferric iron as an electron acceptor has been mentioned for (Sugio *et al.*, 1988) and purified from the membrane fraction of a strain of *A. ferrooxidans* (Sugio *et al.*, 1992). In the said bacterium, the sulfite oxidoreductase could not utilize cytochrome *c* or ferricyanide as an electron acceptor. Additionally, the physiological significance of the enzyme was said to be two-fold: (i) the detoxification of sulfite produced during sulfur oxidation and (ii) production of ferrous iron by the reduction of ferric iron by sulfite and the subsequent oxidation of the ferrous iron produced by iron oxidase to produce energy for the cells.

**Reduction of exogenous ferric iron by formate oxidation.** Formate was oxidized by the bacterium with stoichiometric oxygen consumption ($HCOOH + ½\ O_2 \rightarrow H_2O + CO_2$) (see Part I, Table 11 and Figure 12). Formate oxidation by *A. ferrooxidans* has been previously reported (Pronk *et al.*, 1991). The reduction of exogenous ferric iron by formate oxidation was apparent (Table 8). The degree of coupling increased with increasing ferric iron concentration. However, unlike the reduced sulfur compounds, the degree of coupling with formate was extensive. Nearly 100 % coupling was observed with 4.3 and 8.6 mM ferric iron. The high degree of coupling may indicate a direct enzymatic interaction between formate and exogenous ferric iron reduction. Additionally,

this high degree of coupling also shows that ferric iron is preferred over oxygen even under aerobic incubation

**Reduction of exogenous ferric iron by exogenous substrate oxidation during anaerobic incubation**

It was possible to observe exogenous ferric iron reduction by exogenous substrates during anaerobic incubation (Table 9). The degree of coupling, as previously defined, was greater than that which was observed under aerobic incubation for sulfur and thiosulfate but lower for formate. Additionally, some unexpected results were observed with sulfite.

The degree of coupling with DMSO/sulfur was around 41 %. The mechanism suggested under aerobic incubation for sulfur coupling to ferric iron may not be proposed under anaerobic incubation since oxygen is not available to carry out the initial oxidation of sulfur to sulfite required for the reduction of ferric iron. As a result, the observed ferric iron reduction during anaerobic incubation may indicate a direct enzymatic interaction between sulfur oxidation and exogenous ferric iron reduction. Possibly, a direct enzymatic interaction between sulfur and ferric may not be favored under aerobic conditions and only observed under anaerobic conditions. Both with DMSO/sulfur and Tween 80 sulfur, iron reduction was greater anaerobically than aerobically (Tables 3, 4), supporting the idea of ferric iron reduction during sulfur oxidation to sulfite. The degree of coupling was calculated assuming complete oxidation of substrate during the allotted incubation period (15 min). In the Tween 80 sulfur experiment with excess sulfur it was not possible to determine how much sulfur was oxidized. It is worth noting that a sulfur:

ferric ion oxidoreductase has also been mentioned for (Sugio *et al.*, 1985) and purified from (Sugio *et al.*, 1988) *A. ferrooxidans*. The enzyme purified from the soluble fraction of cell free extracts of the bacterium had a molecular weight of 46 kDa and was composed of two identical subunits ($M_r$ = 23 kDa). The purified enzyme showed a strict requirement for reduced glutathione (GSH) for the oxidation of sulfur. In later reports, the researchers responsible for the purification of the enzyme suggested that $H_2S$ may be the actual substrate for the enzyme and the enzyme should therefore be referred to as hydrogen sulfide: ferric ion oxidoreductase (Sugio *et al.*, 1989; 1992). The putative role of GSH in Sugio's purified enzyme is in agreement with Suzuki's (1965) finding of sulfur oxidation only in the presence of GSH, in cell free systems.

Electron transfer between thiosulfate and ferric iron during anaerobic incubation was more extensive than during aerobic incubation. The degree of coupling under anaerobic incubation was 74 % at 8.6 mM ferric iron (Table 9) whereas the degree of coupling was 34 % at the same ferric iron concentration during aerobic incubation (Table 6). The mechanism suggested during aerobic incubation for thiosulfate coupling to ferric iron may not be proposed under anaerobic incubation since oxygen is not available to carry out the initial oxidation of thiosulfate to the level of sulfite required for the coupling. As a result, the observed coupling may also be a direct enzymatic interaction between thiosulfate oxidation and exogenous ferric iron reduction.

Formate oxidation and coupling with exogenous ferric iron reduction was not as extensive as it was during aerobic incubation. The coupling was around 46 % at 8.6 mM ferric iron (Table 9) compared to near complete coupling at ferric iron concentration of

only 4.3 (Table 8) during aerobic incubation. The results cannot be adequately explained at the present time.

The inability of cells to reduce exogenous ferric iron in the presence of sulfite was unexpected, since the aerobic experiments with DMSO/sulfur and thiosulfate (Tables 3 and 6) indicated that sulfite formed was oxidized with ferric iron. It may be that cells oxidize ferric iron with sulfite formed inside the cells, but perhaps not with externally added sulfite. In general, the data presented in Table 9 illustrates some possibility of direct coupling between sulfur and thiosulfate oxidation and exogenous ferric iron reduction under anaerobic conditions.

The ability of sulfur grown version of *A. thiooxidans* strain ATCC 8085 to couple exogenous substrate oxidation (sulfur, thiosulfate, formate) to exogenous ferric iron reduction was investigated. Results show that sulfur grown cells cannot utilize ferric iron as an alternate electron acceptor during substrate oxidation. Previously, Suzuki *et al.* (1990) showed that sulfur grown version of the bacterium was not able to oxidize sulfur by ferric iron even during anaerobic incubation. A comparative examination of the cytochrome content of thiosulfate and sulfur grown cells revealed that sulfur grown cells lack the extensive cytochrome network present in the thiosulfate grown cells (Figure 14 (a) and (b)). Possibly, the absence of an extensive cytochrome network in the sulfur grown cells may play a crucial role in the inability of these cells to utilize ferric iron as an electron acceptor during exogenous substrate oxidation.

**Implication of results**

Ferric iron reduction by substrate oxidation, both endogenous substrates(s) and exogenous substrates, was an unexpected occurrence in *A. thiooxidans* strain ATCC 8085 since the bacterium does not oxidize ferrous iron.

The coupling of exogenous substrate oxidation to ferric iron reduction may indicate an inherent ability of the bacterium to utilize an electron acceptor other than oxygen. That is, the bacterium may posses the ability to grow under anaerobic conditions using ferric iron as the terminal electron acceptor. To verify this assumption, the ability of *A. thiooxidans* to grow anaerobically, while respiring on ferric iron, must be shown. Coincidentally, this was also proposed by Brock and Gustafson (1976), based on similar observations in their strain of the bacterium. Heeding the work of the earlier researchers, Kino and Usami (1982) were unsuccessful in growing their strain of the bacterium under anaerobic conditions while utilizing ferric iron as the terminal electron acceptor. However, some preliminary evidence for the ability of the present strain to oxidize substrates and couple that to exogenous ferric iron reduction under anaerobic conditions was presented in Table 9. Thus the possibility of growth under these environmental conditions is worth investigating, specifically using this strain of the bacterium.

The observation of ferric iron reduction under aerobic conditions by endogenous substrate(s) was quite peculiar. By using ferric iron as an electron acceptor, the bacterium is relinquishing some energy. The redox potential of the $O_2/H_2O$ couple ($E_o' = 820$ mV) is higher than that of $Fe^{3+}/Fe^{2+}$ couple ($E_o' = 771$ mV), as a result the bacterium can generate more energy by using $O_2$ as a terminal electron acceptor than $Fe^{3+}$. Therefore, the ferrous iron formed may serve an additional purpose on top of its role as a terminal

electron acceptor. Possibly, the ferrous iron formed may serve as a store of reducing equivalents. However, for this assumption to hold true, the bacterium must posses iron oxidase activity. It may be argued that the iron oxidase activity in question cannot be detected under the present experimental conditions. A more reasonable explanation may be that the ferrous iron formed is utilized for the activation of elemental sulfur, in a role analogous to GSH in cell free systems (Suzuki, 1965; Rohwerder and Sand, 2003). Elemental sulfur, which assumes a stable sulfur octet ($S_8$) configuration, is rather inert and biological oxidation is likely to involve an initial activation step in which the $S_8$ structure is made susceptible to further microbial oxidation. The role of GSH in cell free systems is to carry out a nucleophilic attack on elemental sulfur to form glutathione polysulfide chain ($GS\text{-}S_n^-$) in which the terminal sulfur atom can be readily oxidized. Possibly, a similar fate may be proposed for ferrous iron.

# Tables

**Table 1** Summary of apparent kinetic parameter values for exogenous ferric iron reduction by endogenous respiration when cell concentration was increased

| Cell concentration (mg/mL) | $V_{max}$ (nmol/min) | specific $V_{max}$ (nmol/min/mg) | $K_m$ (mM) | $K_i$ (mM) | $[S]_{0.5}$ (mM) | $n_{app}$ |
|---|---|---|---|---|---|---|
| 5 | 0.8 | 0.17 | 0.30 | 1.8 | | |
| 10 | 1.7 | 0.17 | 0.31 | 72 | | |
| 20 | 3.0 | 0.15 | 0.37 | | | |
| 40 | 6.3 | 0.16 | | | 0.5 | 4.8 |
| 80 | 20.9 | 0.26 | | | 1.2 | 4.8 |

Summary of Figures 7,8,9,10,11

**Table 2** Total iron (ferrous + ferric) and ferrous iron in various amounts of cells

| Amount of cells (mg) | Total iron (ferrous + ferric) (nmol) | Total ferrous iron (nmol) | Ferrous iron as a % of total iron | Total iron (ferrous + ferric)/mg of cells (nmol/mg) |
|---|---|---|---|---|
| 5 | 265 | 0 | 0 | 53 |
| 10 | 427 | 0 | 0 | 43 |
| 20 | 1013 | 98 | 10 | 51 |
| 40 | 1807 | 57 | 3 | 45 |
| 80 | 3360 | 154 | 5 | 42 |
| 200 | 8446 | 557 | 7 | 42 |
| | | | 4 | 46 |

Method used for analysis is described in the materials and methods. Iron determination was performed in 0.1 M β-alanine-$H_2SO_4$ pH 3 and contained cells as specified. The volume of the cell suspensions was 1 mL .

**Table 3.** Reduction of exogenous ferric iron by DMSO/sulfur oxidation

| Components of reaction mixture | Concentration of ferric iron (mM) | Total oxygen consumed (nmol) | Total ferrous iron formed (nmol) | Degree of coupling [d] (%) |
|---|---|---|---|---|
| a) Cells + ferric iron + DMSO/sulfur [a] | 0.0 | | 12 | |
| | 1.0 | | 169 | |
| | 2.1 | | 227 | |
| | 4.3 | | 252 | |
| | 8.6 | | 376 | |
| b) Cells + ferric iron + DMSO/sulfur [b] | 0.0 | 234 | 0 | |
| | 1.0 | 210 | 96 | 10 |
| | 2.1 | 200 | 136 | 15 |
| | 4.3 | 184 | 200 | 21 |
| | 8.6 | 160 | 296 | 32 |
| c) Cells + ferric iron | 0.0 | | 5 | |
| | 1.0 | | 49 | |
| | 2.1 | | 89 | |
| | 4.3 | | 63 | |
| | 8.6 | | 59 | |
| d) Ferric iron + DMSO/sulfur | 8.6 | | 1 [c] | |
| e) difference between a) and c) | 0.0 | | 7 | |
| | 1.0 | | 120 | 13 |
| | 2.1 | | 138 | 15 |
| | 4.3 | | 189 | 20 |
| | 8.6 | | 317 | 34 |

The reactions were incubated for 15 min at 25°C in 0.1 M β-alanine-$H_2SO_4$ pH 3 and contained 25 mg of cells, $FeCl_3$ as specified, and 156 nmol of DMSO/sulfur. The volume of the reaction mixtures was 1.4 mL.

a. Colorimetric determination by 1,10-phenanthroline.
b. Calculated from the decrease in the amount of oxygen uptake measured with 156 nmol of DMSO/sulfur.
c. No oxygen consumption observed.
d. Defined as : (Total number of electrons transferred to exogenous ferric iron from the oxidation of DMSO/sulfur ÷ Total number of electrons available from the oxidation of DMSO/sulfur) x 100 %

Electron count based on 4 electrons equivalent to one molecular oxygen consumed ($O_2 + 4e^- + 4H^+ \rightarrow 2H_2O$). Since the complete oxidation of 156 nmol of DMSO/sulfur consumed 234 nmol of oxygen ($S + 1½O_2 + H_2O \rightarrow SO_4^{2-} + 2H^+$), then the consumption of 234 nmol of oxygen was made possible by 936 nmol of electrons.

**Table 4** Reduction of exogenous ferric iron by Tween 80 sulfur oxidation

| Components of reaction mixture | Concentration of ferric iron (mM) | Total oxygen consumed (nmol) | Total ferrous iron formed (nmol) | Degree of coupling [c] (%) |
|---|---|---|---|---|
| a) Cells + ferric iron + Tween 80 sulfur [a] | 0.0 | 200 | 4 | |
| | 1.0 | 200 | 165 | 21 |
| | 2.1 | 200 | 298 | 37 |
| | 4.3 | 200 | 327 | 41 |
| | 8.6 | 200 | 506 | 63 |
| b) Ferric iron + Tween 80 sulfur | 8.6 | | 3 [b] | |

The reactions were incubated at 25°C in 0.1 M β-alanine-$H_2SO_4$ pH 3 and contained 25 mg of cells, $FeCl_3$ as specified, and 1mmol of Tween 80 sulfur. The volume of the reaction mixtures was 1.4 mL.

a. Colorimetric determination by 1,10-phenanthroline. Since excess Tween 80 sulfur was used (1 mmol), the reaction had to be terminated at some point. The reaction was terminated after the consumption of 200 nmol of oxygen, corresponding to 133 nmol of Tween 80 sulfur oxidized. Tween 80 sulfur amount used was similar to the amount of DMSO/sulfur used (156 nmol). Time allotted was too short for any significant amount of ferrous iron to be formed at any of the ferric iron concentrations tested from endogenous respiration.

b. No oxygen consumption observed.

c. Defined as : (Total number of electrons transferred to exogenous ferric iron from the oxidation of Tween 80 sulfur ÷ Total number of electrons available from the oxidation of Tween 80 sulfur) x 100 %

Electron count based on 4 electrons equivalent to one molecular oxygen consumed ($O_2 + 4e^- + 4H^+ \rightarrow 2H_2O$). Since the complete oxidation of 133 nmol of Tween 80 sulfur consumed 200 nmol of oxygen ($S + 1½O_2 + H_2O \rightarrow SO_4^{2-} + 2H^+$), then the consumption of 200 nmol of oxygen was made possible by 800 nmol of electrons.

**Table 5** Summary of total oxygen consumed and the amount of reaction products formed after the reduction of exogenous ferric iron by DMSO/sulfur oxidation

| Components of reaction mixture | Total oxygen consumed (nmol) | Total ferrous iron formed (nmol) | Total sulfite formed (nmol) |
|---|---|---|---|
| Cells + DMSO/sulfur [a] | 234 (234) | 8 | 22 |
| Cells + HQNO [b] + DMSO/sulfur | 175 (156) | 9 | 131 (156) |
| Cells + ferric iron [c] + DMSO/sulfur | 156 | 466 | 4 |
| Cells + ferric iron | 10 | 102 | 11 |
| | 466 – 102 = | 364 (310) | |
| Cells | 25 | 8 | 5 |
| Cells + HQNO | 21 | 18 | 23 |
| Cells + HQNO + ferric iron + DMSO/sulfur [d] | 260 | 12 | 8 |
| HQNO + ferric iron + DMSO/sulfur | 0 | 22 | 6 |

The reactions were incubated for 15 min at 25°C in 0.1 M β-alanine-$H_2SO_4$ pH 3 and contained 32 mg of cells and components as specified. The volume of the reaction mixtures was 1.6 mL.

( ) denotes expected values.

a. 156 nmol. of DMSO/sulfur
b. 3.6 μM of HQNO.
c. 8.6 mM of ferric iron.
d. A distinctively biphasic oxidation pattern was observed. An initial rapid oxidation lasting less than a minute generated a stoichiometry consistent with sulfur oxidation to sulfite. The final slow oxidation pattern was concluded to be a chemical reaction of sulfite with oxygen catalyzed by ferric iron.

**Table 6** Reduction of exogenous ferric iron by thiosulfate oxidation

| Components of reaction mixture | Concentration of ferric iron (mM) | Total oxygen consumed (nmol) | Total ferrous iron formed (nmol) | Degree of coupling [d] (%) |
|---|---|---|---|---|
| a) Cells + ferric iron + thiosulfate [a] | 0.0 | | 15 | |
| | 1.0 | | 139 | |
| | 2.1 | | 191 | |
| | 4.3 | | 263 | |
| | 8.6 | | 333 | |
| b) Cells + ferric iron + thiosulfate [b] | 0.0 | 200 | 0 | |
| | 1.0 | 180 | 80 | 10 |
| | 2.1 | 168 | 128 | 16 |
| | 4.3 | 150 | 200 | 25 |
| | 8.6 | 130 | 280 | 35 |
| c) Cells + ferric iron | 0.0 | | 10 | |
| | 1.0 | | 52 | |
| | 2.1 | | 58 | |
| | 4.3 | | 71 | |
| | 8.6 | | 58 | |
| d) Ferric iron + thiosulfate | 8.6 | | 1 [c] | |
| e) difference between a) and c) | 0.0 | | 5 | |
| | 1.0 | | 87 | 11 |
| | 2.1 | | 133 | 17 |
| | 4.3 | | 192 | 24 |
| | 8.6 | | 275 | 34 |

The reactions were incubated for 15 min at 25°C in 0.1 M β-alanine-$H_2SO_4$ pH 3 and contained 25 mg of cells, $FeCl_3$ as specified, and 100 nmol of thiosulfate. The volume of the reaction mixtures was 1.4 mL.

a. Colorimetric determination by 1,10-phenanthroline.
b. Calculated from the decrease in the amount of oxygen uptake measured with 100 nmol of thiosulfate.
c. No oxygen consumption observed.
d. Defined as : (Total number of electrons transferred to exogenous ferric iron from the oxidation of thiosulfate ÷ Total number of electrons available from the oxidation of thiosulfate) x 100 %

Electron count based on 4 electrons equivalent to one molecular oxygen consumed ($O_2 + 4e^- + 4H^+ \rightarrow 2H_2O$). Since the complete oxidation of 100 nmol of thiosulfate consumed 200 nmol of oxygen ($S_2O_3^{2-} + 2O_2 + H_2O \rightarrow 2SO_4^{2-} + 2H^+$), then the consumption of 200 nmol of oxygen was made possible by 800 nmol of electrons.

**Table 7.** Summary of total oxygen consumed and the amount of reaction products formed after the reduction of exogenous ferric iron by thiosulfate oxidation

| Components of reaction mixture | Total oxygen consumed (nmol) | Total ferrous iron formed (nmol) | Total sulfite formed (nmol) |
|---|---|---|---|
| Cells + thiosulfate [a] | 194 (200) | 4 | 3 |
| Cells + HQNO [b] + thiosulfate | 167 (150) | 5 | 97 (100) |
| Cells + ferric iron [c] + thiosulfate | 130 | 363 | 0 |
| Cells + ferric iron | 10 | 67 | 0 |
| | 363 – 67 = | 296 (280) | |
| Cells | 20 | 8 | 7 |
| Cells + HQNO | 20 | 1 | 5 |
| Cells + HQNO + ferric iron + thiosulfate [d] | 180 | 185 | 0 |
| HQNO + ferric iron + thiosulfate | 0 | 5 | 0 |

The reactions were incubated for 15 min at 25°C in 0.1 M β-alanine-$H_2SO_4$ pH 3 and contained 32 mg of cells and components as specified. The volume of the reaction mixtures was 1.6 mL.

( ) denotes expected values.

a. 100 nmol. thiosulfate.
b. 3.6 μM HQNO.
c. 8.6 mM ferric iron.
d. A distinctively biphasic oxidation pattern was observed. An initial rapid oxidation lasting less than a minute generated a stoichiometry very similar to thiosulfate oxidation via the thiosulfate oxidizing enzyme pathway to sulfite (Pathway B in Masau *et al.*, 2001). The final slow oxidation pattern may be a chemical reaction of sulfite with oxygen catalyzed by ferric iron as reported in Table 5. Reduction of ferric iron was distinct and was observed in all other instances as well. At the present time an adequate explanation cannot be proposed.

**Table 8.** Reduction of exogenous ferric iron by formate oxidation

| Components of reaction mixture | Concentration of ferric iron (mM) | Total oxygen consumed (nmol) | Total ferrous iron formed (nmol) | Degree of coupling [d] (%) |
|---|---|---|---|---|
| a) Cells + ferric iron + formate [a] | 0.0 | | 13 | |
| | 1.0 | | 185 | |
| | 2.1 | | 176 | |
| | 4.3 | | 221 | |
| | 8.6 | | 243 | |
| b) Cells + ferric iron + formate [b] | 0.0 | 50 | 0 | |
| | 1.0 | 30 | 80 | 40 |
| | 2.1 | 26 | 96 | 48 |
| | 4.3 | 20 | 120 | 60 |
| | 8.6 | 12 | 152 | 76 |
| c) Cells + ferric iron | 0.0 | | 1 | |
| | 1.0 | | 19 | |
| | 2.1 | | 20 | |
| | 4.3 | | 29 | |
| | 8.6 | | 49 | |
| d) Ferric iron + formate | 8.6 | | 3 [c] | |
| e) difference between a) and c) | 0.0 | | 12 | |
| | 1.0 | | 166 | 83 |
| | 2.1 | | 156 | 78 |
| | 4.3 | | 192 | 96 |
| | 8.6 | | 194 | 97 |

The reactions were incubated for 15 min at 25°C in 0.1 M β-alanine-$H_2SO_4$ pH 3 and contained 25 mg of cells, $FeCl_3$ as specified, and 100 nmol of formate. The volume of the reaction mixtures was 1.4 mL.

a. Colorimetric determination by 1,10-phenanthroline.
b. Calculated from the decrease in the amount of oxygen uptake measured with 100 nmol of formate.
c. No oxygen consumption observed.
d. Defined as : (Total number of electrons transferred to exogenous ferric iron from the oxidation of formate ÷ Total number of electrons available from the oxidation of formate) x 100 %

Electron count based on 4 electrons equivalent to one molecular oxygen consumed ($O_2 + 4e^- + 4H^+ \rightarrow 2H_2O$). Since the complete oxidation of 100 nmol of formate consumed 50 nmol of oxygen ($HCOOH + \frac{1}{2}O_2 \rightarrow H_2O + CO_2$), then the consumption of 50 nmol of oxygen was made possible by 200 nmol of electrons.

**Table 9** Reduction of exogenous ferric iron by exogenous substrate oxidation during anaerobic incubation

| Components of Reaction mixture | Total ferrous iron formed (nmol) | Degree of coupling [c] (%) |
|---|---|---|
| cells | 7 | |
| cells + ferric iron [a] | 72 | |
| + 156 nmol DMSO/sulfur | 456<br>456 – 72 = 384 | 41 |
| + 1 mmol Tween 80 sulfur | 892<br>892 – 72 = 820 [b] | |
| + 100 nmol thiosulfate | 662<br>662 – 72 = 590 | 74 |
| + 100 nmol formate | 163<br>163 – 72 = 91 | 40 |
| + 100 nmol sulfite | 65 | |

The reactions were incubated for 15 min under $N_{2(g)}$ at 25°C in 0.1 M β-alanine-$H_2SO_4$ pH 3 and contained 20 mg of cells, $FeCl_3$ as specified, and exogenous substrates at the amounts specified. The volume of the reaction mixtures was 1.4 mL. Chemical controls were performed in the absence of whole cells and ferrous iron detected after the 15 min incubation period were negligible.

a. 8.6 mM ferric iron.
b. It was not possible to determine the exact amount of Tween 80 sulfur that reacted during the allotted time (15 min) during anaerobic incubation.
c. Defined as : (Total number of electrons transferred to exogenous ferric iron from the oxidation of an exogenous substrate ÷ Total number of electrons available from the oxidation of an exogenous substrate) x 100 % . Electron count was previously defined in Table 3 for DMSO/sulfur, Table 6 for thiosulfate, and Table 8 for formate.

# Figures

**Figure 1** Exogenous ferric iron reduction by endogenous respiration in various assay buffers. The reactions were performed at 25°C in the buffers specified and contained 20 mg of cells and 4 μmol of $FeCl_3$. The volume of the reaction mixtures was 1 mL . The results were based on 2 separate trials. The error bars are the standard deviation of the 2 trials.

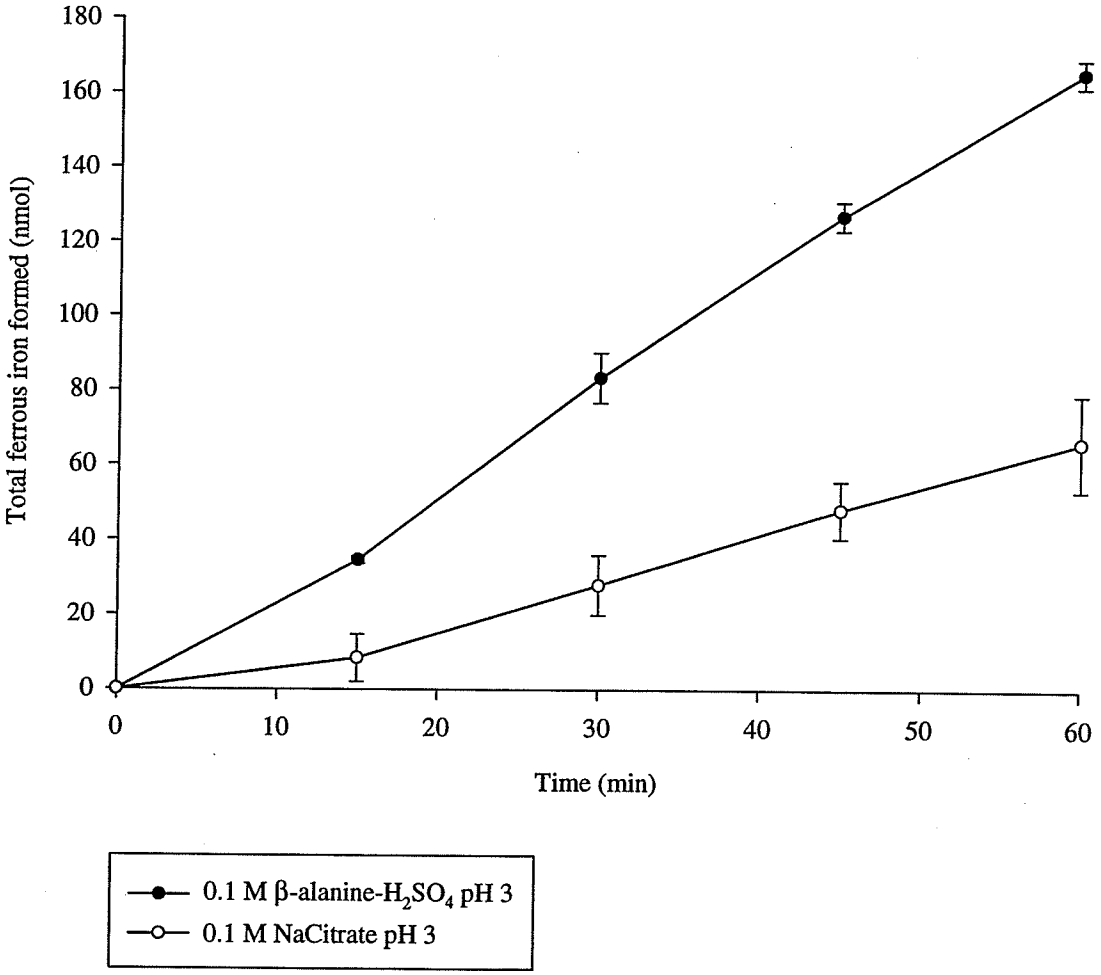
180
160
140
120
100
80
60
40
20
0
Total ferrous iron formed (nmol)
0
10
20
30
40
50
60
Time (min)
0.1 M β-alanine-H2SO4 pH 3
0.1 M NaCitrate pH 3

**Figure 2** Exogenous ferric iron reduction by endogenous respiration in different concentrations of β-alanine-$H_2SO_4$ pH 3 . The reactions were performed at 25°C in β-alanine-$H_2SO_4$ pH 3 buffers of specified concentrations with each containing 20 mg of cells and 4 μmol $FeCl_3$. The volume of the reaction mixtures was 1 mL . The results were based on 2 separate trials. The error bars are the standard deviation of the 2 trials.

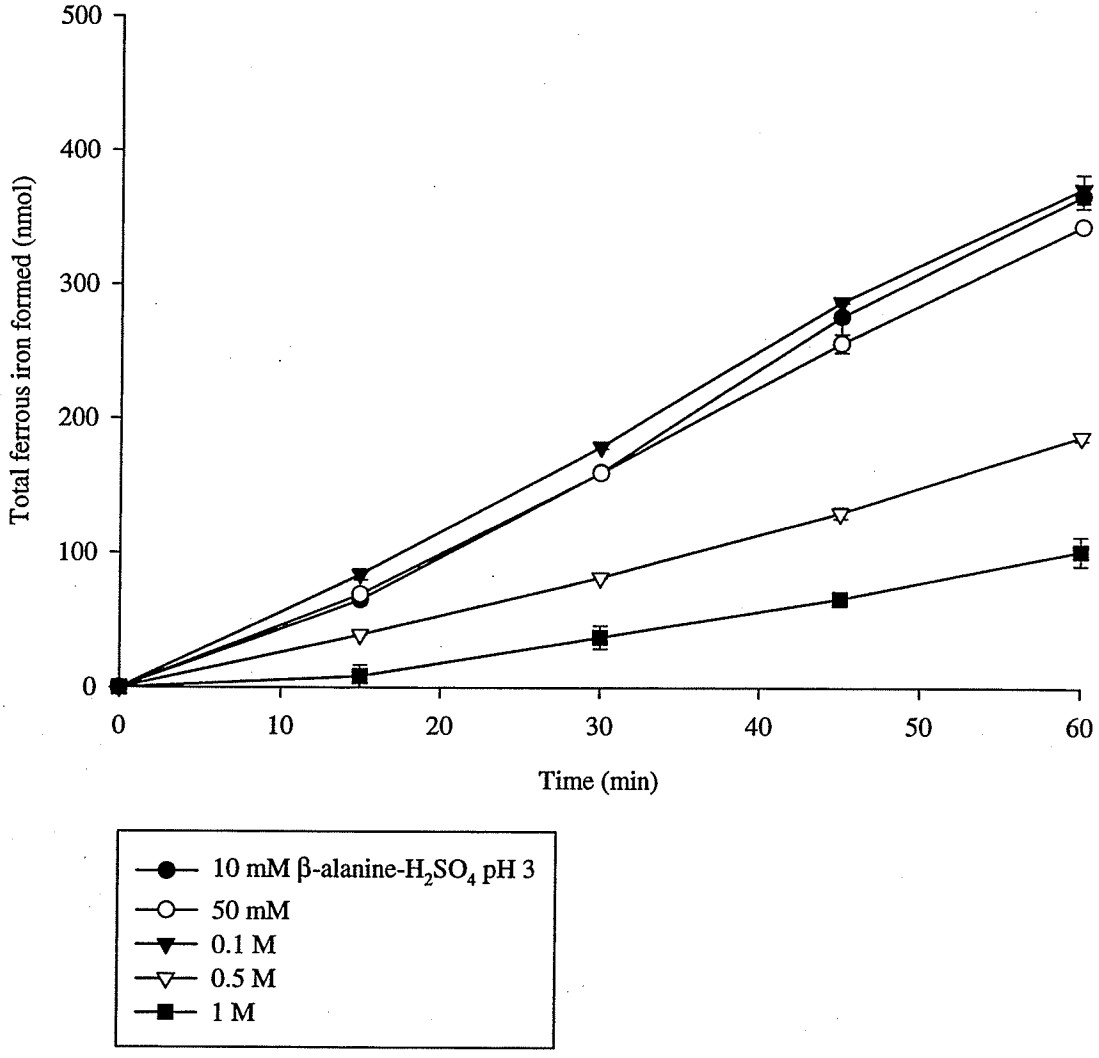
500
400
300
200
100
0
Total ferrous iron formed (nmol)
0
10
20
30
40
50
60
Time (min)
10 mM β-alanine-H2SO4 pH 3
50 mM
0.1 M
0.5 M
1 M

**Figure 3** Endogenous respiration in the presence of increasing concentrations of exogenous ferric iron. **a)** Oxygen consumption by endogenous respiration in the presence of increasing concentrations of exogenous ferric iron. **b)** Ferrous iron formation by endogenous respiration in the presence of increasing concentrations of exogenous ferric iron. Expected ferrous iron formation was also determined based on inhibition of oxygen consumption ($O_2 + 4e^- + 4H^+ \rightarrow 2H_2O$ ; $Fe^{3+} + e^- \rightarrow Fe^{2+}$). The reactions were performed at 25°C in 0.1 M β-alanine-$H_2SO_4$ pH 3 and contained 112 mg of cells and exogenous ferric iron as specified. The volume of the reaction mixtures was 1.4 mL .

3 (a)

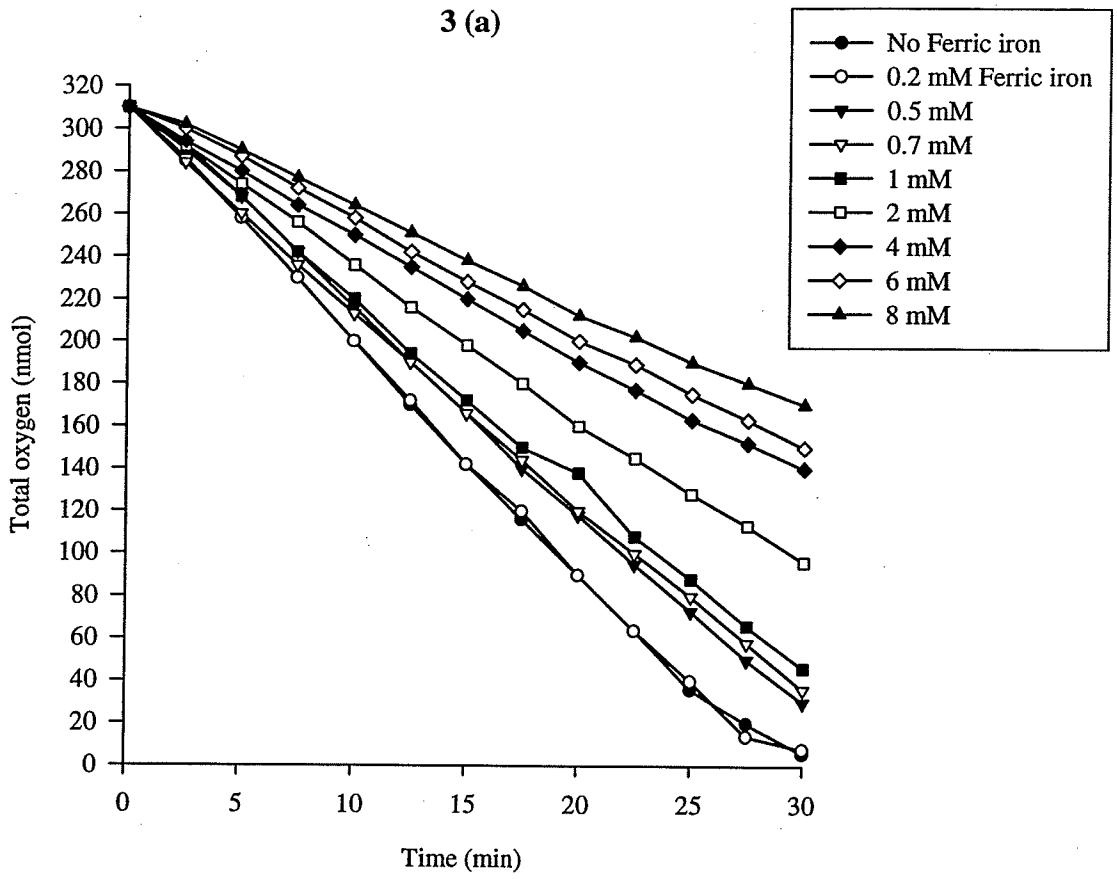
No Ferric iron
0.2 mM Ferric iron
0.5 mM
0.7 mM
1 mM
2 mM
4 mM
6 mM
8 mM
Total oxygen (nmol)
320
300
280
260
240
220
200
180
160
140
120
100
80
60
40
20
0
0
5
10
15
20
25
30
Time (min)

3 (b)

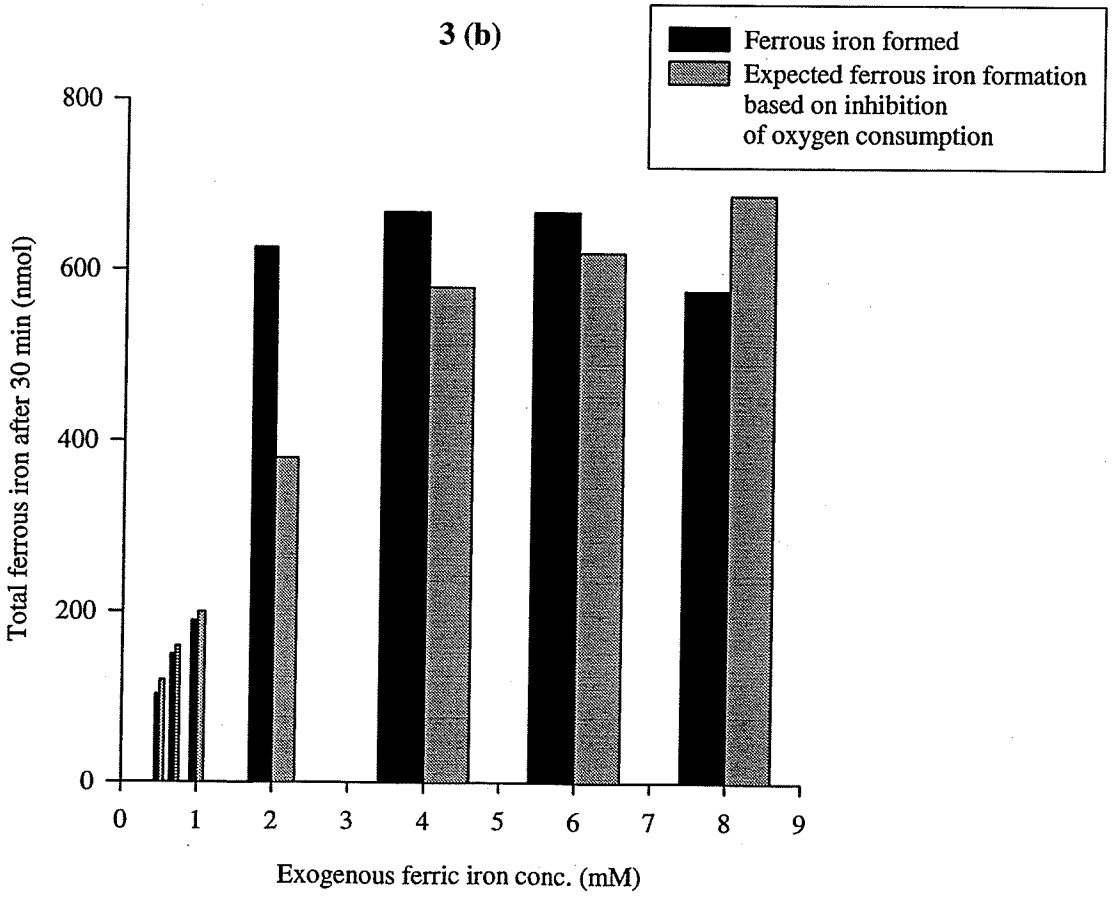
Ferrous iron formed
Expected ferrous iron formation based on inhibition of oxygen consumption
Total ferrous iron after 30 min (nmol)
800
600
400
200
0
0
1
2
3
4
5
6
7
8
9
Exogenous ferric iron conc. (mM)

**Figure 4** Oxygen consumption by endogenous respiration by various cell concentrations. Reactions were performed at 25°C in 0.1 M β-alanine-$H_2SO_4$ pH 3 and contained cell concentrations as specified. The volume of the reaction mixtures was 1.2 mL .

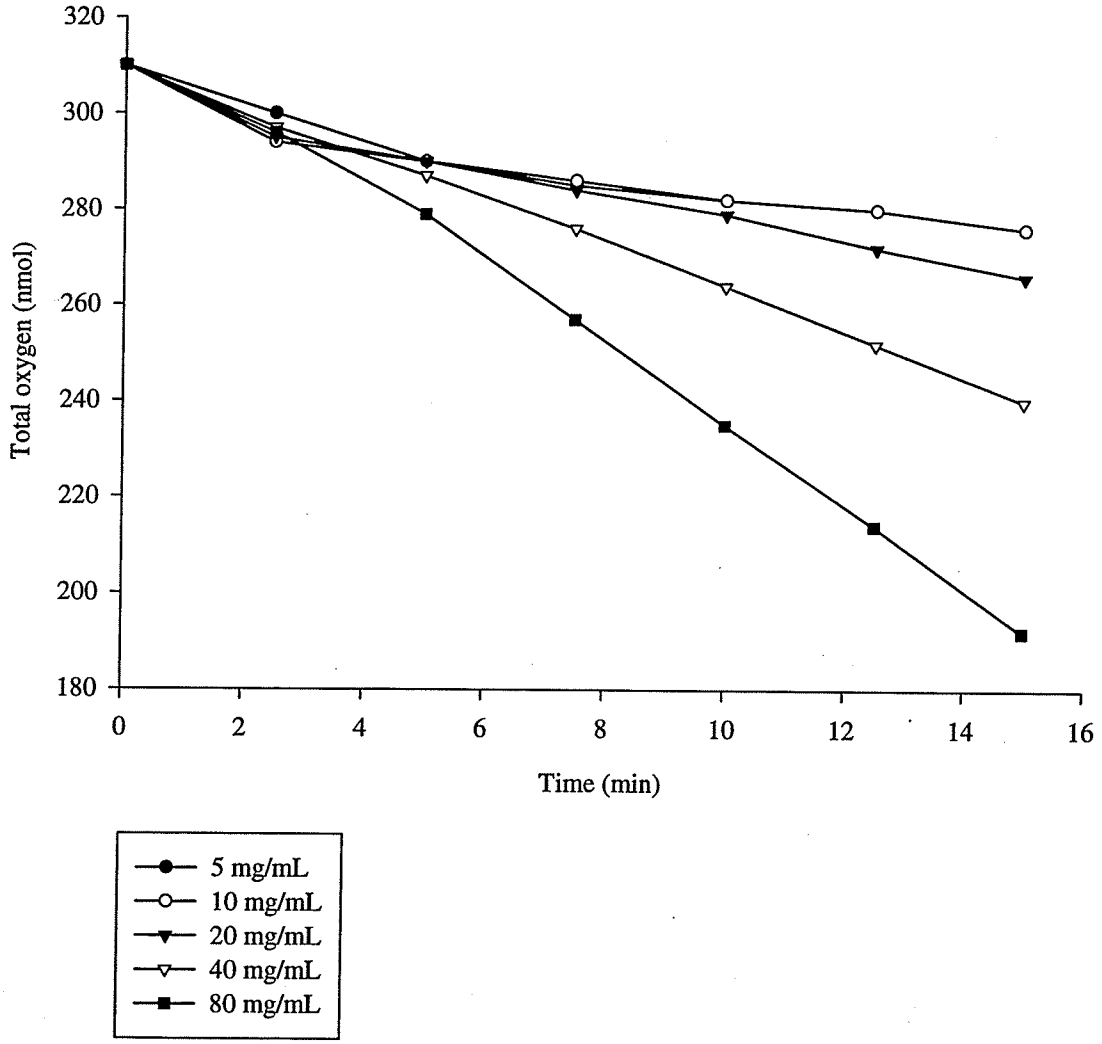
320
300
280
260
240
220
200
180
Total oxygen (nmol)
0
2
4
6
8
10
12
14
16
Time (min)
5 mg/mL
10 mg/mL
20 mg/mL
40 mg/mL
80 mg/mL

**Figure 5** Exogenous ferric iron reduction by endogenous respiration during aerobic and anaerobic incubation (under $N_{2(g)}$). The reactions were performed at 25°C in 0.1 M β-alanine-$H_2SO_4$ pH 3 and contained 20 mg of cells and 4 μmol of $FeCl_3$. The volume of the reaction mixtures was 1 mL . The results were based on 3 separate trials. The error bars are the standard deviation of the 3 trials.

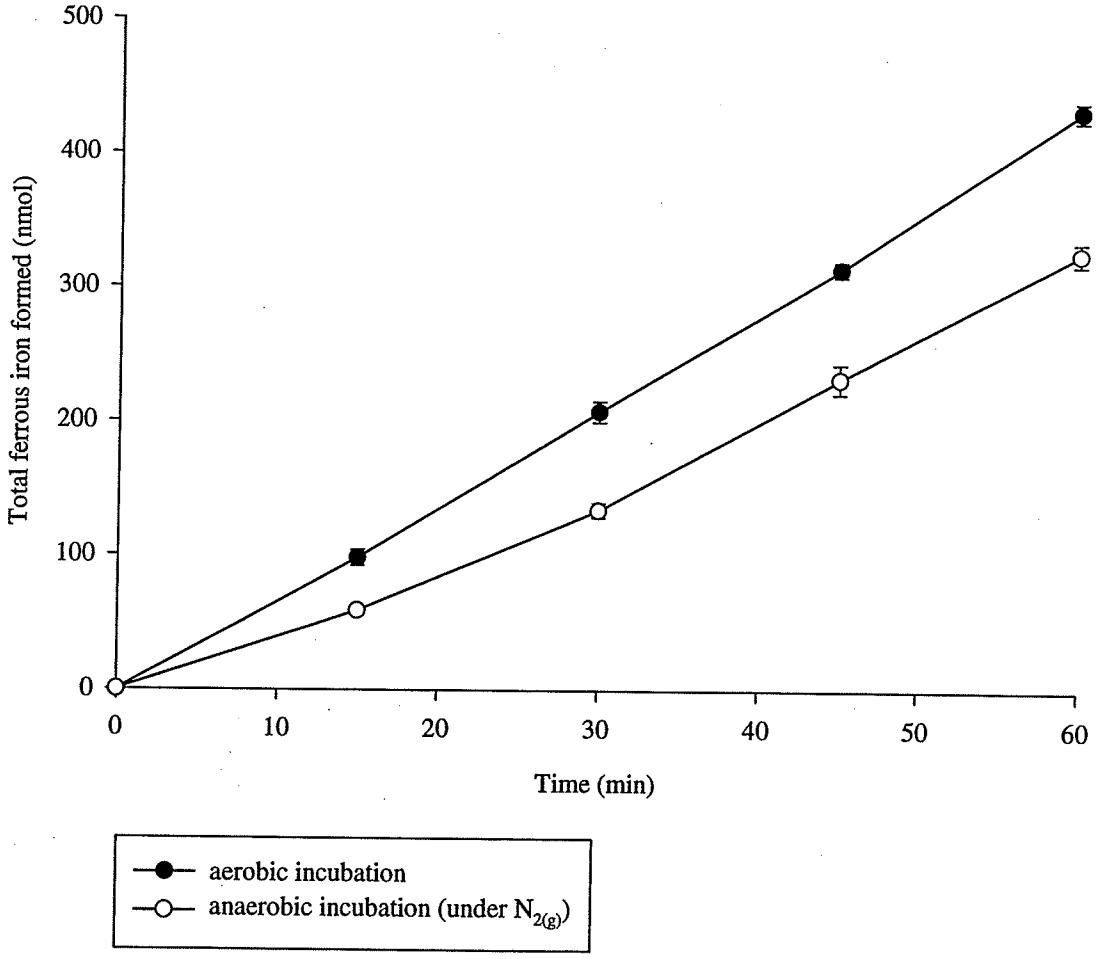
500
400
300
200
100
0
Total ferrous iron formed (nmol)
0
10
20
30
40
50
60
Time (min)
aerobic incubation
anaerobic incubation (under $N_{2(g)}$)

**Figure 6** The effect of varying concentrations of cyanide on endogenous respiration by exogenous ferric iron reduction. The reactions were performed at 25°C in 0.1 M β-alanine-$H_2SO_4$ pH 3 and contained 20 mg of cells, 4 μmol $FeCl_3$, and KCN at the concentrations specified. The volume of the reaction mixtures was 1 mL . The results were based on 2 separate trials. The error bars are the standard deviation of the 2 trials.

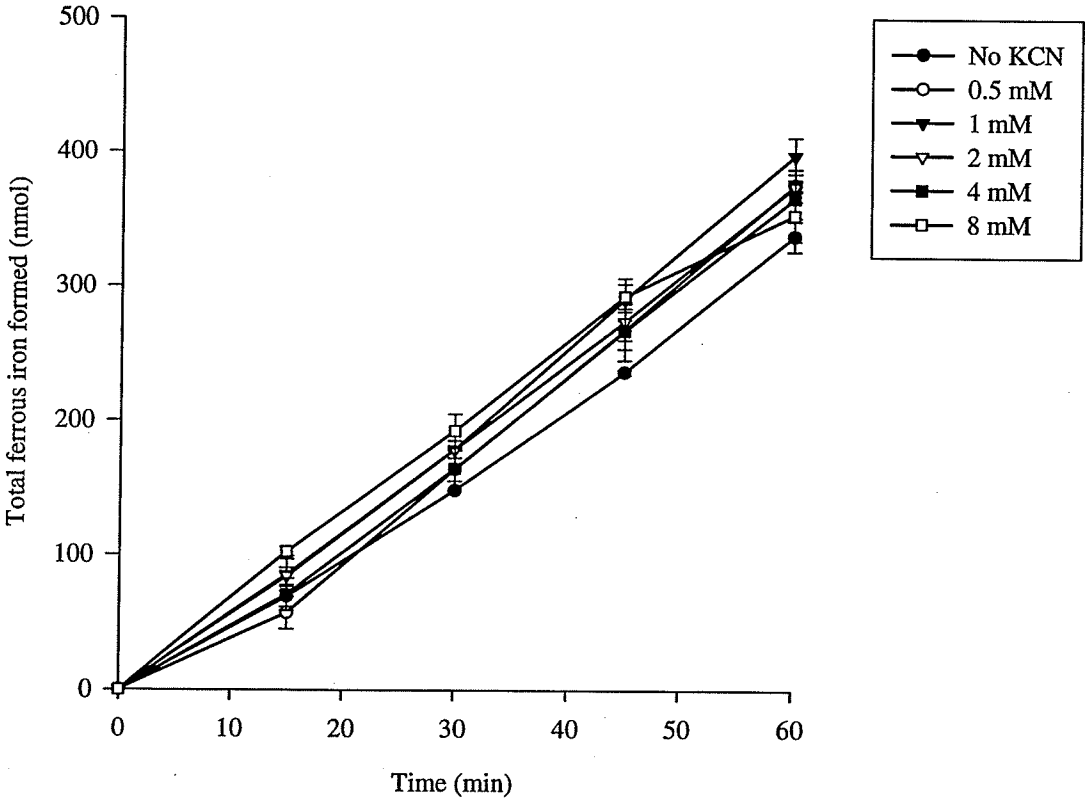
500
400
300
200
100
0
Total ferrous iron formed (nmol)
0
10
20
30
40
50
60
Time (min)
No KCN
0.5 mM
1 mM
2 mM
4 mM
8 mM

**Figure 7** Exogenous ferric iron reduction by endogenous respiration by a 5 mg/mL cell concentration. **a)** Michaelis-Menten Plot. **b)** Lineweaver-Burk Plot. **c)** $K_i$ determination. The reactions were performed at 25°C in 0.1 M β-alanine-$H_2SO_4$ pH 3 and contained 5 mg of cells and $FeCl_3$ as specified. The volume of the reaction mixtures was 1 mL . The results were based on two separate trials. The error bars are the standard deviation of the 2 trials. The rates were corrected for the release of endogenous reduced iron.

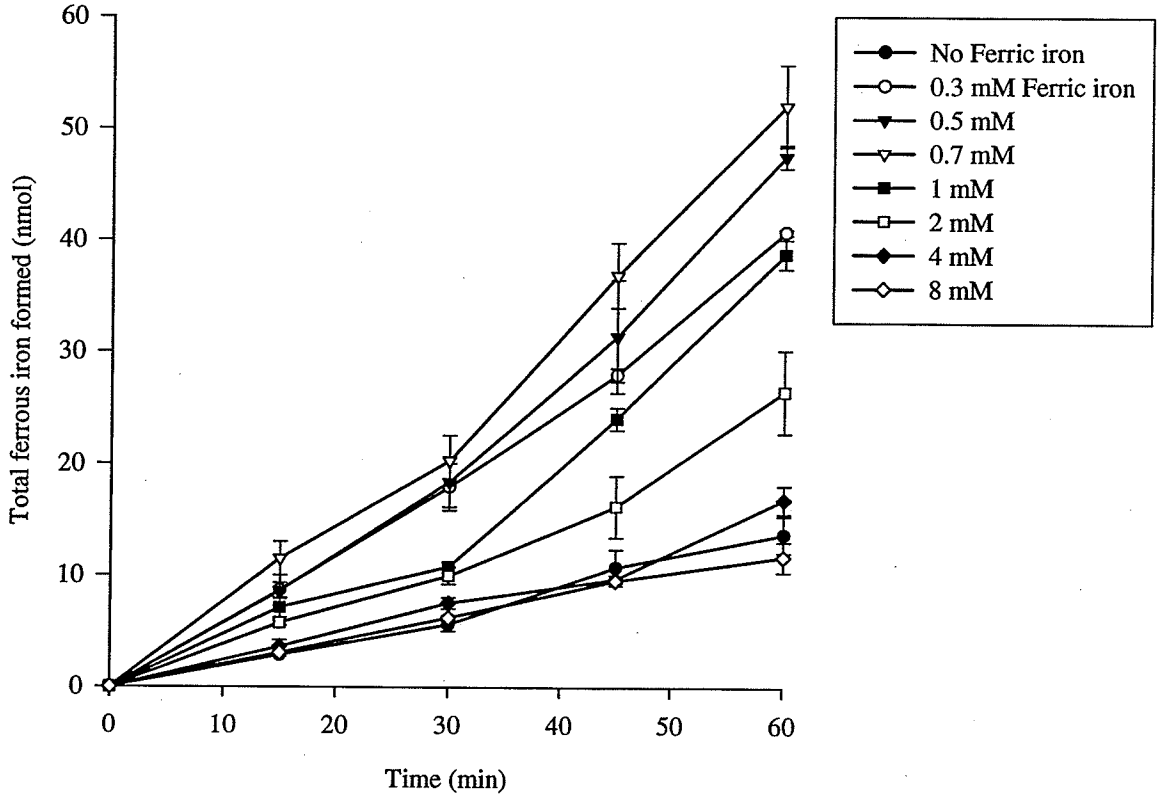


**a) Michaelis-Menten Plot**

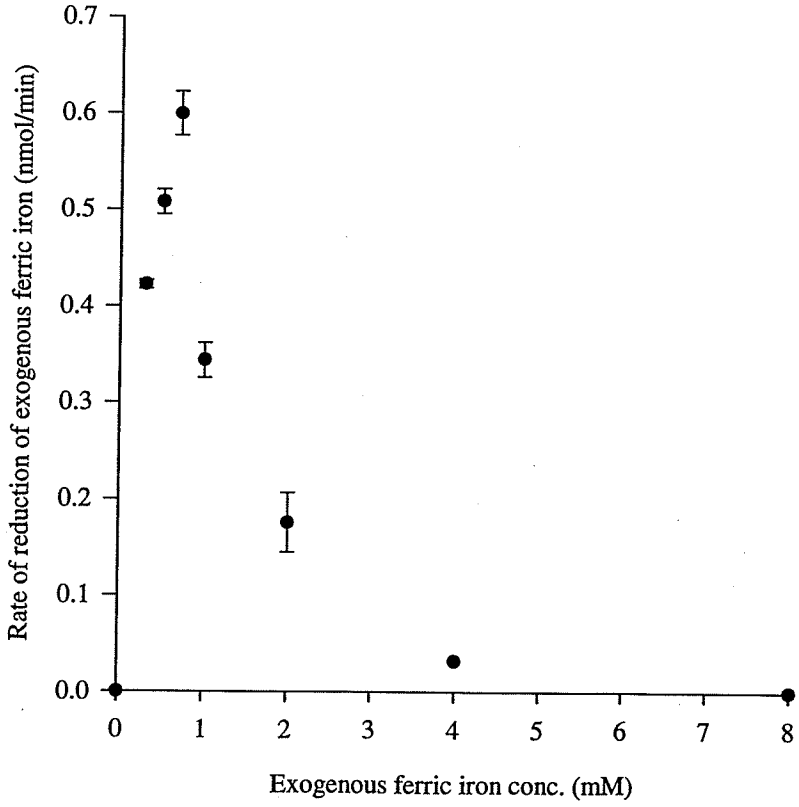

**b) Lineweaver-Burk Plot**

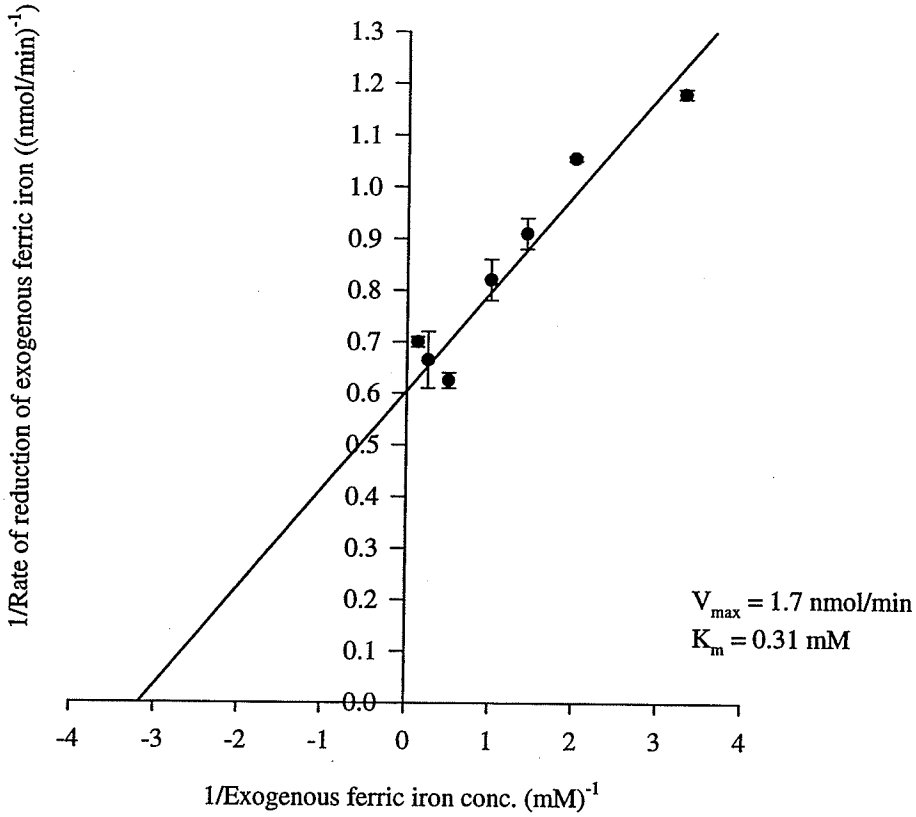


**c) $K_i$ Determination**

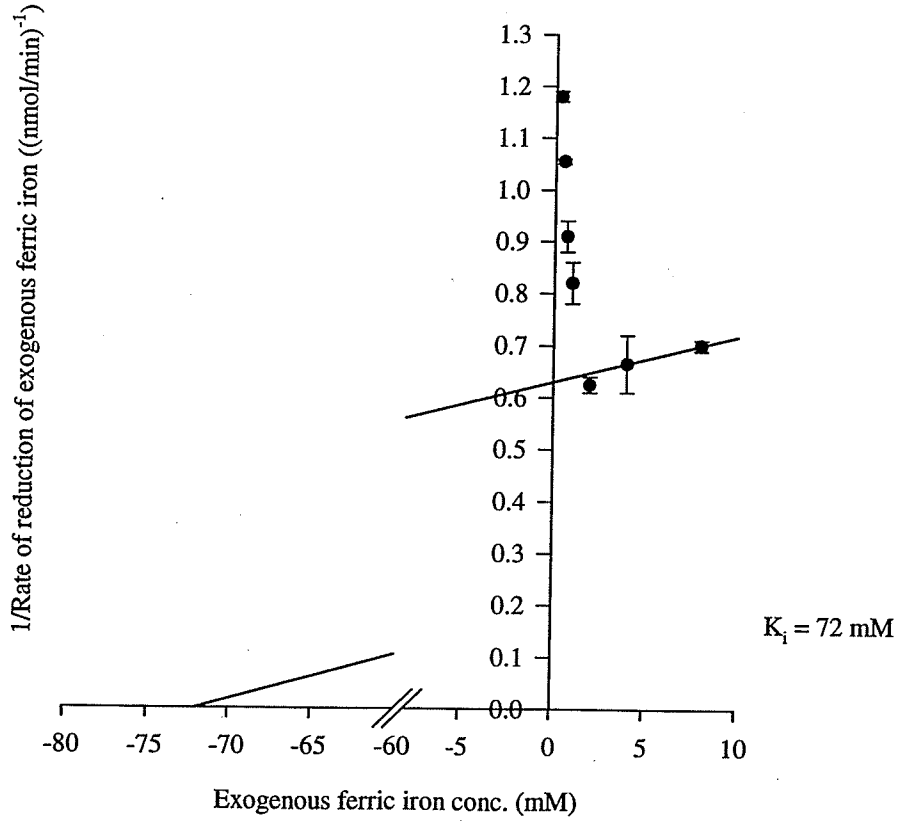

**Figure 8** Exogenous ferric iron reduction by endogenous respiration by a 10 mg/mL cell concentration. **a)** Michaelis-Menten Plot. **b)** Lineweaver-Burk Plot. **c)** $K_i$ determination. The reactions were performed at 25°C in 0.1 M β-alanine-$H_2SO_4$ pH 3 and contained 10 mg of cells and $FeCl_3$ as specified. The volume of the reaction mixtures was 1 mL . The results were based on two separate trials. The error bars are the standard deviation of the 2 trials. The rates were corrected for the release of endogenous reduced iron.

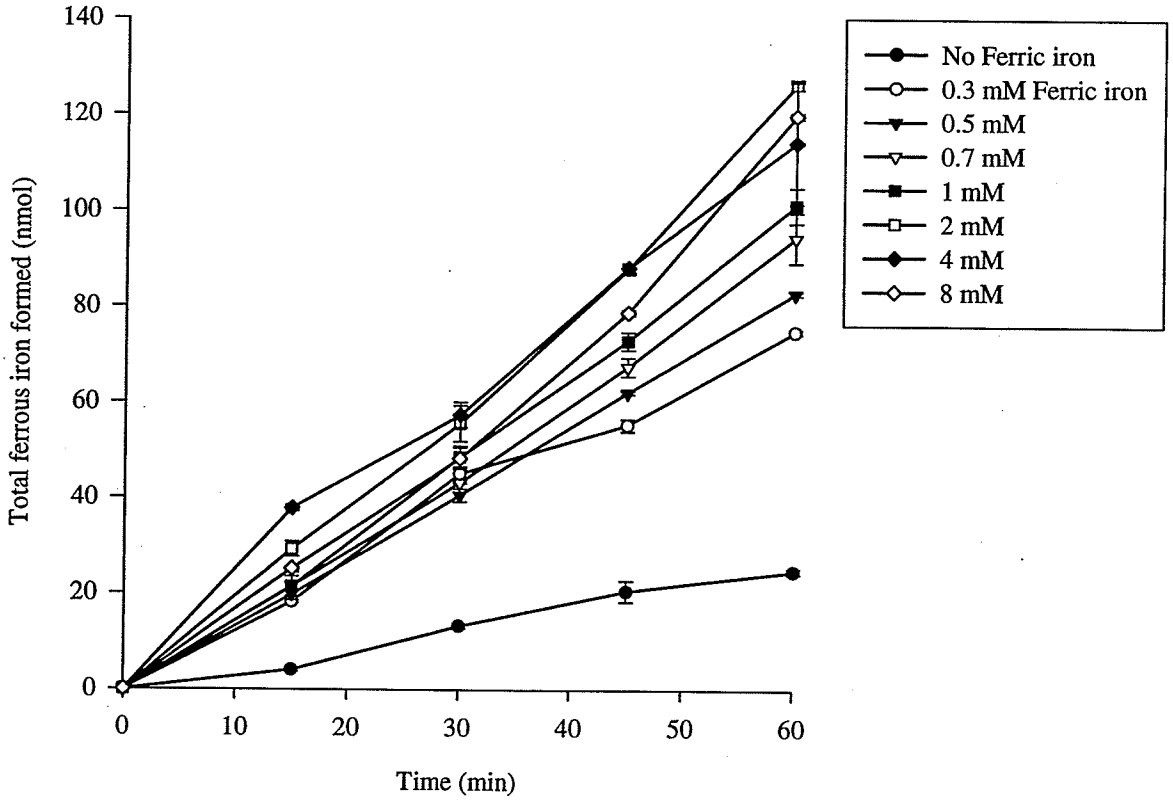


**a) Michaelis-Menten Plot**

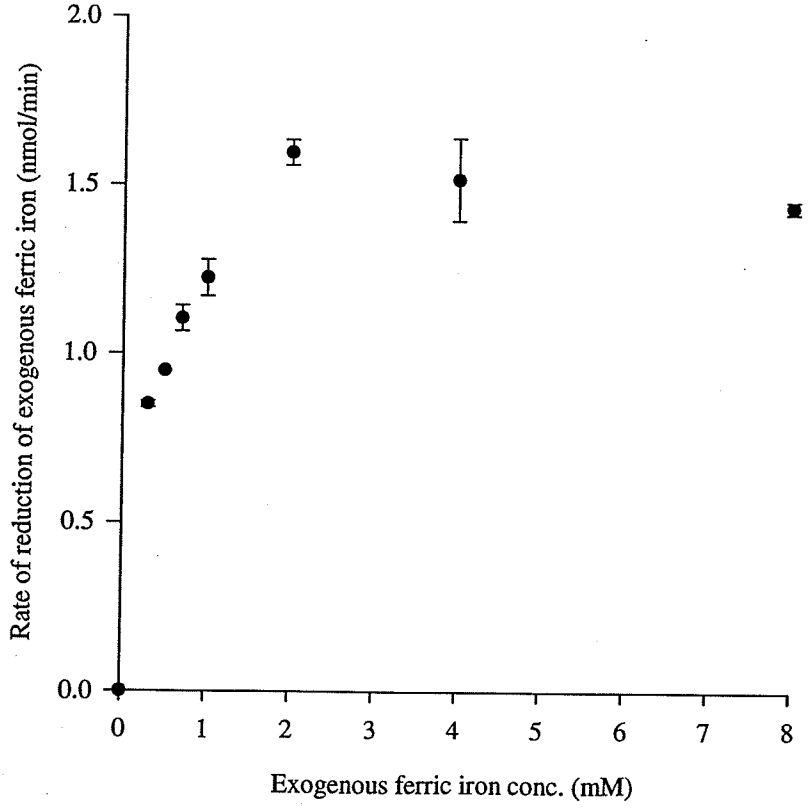

**b) Lineweaver-Burk Plot**

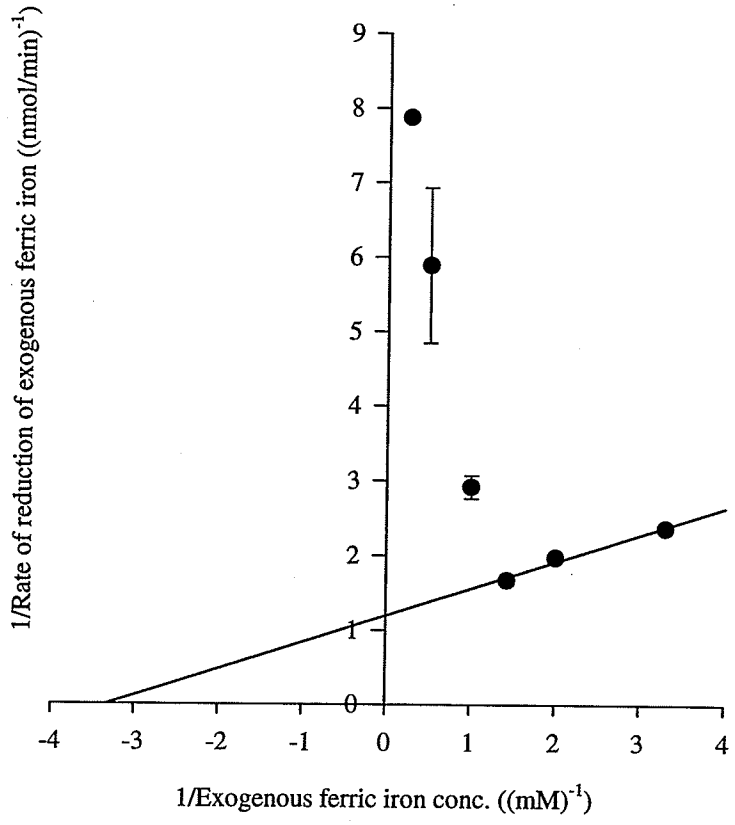


$V_{max}$ = 0.84 nmol/min
$K_m$ = 0.30 mM

**c) $K_i$ Determination**

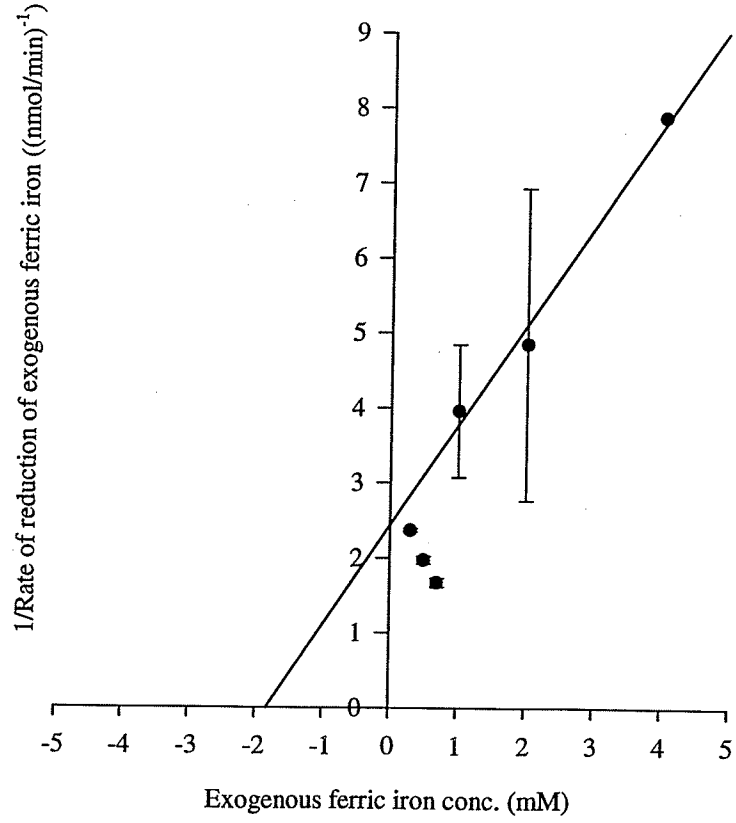


$K_i$ = 1.8 mM

**Figure 9** Exogenous ferric iron reduction by endogenous respiration by a 20 mg/mL cell concentration. **a)** Michaelis-Menten Plot. **b)** Lineweaver-Burk Plot. The reactions were performed at 25°C in 0.1 M β-alanine-$H_2SO_4$ pH 3 and contained 20 mg of cells and $FeCl_3$ as specified. The volume of the reaction mixtures was 1 mL . The results were based on two separate trials. The error bars are the standard deviation of the 2 trials. The rates were corrected for the release of endogenous reduced iron.

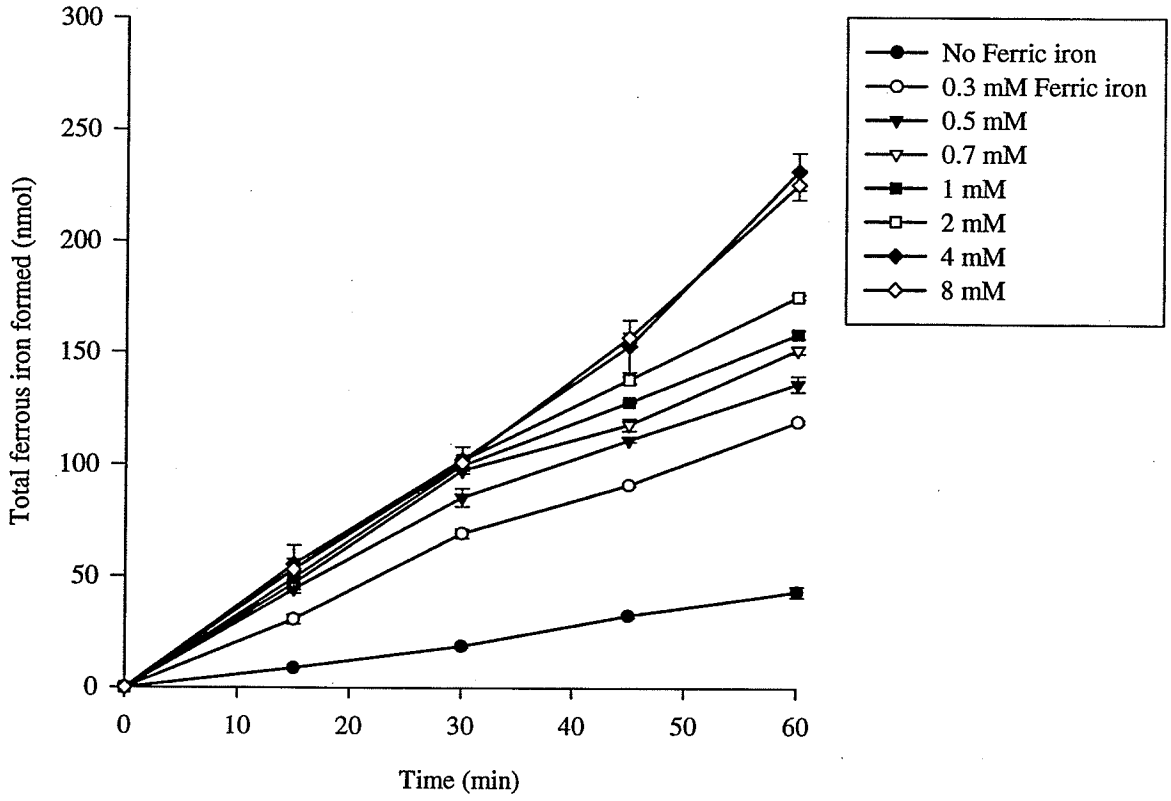


**a) Michaelis-Menten Plot**

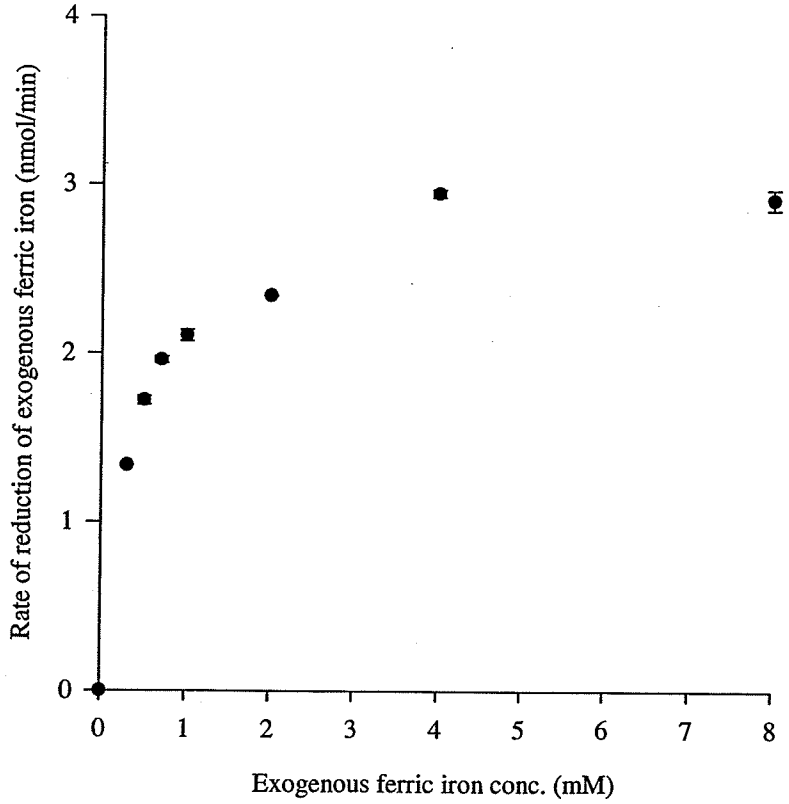

**b) Lineweaver-Burk Plot**

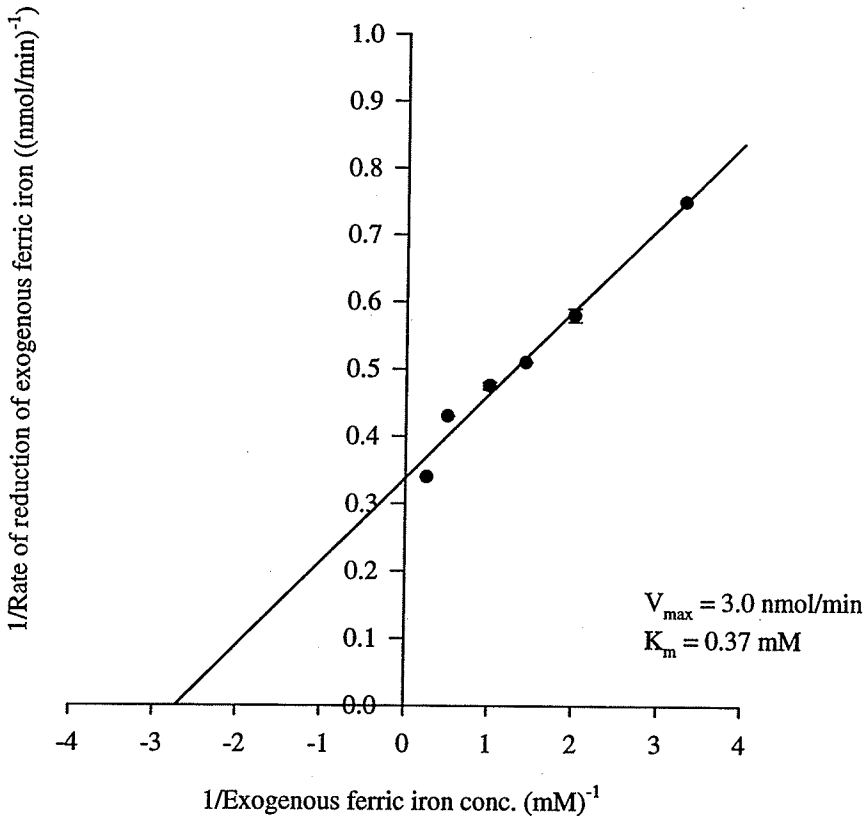

**Figure 10** Exogenous ferric iron reduction by endogenous respiration by a 40 mg/mL cell concentration. **a)** Michaelis-Menten Plot. **b)** Lineweaver-Burk Plot. **c)** Hill Plot. The reactions were performed at 25°C in 0.1 M β-alanine-$H_2SO_4$ pH 3 and contained 40 mg of cells and $FeCl_3$ as specified. The volume of the reaction mixtures was 1 mL . The results were based on two separate trials. The error bars are the standard deviation of the 2 trials. The rates were corrected for the release of endogenous reduced iron.

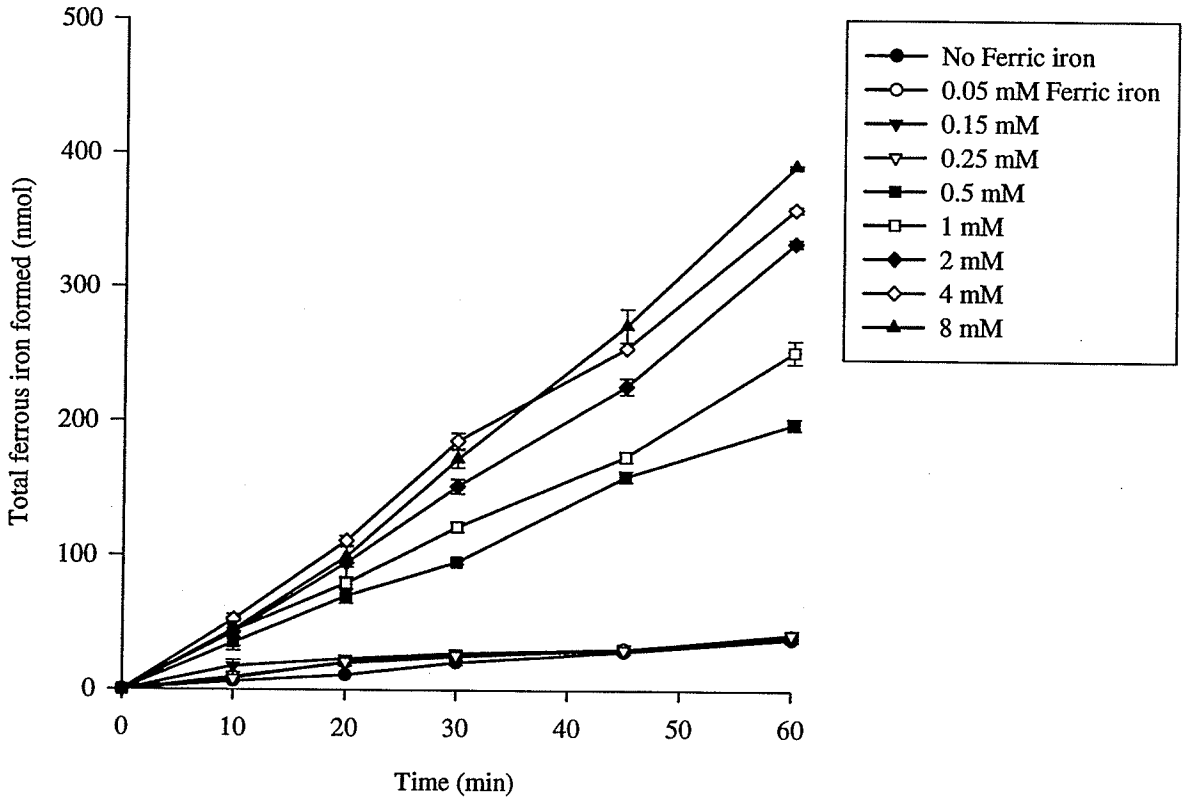


**a) Michaelis-Menten Plot**

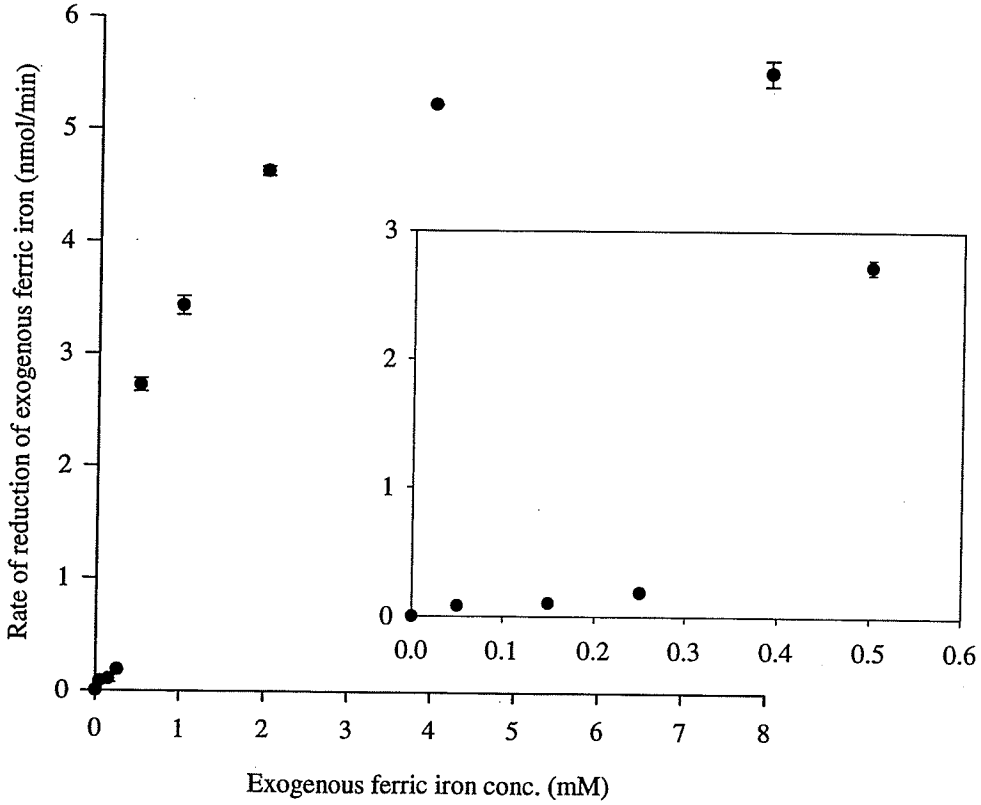

**b) Lineweaver-Burk Plot**

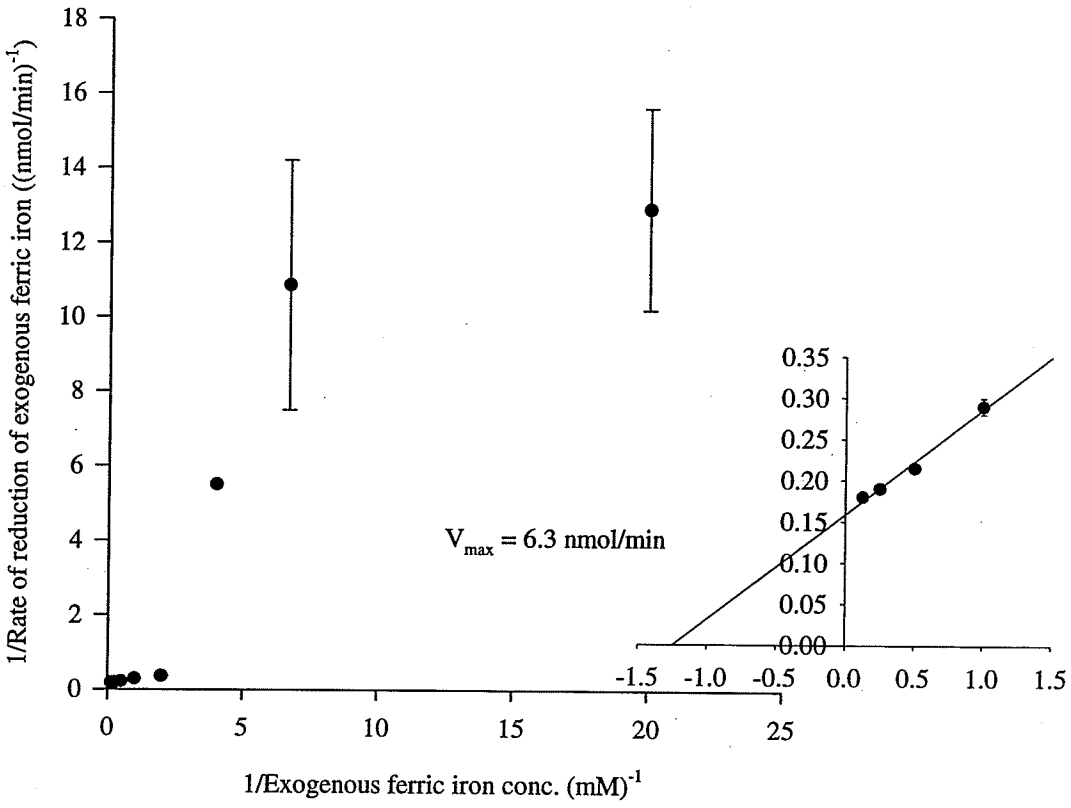


**c) Hill Plot**

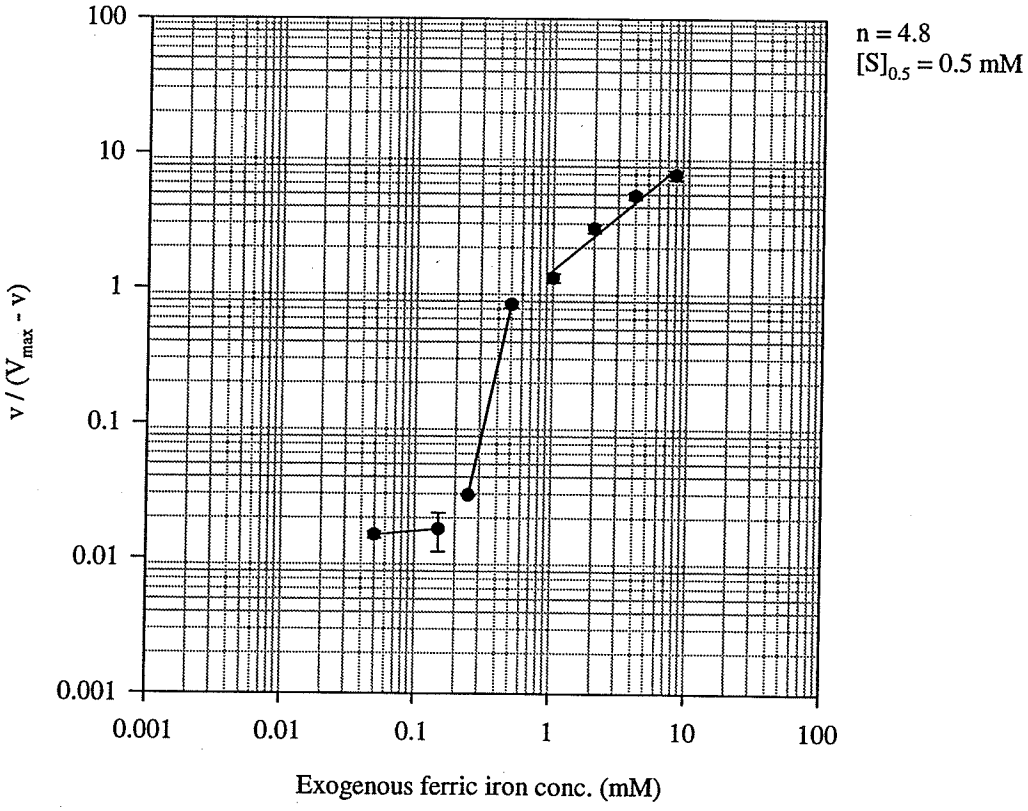

**Figure 11** Exogenous ferric iron reduction by endogenous respiration by a 80 mg/mL cell concentration. **a)** Michaelis-Menten Plot. **b)** Lineweaver-Burk Plot. **c)** Hill Plot.
The reactions were performed at 25°C in 0.1 M β-alanine-$H_2SO_4$ pH 3 and contained 80 mg of cells and $FeCl_3$ as specified. The volume of the reaction mixtures was 1 mL . The results were based on two separate trials. The error bars are the standard deviation of the 2 trials. The rates were corrected for the release of endogenous reduced iron.

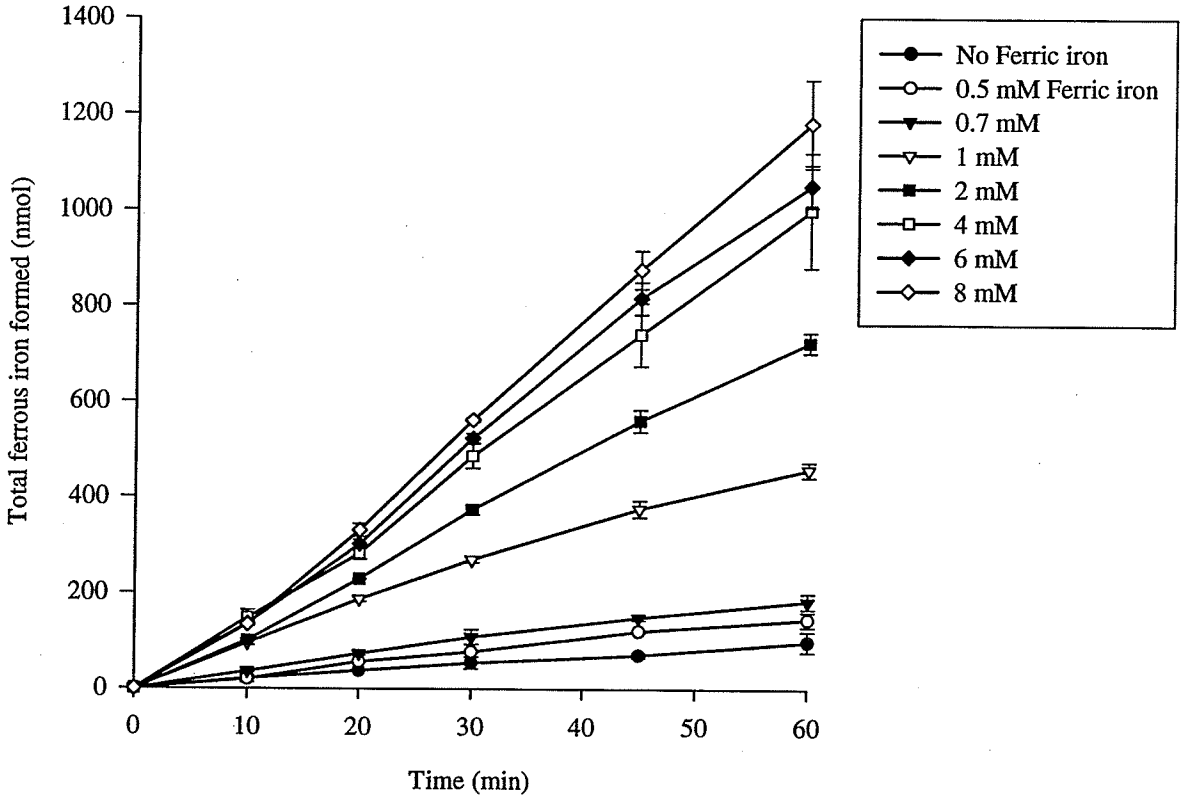


**a) Michaelis-Menten Plot**

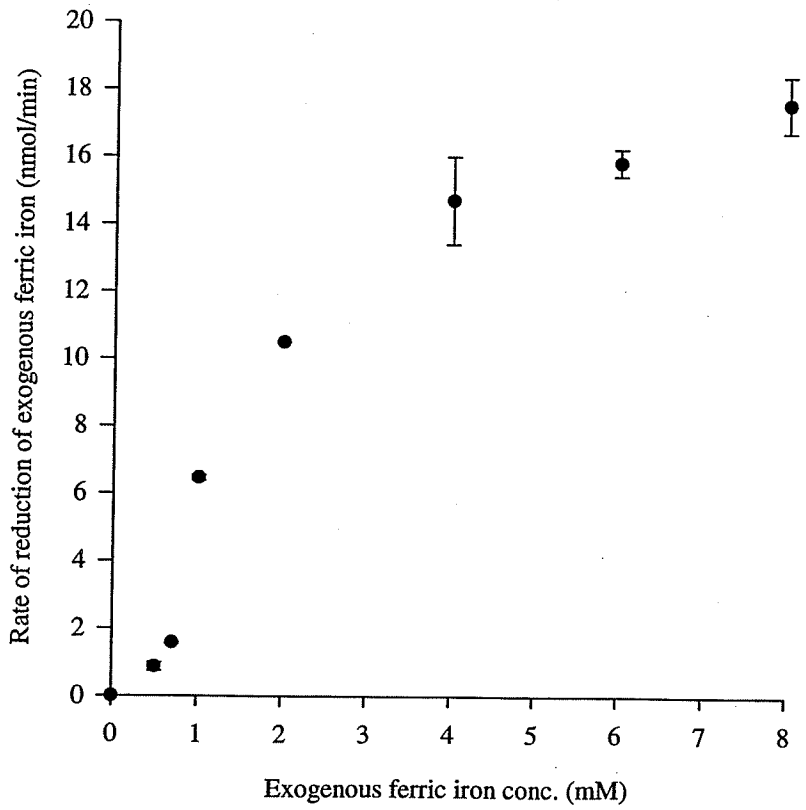

**b) Lineweaver-Burk Plot**

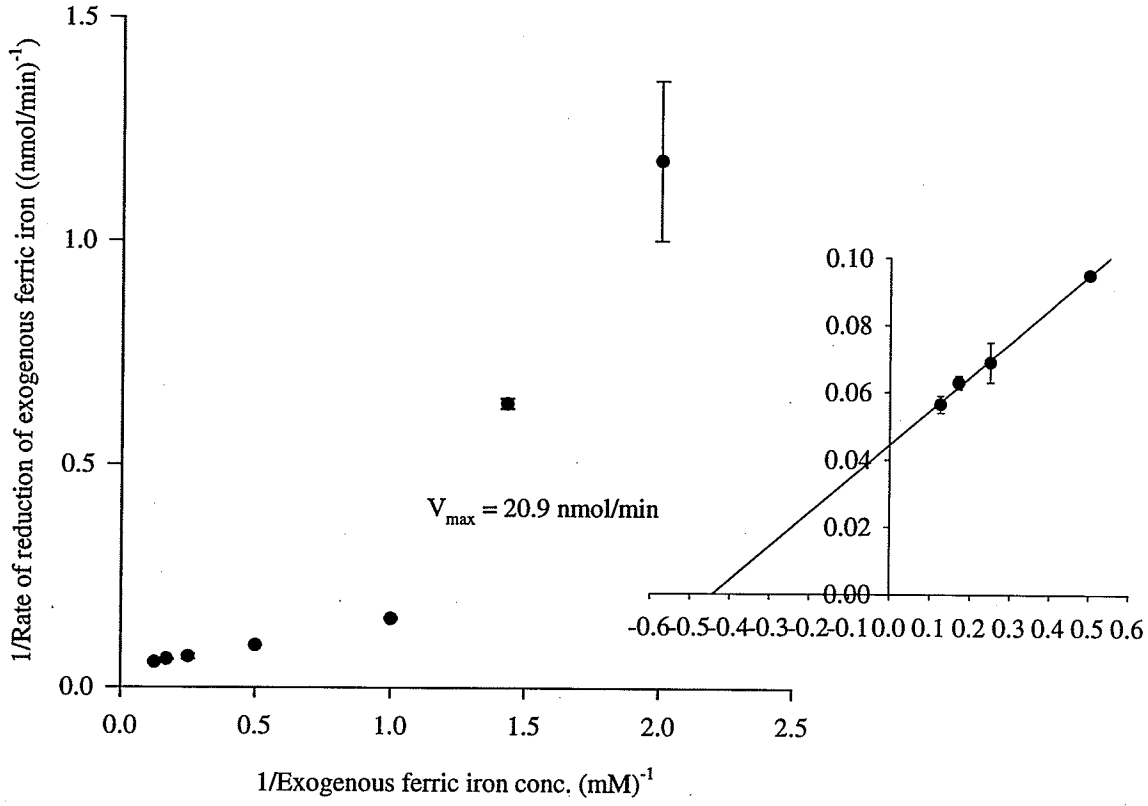


**c) Hill Plot**

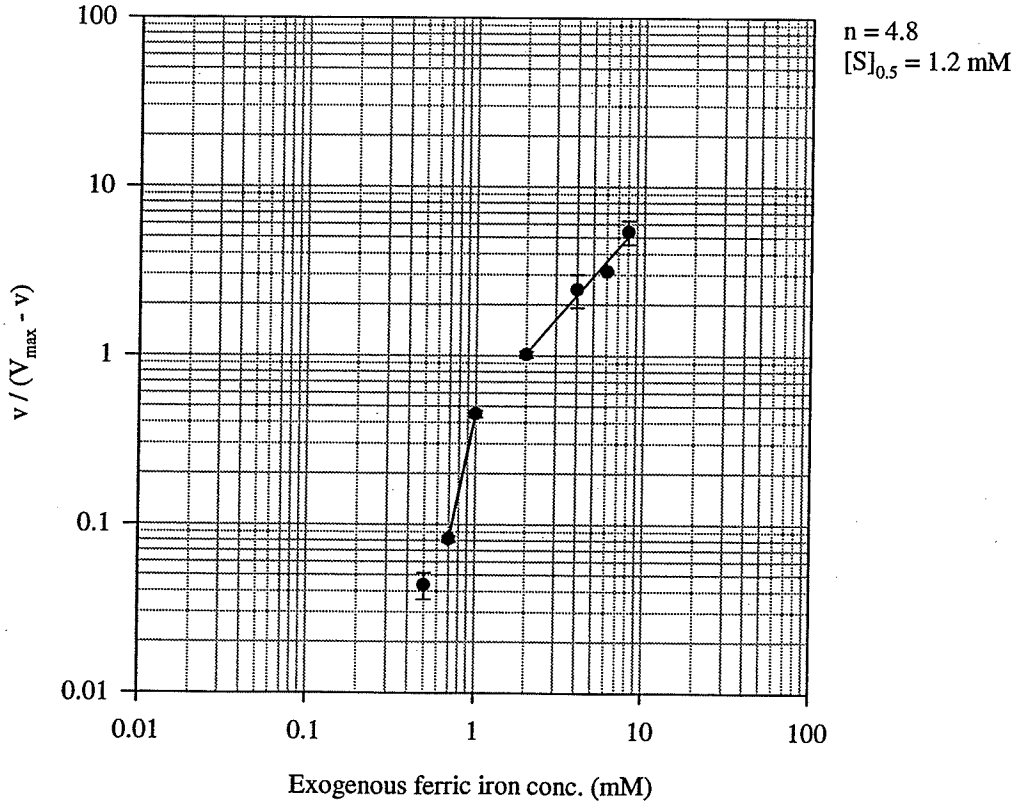

**Figure 12** Endogenous ferric iron reduction by endogenous respiration in various cell concentrations. **a)** Total iron (ferrous + ferric) and ferrous iron in the cell suspension. **b)** Total iron (ferrous + ferric) and ferrous iron in the supernatant of the cell suspension. **c)** Percent increase in ferrous iron in the cell suspension based on 0-time reading. The reactions were performed 25°C in 0.1 M β-alanine-$H_2SO_4$ pH 3 and contained cell concentrations as specified. The volume of the reaction mixture was 1 mL . Results were based on 2 separate trials. The error bars are the standard deviation of the 2 trials.

a)

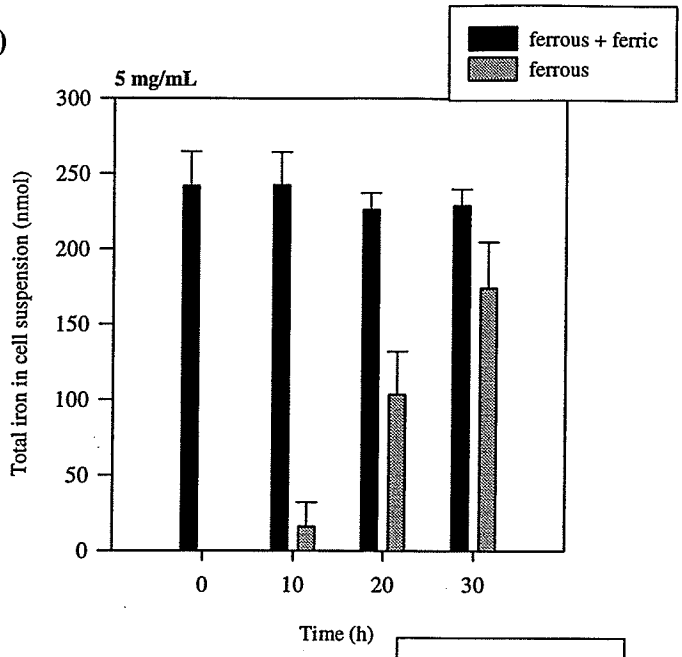
5 mg/mL
ferrous + ferric
ferrous
Total iron in cell suspension (nmol)
300
250
200
150
100
50
0
0
10
20
30
Time (h)

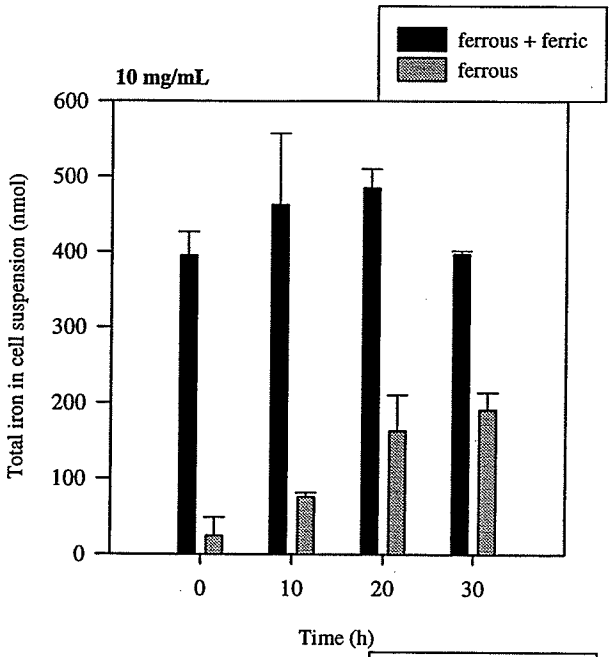
10 mg/mL
ferrous + ferric
ferrous
Total iron in cell suspension (nmol)
600
500
400
300
200
100
0
0
10
20
30
Time (h)

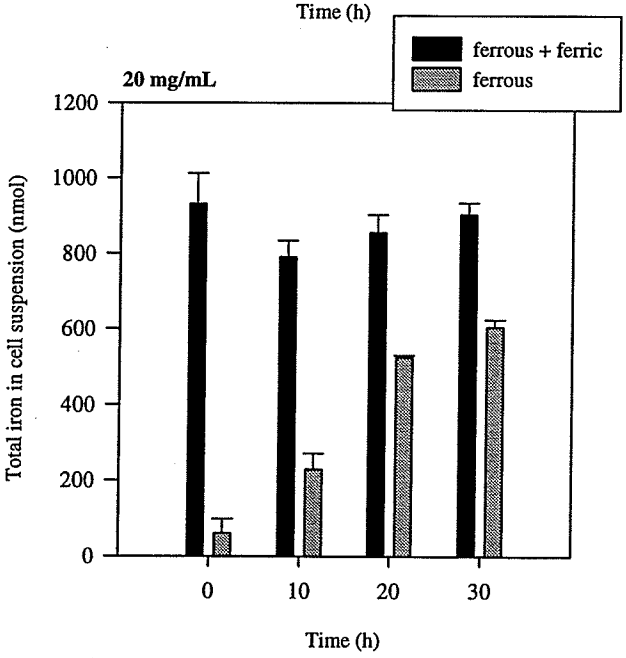
20 mg/mL
ferrous + ferric
ferrous
Total iron in cell suspension (nmol)
1200
1000
800
600
400
200
0
0
10
20
30
Time (h)

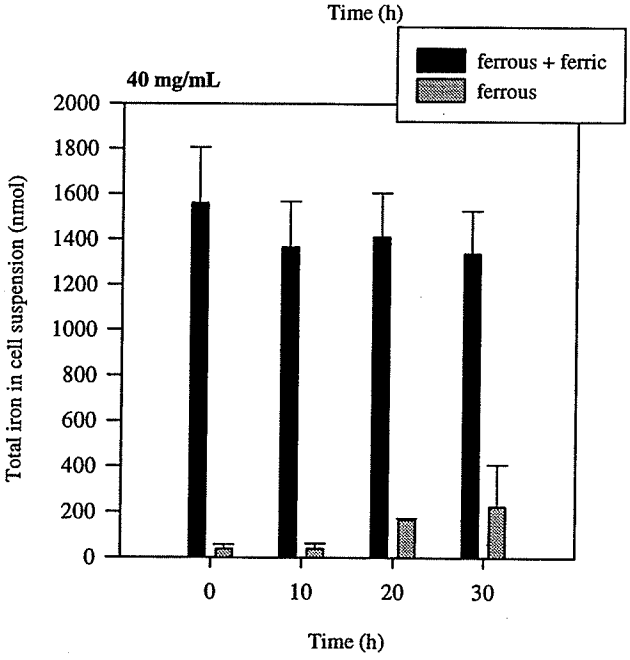
40 mg/mL
ferrous + ferric
ferrous
Total iron in cell suspension (nmol)
2000
1800
1600
1400
1200
1000
800
600
400
200
0
0
10
20
30
Time (h)

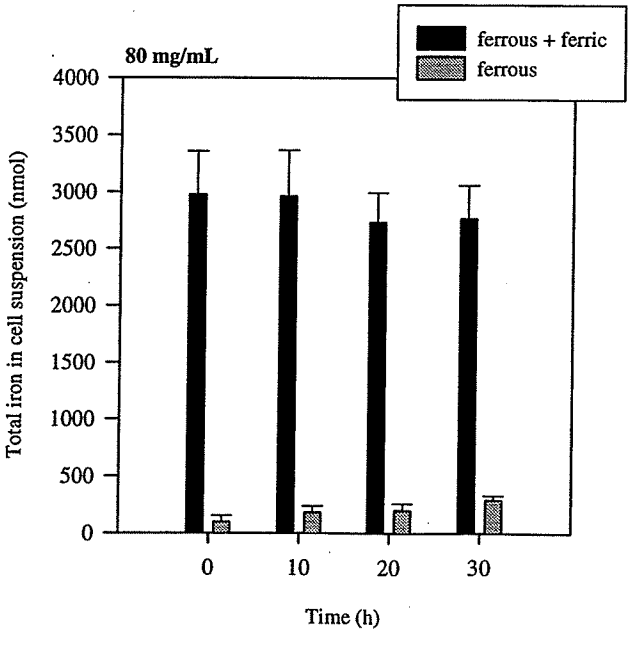
80 mg/mL
ferrous + ferric
ferrous
Total iron in cell suspension (nmol)
4000
3500
3000
2500
2000
1500
1000
500
0
0
10
20
30
Time (h)

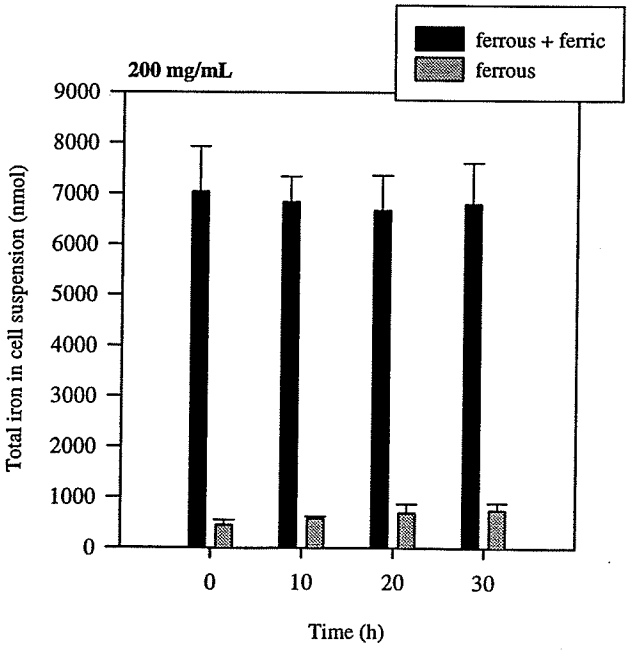
200 mg/mL
ferrous + ferric
ferrous
Total iron in cell suspension (nmol)
9000
8000
7000
6000
5000
4000
3000
2000
1000
0
0
10
20
30
Time (h)

**b)**

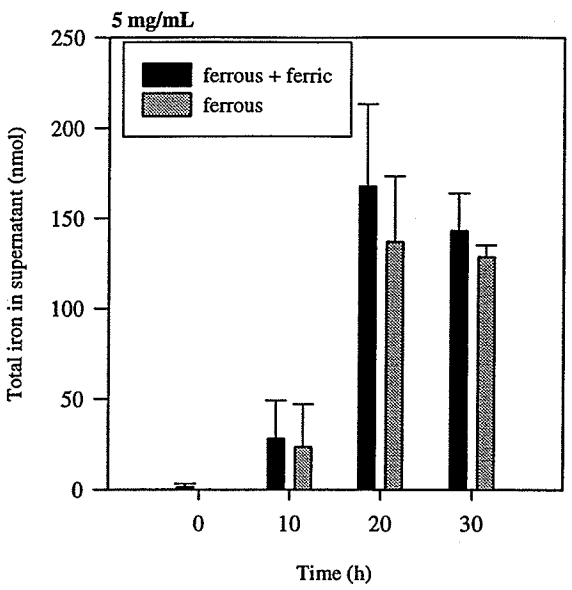
5 mg/mL
ferrous + ferric
ferrous
Total iron in supernatant (nmol)
250
200
150
100
50
0
0
10
20
30
Time (h)

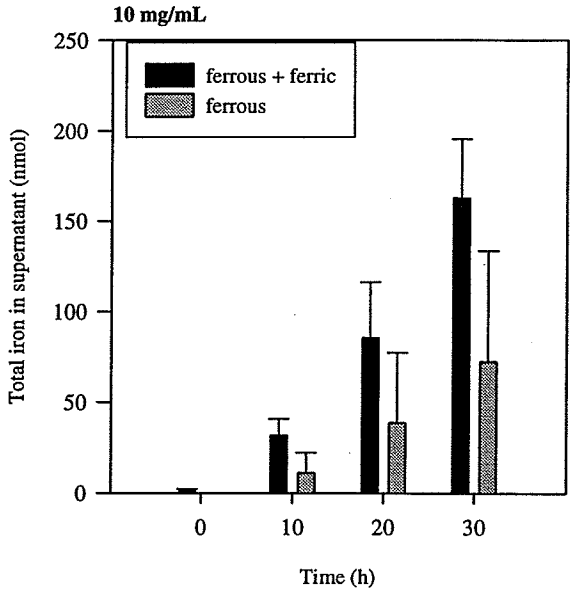
10 mg/mL
ferrous + ferric
ferrous
Total iron in supernatant (nmol)
250
200
150
100
50
0
0
10
20
30
Time (h)

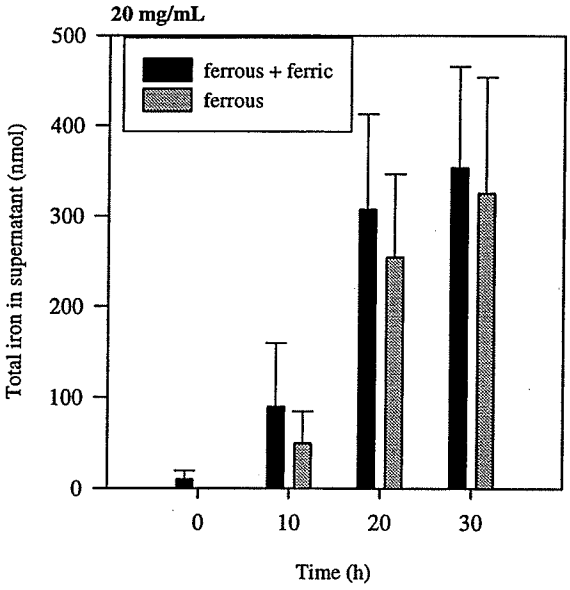
20 mg/mL
ferrous + ferric
ferrous
Total iron in supernatant (nmol)
500
400
300
200
100
0
0
10
20
30
Time (h)

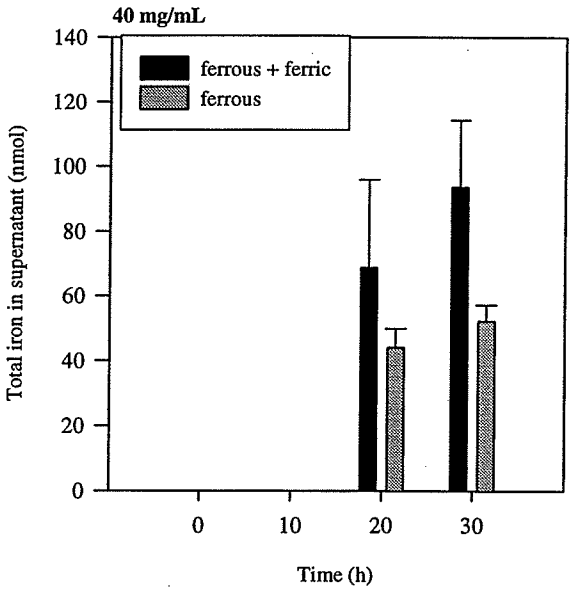
40 mg/mL
ferrous + ferric
ferrous
Total iron in supernatant (nmol)
140
120
100
80
60
40
20
0
0
10
20
30
Time (h)

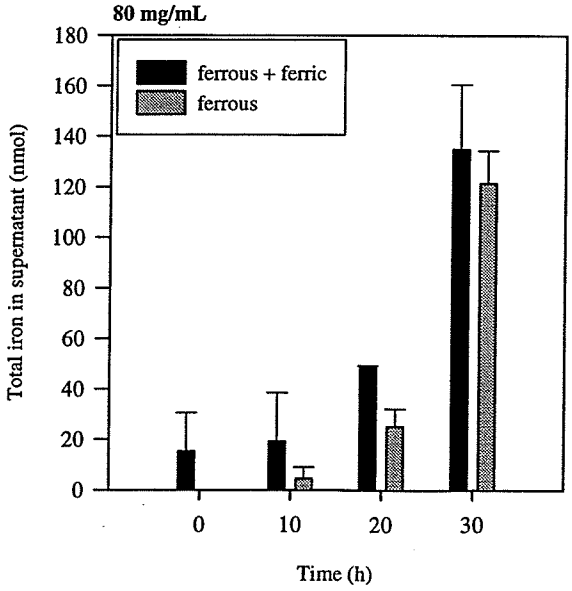
80 mg/mL
ferrous + ferric
ferrous
Total iron in supernatant (nmol)
180
160
140
120
100
80
60
40
20
0
0
10
20
30
Time (h)

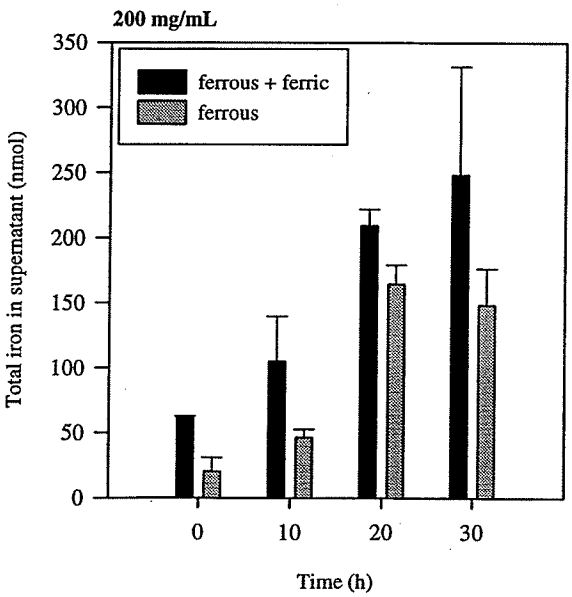
200 mg/mL
ferrous + ferric
ferrous
Total iron in supernatant (nmol)
350
300
250
200
150
100
50
0
0
10
20
30
Time (h)

c)

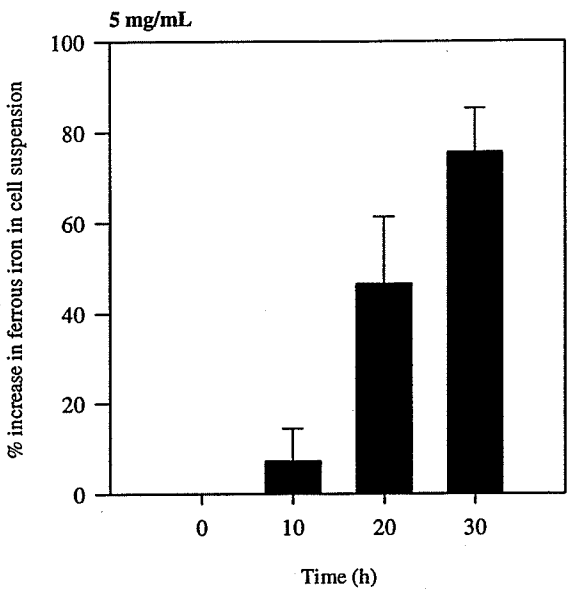
5 mg/mL
% increase in ferrous iron in cell suspension
100
80
60
40
20
0
0
10
20
30
Time (h)

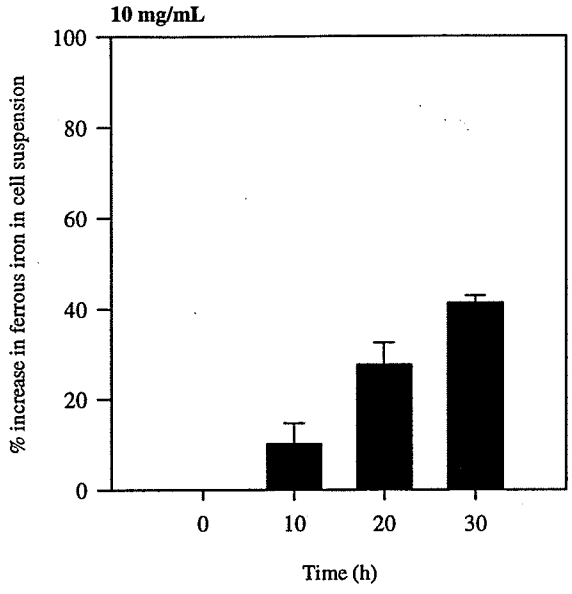
10 mg/mL
% increase in ferrous iron in cell suspension
100
80
60
40
20
0
0
10
20
30
Time (h)

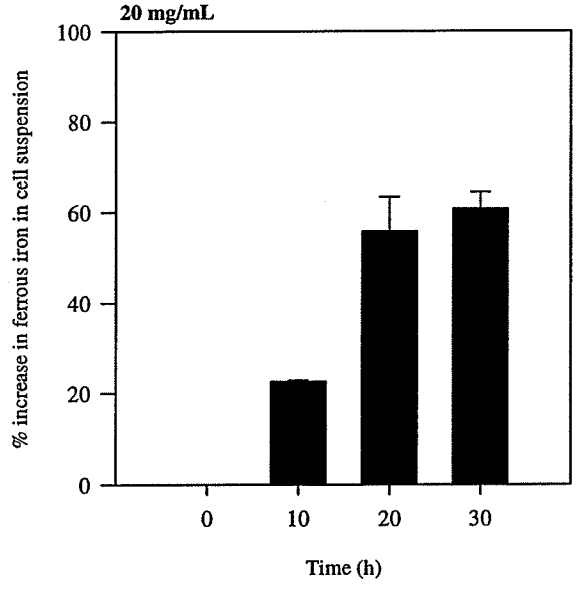
20 mg/mL
% increase in ferrous iron in cell suspension
100
80
60
40
20
0
0
10
20
30
Time (h)

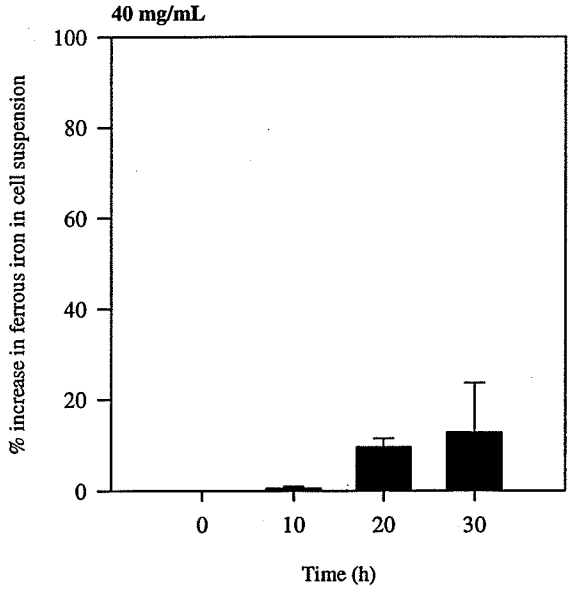
40 mg/mL
% increase in ferrous iron in cell suspension
100
80
60
40
20
0
0
10
20
30
Time (h)

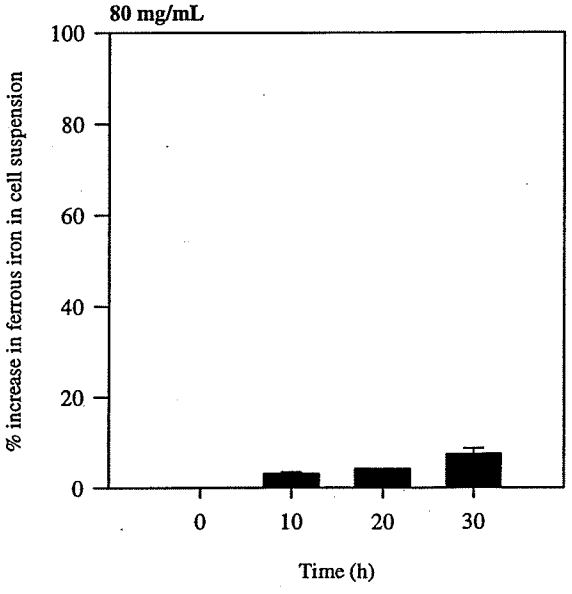
80 mg/mL
% increase in ferrous iron in cell suspension
100
80
60
40
20
0
0
10
20
30
Time (h)

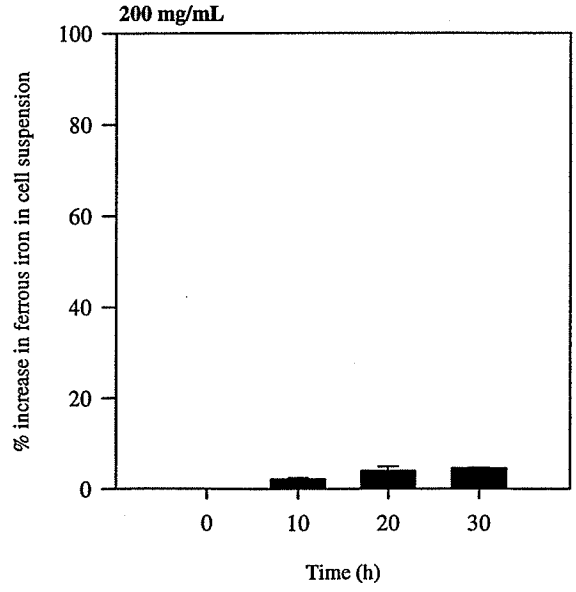
200 mg/mL
% increase in ferrous iron in cell suspension
100
80
60
40
20
0
0
10
20
30
Time (h)

**Figure 13** Endogenous ferric iron reduction by endogenous respiration during anaerobic incubation. The reactions were performed at 25°C in 0.1 M β-alanine-$H_2SO_4$ pH 3 and contained 20 mg of cells and 4 μmol $FeCl_3$. The volume of the reaction mixtures was 1 mL.

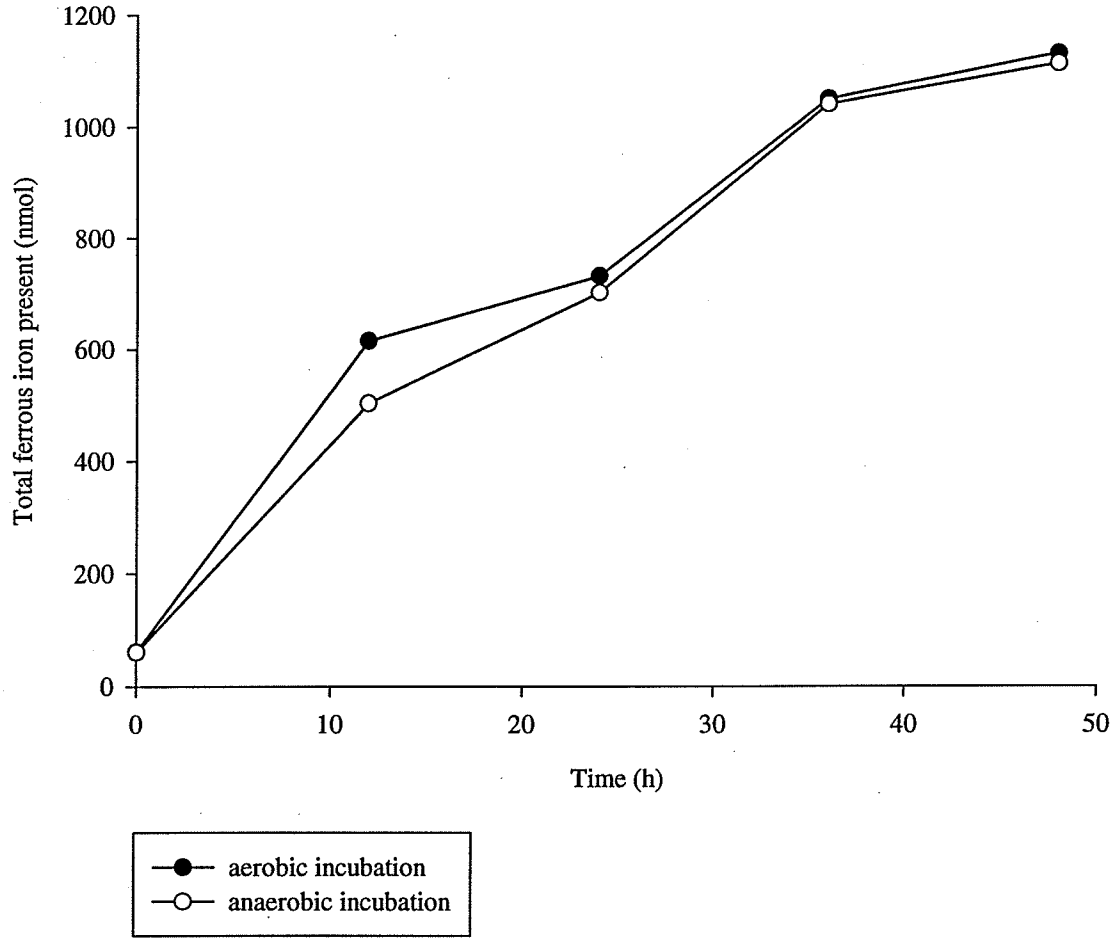
1200
1000
800
600
400
200
0
Total ferrous iron present (nmol)
0
10
20
30
40
50
Time (h)
aerobic incubation
anaerobic incubation

**Figure 14** Dithionite reduced minus oxidized spectrum of cell free crude extracts of **a)** thiosulfate grown cells and **b)** sulfur grown cells. Preparation of cell free extracts and the technique used to obtain the spectra are outlined in materials and methods.

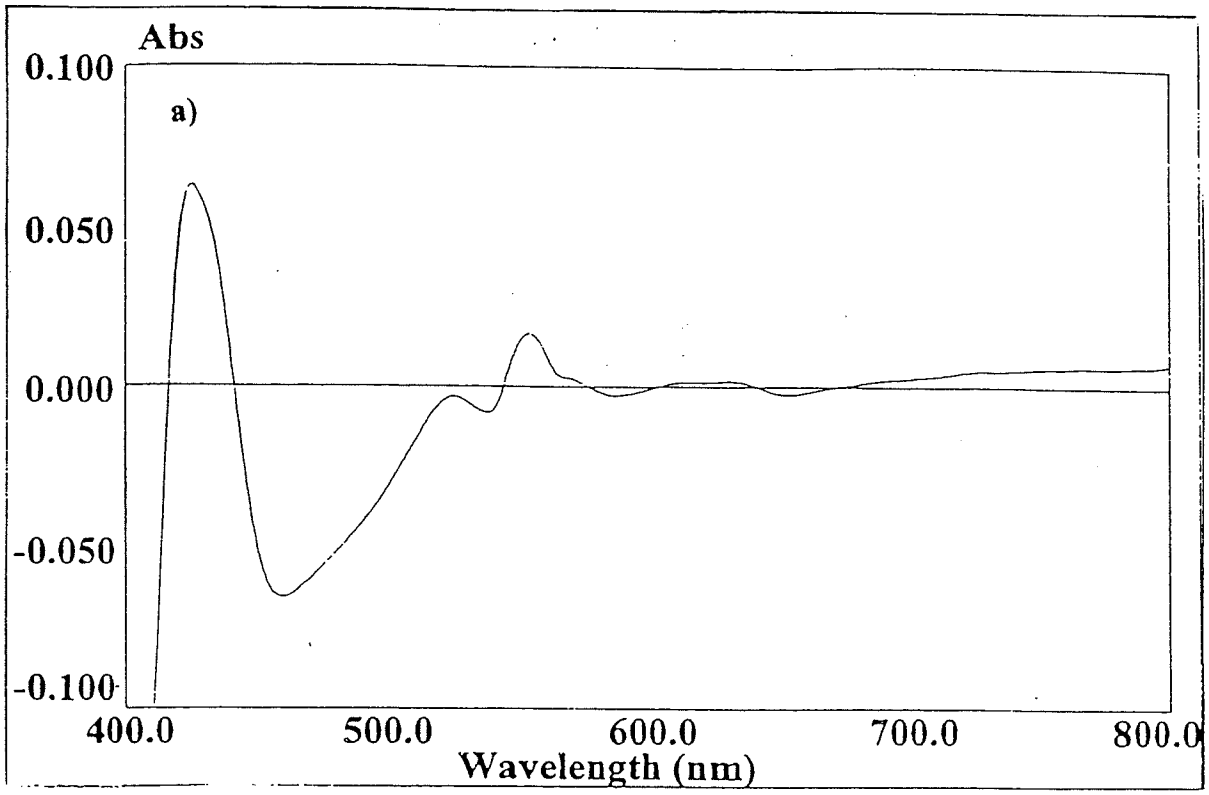
Abs
0.100
a)
0.050
0.000
-0.050
-0.100
400.0
500.0
600.0
700.0
800.0
Wavelength (nm)

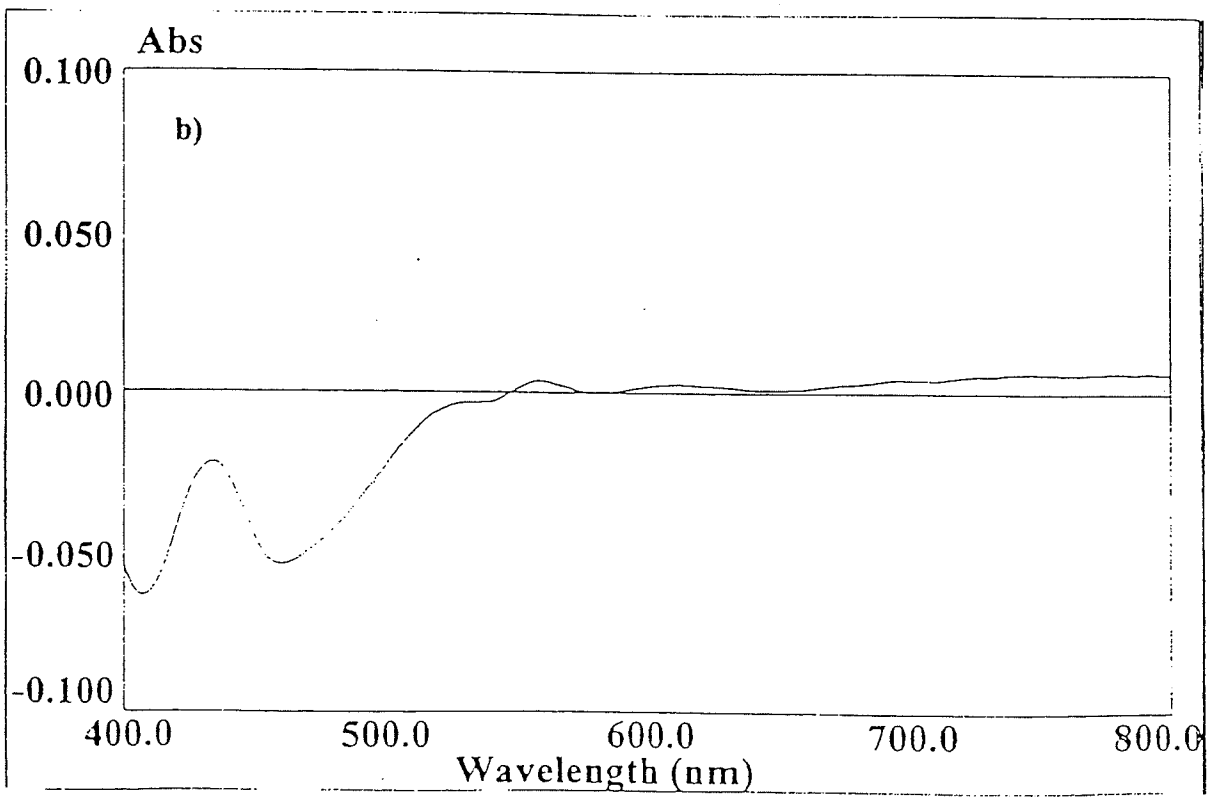
Abs
0.100
b)
0.050
0.000
-0.050
-0.100
400.0
500.0
600.0
700.0
800.0
Wavelength (nm)

# References

Aleem, M.I.H. 1977. Coupling of energy with electron transfer reactions in chemoautotrophic bacteria. *In* Microbial Energetics. *Edited* by B.A. Haddock and W.A. Hamilton. Cambridge University Press, London, U.K. . pp. 351-381.

Aleem, M.I.H. 1969. Generation of reducing power in chemosynthesis. VI. Energy-linked reactions in the chemoautotroph, *Thiobacillus neapolitanus*. Antonie van Leeuwenhock. 35: 379-391.

Aleem, M.I.H., Lees, H., and Nicholas, D.J.D. 1963. Adenosine triphosphate-dependent reduction of nicotinamide adenine dinucleotide by ferro-cytochrom *c* in chemoautotrophic bacteria. Nature. 200: 759-761.

Alexander, B., Leach, S. and Ingledew, W.J. 1987. The relationship between chemiosmotic parameters and sensitivity to anions and organic acids in the acidophile *Thiobacillus ferrooxidans*. J. Gen. Microbiol. 133: 1171-1179.

Ballentine, R. and Burford, D.D. 1957. Determination of metals. *In* Methods Enzymol. Vol 3. *Edited* by S.P. Colowick and N.O. Kaplan. Academic Press, New York, New York, U.S.A. . pp. 1002-1035.

Boonstra, J., Ottema, S., Sips,H., and Konings, W.N. 1979. Uncoupling action of amytal in membrane vesicles from *Escherichia coli*. Eur. J. Biochem. 102: 383-388.

Bray, R.C. 1963. *In* The Enzymes. Vol. 7. *Edited* by P.D. Boyer, H. Lardy, and K. Myrbäck, Academic Press, New York, New York, U.S.A. . pp.533.

Brasseur, G., Bruscella, P., Bonnefoy, V., and Lemesle-Meunier, D.2002. The $bc_1$ complex of the iron-grown acidophilic chemolithotrophic bacterium *Acidithiobacillus ferrooxidans* functions in the reverse but not in the forward direction. Is there a second $bc_1$ complex?. Biochim. Biophys. Acta. 1555: 37-43.

Brock, T.D. and Gustafson,J. 1976. Ferric iron reduction by sulfur- and iron- oxidizing bacteria. Appl. Environ. Microbiol. 32: 567-571.

Brugna, M., Nitschke, W., Asso, M., Guigliarelle, B., Lemesle-Meunier, D., and Schmidt, C. 1999. Redox components of cytochrome bc-type enzymes in acidophilic prokaryotes II. The Rieske protein of phylogentically distant acidophilic organisms. J. Biol. Chem. 274: 16766-16772.

Chappell, J.B. and Greville, G.D. 1954. Effect of silver ions on mitochondrial adenosine triphosphatase. Nature. 174: 930-931.

Charles, A.M. and Suzuki, I. 1966. Purification and properties of sulfite: cytochrome *c* oxidoreductase from *Thiobacillus novellas*. Biochim. Biophys. Acta. 128: 522-534.

Chena, S-C and Liu, J-K. 1999. The respiratory responses to cyanide of a cyanide-resistant *Klebsiella oxytoca* bacterial strain. FEMS Microbiol. Lett. 175: 37-43.
Cohen, H.J., Fridovich, I. and Rajagopalan, K.V. 1971. Hepatic sulfite oxidase: A functional role for molybdenum. J. Biol. Chem. 246: 374-382.

Cobley, J.G. 1976a. Energy-conserving reactions in phosphorylating electron transport particles from *Nitrobacter winogradskyi*. Activation of nitrite oxidation by the electrical component of the proton motive force. Biochem. J. 156: 481-491.

Cobley, J.G. 1976b. Reduction of cytochromes by nitrite in electron-transport particles from *Nitrobacter winogradskyi*. Proposal of a mechanism for $H^+$ translocation. Biochem. J. 156: 493-498.

Cook, T.M. and Umbreit, W.W. 1962. The occurrence of cytochrome and coenzyme Q in *Thiobacillus thiooxidans*. Biochem. 2: 194-196.

Cox, J.C., Nicholls, D.G. and Ingledew, W.J. 1979. Transmembrane electrical potential and transmembrane pH gradient in the acidophile *Thiobacillus ferro-oxidans*. Biochem. J. 178: 195-200.

Darrouzet, E., Valkova-Valchanova, M., Ohnishi, T. and Daldal, F. 1999. Structure and function of the bacterial $bc_1$ complex : Domain movement, subunit interactions, and emerging rationale engineering attempts. J. Bioenerg. Biomembr. 31: 275-288.

Dean, J.A. (*Editor*). 1985. Lange's handbook of chemistry. 13$^{th}$ ed. McGraw-Hill Company, New York, New York, U.S.A. .

Dibrov, P., Dzioba, J., Gosink, K. K. and Häse, C.C. 2002. Chemiosmotic mechanism of antimicrobial activity of $Ag^+$ in *Vibrio cholerae*. Antimicrob. Agents Chemother. 46: 2668-2670.

Dixon, M. and Webb, E.C. 1979. Enzymes. Third Edition. Longman Group Limited, London, U.K. .

Elbehti, A., Brasseur, G., and Lemesle-Meunier, D. 2000. First evidence for the existence of an uphill electron transfer through the *bc*1 and NADH-Q oxidoreductase complexes of the acidophilic obligate chemolithotrophic ferrous ion-oxidizing bacterium *Thiobacillus ferrooxidans*. J. Bacteriol. 182: 3602-3606.

Elbehti, A., Nitschke, W., Tron, P., Michel, C., and Lemesle-Meunier, D. 1999. Redox components of cytochrome *bc*-type enzymes in acidophilic prokaryotes I. Characterization of the cytochrome $bc_1$-type complex of the acidophilic ferrous ion-oxidizing bacterium Thiobacillus ferrooxidans. J. Biol. Chem. 274: 16760-16765.

Enoch, H.G. and Lester, R.C. 1975. The purification and properties of formate dehydrogenase and nitrate reductase from *Escherichia coli*. J. Biol. Chem. 237: 6693-6705.

Giudici-Orticoni, M. –T., Guerlesquin, F., Bruschi, M., and Nitschke, W. 1999. Interaction induced redox switch in the electron transport complex rusticyanin-cytochrome $c_4$. J. Biol. Chem. 274: 30365-30369.

Haddock, B.A. and Jones, C.W. 1977. Bacterial respiration. Bacteriol. Rev. 41: 47-99.

Harahuc, L. and Suzuki, I. 2001. Sulfite oxidation by iron-grown cells of *Thiobacillus ferrooxidans* at pH 3 possibly involves free radicals, iron, and cytochrome oxidase. Can. J. Microbiol. 47: 424-430.

Harrison, A.P. 1982. Genomic and physiological diversity amongst strains of *Thiobacillus ferrooxidans*, and genomic comparison with *Thiobacillus thiooxidans*. Arch. Microbiol. 131: 68-76.

Hsung, J.C. and Haug, A. 1977 a). Membrane potential of *Thermoplasma acidophila*. FEBS Lett. 73: 47-50.

Hsung, J.C. and Haug, A. 1977 b). $\zeta$ – potential and surface charge of *Thermoplasma acidophila*. Biochim. Biophys. Acta. 461: 124-130.

Hunte, C., Palsdottir, H., and Trumpower, B.L. 2003. Protonmotive pathways and mechanisms in the cytochrome bc1 complex. FEBS Lett. 545: 39-46.

Ingledew, W.J. 1982. *Thiobacillus ferrooxidans*: The bioenergetics of an acidophilic chemolithotroph. Biochim. Biophys. Acta. 683: 89-117.

Jackson, J.F., Moriarity, D.J.W., and Nicholas, D.J.D. 1968. Deoxyribonucleic acid base composition and taxonomy of Thiobacilli and some nitrifiying bacteria. J. Gen. Microbiol. 53: 53-60.

Kamimura, K., Fuji, S., and Sugio, T. 2001. Purification and some properties of ubiquinol oxidase from obligately chemolithotrophic iron-oxidizing bacterium, *Thiobacillus ferrooxidans* NASF-1. Biosci. Biotechnol. Biochem. 65: 63-71.

Kappler, U., Bennett, B., Rethmeier, J., Schwarz, G., Deutzmann, R., McEwan, A.G., and Dahl, C. 2000. Sulfite: cytochrome *c* oxidoreductase from *Thiobacillus novellas*: Purification, characterization, and molecular biology of a heterodimeric member of the sulfite oxidase family. J. Biol. Chem. 275: 13202-13212.

Kappler, U. and Dahl, C. 2001. Enzymology and molecular biology of prokaryotic sulfite oxidation. FEMS Microbiol. Lett. 203: 1-9.

Kelly, D.P. and Wood, A.P. 2000. Reclassification of some species of Thiobacillus to the newly designated genera *Acidithiobacillus* gen. nov., *Halothiobacillus* gen. nov. and *Thermithiobacillus* gen. nov. Int. J. Syst. Evol. Microbiol. 50: 511-516.

Kessler, D.L. and Rajagopalan, K.V. 1972. Purification and properties of sulfite oxidase from chicken liver. J. Biol. Chem. 247: 6566-6573.

Kiesow, L.A. 1967. Energy-linked reactions in chemoautotrophic organisms. *In* Current Topics in Bioenergetics. Vol. 2. *Edited* by D.R. Sanadi. Academic Press, New York, New York, U.S.A. . pp. 195-233.

Kino, K. and Usami, S. 1982. Biological reduction of ferric iron by iron- and sulfur-oxidizing bacteria. Agric. Biol. Chem. 46: 803-805.

Knowles, C.J. 1976. Microorganisms and cyanide. Bacteriol. Rev. 40: 652-680.

Knowles, C.J. and Bunch, A.W. 1986. Microbial cyanide metabolism. Adv. Microbiol. Physiol. 27: 73-111.

Kodoma, A., Kodoma, T. and Mori, T. 1970. Studies on the metabolism of a sulfur-oxidizing bacterium VII. Oxidation of sulfite by a cell-free extract of *Thiobacillus thiooxidans*. Plant and Cell Physiol. 11: 701-711.

Leberman, R. and Soper, A.K. 1995. Effect of high salt concentrations on water structure. Nature. 378: 364-366.

Lehninger, A.L., Nelson, D.L. and Cox, M.M. 1993. Princples of Biochemistry. Second Edition. Worth Publishers, Inc. New York, New York, U.S.A. .

Levin, R.A. 1971. Fatty acids of *Thiobacillus thiooxidans*. J. Bacteriol. 108: 992-995.

Lizama, H. M. and Suzuki, I. 1991. Kinetics of sulfur and pyrite oxidation by *Thiobacillus thiooxidans*. Competitive inhibition by increasing concentrations of cells. Can. J. Microbiol. 37: 182-187.

Lofrumento, N.E., Zanotti, F., and Pavone, A. 1979. Effect of ethylmaleimide on the transport of $Ca^+$ and $K^+$ ions across mitochondrial membranes. Boll. Soc. Ital. Biol. Sper. 55: 715-721.

Lofrumento, N.E. and Zanotti, F. 1978. Calcium release induced by N-ethylmaleimide in rat liver mitochondria. FEBS Lett. 87: 186-190.

Lu, W-P. and Kelly, D.P. 1984. Properties and role of sulfite:cytochrome *c* oxidoreductase purified from *Thiobacillus versutus* (A2). J. Gen. Microbiol. 130: 1683-1692.

Lyric, R.M. and Suzuki, I. 1970. Enzymes involved in the metabolism of thiosulfate by Thiobacillus thioparus I. Survey of enzymes and properties of sulfite: cytochrome *c* oxidoreductase. Can. J. Biochem. 48: 334-343.

Marquis, R.E. 1995. Antimicrobial actions of fluoride for oral bacteria. Can. J. Microbiol. 41: 955-964.

Marzulli, D., Zanotti, F. and Lofrumento, N.E. 1985 (a). N-ethylmaleimide as oxidizing agent in biological and non-biological systems. Boll. Soc. Ital. Biol. Sper. 61: 121-127.

Marzulli, D., Zanotti, F. and Lofrumento, N.E. 1985 (b). An indirect and highly sensitive method for the determination of the flow of reducing equivalents in the respiratory chain. Boll. Soc. Ital. Biol. Sper. 61: 129-135.

Masau, R.J.Y., Oh, J.K., and Suzuki, I. 2001. Mechanism of oxidation of inorganic sulfur compounds by thiosulfate-grown *Thiobacillus thiooxidans*. Can. J. Microbiol. 47: 348-358.

Matin, A., Wilson, B., Zychlinsky, E., and Matin, M. 1982. Proton motive force and physiological basis of delta pH maintenance in *Thiobacillus acidophilus*. J. Bacteriol. 150: 582-591.

Mitchell, P. 1976. Possible molecular mechanisms of the protonmotive function of cytochrome systems. J. Theoret. Biol. 62: 327-367.

Miyoshi, H. 1998. Structure-activity relationships of some complex I inhibitors. Biochemica et Biophysica Acta. 1364: 236-244.

Nakamura, K., Kuribayashi, S., Kurosawa, H. and Amano, Y. 1992. Pathway of sulfite oxidation in *Thiobacillus thiooxidans* JCM 784. Biosci. Biotech. Biochem. 56: 261-263.

Nakamura, K., Miki, H., and Amano, Y. 1990. Cell growth and accumulation of *Thiobacillus thiooxidans* S3 in a ph-controlled thiosulfate medium. J. Gen. Appl. Microbiol. 36: 369-376.

Nakamura, K., Yoshikawa, H., Okubo, S., Kurosawa, H., and Amano, Y. 1995. Purification and properties of membrane-bound sulfite dehydrogenase from *Thiobacillus thiooxidans* JCM7814. Biosci. Biotech. Biochem. 59: 11-15.

Nicholls, D.G. and Ferguson, S.J. 1992. Bioenergetics 2. Academic Press Inc. San Diego, California, U.S.A.

Nogami, Y., Maeda, T., Negishi, A., and Sugio, T. 1997. Inhibition of sulfur oxidizing activity by nickel ion in *Thiobacillus thiooxidans* NB1-3 isolated from the corroded concrete. Biosci. Biotech. Biochem. 61: 1373-1375.

Oleskin, A.V. and Samuilov, V.D. 1988. Side effects of $bc_1$ cytochrome complex inhibitors in energy-transducing biomembranes. Biokhim. 53: 1803-1809.

Oshima, T., Arakawa, H. and Baba, M. 1977. Biochemical studies on an acidophilic, thermophilic bacterium, *Bacillus acidocaldarius*: Isolation of bacteria, intracellular pH, and stabilities of biopolymers. J. Biochem. 81: 1107-1113.

Parasegian, V.A. 1995. Hopes for Hofmeister. Nature. 378: 335-336.
Pinset, J. 1954. The need for selenite and molybdate in the formation of formic dehydrogenase by members of the *Coli-aerogenes* group of bacteria. Biochem. J. 57:10-16.

Pinset, J. 1954. The need for selenite and molybdate in the formation of formic dehydrogenase by members of the *Coli-aerogenes* group of bacteria. Biochem. J. 57: 10-16.

Pronk, J.T. and Johnson, D.B. 1992. Oxidation and reduction of iron by acidophilic bacteria. Geomicrobiol. J. 10: 153-171.

Pronk, J.T., Meijer, W.M., Hazeu, W., van Dijken, J.P., Bos, P., and Kuenen, J.G. 1991. Growth of Thiobacillus ferroxidans on formic acid. Appl. Environ. Microbiol. 57: 2057-2062.

Rajagopalan, K.V., Fridovich, I., and Handler, P. 1962. Hepatic aldehyde oxidase: I Purification and properties. J. Biol. Chem. 273: 922-928.

Rohwerder, T. and Sand, W. 2003. The sulfane sulfur of persulfides in the actual substrate of the sulfur-oxidizing enzyme from *Acidithiobacillus* and *Acidiphilium* spp. Microbiol. 149: 1699-1709.

Roth, C.W., Hempfling, W.P., Conners, J.N., and Vishniac, W.V. 1973. Thiosulfate- and sulfide-dependent pyridine nucleotide reduction and gluconeogenesis in intact *Thiobacillus neapolitanus*. J. Bacteriol. 114: 592-599.

Rudolph, M.J., Johnson, J.L., Rajagopalan, K.V., and Kisker, C. 2003. The 1.2 Å structure of the human sulfite oxidase cytochrome $b_5$ domain. Acta. Cryst. D59: 1183-1191.

Saxena, J. and Aleem, M.I.H. 1972. Generation of reducing power in chemosynthesis VII. Mechanism of pyridine nucleotide reduction by thiosulfate in the chemoautotroph *Thiobacillus neapolitanus*. Arch. Mikrobiol. 84: 317-326.

Searcy, D.G. 1976. *Thermoplasma acidophilum*: Intracellular pH and potassium concentration. Biochim. Biophys. Acta. 451: 278-286.

Segel, I.H. 1975. Enzyme Kinetics. John Wiley and Sons Inc. New York, New York, U.S.A. .

Shively, J.M., Devore, W., Stratford, L., Porter, L., Medlin, L., and Stevens, S.E. 1986. Molecular evolution of the large subunit of ribulose-1,5-bisphosphate carboxylase/oxygenase (RuBisCo). FEMS Microbiol. Lett. 37: 251-257.

Shively, J.M., van Keulen, G., and Meijer, W.G. 1998. Something from almost nothing: Carbon dioxide fixation in chemoautotrophs. Annu. Rev. Microbiol. 52: 191-230.

Silverman, M.P. and Lundgren, D.G. 1959. Studies on the chemoautotrophic iron bacteria *Ferrobacillus ferrooxidans* I An improved medium and a harvesting procedure for securing high cell yields. J. Bacteriol. 77: 642-647.

Sugio, T., Domatsu, C., Munakata, O., Tano, T., and Imai, K. 1985. Role of ferric iron-reducing system in sulfur oxidation of *Thiobacillus ferrooxidans*. Appl. Environ. Microbiol. 49: 1401-1406.

Sugio, T., Hirose, T., Li-Zhen, Y., and Tano, T. 1992. Purification and some properties of sulfite: ferric ion oxidoreductase from *Thiobacillus ferrooxidans*. J. Bacteriol. 174: 4189-4192.

Sugio, T., Katagiri, T., Inagaki, K., and Tano, T. 1989. Actual substrate for elemental sulfur oxidation by sulfur:ferric ion oxidoreductase purified from *Thiobacillus ferrooxidans*. Biochim. Biophys. Acta. 973: 250-256.

Sugio, T., Katagiri, T., Moriyama, M., Zhēn, Y.L., Inagaki, K., and Tano, T. 1988. Existence of a new type of sulfite oxidase which utilizes ferric ions as an electron acceptor in *Thiobacillus ferrooxidans*. Appl. Environ. Microbiol. 54: 153-157.

Sugio, T., Noguchi, M., and Tano, T. 1987. Detoxification of sulfite produced during the oxidation of elemental sulfur by *Thiobacillus ferrooxidans*. Agric. Biol. Chem. 51: 1431-1433.

Sugio, T., Mizunaski, W., Inagaki, K., and Tano, T. 1987. Purification and some properties of sulfur: ferric ion oxidoreductase from *Thiobacillus ferroxidans*. J. Bacteriol. 169: 4916-4922.

Sugio, T., White, K.J., Shute, E., Choate, D., and Blake II, R.C. 1992. Existence of a hydrogen sulfide: ferric ion oxidoreductase in iron-oxidizing bacteria. Appl. Environ. Microbiol. 58: 431-433.

Suzuki, I., Chan, C.W., and Takeuchi, T.L. 1992. Oxidation of elemental sulfur to sulfite by *Thiobacillus thiooxidans* cells. Appl. Environ. Microbiol. 58: 3767-3769.

Suzuki, I., Lee, D., Mackay, B., Harahuc, L. and Oh, J.K. 1999. Effect of various ions, pH, and osmotic pressure on oxidation of elemental sulfur by *Thiobacillus thiooxidans*. Appl. Environ. Microbiol. 65: 5163-5168.

Suzuki, I., Takeuchi, T.L., Yuthasastrkosol, T.D., and Oh, J.K. 1990. Ferrous iron and sulfur oxidation and ferric iron reduction activities of *Thiobacillus ferrooxidans* are affected by growth on ferrous iron, sulfur, or a sulfide ore. Appl. Environ. Microbiol. 56: 1620-1626.

Suzuki, I. 1999. Oxidation of inorganic sulfur compounds: Chemical and enzymatic reactions. Can. J. Microbiol. 45: 97-105.

Suzuki, I. 1994. Sulfite: cytochrome *c* oxidoreductase of Thiobacilli. *In* Methods Enzymol. Vol. 243. *Edited* by H.D. Peck Jr. and J. LeGall, Academic Press, New York, New York, U.S.A. . pp.447-454.

Suzuki, I. 1974. Mechanism of inorganic oxidation and energy coupling. Annu. Rev. Microbiol. 28: 85-101.

Suzuki, I. 1965. Oxidation of elemental sulfur by an enzyme system of Thiobacillus thiooxidans. Biochim. Biophys. Acta. 104: 359-371.

Takakuwa, S. 1976. Studies on the metabolism of a sulfur-oxidizing bacterium IX. Electron transfer and the terminal oxidase system in sulfite oxidation of *Thiobacillus thiooxidans*. Plant and Cell Physiol. 17: 103-110.

Takakuwa, S., Nishiwaki, T., Hosoda, K., Tominaga, N., and Iwasaki, H. 1977. Promoting effect of molybdate on the growth of sulfur-oxidizing bacterium, *Thiobacillus thiooxidans*. J. Gen. Appl. Microbiol. 23: 163-173.

Takeuchi, T.L. and Suzuki, I. 1994. Effect of pH on sulfite oxidation by *Thiobacillus thiooxidans* cells with sulfurous acid or sulfur dioxide as a possible substrate. J. Bacteriol. 176: 913-916.

Tano, T., Ito, T., Takesue, H., Sugio, T. and Imai, K. 1982. *b*-type cytochrome, an electron carrier in the sulfite-oxidation system of *Thiobacillus thiooxidans*. J. Ferment. Technol. 60: 181-187.

Tikhonova, G.V., Lisenkova, L.L., Doman, N.G., and Skulachev, V.P. 1967. Electron transport pathways in *T. ferrooxidans*. Biokhim. 32: 725-733.

Thöny-Meyer, L. 1997. Biogenesis of respiratory cytochromes in bacteria. Microbiol. Mol. Biol. Rev. 61: 337-376.

Toghrol, F and Southerland, W.M.. 1983. Sulfite oxidase activity in *Thiobacillus novellas*. J. Bacteriol. 156: 941-944.

Vestal, J.R. and Lundgren, D.G. 1971. The sulfite oxidase of *Thiobacillus ferrooxidans* (*Ferrobacillus ferrooxidans*). Can. J. Biochem. 49: 1125-1130.

Vogler, K.G., LePage, G.A., and Umbreit, W.W. 1942. Studies on the metabolism of autotrophic bacteria. I. The respiration of *Thiobacillus thiooxidans* on sulfur. J. Gen. Physiol. 26: 89-102.

von Jagow, G. and Link, T.A. 1986. Use of specific inhibitors on the mitochondrial $bc_1$ complex. *In* Methods Enzymol. Vol. 126. *Edited* by S. Fleischer and B. Fleischer. Academic Press, New York, New York, U.S.A. . pp. 253-271.

Waksman, S.A. and Joffe, J.S. 1922. Microorganisms concerned in the oxidation of sulfur in the soil. II. Thiobacillus thiooxidans, a new sulfur oxidizing organism, isolated from soil. J. Bacteriol. 7: 239-256.

West, P.W. and Gaeke, G.C. 1956. Fixation of sulfur dioxide as disulfitomercurate and subsequent colorimetric estimation. Anal. Chem. 28: 1816-1819.

Yamanaka, T. 1992. The biochemistry of bacterial cytochromes. Springer-Verlag, Berlin, Germany.

Yamanaka, T., Yoshioka, T., and Kimura, K. 1981. Purification of sulphite-cytochrome c reductase of Thiobacillus novellas and reconstitution of its sulphite oxidase system with the purified constitutents. Plant Cell. Physiol. 22: 613-622.

Zanotti, F., Marzulli, D. and Lofrumento, N.E. 1985. The effect of some sulfhydryl reagents on the respiratory chain activity. Boll. Soc. Ital. Biol. Sper. 61: 113-20.